AD-A200 758

ENDOCHRONIC PLASTICITY

DTIC FILE COPY

Kirk C. Valanis

President, ENDOCHRONICS, INC.
Vancouver, Washington
and
Research Professor, Applied Science Center
University of Portland
Portland, Oregon

Harold E. Read

Manager, Applied Mechanics
S-CUBED
La Jolla, California

DTIC
SELECTE
OCT 1 7 1988
S D

December, 1987

88 9 27 134

ENDOCHRONIC PLASTICITY

Kirk C. Valanis

President, ENDOCHRONICS, INC.
Vancouver, Washington
and
Research Professor, Applied Science Center
University of Portland
Portland, Oregon

Harold E. Read

Manager, Applied Mechanics
S-CUBED
La Jolla, California

December, 1987

PREFACE

In this book we have attempted to give an analytical, thorough account of the progress that has been made in the field of Endochronic Plasticity* during the the last sixteen years since its inception. We believe that anyone with advanced knowledge in the field of solid mechanics will have little difficulty following the analytical exposition. Often we have given simple worked examples to aid the reader, even though we suspect that at times we may have been somewhat concise.

It is our hope that the large number of applications to real material behavior and the copious instances of favorable comparison with experiment presented herein will convince, even the most casual reader that the theory has indeed a "natural" basic and intrinsic capability for describing remarkably well the plastic behavior of materials. Furthermore it is a theory that can be taught in the classroom in a rational and sequential manner, particularly since the material functions can be determined from well-defined experiments. Furthermore, it also contains classical von Mises plasticity as a special case.

We do not doubt that there exist cases — and more will be found -- where the theory will not describe the observed behavior with the kind of accuracy presented here. For instance, hardening of face-centered cubic metals in cyclic paths in more than one dimension may be one such case. We believe that what will be called for here is not a new theory but a modification of the hardening function, possibly from scalar to tensorial. Thus the fundamental constructs of the theory will remain unchanged.

Throughout the evolution and development of the theory we have tried to retain a central unity, simplicity and an economy of form whereby various manifestations of the mechanical response of a material are merely "projections" of the constitutive equation on that "response plane". We have, in fact, refrained from "dichotomies" whereby one form of a constitutive equation of a material would be applicable to one class of strain histories and another form to another. The benefit of this approach, apart from its esthetic value, is that if a constitutive equation has a broad validity then it must be representative of physical reality and can form a basis for the understanding of the internal physical processes that underlie the observed phenomena. We feel that the examples presented in this book, to illustrate the application of the

---

* The term "Endochronic" was coined by Valanis from the Greek language and means internal (endo) time (chronos).

i

theory, provide strong support for this approach.

There are a number of interesting topics pertinent to the endochronic theory that have not been discussed in this book. These include large deformations, rate-dependence and creep, damage and fracture, dilatancy, and numerical methods for treating endochronic models in large finite element or finite difference computer codes. These topics will be covered in an upcoming second volume of Endochronic Plasticity by the same co-authors.

ACKNOWLEDGEMENT

TABLE OF CONTENTS

TABLE OF CONTENTS

TABLE OF CONTENTS

Section   **Page**

TABLE OF CONTENTS

1. INTRODUCTION.

1.1 Plasticity and Thermodynamics.

In 1970. the year when the first two papers [1.1, 1.2] on endochronic plasticity were actually conceived. the foundations of the existing theory of plasticity. which is a mathematical theory for rate-indifferent behavior. were basically mechanical. The fundamental hypothesis upon which this theory rested was, and still is, that there exists a yield surface in stress space which determines whether a change in the stress state in a material neighborhood will (a) give or (b) not give rise to a plastic deformation of that neighborhood. See, for instance Fung [1.3] for the climate of thought at that time.

It was further postulated that, in the event that (a) is true, the increment in plastic strain is normal to a potential surface in stress space. In the "associated flow rule" theories the yield surface and the potential surface are identical. The shape and size of these surfaces is generally assumed to depend on the state of stress, the temperature and the history of plastic deformation. The precise nature of this dependence was a matter of conjecture and simple models such as "isotropic" or "linear kinematic" hardening. or combinations thereof were introduced in the literature in the course of time.

Experimental programs undertaken by a number of investigators to resolve this question revealed that different definitions of yield give rise to differing modes of the manner in which the topology of the yield surface changes with deformation. Since the onset of yield is not a well-defined physical phenomenon and depends a great deal on the sensitivity of experimental measurement the question must be asked of whether yield is an *a priori* essential ingredient in a constitutive formulation of the mechanical response of metals. or merely a convenient *a posteriori* idealization. Furthermore. despite extensive experimentation. notably by Phillips. the experimental determination of the precise constitutive dependence of the geometry of the yield surface on the history of plastic deformation remained unresolved. (As it happens the endochronic theory answered this question explicitly by determining that the back stress is a linear functional of the plastic strain history. but more will be said about this later in Chapter 3.)

From the physical perspective. experimental observation suggests that in the presence of monotonically increasing deformation at constant strain rate. the stress response of metals at <u>room temperature</u> shows little sensitivity to the actual value of

the strain rate over a fairly broad range (10^{-5} - 10^{-1} sec^{-1}). Under these conditions plasticity appears to be an appropriate theory insofar as rate insensitivity is concerned.

On the other hand, as the temperature increases strain rate sensitivity becomes more pronounced to the point where viscoelasticity (without yield and albeit non-linear) appeared to experimenters to be a more appropriate theory for the mechanical behavior of metals. Seemingly, temperature appears to play an important role in determining whether "yield" is an essential constitutive ingredient in a theoretical formulation of metal behavior. Moreover there was the nagging question as to why thermodynamics could not play a more central role in the formulation of a constitutive theory for metal plasticity.

The decade of the sixties saw a rapid development of the theory of irreversible thermodynamics of internal variables as a rigorous branch of phenomenological science pertaining to the deformation of materials, even though its impact was not realized until a decade later. See typically Refs. [1.4] to [1.11]. Until then, irreversible thermodynamics remained an obscure field of science where the "equilibrium state" played a basic role and irreversibility was understood only as a small deviation from this state. So long as a system (or process, or both) was near equilibrium, thermodynamic equilibrium relations applied, approximately (but not otherwise).

At the beginning the internal variable theory was developed in conjunction with linear systems (linear rate equations) with the implicit assumption that this was a theory of irreversible systems near equilibrium (see Refs. [1.4] to [1.8]). Even after the removal of this limitation by Valanis and Coleman [1.9, 1.10, 1.11] there was still not a clear distinction between an equilibrium state and a thermodynamic state and a recognition that in the new context, a thermodynamic state is not necessarily an equilibrium state or a near-equilibrium state. This was probably due to the fact that the existence of entropy for systems far for equilibrium was still open to doubt and was accepted grudgingly only for systems (or processes) near equilibrium. Insofar as plasticity of metals was concerned the internal variable theory was still regarded as an approximation at best [1.12].

From an historical perspective Coleman [1.13], in developing his _functional_ _thermodynamics_, must be credited for taking the bold step in assuming without proof that an entropy function exists for systems far from equilibrium. The question of

existence of entropy, however, still remained. In 1971, Valanis [1.14] published a proof of existence of entropy for systems far from equilibrium making use of Caratheodory's axiom of inaccessibility of thermodynamic states along reversible paths [1.15]. In 1981 a more rigorous proof along similar lines was given by Valanis [1.16] with a clear physical justification for the axiom of inaccessibility. The way was now clear to apply the theory of irreversible thermodynamics of internal variables to material systems far from equilbrium.

1.2 The Concept of Intrinsic Time.

Time is a measure of change. A change in the position of a pendulum from one extreme to the other measures half a period. If the period of oscillation is one second, then half a second is a measure of change in the above positions. In an ideal pendulum the period is invariant, i.e., the temporal distance between two specific events (in this case the two extreme positions) is always constant. If now one marks off on the real line points corresponding to the ends of half periods (or periods) these points are all equidistant. A continuous time scale is now created by assuming that the density of events between any two points is, in fact, constant. As it happens the motion of the pendulum relative to its own time scale satisfies Newton's second law of motion.

Consider now another system which is not cognizant of a Newtonian time scale. A metal whose stress response is strain rate insensitive is such a system. The internal changes that determine the stress state begin at the onset of deformation and end when the deformation stops. No further internal changes will take place unless the state of deformation changes.

This is another instance in which time is a measure of change. In this case, however, if there is no internal change there is no time change. Since the stress is, inevitably, determined by the history of internal change, it is obvious that this history cannot be defined with respect to the Newtonian time scale <u>but by one that is determined by the internal material changes brought about by the deformation</u>. Such a time scale is obviously <u>intrinsic</u> to the material at hand. Initially, "internal change" was regarded in the broadest possible terms. For instance an affine rearrangement of the atoms due to deformation was considered an internal change.

However, from a strictly phenomenological viewpoint, insofar as a material neighborhood is concerned, all one can measure is the state of stress corresponding to the current state of strain. More generally, and in geometric terms, to every strain path in a nine-dimensional strain space (with an appropriate metric), there corresponds a stress path in a nine-dimensional stress space. Thus if strain is regarded as the input then the strain path would appear to qualify as an appropriate time scale with respect to which the strain history (which determines the stress) could be defined.

This is indeed the position that Valanis took in 1970 in the work subsequently published in Refs. [1.1] and [1.2]) where he defined the intrinsic time measure $d\varsigma$ as the increment of distance along the total strain path in a strain space with a (material) metric $\underset{\sim}{P}$. Thus for small strains

$$(d\varsigma)^2 = d\underset{\sim}{\varepsilon} \cdot \underset{\sim}{P} \cdot d\underset{\sim}{\varepsilon} \quad , \tag{1-1}$$

where $\underset{\sim}{\varepsilon}$ is the small strain tensor. Of course nothing is ever totally new under the sun. Il'iushin [1.17] broached the idea of path dependence in terms of a path s where

$$ds^2 = d\underset{\sim}{\varepsilon} \cdot d\underset{\sim}{\varepsilon} \quad , \tag{1-2}$$

and Pipkin and Rivlin [1.18] examined the mathematics of functionals defined in terms of this path but stopped short of testing the applicability of their equations to real systems.

It should be pointed out that the Il'iushin measure ds is a very particular case of $d\varsigma$ when $\underset{\sim}{P}$ is isotropic and has the very restricted form

$$P_{ijk\ell} = \delta_{ik} \, \delta_{j\ell} \tag{1-3}$$

Therefore ds is not intrinsic to the material at hand and is not applicable to materials that are compressible and/or anisotropic.

Subsequent work by Valanis [1.19] revealed that Eq. (1-1) gave rise to one-dimensional stress-strain behavior which, at the onset of unloading, was not in agreement with observation. Specifically in metals, the slope of the uniaxial stress-strain curve at the onset of unloading was higher than the elastic slope, observed in experiment. Also small hysteresis loops in the first quadrant of the uniaxial stress-strain space did not close as is invariably observed.

These inadequacies of the theory were removed by Valanis [1.20, 1.21] upon defining the intrinsic time measure in terms of the increment in <u>plastic</u> strain. Thus

$$d\zeta^2 = d\underset{\sim}{\varepsilon}^P \cdot \underset{\sim}{P} \cdot d\underset{\sim}{\varepsilon}^P \qquad (1-4)$$

For an extensive discussion of this issue see Section 2.3.

1.3 Endochronic Plasticity and Experiment.

The definition of intrinsic time given in Eq. (1-4), in conjunction with plastic incompressibility and a weakly singular deviatoric memory kernel, gives rise to theoretically predicted behavior of metals that matches closely that which is observed in experiment. For instance the continuous transition from elastic to plastic behavior that one observes in most metals (one exception is mild steel at slow strain rates) is now given by the theory by virtue of the continuity of the (deviatoric) memory kernel at all z except $z = 0$. The singularity of the kernel at $z = 0$ ensures that the slope of the uniaxial (or shear) stress-strain curve at the onset of unloading or reloading is elastic.

No yield surface exists and, as a result, no experiments need be done to determine such a surface and its wanderings in stress space. The two fundamental and only material functions i.e., the deviatoric memory kernel $\rho(z)$ and the hardening function $F_s(\zeta)$ -- that determine completely, in any number of dimensions, the stress response of isotropic plastically incompressible materials -- can be found by means of a uniaxial test, or shear test for that matter. If a yield point, i.e., a sharp transition between elastic and plastic behavior exists, this can be accounted for by the presence of a delta function in the memory kernel at $z = 0$. <u>The strength of the delta function is the yield stress.</u> <u>The continuous part of the kernel then determines the evolution of the back stress.</u> These points are discussed extensively in Chapter 3.

1.4 The Book.

The book consists of ten chapters, Chapter 1 being the Introduction.

Chapter 2 deals with the constitutive development of the endochronic theory. Section 2.1 deals with the basic thermodynamics of the endochronic theory, particularly with the concepts that underlie the irreversible thermodynamics of internal variables, and the derivation of constitutive equations for isotropic, plastically compressible solids, in isothermal small strain fields. Section 2.2 deals with the concept of intrinsic time and the necessity and sufficiency of its definition in terms of Eq. (1-4).

Chapter 3 is devoted to the treatment of plastically incompressible bodies. To begin, a simple worked example is given in Section 3.2. In the same section the properties of the deviatoric memory kernel and specifically the weak singularity in its functional form are dealt with in some detail. Section 3.3 deals with the analysis of the stress response to complex uniaxial strain paths involving arbitrary sequential segments of loading and unloading. Extensive comparison with experimental data is made in the case where the memory kernel is given by a simple weakly singular power form and remarkable agreement is demonstrated for a number of very complex such paths. Section 3.4 deals with the very important question of the experimental determination of the two basic material functions of plastically incompressible bodies: the memory function $\rho(z)$ and the hardening function $F_s(\varsigma)$. It is shown that both these functions can be determined from a uniaxial (or pure shear) experiment. Section 3.5 deals with applications of the theory in more than one dimension. Experimental evidence of the predictive capability of the theory is demonstrated in heterogeneous two-dimensional strain fields, created in a plate with two symmetrically placed edge cracks, by pulling in the axial direction, pulling and unloading, then compressing, unloading and pulling and so on. Also in this section the ability of the theory to predict the experimentally observed stress in the case of a number of nonproportional strain paths in two dimensions, specifically tension-torsion, is clearly demonstrated. Section 3.6 is devoted to endochronic plasticity with a yield surface.

This is an important section where it is demonstrated that if the memory kernel $\rho(z)$ contains a delta function (as it must when the number of internal variables is finite! [1.2]), then the endochronic theory takes the special form of a von Mises yield surface theory with non-linear kinematic-cum-isotropic hardening. Furthermore the theory gives as a derived result, and for the first time in the history of plasticity, that the "back stress" is a linear functional of the history of plastic strain. This result was obtained by Valanis in 1980. See Ref. [1.21].

At the 1984 symposium on plasticity in Udine (see Ref. [1.22]) E. H. Lee made an argument, later published as a discussion in the proceedings of the symposium, p. 175, that "the back stress must be a function of the plastic strain" and merely referenced himself [1.23]. A study of this reference, however, failed to reveal a demonstration that the back stress is a functional of the history of plastic strain.

Chapter 4 is devoted to the theory of compressible plastic isotropic solids, such as soils and concrete. The full constitutive equation is reviewed and the various consequences of plastic compressibility are illustrated. There are now four basic material functions to be determined: the deviatoric and hydrostatic memory functions ρ and ϕ, respectively, and the deviatoric and hydrostatic hardening functions F_s and F_H. A straightforward experimental technique for their determination is given. It must be noted that this particular constitutive equation does not account for dilatancy but a more general equation with dilatant capability has been derived recently by Valanis and Peters [1.24] and applied to soils by Peters [1.25] and Valanis and Read [1.26].

Chapter 5 deals with some general topics of central interest to plasticity. The results, by Valanis, are totally new and have not appeared previously in the literature. Section 5.1 treats the problem of history induced anisotropy. It is demonstrated that in the case of a plastically incompressible solid, any plastic strain history with a terminal zero stress will give rise to anisotropy, if the terminal state is regarded as a reference state of a subsequent plastic strain history. Sections 5.2 and 5.3 are devoted to the Drucker and Il'iushin postulates. Contrary to accepted opinion, it is proved that both of these postulates have a thermodynamic origin and are, in fact, variants of one and the same postulate to the effect that:

The irreversible entropy production during an isothermal cycle, closed either with respect to stress or strain, is greater than the free energy release at the end of the cycle.

Section 5.4 examines the question of uniqueness of the solution of the initial and boundary value problems of plastically incompressible bodies. It is shown in this section that the solutions of the above problems are unique when the constitutive equation given in Chapter 2 governs the material behavior of the continuum -- with or without a yield surface.

Chapter 6 gives an overall discussion of the flow rules of endochronic plasticity in the presence of plastic incompressibility. The essence of a "flow rule" is contained in the following question:

Given an increment of stress or strain, what is the corresponding increment of plastic strain?

In a strict sense, the flow rules of endochronic plasticity are _implicit_ in that the plastic strain increment, corresponding to a stress or strain increment, can be calculated directly from the constitutive equation. However, further analysis reveals that simple rules exist -- known as "flow rules" -- which give the information on the magnitude and direction of the plastic strain increment, without the need for a computation involving the endochronic constitutive equation. These bear resemblance -- but are not identical -- to the flow rules of classical plasticity and are a direct consequence of the singularity of the deviatoric memory kernel.

Chapters 7 and 8 give two different analyses for determining the flow rules of endochronic plasticity -- in the presence of plastic incompressibility. The reasons behind the two analyses are historical, as explained below. At the time the writing of this book began, the flow rules in existence were those derived by Murakami and Read in Refs. [1.27] and [1.28]. They considered the case of an arbitrary change in the direction of a stress path which was previously smooth. The explicit orientation of the plastic strain increment relative to the stress increment, however, was not determined. The analysis by Murakami and Read, which also gives the orientation of

the plastic strain increment relative to the ultimate surface. is given in Chapter 8.

In the course of writing Chapter 5. Valanis saw the possibility of an analysis which determines the flow rules in general situations and proves that the plastic strain path is continuous and has a continuous derivative at "loading" points but a discontinuous derivative at "unloading" points. This analysis is given in Chapter 7. Because the methods of derivation are fundamentally different we felt that the reader will benefit from both expositions. Needless to say. the results by both methods agree when the appropriate conditions apply.

Chapter 9 pertains to the application of the endochronic theory of plastically compressible solids to plain concrete. This work became possible by virtue of some excellent three-dimensional experiments carried out at the University of Colorado [1.29]. In spite of the susceptibility of plain concrete to cracking. the material at hand. and the nature of the experiments. were such that no significant damage to the concrete was observed. The extremely complex behavior of this material notwithstanding. it is demonstrated in this chapter that the theory has a remarkable capability for predicting the observed response in cases of intricate. non-proportional three-dimensional stress paths. In particular the phenomenon of shear-induced densification in the presence of constant pressure is predicted. with great analytical economy. in closed form.

Finally. Chapter 10 deals briefly with analytical techniques for integrating numerically the constitutive equation in the presence of arbitrary stress or strain paths.

Before closing we would like to beg the indulgence of the many other contributors to the endochronic theory. namely. Professor Han Chin Wu. Dr. H. C. Lin. Dr. M. C. Yip. Professor Z. P. Bazant and more recently. Professor S. N. Atluri. to name a few. whose contributions are now part of the technical literature. Pressure of time has prevented us from discussing their work in this volume.

REFERENCES FOR CHAPTER 1.

1.1   Valanis. K. C., "A Theory of Viscoplasticity Without a Yield Surface: General Theory." *Arch. Mechs.*, 23 (1971). 517.

1.2   Valanis. K. C., "A Theory of Viscoplasticity Without a Yield Surface: Application to Metals." *Arch. Mechs.*, 23 (1971), 535.

1.3   Fung. Y. C., "Foundations of Solid Mechanics." Prentice Hall. N.J., (1965).

1.4   Biot. M. A., "Theory of Stress-Strain Relations in Anisotropic Viscoelastic and Relaxation Phenomena. *J. Appl. Phys.*, 25, 1385 (1954).

1.5   Biot. M. A., "Variational Principle in Irreversible Thermodynamics with Application to Viscoelasticity." *Phys. Rev.*, 97, 1463 (1955).

1.6   Biot. M. A., "Thermoelasticity and Irreversible Thermodynamics." *J. App. Phys.*, 27, 240 (1956).

1.7   Biot. M. A., "Linear Thermodynamics and the Mechanics of Solids." *Proc. Third U.S. National Congress of Appl. Mech.*, A.S.M.E., NY (1958).

1.8   Schapery. R. A., "Application of Thermodynamics to Thermomechanical Fracture and Birefringent Phenomena in Viscoelastic Media." *J. Appl. Phys.*, 35, 1941 (1964).

1.9   Valanis. K. C., "The Viscoelastic Potential and Its Thermodynamic Foundations. Iowa State University. ERI Report 52 (1967). *J. Math. and Phys.*, 47, 262 (1968).

1.10   Valanis. K. C., "Unified Theory of Thermomechanical Behavior of Viscoelastic Materials." *Proc. Mechanical Behavior of Materials Under Dynamic Loads.* Ed. U.S. Lindholm. Springer Verlag. NY (1968).

1.11   Coleman. B. D., and M. Gurtin. "Thermodynamics with Internal Variables." *J. Chem. Phys.*,)47, 597 (1971).

1.12   Rice. J. R.., "On The Structure of Stress-Strain Relations for Time-Dependent Plastic Deformation of Metals." *J. App. Mechs.*, 37, 728 (1970).

1.13   Coleman. B. D., "Thermodynamics of Materials with Memory." *Arch. of Rational Mechanics and Analysis.* 17, 1 (1964).

1.14   Valanis. K. C., "Irreversibility and Existence of Entropy." *Intl. J. Non-linear Mechs.*, 6, 337 (1971).

1.15   Caratheodory, C., "Untersuchungen Über die Grundlagen der Thermodynamic," *Math. Annalen.* 67, 355 (1909).

1.16   Valanis, K. C., "Partial Integrability as a Basis of Existence of Entropy in Irreversible Systems," *ZAMM.* 63, 73 (1983).

1.17   Il'iushin, A. A., "On the Relation Between Stresses and Small Deformations in the Mechanics of Continuous Media," *Prikl. Math. Mekh.,* 18, 641 (1954).

1.18   Pipkin, A. C., and R. S. Rivlin, "Mechanics of Rate-Independent Materials," *ZAMP,* 16, 313 (1965).

1.19   Valanis, K. C., "On the Foundations of the Endochronic Theory of Plasticity," *Arch. of Mech.,* 27, 857 (1975).

1.20   Valanis, K. C., "Fundamental Consequences of a New Intrinsic Time Measure. Plasticity as a Limit of the Endochronic Theory," University of Iowa Report G 224-DME-78-001 (1978).

1.21   Valanis, K. C., "Some Fundamental Consequences of a New Intrinsic Time Measure. Plasticity as a Limit of the Endochronic Theory," *Arch. Mechs.,* 32, 181 (1980).

1.22   Sawczuk, A., and G. Bianchi, Proceedings, International Symposium on "Plasticity Today. Modeling, Methods and Applications," Udine, Italy (1983). Elsevier Applied Science Publishers, London (1985).

1.23   Lee, E. H., "Elastic-Plastic Deformation at Finite Strains," *J. Appl. Mechs.,* 36, 1 (1969).

1.24   Valanis, K. C., and J. Peters, "A Constitutive Theory of Soils with Dilatant Capability," Waterways Experiment Station Report WES xxx-xxxx (1987).

1.25   Peters, J., "Internal Variable Model for Frictional Materials," *Proceedings, International Workshop on Constitutive Equations for Granular Non-Cohesive Materials,* Ed. A. Saada, Case Western Reserve University (1987).

1.26   Valanis, K. C., and H. E. Read, "An Endochronic Constitutive Model for ISST Soils," S-CUBED Report in preparation (1987).

1.27   Murakami, H., and H. E. Read, "Endochronic Plasticity: Some Basic Properties of Plastic Flow and Failure, *Intl. J. Solids and Structs.,* 23(1), 133 (1987).

1.28   Murakami, H., and H. E. Read. "Plastic Flow Properties of an Endochronic Model with a Third-Invariant Ultimate Surface." to appear.

1.29   Scavuzzo, R., T. Stankowski, K. H. Gerstle and H. Y. Ko. "Stress-Strain Curves for Concrete Under Multi-Axial Load Histories." CEAE Dept. University of Colorado, Boulder, Colorado (1983).

2. THEORETICAL FOUNDATIONS OF THE THEORY

2.1 Basic Thermodynamics.

From a thermodynamic standpoint materials are divided into two basic and distinct classes: reversible and irreversible (or dissipative). In reversible materials the work done during homogeneous deformation and temperature is completely recoverable and in a cycle of such thermomechanical process the material returns to its initial state. Thus if temperature and strain denote the thermodynamic state of the system then the internal energy and stress are "functions of state" in the sense that they are determined by the current values of temperature and strain.

In this book, however, we shall deal with thermodynamics of <u>dissipative</u> materials. The word "dissipative" is meant to denote that class of materials with the following property: <u>the work done during homogeneous deformation and temperature is not completely recoverable in the sense that a measurable portion of it is converted into "heat", i.e., random vibrational energy of the constituent atoms of the material</u>. Because the loss of recoverable energy is a function of the strain (stress) and temperature histories, the material response is also a function of the strain (stress) and temperature histories. The above statement is tantamount to saying that the stress (strain) at time t is <u>not</u> determined by the value of the strain (stress) and temperature at time t.

In thermodynamic language, the stress (strain) in dissipative materials is not a state function of strain (stress) and temperature and similarly other thermodynamic functions such as internal energy and free energy are not either. Note that in the above discussion strain and stress are used interchangeably depending on which is regarded as the independent thermodynamic variable.

In the theory of irreversible thermodynamics of internal variables "dissipative" behavior is accounted for by introducing additional thermodynamic variables which are not macroscopically measurable but whose physical existence is necessary for the description of the observed physical phenomena. These variables are called <u>internal</u> variables or <u>internal state</u> variables and are denoted by q_r. In the present treatment they will be regarded as second order symmetric tensors. Their number will depend on the complexity of the material in question and on the degree of accuracy with which one wishes to describe the material response.

In a descriptive sense they could signify conformations of dislocations as would be the case in metals or, more generally, non-affine motions of atoms and internal flaws. Of significance is the observation that the internal variables cannot be functions of state, otherwise their introduction would be redundant. As we shall show they are in fact functions of the history of strain (stress) and temperature as well, but we shall not be concerned with thermal effects in this book, even though the general equations will be derived in the presence of a temperature field.

2.1.1 First Law of Thermodynamics.

The first law of thermodynamics is, in essence, a statement of conservation of energy of a material system. The global form of the law concerns large material systems whereas the local form pertains to infinitesimally small systems. The latter is less general than the former in that it may be derived from it when conditions of continuity and differentiability apply.

Given a finite material domain the First Law is a statement to the fact that:

The Rate of Change of Internal Energy + The Rate of Change of Kinetic Energy = The Rate of Work Done by the Surface Forces + The Rate of Work Done by the Body Forces + The Rate of Heat Supply by Conduction, Radiation and Internal Heat Sources.

It is shown in standard textbooks on continuum mechanics (see [2.1], for example) that when the First Law is applied to an infinitesimal system, the rate of work done by the forces on the system by virtue of its rigid body motion, is exactly equal to the rate of change of its kinetic energy so that the local form is now the following:

The Rate of Change of Internal Energy = The Rate of Work Done by the Stresses by Virtue of the Velocity Gradients + The Rate of Heat Supply by Conduction, Radiation, and Heat Sources.

The appropriate analytical expression for the local form in the presence of a small strain field is, then, the following:

$$\dot{e} = \sigma_{ij} \, \dot{\epsilon}_{ij} - h_{i,i} + \dot{q} \tag{2-1}$$

2-2

where e is the internal energy per unit undeformed volume, σ_{ij} the stress tensor, ϵ_{ij} the small strain tensor, h_i the heat flux vector, q the heat supply per unit undeformed volume and a dot over a quantity denotes differentiation with respect to time. One may now proceed to define a quantity Q such that $\dot{Q}$ is the rate of total heat supply to the system by means of conduction and internal heat sources, that is

$$\dot{Q} = - h_{i,i} + \dot{q} \tag{2-2}$$

so that the First Law now becomes

$$\dot{e} = \sigma_{ij} \dot{\epsilon}_{ij} + \dot{Q} \quad . \tag{2-3}$$

2.1.2 Second Law of Thermodynamics - Entropy.

Reversible Systems.

A fundamental issue of thermodynamics has been the question of existence of entropy as a state function. This, of course, is a vast subject and we cannot do it justice in this book, whose scope and purposes are different. We felt, however, that a short discussion will be of value to the reader.

In reversible systems, entropy has not been in doubt ever since Caratheodory [2.2] argued its existence on the basis of inaccessibility of thermodynamic states during quasistatic changes of state. Valanis [2.3,2.4] showed that in the case of reversible systems entropy exists for the thermodynamic changes of state that are not necessarily quasistatic on the basis of the physical observation that in a reversible system under adiabatic conditions the temperature is a function of strain. Under these conditions and on the basis that the internal energy e and the stress σ are state functions of strain ϵ and temperature T, "the First Law is integrable" in the sense that if one writes Eq. (2-1) in the form

$$\dot{e} - \sigma_{ij} \dot{\epsilon}_{ij} = \dot{Q} \quad , \tag{2-4}$$

there exists an integrating denominator θ, (a generalized temperature) such that

$$\frac{\dot{e} - \sigma_{ij} \dot{\epsilon}_{ij}}{\theta} = \dot{\eta} \tag{2-5a}$$

2-3

or

$$\dot{e} = \sigma_{ij} \, \dot{\epsilon}_{ij} + \theta \dot{\eta} \, , \qquad\qquad (2\text{-}5b)$$

where η, the ENTROPY, <u>is a state function of strain and temperature</u>. Thus, in view of Eqs. (2-4) and (2-5),

$$\dot{\eta} = \frac{\dot{q}}{\theta} \quad\text{or}\quad \theta\dot{\eta} = \dot{q} \, . \qquad\qquad (2\text{-}6)$$

Equation (2-6) is known as the <u>Second Law of Thermodynamics</u>.

Irreversible Systems.

In the case of irreversible systems e and q are functions of strain, temperature and n internal variables g_r, i.e.,

$$e = e(c, T, g_r) \, , \quad q = (\xi, T, g_r) \, . \qquad\qquad (2\text{-}7a,b)$$

It has been shown by Valanis [2.3.2.4], that in irreversible systems <u>also</u>, an entropy function η exists, by virtue of Caratheodory's theorem of inaccessibility of states and the First Law. In this case η is related to other thermodynamic quantities by means of the following relation:

$$\dot{e}\Big|_q = \sigma_{ij}\dot{\epsilon}_{ij} + \theta\dot{\eta}\Big|_q \, , \qquad\qquad (2\text{-}8)$$

where θ is a generalized temperature and the subscript q denotes the variation of a quantity while the internal variables are kept constant. Of importance is the fact that now η is a function of q, T (or θ) and g_r:

$$\eta = \eta(\xi, T, g_r) \quad\text{or}\quad \eta = \eta[\epsilon(\theta, q)_{r}] \qquad\qquad (2\text{-}9a,b)$$

We point out the essential difference between Eqs. (2-5a) and (2-8). In the case of the former the rate of change of internal energy is equal to the rate of work plus the temperature times the rate of change of entropy. In the case of the latter, the rate of change on internal energy <u>at constant</u> g_r is equal to the rate of work plus the temperature times the rate of change of entropy <u>at constant</u> g_r. As we shall see

2-4

later this difference is going to make itself felt upon substitution of Eq. (2-8) in the first law of thermodynamics. See Ref.[2.3].

If now one substitutes Eqs. (2-7) and (2-9) in Eq. (2-8), relations (2-10) follow:

$$\sigma_{ij} = \frac{\partial}{\partial \epsilon_{ij}} (e - \theta\eta)\Big|_{T,q} \quad , \tag{2-10}$$

$$\theta\frac{\partial \eta}{\partial T}\Big|_{\epsilon,q} = \frac{\partial e}{\partial T}\Big|_{\epsilon,q} \quad , \tag{2-11}$$

where subscripts to the right of a vertical bar imply differentiation with the corresponding quantities held constant.

Simpler results follow if one introduces the transformation

$$\theta = \theta(T) \tag{2-12}$$

and use θ as an independent variable in Eqs. (2-10) and (2-11). In this case,

$$\sigma_{ij} = \frac{\partial}{\partial \epsilon_{ij}} (e - \theta\eta)\Big|_{\theta,q} \tag{2-13}$$

$$\theta\frac{\partial \eta}{\partial \theta}\Big|_{T,q} = \frac{\partial e}{\partial \theta}\Big|_{T,q} \quad . \tag{2-14}$$

Equation (2-13) suggests a new thermodynamic function ψ (the Helmholtz free energy) where

$$\psi = e - \theta\eta \quad . \tag{2-15}$$

When use is made of this last relation in Eqs. (2-13) and (2-14), one finds the "standard" thermodynamic equations:

$$\sigma_{ij} = \frac{\partial \psi}{\partial \epsilon_{ij}}\Big|_{\theta,q} \quad , \tag{2-16}$$

$$\theta = -\left.\frac{\partial \psi}{\partial \theta}\right|_{\epsilon,q} \quad , \tag{2-17}$$

which, insofar as solids are concerned, first appeared in the work of Biot [2.5, 2.6, 2.7, 2.8] and later Schapery [2.9] in the narrower context of $\theta = T$, their derivation differing in that the existence of entropy was assumed. In the form given above, they first appeared in the work of Valanis [2.3, 2.4] on the proof of existence of entropy in irreversible systems.

The Clausius - Duhem Inequality.

Substitution of Eqs. (2-15), (2-16) and (2-17) into the First Law, Eq. (2-3), gives the following result which is fundamental to the behavior of irreversible systems:

$$\theta \dot{\eta} + \frac{\partial \psi}{\partial g_r} \cdot \dot{g}_r = \dot{Q} \quad . \tag{2-18}$$

Note the difference between Eqs. (2-6), for reversible systems, and Eq. (2-18) for irreversible systems, particularly as they relate the rate of increase of entropy to the rate of heat supply. In the case of irreversible systems there is an extra term: $\partial\psi/\partial g_r \cdot \dot{g}_r$. The algebraic sign of this term is of central significance to irreversible behavior.

We note that

$$\frac{\partial \psi}{\partial g_r} \cdot \dot{g}_r = \left.\dot{\psi}\right|_{\epsilon,\theta} \quad . \tag{2-19}$$

In other words, the left-hand side of Eq. (2-19) i.e., the "extra term", is equal to the rate of change of the free energy under constant temperature and fixed strain. The constancy of temperature implies that no heat is being added to the system while the fixed strain precludes work from being done on the system. Under these conditions the free energy cannot increase since this "spontaneous" increase would imply an increased capability to do work and the system would then serve as a continuous source of mechanical energy, in the absence of external interference. Since such systems are not observed in nature, we are forced to conclude that

$$\dot{\psi}\Big|_{\xi,\theta} < 0 \quad , \tag{2-20}$$

so long as $\|\dot{g}_r\| \neq 0$, an inequality which is characteristic of thermodynamically **stable** systems. Use of inequality (2-20) in Eq. (2-18) gives rise to a second inequality, more commonly quoted,

$$\theta\dot{\eta} > \dot{Q} \tag{2-21}$$

when $\|\dot{g}_r\| \neq 0$, which is the Clausius-Duhem inequality, that applies to **irreversible** systems.

2.1.3 Evolution Equations for the Internal Variables.

One of the central consequences of Ineq. (2-20) and the associated Eq. (2-19) is the following inequality:

$$-\frac{\partial\psi}{\partial g_r} \cdot \dot{g}_r > 0 , \quad \text{(r not summed)} \tag{2-22}$$

for all g_r such that $\|\dot{g}_r\| \neq 0$. This, of course, is because g_r are independent variables, in which case, a specific g_r may be varied while the remaining may be kept constant. The implications of Ineq. (2-22) are profound. One main conclusion is that $- \partial\psi/\partial g_r$, on one hand, and $\dot{g}_r$, on the other, must be functionally related, otherwise they could be varied independently so as to violate Ineq. (2-22). This observation was made by Valanis [2.10, 2.11] who proceeded to suggest a general set of evolution equations for g_r of the type

$$\dot{g}_r = f_r(\zeta, g_r) \quad , \quad (r = 1,2 \dots n) \tag{2-23}$$

where ζ is a deformation measure (Right Cauchy - Green tensor) not necessarily pertaining to small deformation. These equations are commonly referred to in the literature as the "Coleman" equations, because Coleman and Gurtin also proposed them in Ref. [2.12]. However, they point out in that reference that while their manuscript was in progress Valanis had **already** proposed Eqs. (2-23) in Ref. [2.10]. We feel that we should make this comment so that the record can be corrected.

Of course the form of Eqs. (2-23) cannot be arbitrary but must satisfy the following inequality:

$$- \underset{\sim}{f}_r \cdot \frac{\partial \psi}{\partial \underset{\sim}{g}_r} > 0 \quad . \tag{2-24}$$

If one is dealing with a small deformation theory as is the case here, Eqs. (2-23) become

$$\dot{\underset{\sim}{g}}_r = \underset{\sim}{f}_r\left(\underset{\sim}{\varepsilon}, \underset{\sim}{g}_r\right) \quad , \tag{2-25}$$

where $\underset{\sim}{\varepsilon}$ is the small strain tensor.

A slightly different approach suggests itself if one recognizes that $- \partial \psi / \partial \underset{\sim}{g}_r$ are internal thermodynamic forces associated with the internal mechanism r and seeks a direct relationship between $\dot{\underset{\sim}{g}}_r$ and $- \partial \psi / \partial \underset{\sim}{g}_r$. In this case one may set

$$\dot{\underset{\sim}{g}}_r = - \underset{\sim}{f}_r\left(\frac{\partial \psi}{\partial \underset{\sim}{g}_s}\right) \tag{2-26}$$

The negative sign has been chosen for convenience so that the functions $\underset{\sim}{f}_r$ satisfy the inequalities:

$$\frac{\partial \psi}{\partial \underset{\sim}{g}_r} \cdot \underset{\sim}{f}_r > 0 \quad . \tag{2-27}$$

2.1.4 The Intrinsic Time Scale.

The concept of intrinsic time and its role in the constitutive theory of solids and, later liquids, was introduced in conjunction with the plasticity theory of metals by Valanis [2.13]. The basis of the concept lies in the proposition that a material senses rates of change associated with its constitution, not with respect to the Newtonian time t but an intrinsic time z, which is a property of the material at hand. Related ideas have stemmed from the observation that in certain cases the constitutive response of a material is most precisely and elegantly formulated by not using the actual time but a "reduced" time in the formulation. For instance this is the case in the "WLF equation" in polymers [2.15] where the "reduced" time ξ is related to the Newtonian time t by the relation

$$d\xi = \frac{dt}{a_T} \quad , \qquad\qquad (2\text{-}28)$$

where a_T is a function of temperature. The term "reduced" was actually introduced by Schapery [2.16] who used it in relation to a definition of $d\xi$ given in one dimension by the expression:

$$d\xi = \frac{dt}{a(T,\sigma,\dot{\epsilon})} \quad , \qquad\qquad (2\text{-}29)$$

where σ is the stress and $\dot{\epsilon}$ the strain rate. However, the very philosophy of Eq. (2-29) suggests an effect of the field (temperature, stress or strain rate field) on the time scale rather than a material time per se, i.e., an intrinsic time which is a material property of the substance at hand.

The subject will be discussed again at much greater length in Section 2.3 where a derivation of the intrinsic time scale is given. The significance of the proposition in so far as thermodynamics of evolution equations for g_r is concerned is that in Eq. (2-26) the rate of change of g_r is with regard to the intrinsic time z, so that the evolution equation for g_r now becomes

$$\frac{dg_r}{dz} + \mathcal{L}_r\left[\frac{\partial\psi}{\partial g_s}\right] = 0 \quad . \qquad\qquad (2\text{-}30)$$

Of particular interest in the linear form of Eqs. (2-30) which will be the basis of the theory presented in this book. This form is obtained on the basis of the proposition of classical irreversible thermodynamics, whereby the "internal forces" $\partial\psi/\partial g_r$, are proportional to the "fluxes", in this case the rates of the internal variables g_r, and is given by the equations:

$$\frac{\partial\psi}{\partial g_r} + \underset{\sim}{b}^{(r)} \cdot \frac{dg_r}{dz} = 0 \qquad\qquad (2\text{-}31)$$

Here $b^{(r)}$ is a fourth-order tensor, symmetric, and positive definite, the last property being necessary to satisfy the Clausius-Duhem inequality (2-22). The tensor $b^{(r)}$ is called the "dissipation", or resistance tensor for obvious reasons.

2.1.5 Recapitulation.

The thermodynamic formulation of constitutive equations of dissipative materials consists of the following steps.

(i)   Specifying the form of the Helmholtz free energy ψ where

$$\psi = \psi\left(\underset{\sim}{\varepsilon}, \theta, \mathbf{g}_r\right) \tag{2-32}$$

        Insofar as small strain theory is concerned the form of Eq. (2-32) is discussed at length in subsequent sections.

(ii)   Using Eqs. (2-16) and (2-17) to determine the stress and the entropy in terms of $\underset{\sim}{\varepsilon}$, θ and $\mathbf{g}_r$.

(iii)   Solving Eq. (2-31) to obtain the $\mathbf{g}_r$ as a function of the history of strain and temperature relative to the intrinsic time scale z.

(iv)   Determining the intrinsic time scale. This last step will be discussed in Section 2.3 for the case of rate independent materials.

2.2 Formulation of the Theory for Isothermal Small Strain Problems.

2.2.1 Basic Equations.

In the presence of small strain and uniform temperature fields we write the free energy density ψ in the quadratic form given below with the upper index of summation left unspecified.

$$\psi = \frac{1}{2} \sum_r \left(\underset{\sim}{\varepsilon} - \mathbf{g}_r\right) \cdot \underset{\sim}{A}^r \cdot \left(\underset{\sim}{\varepsilon} - \mathbf{g}_r\right) \ . \tag{2-33}$$

where $\mathbf{g}_r$ are the internal variables of the material system. $\underset{\sim}{\varepsilon}$ is the strain tensor and $\underset{\sim}{A}^r$ is the elastic stiffness tensor associated with the mechanism r. The physics of Eq. (2-33) become apparent upon the following observations.

Let internal constraints be applied to the system so that the quantities $(\underset{\sim}{\varepsilon} - \underset{\sim}{g}_r)$ vanish for all r except when $r = n$. In this case

$$\psi = \tfrac{1}{2}\left(\underset{\sim}{\varepsilon} - \underset{\sim}{g}_n\right) \cdot \underset{\sim}{A}^n \cdot \left(\underset{\sim}{\varepsilon} - \underset{\sim}{g}_n\right) \; . \tag{2-34}$$

Since at constant temperature the Helmholtz free energy has the physical significance of the <u>elastic</u> (recoverable) energy, it follows that $\underset{\sim}{A}^n$ is the elastic stiffness tensor associated with the deformation of mechanism n and

$$\underset{\sim}{\varepsilon} - \underset{\sim}{g}_n = \underset{\sim}{\varepsilon}_n^e \; , \tag{2-35}$$

where $\underset{\sim}{\varepsilon}_n^e$ is the elastic strain of the material system when only the nth mechanism is operative. Thus Eq. (2-34) becomes

$$\psi = \tfrac{1}{2} \, \underset{\sim}{\varepsilon}_n^e \cdot \underset{\sim}{A}^n \cdot \underset{\sim}{\varepsilon}_n^e \; , \tag{2-36}$$

so that ψ in Eq. (2-36) is the strain energy associated with the deformation related to the mechanism n. In conventional plasticity terms, $\underset{\sim}{g}_n$ is the plastic strain associated with mechanism n since indeed by definition

$$\underset{\sim}{\varepsilon}_n^p = \underset{\sim}{\varepsilon} - \underset{\sim}{\varepsilon}_n^e = \underset{\sim}{g}_n \; , \tag{2-37}$$

the strain $\underset{\sim}{\varepsilon}$ being common to all mechanisms.

The basic thermodynamic relations of interest are:

$$\underset{\sim}{\sigma} = \frac{\partial \psi}{\partial \underset{\sim}{\varepsilon}} = \sum_r \underset{\sim}{A}^r \cdot \left(\underset{\sim}{\varepsilon} - \underset{\sim}{g}_r\right) \tag{2-38}$$

$$\frac{\partial \psi}{\partial \underset{\sim}{g}_r} + \underset{\sim}{b}^r \cdot \frac{d\underset{\sim}{g}_r}{dz} = 0 \tag{2-39}$$

and thus in view of Eq. (2-33) we have:

$$\underset{\sim}{A}^r \cdot \left(\underset{\sim}{\varepsilon} - \underset{\sim}{g}_r \right) = \underset{\sim}{b}^r \cdot \frac{d\underset{\sim}{g}_r}{dz} \quad , \tag{2-40}$$

where z is an intrinsic time scale. which for the moment we leave undefined. and $\underset{\sim}{b}_r$ is the resistance (or dissipation) tensor associated with mechanism r.

It may be shown straightfowardly that if both $\underset{\sim}{A}^r$ and $\underset{\sim}{b}^r$ have isotropic forms for all r. then Eqs. (2-38) and (2-40) uncouple into hydrostatic and deviatoric forms in the following fashion:

$$\underset{\sim}{\varrho} = \underset{\approx}{s} + \sigma \underset{\approx}{I} \quad , \quad \underset{\sim}{\varepsilon} = \underset{\approx}{e} + \epsilon \underset{\approx}{I} \quad , \quad \underset{\sim}{g} = \underset{\approx}{g} + q \underset{\approx}{I} \tag{2-41a,b,c}$$

$$\psi = \psi_s + \psi_H \tag{2-42}$$

$$\psi_s = \frac{1}{2} \sum_r \mu_r \left|\left| \underset{\approx}{e} - \underset{\approx}{g}_r \right|\right|^2 \quad , \quad \psi_H = \frac{1}{2} \sum_r K_r \left| \epsilon - q_r \right|^2 \tag{2-43a,b}$$

$$\underset{\approx}{s} = \frac{\partial \psi_s}{\partial \underset{\approx}{e}} \quad , \quad \sigma = \frac{\partial \psi_H}{\partial \epsilon} \tag{2-44a,b}$$

$$\frac{\partial \psi_D}{\partial \underset{\approx}{g}_r} + b_1^r \frac{\partial \underset{\approx}{g}_r}{\partial z} = 0 \quad , \quad \frac{\partial \psi_H}{\partial q_r} + b_o^r \frac{\partial q_r}{\partial z} = 0 \tag{2-45a,b}$$

where

$$A_{ijk\ell}^r = A_1^r \, \delta_{ij}\delta_{k\ell} + A_2^r \, \delta_{ik}\delta_{j\ell} \tag{2-46}$$

$$b_{ijk\ell}^r = b_1^r \, \delta_{ij}\delta_{k\ell} + b_2^r \delta_{ik}\delta_{j\ell} \tag{2-47}$$

$$\mu_r = A_2^r \quad , \quad K_r = A_1^r + \frac{A_2^r}{3} \tag{2-48a,b}$$

2-12

$$b_0^r = b_1^r + \frac{b_2^r}{3} \qquad (2\text{-}49)$$

If at this juncture, one defines _internal_ _forces_ by the relations

$$\mathbf{g}_r = -\frac{\partial \psi_s}{\partial g_r} \ , \quad \mathbf{q}_r = -\frac{\partial \psi_H}{\partial q_r} \ , \qquad (2\text{-}50a,b)$$

the evolution equations (2-45a,b), in conjunction with the energy relations (2-43a,b), give rise to the following "rate" equations for the internal forces:

$$\frac{\mu_r}{b_1^r}\,\mathbf{g}_r \ + \frac{d\mathbf{g}_r}{dz} = \mu_r\,\frac{d\mathbf{g}}{dz} \qquad (2\text{-}51)$$

$$\frac{K_r}{b_o^r}\,\mathbf{q}_r \ + \frac{d\mathbf{q}_r}{dz} = K_r\,\frac{d\epsilon}{dz} \quad , \qquad (2\text{-}52)$$

while Eqs. (2-44a,b) become:

$$\mathbf{s} = \sum_r \mathbf{g}_r \qquad (2\text{-}53)$$

$$\sigma = \sum_r \mathbf{q}_r \qquad (2\text{-}54)$$

Thus following the above analysis, the constitutive response of the material system is _completely_ defined by Eqs. (2-51), (2-52), (2-53) and (2-54).

In general the resistance coefficients b_0^r and b_1^r are not constant but depend on the stress field and/or the strain field and the temperature field histories in a fashion which for the time being we leave unspecified. However, we introduce this dependence by means of the functions F_S and F_H which are such that

$$b_1^r = b_{10}^r F_S \ , \quad b_0^r = b_{00}^r F_H, \qquad (2\text{-}55a,b)$$

and introduce the notation

$$\frac{\mu_r}{b_{10}^r} = \alpha_r \quad , \quad \frac{K_r}{b_{00}^r} = \lambda_r \qquad\qquad (2\text{-}56a,b)$$

$$dz_S = \frac{dz}{F_S} \quad , \quad dz_H = \frac{dz}{kF_H} \qquad\qquad (2\text{-}57a,b)$$

where μ_r, b_{10}^r, K_r, b_{00}^r and k are positive material constants. The significance of the constant k will be discussed in Chapter 4. In terms of the above notation Eqs. (2-51) and (2-52) are now linear and have the forms

$$\alpha_r \, \mathbf{g}_r + \frac{d\mathbf{g}_r}{dz_s} = \mu_r \frac{d\mathbf{g}}{dz_s} \qquad\qquad (2\text{-}58)$$

$$\lambda_r q_r + \frac{dq_r}{dz_H} = K_r \frac{d\epsilon}{dz_H} \qquad\qquad (2\text{-}59)$$

Equations (2-58) and (2-59) may be integrated and the results substituted in Eqs. (2-53) and (2-54) respectively, to obtain constitutive equations in explicit integral form, which relate the current stress to the history of strain.

Insofar as the internal forces $\mathbf{g}_r$ and q_r are concerned, they are given by Eqs. (2-60) and (2-61) where it is shown that $\mathbf{g}_r$ and q_r are linear functionals of the deviatoric and hydrostatic strain histories, respectively. The memory kernels are positive decaying exponential functions which endow these forces with the characteristic of fading memory.

$$\mathbf{g}_r = \mu_r \int_0^{z_s} e^{-\alpha_r(z_s - z')} \frac{d\mathbf{g}}{dz'} \, dz \qquad\qquad (2\text{-}60)$$

$$Q_r = K_r \int_0^{z_H} e^{-\lambda_r (z_H - z')} \frac{d\epsilon}{dz'} \, dz \qquad (2\text{-}61)$$

Substitution of Eqs. (2-60) and (2-61) in Eqs. (2-53) and (2-54) respectively gives the explicit constitutive representation of the stress response in terms of Eqs. (2-62) and (2-63) where on one hand the deviatoric stress $\underset{\sim}{s}$ is a linear functional of the history of the deviatoric strain while on the other, the hydrostatic stress σ is a linear functional of the history of hydrostatic (volumetric) strain.

$$\underset{\sim}{s} = 2 \int_0^{z_s} \mu \left(z_s - z' \right) \frac{d\underset{\sim}{e}}{dz'} \, dz' \qquad (2\text{-}62)$$

$$\sigma = \int_0^{z_H} K \left(z_H - z' \right) \frac{d\epsilon}{dz'} \, dz' \qquad (2\text{-}63)$$

The corresponding kernels $\mu(z_s)$ and $K(z_H)$ are given in terms of sums of positive decaying exponentials (Dirichlet series) according to the following equations:

$$\mu \left(z_s \right) = \sum_r \mu_r \, e^{-\alpha_r z_s} \qquad (2\text{-}64)$$

$$K \left(z_H \right) = \sum_r K_r e^{-\lambda_r z_H} \qquad (2\text{-}65)$$

The set of Eqs. (2-53), (2-54), (2-58) and (2-59) as well as the set of Eqs. (2-62), (2-63), (2-64) and (2-65) constitute alternative representations of the stress response to a history of strain with respect to the intrinsic time scale z, which is still undefined. See Refs. [2.17, 2.18, 2.19].

2.2.2 Plastic Strain as an Independent Variable.

The definition of plastic strain, (already used in Eq. (2-37) when only one mechanism was operative), is given by the expressions:

$$\underset{\sim}{e}^{P} = \underset{\sim}{e} - \underset{\sim}{e}^{e} \qquad (2\text{-}66a)$$

$$\epsilon^{P} = \epsilon - \epsilon^{e} \qquad (2\text{-}66b)$$

where

$$d\underset{\sim}{e}^{e} = \frac{d\underset{\sim}{s}}{2\mu_{o}} \quad , \quad d\epsilon^{e} = \frac{d\sigma}{K_{o}} \qquad (2\text{-}67a,b)$$

and μ_{o} and K_{o} are, respectively, the elastic shear and elastic bulk moduli. At this point we make certain observations. If, as is customary, we define $2\mu_{o}$ as the initial slope of the shear stress-strain curve, then it follows from Eq. (2-62) that

$$\mu_{o} = \mu(0) \quad , \qquad (2\text{-}68)$$

since at vanishingly small z_{s},

$$\underset{\sim}{s} = 2\mu(0)\underset{\sim}{e} \quad . \qquad (2\text{-}69)$$

Similarly,

$$K_{o} = K(0) \quad , \qquad (2\text{-}70)$$

on the basis of Eq. (2-63). Thus in that which follows, and without further comment, we take $\mu_{o} = \mu(0)$ and $K_{o} = K(0)$.

With specific reference to the shear response, it is shown in Ref. [2.14] that if one substitutes for $\underset{\sim}{e}$ in Eq. (2-62) using Eq. (2-61a) one obtains the shear response, as an __explicit linear functional of the plastic deviatoric strain history__, in the following form:

$$s = \int_0^{z_s} \rho\left(z_s - z'\right) \frac{d\varrho^p}{dz'}\, dz' \; , \tag{2-71}$$

where $\rho(z_s)$ is related to $\mu(z_s)$ by the integral equation given below:

$$\rho\left(z_s\right) - \frac{1}{\mu_o} \int_0^{z_s} \mu\left(z_s - z'\right) \frac{d\rho}{dz'} dz' = 2\mu\left(z_s\right) \tag{2-72}$$

Here $\mu(z_s)$ is given in series form by Eq. (2-64). Without solving for $\rho(z_s)$ explicitly, it is important to consider the effect on the functional form of $\rho(z_s)$ of the constraint

$$\mu_o = \mu(0) \quad . \tag{2-73}$$

In view of the fact that $\mu(z_s)$ consists of a series of decaying exponential terms it may be written in the form

$$\mu\left(z_s\right) = \mu(0)\, H\left(z_s\right) + \mu*\left(z_s\right) \; , \tag{2-74}$$

where $H(z_s)$ is the Heaviside unit step function and μ^* is differentiable at the origin. i.e., $d\mu^*/dz_s$ at $z_s = 0$ is finite. Substitution of Eq. (2-74b) in Eq. (2-72) yields the result:

$$\rho - \frac{\mu(0)}{\mu_o}\, \rho\left(z_s\right) - \frac{1}{\mu_o} \int_0^{z_s} \rho\left(z_s - z'\right) \frac{d\mu*}{dz'}\, dz' = \mu\left(z_s\right) \tag{2-75}$$

Thus at $z_s = 0$,

$$\rho(0) - \frac{\mu(0)}{\mu_o}\, \rho(0) = \mu(0) \tag{2-76}$$

2-17

or

$$\rho(0) = \frac{\mu(0)}{1 - \frac{\mu(0)}{\mu_o}} \qquad (2\text{-}77)$$

In view of the constraint (2-73a), it follows that

$$\rho(0) = \infty \qquad (2\text{-}78)$$

In Ref. [2.14] Eq. (2-72) was solved explicitly when the number of terms on the right-hand side of Eq. (2-64) is finite and equal to n (i.e., when the number of internal variables is finite). It was then shown that $\rho(z_s)$ is given by the expression:

$$\rho(z_s) = \rho_o \delta(z_s) + \sum_{r=1}^{n-1} \rho_r e^{-\beta_r z_s} \qquad (2\text{-}79)$$

where r_o, ρ_r and β_r are all positive. In other words, the memory kernel $\rho(z_s)$ consists of a singular part which contains the Dirac delta function, and a well behaved part, which is the sum of a finite number of positive, decaying exponential terms. Note that the above result is independent of the definition of the time scale z_s which, in special cases, could be identical to the ordinary time t, as in viscoelasticity, for instance.

Substitution of Eq. (2-79) in Eq. (2-71) gives the explicit result

$$\underset{\approx}{s} = \rho_o \frac{d\underset{\approx}{e}^p}{dz_s} + \int_0^{z_s} \rho_1(z_s - z') \frac{d\underset{\approx}{e}^p}{dz'} dz' \quad , \qquad (2\text{-}80)$$

where

$$\rho_1(z) = \sum_{r=1}^{n-1} \rho_r e^{-\beta_r z} \quad . \qquad (2\text{-}81)$$

The same argument applies also to the hydrostatic response. Specifically, when the number of hydrostatic internal variables is finite, we can write:

$$\sigma = \phi_o \frac{d\epsilon^p}{dz_H} + \int_0^{z_H} \phi_1(z_H - z')\frac{d\epsilon^p}{dz'}\, dz' \qquad (2\text{-}82)$$

In other words there exists a function $\phi(z_H)$ such that

$$\phi(z_H) = \phi_o \delta(z_H) + \phi_1(z_H) \quad , \qquad (2\text{-}83)$$

where ϕ_o is positive and $\phi_1(z_H)$ consists of a sum of positive decaying exponentials, i.e.,

$$\phi_1(z_H) = \sum_r \phi_r e^{-\xi_r z_H} \qquad (2\text{-}84)$$

The function $\phi(z_H)$ is related to the function $K(z_H)$ (Eq. (2-65)) by the integral equation

$$\phi(z_H) - \frac{1}{K_o} \int_0^{z_H} K(z_H - z')\frac{d\phi}{dz'}\, dz' = K(z_H) \qquad (2\text{-}85)$$

A significant characteristic of Eq. (2-80) (or, Eq. (2-82)) is that the stress $\underset{\sim}{s}$ is non-zero at the onset of deformation, i.e., at $z_s = 0$ we have:

$$\underset{\sim}{s} = \rho_o \left.\frac{d\underset{\sim}{\epsilon}^p}{dz_s}\right|_0 \quad , \qquad (2\text{-}86)$$

where the right-hand side of this equation has the significance of a yield stress. Thus the shear stress-plastic strain curve is discontinuous and has an infinite slope at the origin of plastic deformation. Similar conclusions also apply to the hydrostatic stress-plastic strain curve.

2-19

2.2.3 Discussion of the Above Results.

Let us now examine the physical, mathematical and thermodynamic significance of the above results. The physical significance is illustrated in the mechanical model of Figure 2.1.

The strain $\underset{\sim}{\varepsilon}$ admits the decomposition shown in Eq. (2-66a) provided that the elastic stiffness $2\mu_0$ of the spring is also the elastic stiffness of the <u>entire</u> system, and the plastic solid, in series with the spring, is a rigid-plastic solid, in the sense that the slope of its stress-plastic strain curve is infinite at the onset of deformation. In this event the stress response of the rigid-plastic solid is given solely in terms of the history of the plastic strain, $\underset{\sim}{\varepsilon}^p$.

In mathematical terms, given the constitutive equation (2-62) which relates the stress to the history of <u>total</u> strain in terms of a kernel $\mu(z_s)$, given by Eq. (2-64), there exists an equivalent set of constitutive equations (2-66a), (2-67a) and Eq. (2-71), which relates the stress to the history of <u>plastic</u> strain through another kernel $\rho(z_s)$ such that $\rho(o) = \infty$. The two kernels ρ and μ are related by means of Eq. (2-72). Of importance is the fact that one need not begin with Eq. (2-62) but with Eq. (2-71) and the kernel $\rho(z_s)$ of the rigid-plastic solid and obtain $\mu(z_s)$, which pertains to the entire system, upon use of Eq. (2-72).

The thermodynamic significance is equally important. The rigid-plastic body may now be treated as a separate thermodynamic system, whose strain state is represented by the deviatoric plastic strain tensor $\underset{\sim}{\varepsilon}^p$. Thus the thermodynamic treatment developed in this chapter beginning with Eq. (2-33) applies to the rigid-plastic body, except that $\underset{\sim}{\varepsilon}$ is replaced by $\underset{\sim}{\varepsilon}^p$. Thus equations analogous to Eqs. (2-62) and (2-63) are derived, following the indicated procedure, which now have the form

$$\underset{\sim}{s} = \int_0^{z_s} \rho\left(z_s - z'\right)\frac{d\underset{\sim}{e}^p}{dz'}\, dz' \tag{2-87}$$

and
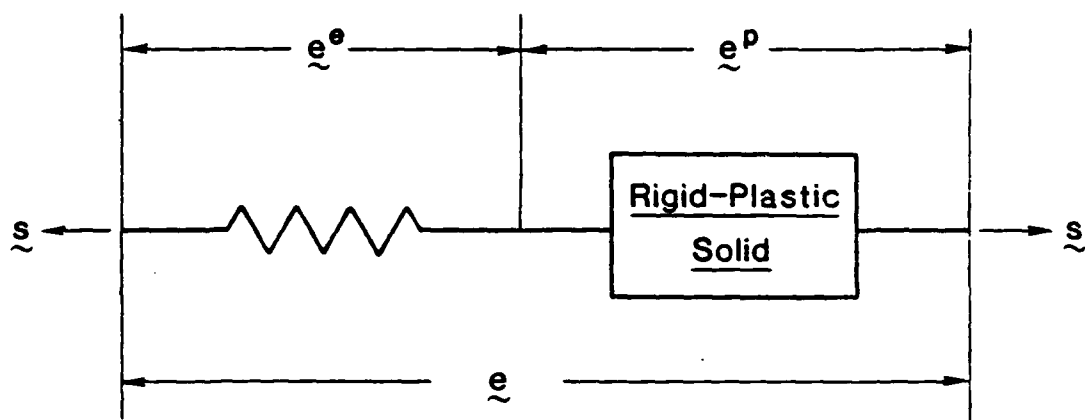
Figure 2.1   Appropriate physical model.

$$\sigma = \int_0^{z_H} \phi\!\left(z_H - z'\right)\frac{d\epsilon^p}{dz'}\, dz' \quad , \tag{2-88}$$

the only condition being that $\rho(0) = \phi(0) = \infty$. Of course $\rho(z_s)$ and $\phi(z_H)$ must be integrable over any finite domain to ensure that $\underset{\sim}{s}$ and σ are bounded. The necessary and sufficient condition that this should be the case, is

$$\int_0^{z_s} \rho(z') < \infty \; , \quad \int_0^{z_H} \phi(z')dz' < \infty \tag{2-89}$$

for all finite z_s and z_H, as will be shown in the following section.

It was shown earlier in this chapter that the rigid-plastic solid can be treated as a separate thermodynamic entity whose strain state is given by the plastic strain tensor. For the sake of discussion we consider the case of the deviatoric response given by Eq. (2-71). The deviatoric thermodynamic state of the system may be described by the deviatoric plastic strain tensor and n internal variables, the number of which may be finite or infinite. We shall show that the choice has significant effect on the form of the kernel function $\rho(z_s)$. However, in any event, the function ρ will consist of a series of decaying exponential terms, the number of which we leave unspecified for the time being. In effect

$$\rho\!\left(z_s\right) = \sum_r R_r e^{-\beta_r z_s} \tag{2-90}$$

We now investigate the constraints on the form of the exponential terms imposed by the infinite value of ρ at $z_s = 0$. We first examine the case where the number of internal variables, i.e., the number of terms in the series is finite. We recall that the analysis in Section 2.2.2 demands that $\rho(z_s)$ must, in this case, contain a delta function. Thus one of the terms in the series (2-90) must be a delta function. This does not pose a difficulty since a delta function is the asymptotic representation of an

exponential function $R_r e^{-\beta_r z}$, whose amplitude R_r and exponent β_r tend to infinity simultaneously while their ratio remains constant. This ratio is in fact the strength of the delta function.

Thus in the case of a finite number of internal variables one satisfies the condition $\rho(o) = \infty$, by letting at least one member of the series become a delta function by means of the asymptotic process discussed above. In fact, this is the only possible avenue since if all R_r are finite then $\rho(o)(=\Sigma R_r)$ is also finite. We note again that in this case the stress-plastic strain curve is discontinuous at the origin of plastic strain. In other words, the rigid-plastic solid with a finite number of internal variables will always exhibit a yield stress.

The case of an infinite number of terms in the series offers different possibilities in the sense that one, now, has a choice. To satisfy the condition $\rho(o) = \infty$ one may again set one (or more) exponential terms equal to a delta function, as in the case of the finite number of terms, but now there is another choice, since one may set

$$\rho(0) = \sum_{r=1}^{\infty} K_r = \infty \qquad (2\text{-}91)$$

by requiring that the series in Eq. (2-91) diverge. In addition, the boundedness of the stress response must be considered. To this end let s be a typical component of $\underset{\sim}{s}$ and e^p the corresponding component of $\underset{\sim}{e}^p$. Then, from Eq. (2-71), we have:

$$s = \int_0^{z_s} \rho(z_s - z') \frac{de^p}{dz'} dz' \qquad (2\text{-}92)$$

Consider the class of histories for which de^p/dz is a constant and equal to θ. In the absence of hydrostatic stress a monotonic constant strain rate history would be a member of this class. Then in view of Eq. (2-92)

$$s = \theta \int_0^{z_s} \rho(z_s - z') \, dz' = \theta \int_0^{z_s} \rho(z') dz' \tag{2-93}$$

Thus boundedness of stress response necessitates that

$$\int_0^{z_s} \rho(z') dz' < \infty \ , \ z_s < \infty \tag{2-94}$$

To prove sufficiency for general strain histories we recall Eq. (2-71) and note the integral inequality, which is a direct consequence of the triangle inequality.

$$\left| \left| \underset{\sim}{s} \right| \right| \leq \left| \left| \frac{d\underset{\sim}{\varepsilon}^p}{dz_s} \right| \right|_{max} \int_0^{z_s} \rho(z_s - z') dz' \tag{2-95}$$

Thus, in view of Ineq. (2-94) $||\underset{\sim}{s}||$ will be bounded for all bounded $||d\underset{\sim}{\varepsilon}^p/dz_s||$. In conclusion, the necessary and sufficient condition that $\underset{\sim}{s}$ be bounded for all bounded strain histories -- in the sense that $||d\underset{\sim}{\varepsilon}^p/dz_s|| < \infty$ -- is that Ineq. (2-94) is satisfied, for all kernels $\rho(z_s)$ that satisfy the Ineq. (2-94). Returning to Eq. (2-90) the corresponding constraint on R_r and β_r is that

$$\sum_{r=1}^{\infty} \frac{R_r}{\beta_r} < \infty \tag{2-96}$$

One can verify that the conditions (2-91), (2-96) are satisfied for a general class of functions $\rho(z_s)$ such that

$$R_r = \frac{R_o}{r^{1-\alpha}} \quad (0 < \alpha < 1) \tag{2-97}$$

and

$$\beta_r = \beta_0(r + K) \quad , \tag{2-98}$$

where β_0 is a positive constant and K a positive integer. Thus.

$$\rho(z_s) = e^{-k\beta_0 z_s} \sum_{r=1}^{\infty} \frac{R_0}{r^{1-\alpha}} e^{-\beta_0 r z_s} \tag{2-99}$$

The importance of this class of kernels lies in the fact that the stress is zero at the onset of plastic deformation. This may be seen directly from Ineq. (2-95) which shows that

$$||\underset{\sim}{s}(0)|| = 0 \quad , \tag{2-100}$$

since, at $z_s = 0$. the integral on the right-hand side of the inequality vanishes. Thus kernels of this type apply to materials that do not exhibit an abrupt transition from elastic to plastic behavior. i.e.. do not exhibit a finite yield stress. Instead. plastic effects take place immediately upon deformation and there is gradual transition from a predominantly elastic to predominantly plastic behavior.

The above cases are summarized in the following form of the kernel ρ:

$$\rho(z_s) = \rho_0 \delta(z_s) + \rho_1(z_s) \tag{2-101}$$

Case (i): $\rho_0 \neq 0, \qquad \rho_1(0) < \infty$

In this case a yield stress exists and the slope of the stress-strain curve at the onset of plastic strain is finite. Thus there exists a "kink" in the stress-strain curve at the yield point as shown in Figure 2.2.

Case (ii): $\rho_0 \neq 0. \rho_1(0) = \infty$

A yield stress exists and the slope of the stress-plastic strain curve is infinite at the onset of plastic strain. Thus the stress-strain curve at the onset of yield is continuous.
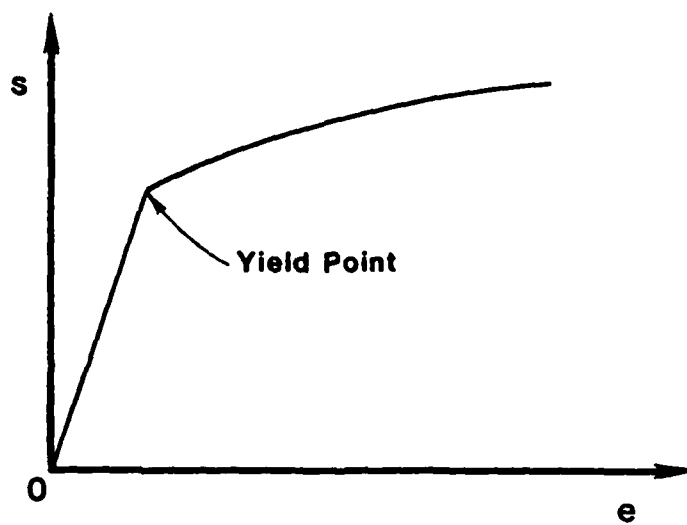
Figure 2.2 Stress-strain curve with a kink at the yield point.

Case (iii): $\rho_0 = 0$, $\rho_1(0) = \infty$

A yield stress does **not** exist. There is a gradual transition from predominantly elastic to predominantly plastic behavior.

2.2.4 Integral Representation of the Memory Kernels.

With reference to $\rho(z_s)$ consider the representation of this kernel by an infinite number of terms. i.e., let

$$\rho(z_s) = \sum_{r=1}^{\infty} R_r e^{-\beta_r z_s} \quad .. \tag{2-102}$$

Furthermore. let $R_r = \beta_0 R(r)$ and $\beta_r = \beta_0 r$. Then Eq. (2-102) becomes

$$\rho(z_s) = \sum_{r=1}^{\infty} \beta_0 R(\beta_0 r) e^{-\beta_0 r z_s} \quad . \tag{2-103}$$

Let the exponentials be "very closely packed" in the sense that β_0 is a small quantity which we denote by Δx. Then Eq. (2-103) becomes

$$\rho(z_s) = \sum_{r=1}^{\infty} \Delta x R(r \Delta x) e^{-r \Delta x z_s} \quad . \tag{2-104}$$

But

$$\lim_{\Delta x \to o} \sum_{r=1}^{\infty} \Delta x R(r \Delta x) e^{-r \Delta x z_s} = \int_0^{\infty} R(x) e^{-x z_s} dx \tag{2-105}$$

whenever the integral exists.

Thus in the limit of vanishingly small β_0 i.e.. infinitely closely packed exponential terms $\rho(z_s)$ is given by an integral. i.e..

$$\rho(z_s) = \int_0^{\infty} R(r) e^{-r z_s} dr \quad . \tag{2-106}$$

Thus $\rho(z_s)$ is the Laplace transform of $R(r)$. the latter being <u>the spectrum</u> of the memory function $\rho(z_s)$.

We give a number of examples below to illustrate the structure of the integral representation given by Eq. (2-106). To fix ideas let

$$R(r) = R_o \, \delta(r - r_o) \tag{2-107}$$

i.e.. the distribution $R(r)$ is given by a δ-function of strength R_o and located at $r = r_o$. In this case Eq. (2-106) gives

$$\rho(z_s) = R_o e^{-r_o z_s} \tag{2-108}$$

i.e.. $\rho(z_s)$ is given by a single exponential.

Now let $R(r)$ have the "power form" representation

$$R(r) = \begin{cases} 0 \, , \, r \leq r_0 \\[2ex] R_o(r - r_o)^{\alpha-1}, \, o < \alpha < 1 \end{cases} \tag{2-109}$$

Then

$$\rho(z_s) = \int_{r_o}^{\infty} R_o(r - r_o)^{\alpha-1} e^{-rz_s} \, dr \tag{2-110}$$

Let $r - r_o = x$. Then

$$\rho(z_s) = e^{-r_o z_s} \int_0^{\infty} R_o x^{\alpha-1} e^{-xz_s} \, dx \quad .$$

Thus,

$$\rho(z_s) = e^{-r_o z_s} \frac{R_o \Gamma(\alpha)}{z_s^{\alpha}} \quad , \tag{2-111}$$

where $\Gamma(\alpha)$ is the complete Gamma function. The form on the right-hand side of Eq. (2-111) is an excellent analytical representation of the deviatoric <u>and</u> hydrostatic memory kernels in metals, soils and concrete.

2.3 The Concept of Intrinsic Time.

2.3.1 Strain Rate Indifference. Elasticity at Reversal Points.

There are two essential features of the mechanical response of metals at room temperature and in a range of strain rates of about 10^{-4} to 10^{-1} sec^{-1}, which impose useful constraints on the form of the intrinsic time z. In an idealized form (in the sense that small deviations from this form are observed) these are:

(a)   Strain rate indifference.

(b)   Elastic behavior at reversal (unloading-reloading) points in a one-dimensional stress-strain path as well as in other paths associated with proportional straining histories.

Strain-rate Indifference. When the history of strain is given by the relation $\epsilon = \phi(t)$ let the stress response σ be given by the function g(t). Elimination of the parameter t leads to the relation

$$\sigma = G_\phi(\epsilon) , \qquad\qquad (2-112)$$

where the response function G_ϕ depends obviously on the history of strain $\phi(t)$. Note that G_ϕ need not be a single-valued function. For instance in a uniaxial cyclic loading G_ϕ will be a multivalued function and will give the various levels of cyclic stress at the same strain level ϵ.

Definition. Rate indifference is the invariance of the function G_ϕ under the transformation $t \rightarrow F(t); \dot{F} > 0$. We note in passing that in elastic materials, $G_\phi = G$ for all ϕ.

Elasticity at Reversal Points. This material property can be discussed simply and meaningfully in the context of strain rate indifference.

2-29

In one dimension, the physical phenomenon is depicted in Figure 2.3 where a uniaxial stress-strain test is shown in schematic form. The slope of the stress-strain diagram at 0, the point of initiation of the loading, is E_o. The stress-strain curve need not contain a finite elastic region. The points A and B are reversal points. What is meant by elasticity at reversal points is that the slope of the stress-strain diagram of point A and B is E_o, i.e.,

$$\frac{d\sigma}{d\epsilon}\bigg|_0 = \frac{d\sigma}{d\epsilon}\bigg|_A = \frac{d\sigma}{d\epsilon}\bigg|_B = E_o \quad , \tag{2-113}$$

where reversal points (such as A and B) are defined by the property that at such points the ratio, $d\epsilon/|d\epsilon|$, charges discontinuously from +1 to -1 or vice-versa.

In <u>three</u> dimensions the situation is similar. Let $\epsilon_{ij}(t)$ be a strain history and t_o the time of occurrence of a reversal point. Denote by t_{o-} the time that precedes t_o by a vanishingly small time increment and t_{o+} the time that succeeds t_o also by a vanishingly small time increment. A point on the strain path in a nine-dimensional strain space at time t_o is said to be a reversal point if:

$$\frac{d\epsilon_{ij}}{||d\epsilon_{ij}||}\bigg|_{t_{o-}} = - \frac{d\epsilon_{ij}}{||d\epsilon_{ij}||}\bigg|_{t_{o+}} \quad , \tag{2-114}$$

where double bars denote the norm in the usual fashion. In three dimensions, elasticity at reversal points implies that at such points

$$d\sigma_{ij} = C_{ijk\ell}d\epsilon_{k\ell} \quad , \tag{2-115}$$

where $C_{ijk\ell}$ is the elasticity tensor. In the specific case where the material is elastically isotropic Eq. (2-115) has the more particular form

$$d\sigma_{ij} = \lambda_o \delta_{ij}d\epsilon_{kk} + 2\mu_o d\epsilon_{ij} \tag{2-116}$$

or, the alternative uncoupled form
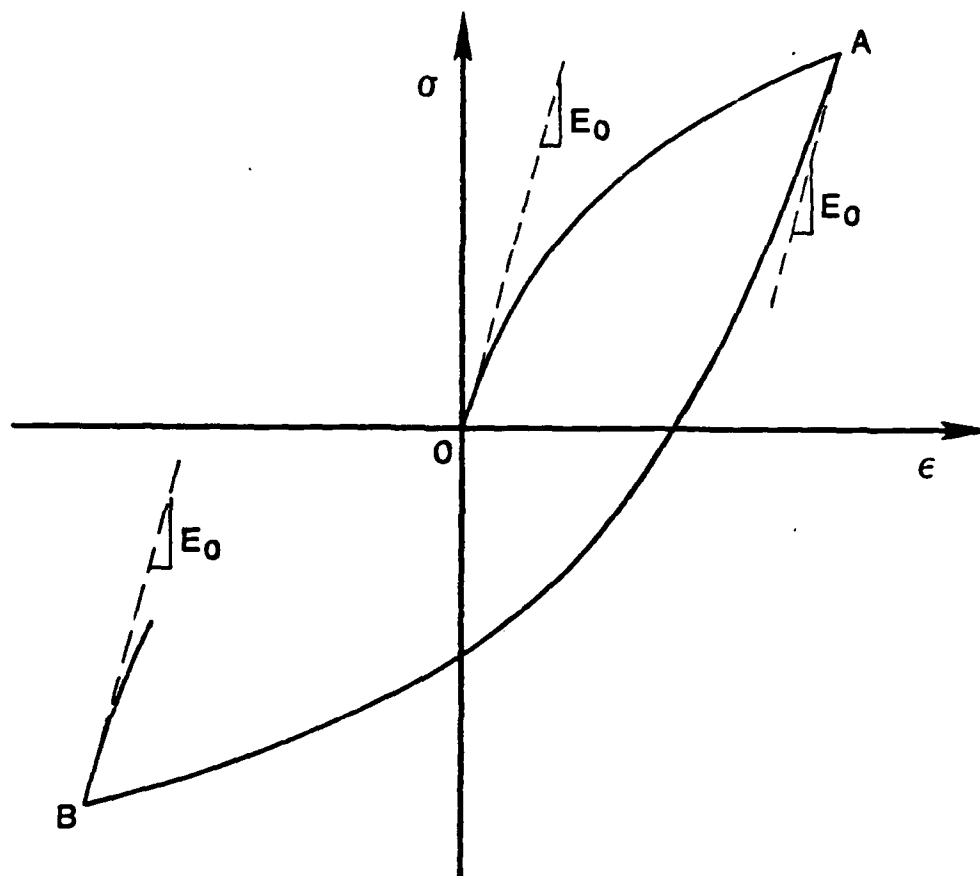
Figure 2.3   Typical uniaxial stress-strain curve showing elastic response at reversal points A and B.

$$d\sigma_{kk} = 3K_o d\epsilon_{kk} \quad , \tag{2-117}$$

$$ds_{ij} = 2\mu_o de_{ij} \quad , \tag{2-118}$$

in the usual notation s and e being the stress and strain deviators respectively.

2.3.2 The Intrinsic Time Scale.

The concept of the intrinsic time scale was developed on physical and mathematical grounds which we proceed to summarize. In metals such as aluminum, copper, high tensile steels, etc., where plastic effects appear immediately upon loading, the onset of yield is difficult to define. Such a concept may even be inappropriate for such materials, except possibly as an approximation.

Classical theories, where the yield surface is used as an essential constitutive element, lie outside the domain of functional theories, that are used in the mathematical representation of the constitutive response of other materials. On the other hand, at higher temperatures where metals evince strain rate effects, functional theories are used for the representation of their mechanical behavior. One cannot but conclude that "yield" may not be an essential element in the formulation of constitutive equations for metals.

Thus within the domain of rate indifferent yet history dependent, where the stress response is a function of the strain path, the definition of the appropriate path, seems to be a more fundamental physical task than the definition of yield point. Thoughts along these lines, although less specific, can be found in the literature. In 1954, Il'iushin [2.20] introduced such a path s, where ds was defined as the norm of the increment of the strain tensor, i.e.

$$ds = ||d\underset{\sim}{e}|| \quad , \tag{2-119}$$

as "useful" in describing plasticity phenomena. Pipkin and Rivlin [2.21] constructed an elaborate mathematical theory using that path in 1964. The relation of their theory to the observed behavior of metals, however, was not pursued.

In 1971 Valanis [2.13] introduced the concept of endochronic plasticity by means of the intrinsic time measure $d\varsigma$ such that

$$d\varsigma^2 = d\underset{\sim}{\varepsilon} \cdot \underset{\sim}{P} \cdot d\underset{\sim}{\varepsilon} \quad , \tag{2-120}$$

where $\underset{\sim}{P}$ is a fourth order material tensor.

One can see immediately that there are substantial conceptual differences between the Il'iushin concept and the endochronic theory. In the Il'iushin approach the path cannot accommodate material symmetries -- isotropy, orthotropy, etc. In the endochronic theory, however, the material symmetries must be reflected in $\underset{\sim}{P}$. In other words an isotropic material requires an isotropic tensor $\underset{\sim}{P}$, an orthotropic material similarly requires that $\underset{\sim}{P}$ be orthotropic and so on.

An intrinsic time scale z was then defined by the relation

$$dz = \frac{d\varsigma}{f(\varsigma)} \tag{2-121}$$

where in physical terms $f(\varsigma)$ plays the role of a hardening function.

In one dimension (in a pure shear test say) Eq. (2-120), within an arbitrary multiplicative constant, assumes the form

$$d\varsigma = |d\gamma| \tag{2-122}$$

where γ is the shear strain. One may use Eqs. (2-121) and (2-122) in conjunction with Eq. (2-115) to predict theoretically the stress-strain response in shear to a strain history including loading, unloading, and reloading. The predicted response is shown schematically in Figure 2.4.

Some features of the theoretically predicted response are worth pointing out. The slope at the unloading point A is not equal to E_o but to $2E_o - E_t$, where E_t is the tangent modulus at A. Upon reloading at B one obtains an open hysteresis loop, because the slope of the reloading curve BC at B is less than the slope of unloading curve AB at B. While these features are not in themselves disturbing and may be

2-33
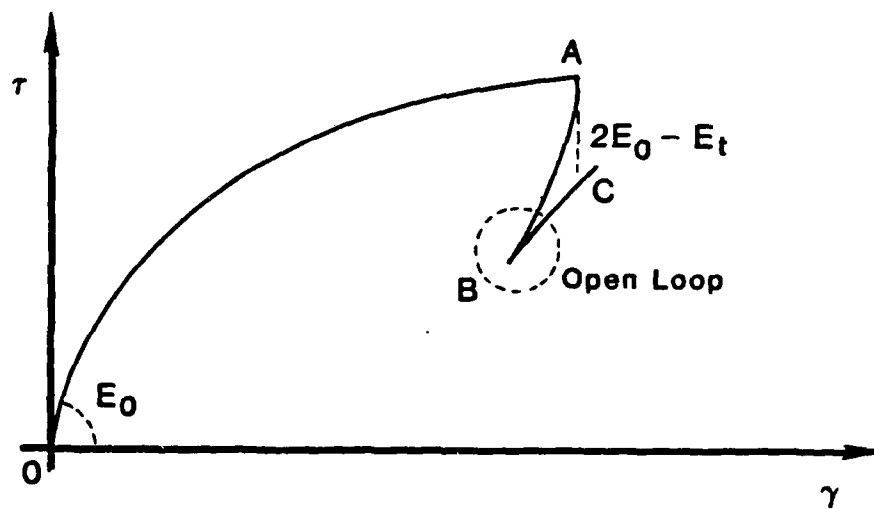
Figure 2.4   Typical response of model when $d\varsigma$ is defined according to Eq. (2-120).

qualitatively characteristic of granular materials, they certainly do not pertain to the behavior of materials which unload elastically in the sense of Section 2.2. Evidently the definition of intrinsic time given by Eq. (2-120) is not characteristic of metals. We also point out that a definition of intrinsic time in terms of the stress tensor such as

$$d\varsigma_\sigma^2 = d\varrho \cdot \underset{\sim}{\mathbf{0}} \cdot d\varrho \tag{2-123}$$

leads to similar difficulties.

The problem of defining the intrinsic time was resolved in Ref. [2.22] where it was demonstrated that the appropriate endochronic time measure is equal to an increment in length of the plastic strain path in plastic strain space. In that which follows, we give the analysis in detail.

2.3.3 The Intrinsic Time in One Dimension.

We shall discuss the question in some detail in one dimension. The resolution of the problem in three dimensions follows similar lines. The philosophical problem that poses itself is the following: We have a (material) system that has no cognizance of Newtonian time. Moreover, given a sequence of strain states the system will "respond" in terms of a sequence of stress states. However, insofar as the material response is concerned, the distance between two strain events cannot be defined in terms of $|d\gamma|$ by means of Eq. (2-120) and similarly the distance between two stress events cannot be defined in terms of $|d\tau|$ by means of Eq. (2-123). In other words, neither the stress history (stress path) nor the strain history (strain path) lie in their own space, in the sense that neither Eq. (2-120) nor Eq. (2-123) are appropriate for the definition of intrinsic time. Since neither a path in (one dimensional) strain- nor stress-space seems appropriate, we proceed to explore the possibilities of a path in the co-joint stress-strain space (τ, γ). Specifically in one dimension let f stand for a strain component and g for a corresponding stress component. We define the intrinsic time scale z by the relationship

$$dz^2 = \alpha df^2 - 2\beta dg df + \gamma dg^2 \tag{2-124}$$

Evidently z is a path in co-joint space (g,f) with the non-negative metric

$$\begin{bmatrix} \alpha & \beta \\ -\beta & \gamma \end{bmatrix} \tag{2-125}$$

Of course since dz^2 cannot be negative, the following inequalities must hold

$$\alpha > 0, \quad \gamma > 0 \tag{2-126}$$

$$\beta^2 \leq \alpha\gamma \tag{2-127}$$

Let the functional relationship between g and f be

$$g = \int_0^z \lambda(z - z')\frac{df}{dz'} \, dz \tag{2-128}$$

where λ is the appropriate kernel (2μ if g is deviatoric, K if hydrostatic, as per Eqs. (2-62) and (2-63).

It follows from Eq. (2-128) that

$$dg = \lambda_0 df + dz\int_0^z \lambda'(z - z')\frac{df}{dz'} \, dz' \quad , \tag{2-129}$$

where $\lambda_0 = \lambda(0)$ (the initial slope of the f-g diagram) and $\lambda'(z) = d\lambda/dz$. Elastic response at reversal points demands that at such points

$$dg = \lambda_0 df. \tag{2-130}$$

It follows from Eq. (2-121) that at such points

$$dz = 0. \tag{2-131}$$

Thus, Eq. (2-130) is true whenever $dz = 0$ and vice-versa. When use of this condition is made in Eq. (2-124) the following relation is obtained

$$\alpha - 2\beta\lambda_o + \gamma\lambda_o^2 = 0 \quad . \tag{2-132}$$

However, λ_o must be real and positive for all choices of α, β and γ. Hence, in addition to Ineqs. (2-126) and (2-127), the following inequalities must hold

$$\beta^2 \geq \alpha\gamma \tag{2-133}$$

$$\beta > 0 \quad . \tag{2-134}$$

We now observe that Ineqs. (2-127) and (2-133) can be satisfied simultaneously, if and only if

$$\beta^2 = \alpha\gamma \quad . \tag{2-135}$$

in which case, when use is made of Equation (2-135) in Equation (2-124), one finds that,

$$dz^2 = \alpha\left(df - \frac{dg}{\lambda_o}\right)^2 \quad . \tag{2-136}$$

Note that the term in the bracket on the right-hand side of Eq. (2-136) is the "plastic strain" increment df_p corresponding to the strain increment df. Thus

$$dz = \sqrt{\alpha(\varsigma)} \cdot d\varsigma \tag{2-137}$$

$$d\varsigma = |df_p| \tag{2-138}$$

since, in general, α may depend on ς.

Conclusion:

On the basis of Eq. (2-124), the requirement of elastic response at reversal points in one dimension leads to a definition of intrinsic time in terms of the plastic strain.

2.3.4 Generalization to Three Dimensions.

We apply the analysis to initially isotropic compressible non-dilatant materials of the type discussed in Section 2.2. The relevant constitutive equations are

$$\underset{\sim}{s} = 2 \int_0^{z_s} \mu(z_s - z')\frac{d\underset{\sim}{e}}{dz'} \, dz' \qquad (2\text{-}139)$$

and

$$\sigma = \int_0^{z_H} K(z_H - z')\frac{d\epsilon}{dz'} \, dz' \quad . \qquad (2\text{-}140)$$

Following the procedure adopted in the one-dimensional case we wrote the above equations in incremental form whereupon

$$d\underset{\sim}{s} = 2\mu(0)d\underset{\sim}{e} + 2dz_s \int_0^{z_s} \mu'(z_s - z')\frac{d\underset{\sim}{e}}{dz'} \, dz' \qquad (2\text{-}141)$$

$$d\sigma = K(0)d\epsilon + dz_H \int_0^{z_H} K(z_H - z')\frac{d\epsilon}{dz'} \, dz' \quad . \qquad (2\text{-}142)$$

If the material is to behave elastically at reversal points the following conditions must apply:

$$dz_s = dz_H = 0 \qquad (2\text{-}143)$$

and $\mu(0)$ and $K(0)$ must be elastic shear and bulk modulus, respectively. However, given the fact that

$$dz_s = \frac{d\varsigma}{F_s} \, , \quad dz_H = \frac{d\varsigma}{kF_H} \, , \qquad (2\text{-}144a,b)$$

the condition (2-143) is satisfied if $d\varsigma = 0$.

The three-dimensional counterpart of Eq. (2-124) is

$$d\varsigma^2 = d\underset{\sim}{\xi} \cdot \underset{\sim}{\alpha} \cdot d\underset{\sim}{\xi} - 2d\underset{\sim}{\xi} \cdot \underset{\sim}{\beta} \cdot d\underset{\sim}{q} + d\underset{\sim}{q} \cdot \underset{\sim}{\gamma} d\underset{\sim}{q} \tag{2-145}$$

In the case of isotropic materials, of interest here, the right-hand side of Eq. (2-145) reduces to the form

$$d\varsigma^2 = \left(\alpha_1 d\underset{\sim}{e} \cdot d\underset{\sim}{e} - 2\beta_1 d\underset{\sim}{e} \cdot d\underset{\sim}{s} + \gamma_1 d\underset{\sim}{s} \cdot d\underset{\sim}{s} \right)$$

$$+ \left(\alpha_2 d\epsilon^2 - 2\beta_2 d\sigma d\epsilon + \gamma_2 d\sigma^2 \right) , \tag{2-146}$$

in the previous notation where the right-hand side of Eq. (2-146) is the addition of a deviatoric and a hydrostatic term in brackets. Since the previous "one-dimensional" argument may apply either to the hydrostatic or deviatoric case, it follows readily that elastic unloading in both hydrostatic and deviatoric histories demands that

$$d\varsigma^2 = \alpha_1 \left| \left| d\underset{\sim}{e}^P \right| \right|^2 + \alpha_2 d\epsilon_p^2 \tag{2-147}$$

where

$$d\underset{\sim}{e}^P = d\underset{\sim}{e} - \frac{d\underset{\sim}{s}}{2\mu_o} \tag{2-148}$$

$$d\epsilon^P = d\epsilon - \frac{d\sigma}{K_o} \tag{2-149}$$

where $2\mu_o$ and K_o are, respectively, the initial slope of the monotonic, shear stress -- (tensorial) shear strain and the hydrostatic stress -- volumetric strain, constitutive response curves, and α_1 and α_2 are functions of ς. A more detailed proof of the above result is given below.

Since the deviatoric deformation is assumed to be independent of its hydrostatic counterpart and vice-versa, both brackets in Eq. (2-146) must be positive semi-definite i.e.,

$$a_1 \, d\underset{\sim}{e} \cdot d\underset{\sim}{e} - 2\beta_1 \, d\underset{\sim}{e} \cdot d\underset{\sim}{s} + \gamma_1 \, d\underset{\sim}{s} \cdot d\underset{\sim}{s} \geq 0 \qquad (2\text{-}150\text{a})$$

$$a_2 \, d\epsilon^2 - 2\beta_2 \, d\epsilon d\sigma + \gamma_2 \, d\sigma^2 \geq 0 \quad . \qquad (2\text{-}150\text{b})$$

Because the hydrostatic response is one-dimensional it need not be discussed again as it was dealt with previously. It remains, therefore, to consider the deviatoric response, i.e., Ineq. (2-150a). To this end let

$$d\underset{\sim}{e} \cdot d\underset{\sim}{s} = ||d\underset{\sim}{e}|| \; ||d\underset{\sim}{s}|| \; \cos\theta \qquad (2\text{-}151)$$

where in a nine-dimensional vector space θ is the angle between the incremental vectors $d\underset{\sim}{e}$ and $d\underset{\sim}{s}$.

Also for simplicity of notation let $||d\underset{\sim}{s}|| = ds$ and $||d\underset{\sim}{e}|| = de$. Then Ineq. (2-150a) becomes

$$a_1 \, de^2 - 2\beta_1 \, \cos\theta \, deds + \gamma_1 ds^2 \geq 0 \qquad (2\text{-}152)$$

for all positive ds and de. Obviously the discriminant of the quadratic on the left-hand side of Eq. (2-152) cannot be positive in which case

$$a_1 \gamma_1 - \beta_1^2 \, \cos^2\theta \geq 0 \qquad (2\text{-}153)$$

for all θ. The worst case is $\theta = 0$, in which case the necessary condition that Ineq. (2-152) not be violated is

$$\beta_1^2 \leq a_1 \gamma_1 \qquad (2\text{-}154)$$

which is precisely analogous to the one-dimensional relation (2-127).

Consider now a reversal point under deviatoric strain conditions. In this case $dz_s = 0$ and because of Eq. (2-141)

$$d\underset{\sim}{s} = 2\mu(0)\,d\underset{\sim}{e} \qquad\qquad\qquad (2\text{-}155a)$$

or

$$ds = 2\mu(0)\,de \quad . \qquad\qquad\qquad (2\text{-}155b)$$

Thus at reversal points we require that $\theta = 0$, in view of Eq. (2-155a). Furthermore the equality sign in Ineq. (2-152) must apply. Thus letting $\mu(0) = \mu_o$, the following relation between μ_o and the constants α_1^o, β_1 and γ_1 is obtained:

$$\gamma_1\left(2\mu_o\right)^2 - 2\beta_1\left(2\mu_o\right) + \alpha_1 = 0 \quad . \qquad\qquad\qquad (2\text{-}156)$$

Thus,

$$2\mu_o = \frac{\beta_1 + \sqrt{\beta_1^2 - \alpha_1\gamma_1}}{\gamma_1} \quad . \qquad\qquad\qquad (2\text{-}157)$$

However, μ_o must be real and positive. Thus the following inequalities must hold.

$$\beta_1^2 \geq \alpha_1\gamma_1 \qquad\qquad\qquad (2\text{-}158a)$$

$$\beta_1 > 0 \quad . \qquad\qquad\qquad (2\text{-}158b)$$

Inequalities (2-154) and (2-158a) can be satisfied simultaneously if and only if

$$\beta_1^2 = \alpha_1\gamma_1 \quad . \qquad\qquad\qquad (2\text{-}159)$$

Furthermore, in view of Eqs. (2-157) and (2-159)

$$\beta_2^2 = \alpha_2\gamma_2 \qquad\qquad\qquad (2\text{-}160)$$

$$K_o = \frac{\beta_2}{\gamma_2} = \sqrt{\frac{\alpha_2}{\gamma_2}} \quad . \qquad\qquad\qquad (2\text{-}161)$$

Thus, Eqs. (2-147), (2-148) and (2-149) follow.

REFERENCES FOR CHAPTER 2

2.1   Malvern, L. E., INTRODUCTION TO THE MECHANICS OF A CONTINUOUS MEDIUM, Prentice-Hall, Inc., Englewood Cliffs, New Jersey (1969).

2.2   Caratheodory, C., "Untersuchungen Über die Grundlagen der Thermodynamic," *Math. Annalen*, **67**, 355 (1909).

2.3   Valanis, K. C., "Irreversibility and Existence of Entropy," *Int. J. Non-Lin. Mech.*, **6**, 337 (1971).

2.4   Valanis, K. C., "Partial Integrability as a Basis of Existence of Entropy in Irreversible Systems," *ZAMM*, **63**, 73 (1983).

2.5   Biot, M. A., "Theory of Stress-Strain Relations in Anisotropic Viscoelastic and Relaxation Phenomena," *J. Appl. Phys.*, **25**, 1385 (1954).

2.6   Biot, M. A., "Variational Principle in Irreversible Thermodynamics with Application to Viscoelasticity," *Phys. Rev.*, **97**, 1463 (1955).

2.7   Biot, M. A., "Thermoelasticity and Irreversible Thermodynamics," *J. App. Phys.*, **27**, 240 (1956).

2.8   Biot, M. A., "Linear Thermodynamics and the Mechanics of Solids," *Proc. Third U.S. National Congress of Appl. Mech.*, A.S.M.E., NY (1958).

2.9   Schapery, R. A., "Application of Thermodynamics to Thermomechanical Fracture and Birefringent Phenomena in Viscoelastic Media," *J. App. Phys.*, **35** 1941 (1964).

2.10   Valanis, K. C., "The Viscoelastic Potential and Its Thermodynamic Foundations," Iowa State University, ERI Report 52 (1967), *J. Math. and Phys.*, **47**, 262 (1968).

2.11   Valanis, K. C., "Unified Theory of Thermomechanical Behavior of Viscoelastic Materials," *Proc. Mechanical Behavior of Materials Under Dynamic Loads*, Ed. U.S. Lindholm, Springer Verlag, NY (1968).

2.12   Coleman, B. D., and Gurtin, M., "Thermodynamics with Internal Variables," *J. Chem. Phys.*, **47**, 597 (1971).

2.13   Valanis, K. C., "A Theory of Viscoplasticity Without a Yield Surface," *Arch. Mech.*, **23**, 517 (1971).

2.14   Valanis, K. C., "Some Fundamental Consequences of a New Intrinsic Time Measure," *Arch. Mech.*, **32**, 181 (1980).

2.15   Ferry, J. D., VISCOELASTIC PROPERTIES OF POLYMERS, John Wiley and Sons, Inc., NY, (1961).

2.16   Schapery, R. A., "Mechanical Characterization of Nonlinear Materials in Terms of Linear Viscoelastic Functions," *Workshop on Applied Thermoviscoplasticity*, Ed. S. Nemat-Nasser, Northwestern University (1975).

2.17   Valanis, K. C., "Endochronic Theory with Proper Loop Closure Properties," S-CUBED Report SSS-R-80-4182, (August, 1979).

2.18   Valanis, K. C., and H. E. Read, "A New Endochronic Model for Soils," *Soil Mechanics - Transient and Cyclic Loads*, Ed. G. N. Pande and O. C. Zienkiewicz, John Wiley and Sons (1982).

2.19   Valanis, K. C., and C. F. Lee, "Some Recent Developments of the Endochronic Theory with Applications, *Nuclear Engineering and Design*, 69, 327 (1982).

2.20   Il'iushin, A. A., "On the Relation Between Stresses and Small Deformation in the Mechanics of Continuous Media," *Prikl. Math. Meh.*, 18 641 (1954).

2.21   Pipkin, A. C., and R. S. Rivlin, *ZAMP*, 16 313 (1964).

2.22   Valanis, K. C., "Continuum Foundations of Endochronic Plasticity," *J. Engin. Materials and Tech.*, 106, 366 (1984).

3. THEORY OF INCOMPRESSIBLE PLASTIC ISOTROPIC SOLIDS

In this chapter, we consider the special form that the general theory presented in Chapter 2 reduces to for solids which are plastically incompressible. i.e., their hydrostatic behavior is purely elastic. After a brief summary of the basic equations of the general theory, some basic features of the governing equations for plastically incompressible solids are discussed, after which the equations governing uniaxial loading are developed and applied to cyclic and complex strain histories. Procedures for determining the material functions $\rho(z)$ and $F_s(z)$ are given. To illustrate the application and predictive capability of the theory in more than one dimension, two multi-dimensional problems are considered, namely, a flat plate with two edge cracks under uniformly applied tension and a cylindrical tube subjected to a homogeneous, two-dimensional, non-proportional stress field. In both cases, comparisons between predictions based on the theory and corresponding experimental data are given. Finally, the version of the theory which exhibits a yield surface and was introduced earlier in Chapter 2 is considered in greater detail, particularly for the case of plastically incompressible solids.

3.1 Summary of Basic Equations for Compressible Plastic Solids.

The equations that describe the behavior of <u>compressible</u> plastic solids (without dilatant capability) were given in the previous section. Here we recall these relations for reference. They consist of (i) the shear and volumetric constitutive response Eqs. (3-1) and (3-2) -- previously Eqs. (2-87) and (2-88):

$$\underset{\sim}{s} = \int_0^{z_s} \rho\left(z_s - z'\right)\frac{d\underset{\sim}{e}^p}{dz'} \, dz' \tag{3-1}$$

$$\sigma = \int_0^{z_H} \phi\left(z_H - z'\right)\frac{d\epsilon^p}{dz'} \, dz' \quad , \tag{3-2}$$

subject to the constraints:

$$\rho(o) = \phi(o) = \infty \tag{3-3}$$

and

$$\int_0^{z_s} \rho(z')dz' < \infty \quad , \quad \int_0^{z_H} \phi(z')dz' < \infty \tag{3-4}$$

for all finite z_s and z_H: (ii) the equations relating the increment in the plastic strain tensor to the increment of the total strain tensor -- previously Eqs. (2-66a). (2-66b) and (2-67a,b):

$$d\underset{\sim}{e}^P = d\underset{\sim}{e} - d\underset{\sim}{s}/2\mu_o \tag{3-5}$$

$$d\epsilon^P = d\epsilon - d\sigma/K_o \tag{3-6}$$

where μ_o is the elastic shear modulus and K_o the elastic bulk modulus. both of which need not be constant: (iii) the definition of intrinsic time for rate independent. isotropic. materials -- previously Eq. (2-147) -- which we write in the form:

$$dz^2 = \left|\left|d\underset{\sim}{e}^P\right|\right|^2 + k^2 |d\epsilon^P|^2 \tag{3-7}$$

where α_1 was set equal to unity[*] and $\alpha_2 = k$: and, (iv) the equations defining the intrinsic time scales z_s and z_H -- previously Eqs. (2-57a,b):

$$dz_s = \frac{dz}{F_s} \quad ; \quad dz_H = \frac{dz}{kF_H} \quad . \tag{3-8a,b}$$

The presence of k in Eq. (3-8b) insures that the hydrostatic response is independent of the value of k.

---

[*] Setting α_1 equal to unity merely defines the unit of intrinsic time. just as the "second" defines the unit of time in the Newtonian time scale.

3.2 Equations for Incompressible Plastic Isotropic Solids.

3.2.1 General Considerations.

These solids are idealizations of reaiity in the sense that they are infinitely resistant to hydrostatic plastic deformation. They provide a good representation of the hydrostatic response of metals. Thus they are characterized by the property

$$\epsilon^P = 0 \tag{3-9}$$

and

$$\phi(z_H) = \infty \quad . \tag{3.10}$$

The integral on the right-hand side of Eq. (3-2), therefore, becomes indeterminate and σ is determined from the elastic hydrostatic response, which is given in Eq. (3-6), by setting $d\epsilon^P = 0$, i.e.,

$$d\sigma = K_o d\epsilon \quad . \tag{3-11}$$

Also the hydrostatic time scale z_H becomes redundant and Eqs. (3-1) to (3-8) simplify considerably into the form of Eqs. (3-12) to (3-16):

$$\underset{\sim}{s} = \int_0^{z_s} \rho(z_s - z') \frac{d\underset{\sim}{e}^P}{dz'} dz' \tag{3-12}$$

$$d\sigma = K_o d\epsilon \tag{3-13}$$

$$d\underset{\sim}{e}^P = d\underset{\sim}{e} - \frac{d\underset{\sim}{s}}{2\mu_o} \tag{3-14}$$

$$dz = \left|\left|d\underset{\sim}{e}^P\right|\right| \tag{3-15}$$

$$dz_s = dz/F_s \quad . \tag{3-16}$$

Certain observations are in order. Equations (3-13) and (3-14) allow for non-linear (albeit elastic) shear and/or hydrostatic response in that μ_o and K_o may be functions of the invariants of the elastic strain tensor. In metals, to which the above equations are applied most frequently μ_o and K_o are considered constants. In the case of elastic-plastic interaction μ_o and K_o may also depend on other quantities associated with plastic deformation, the only constraint being that they should remain invariant with a rotation of the material frame of reference to satisfy the condition of isotropy in the reference configuration.

Equation (3-16) allows for hardening and/or dependence of the shear response on the hydrostatic stress. This is done simply by setting

$$F_s = F_s(\sigma, z) \quad . \tag{3-17}$$

In the case of metals, the shear response is virtually independent of the current hydrostatic stress particularly for small levels of the latter, so that with good accuracy one can set

$$F_s = F_s(z) \quad . \tag{3-18}$$

The above comments pertaining to metals can be summarized by the following three realistic hypotheses which are generally adopted in theories of plasticity of metals:

(i) Under moderate hydrostatic stress (of the order of the yield stress in tension) the hydrostatic response of metals is elastic. Thus in constitutive terms:

σ = function of invariants of $\underline{\varepsilon}$.

In the literature, Eq. (3-13) is usually adopted where K_o is a constant.

(ii) A moderate hydrostatic stress does not affect the mechanical response in shear. Thus:

F_s is not a function of σ.

(iii)　　Shearing at constant hydrostatic stress does not cause a change in the hydrostatic strain. Again in constitutive terms. this is a consequence of the fact that

$$dz = \left|\left|d\underset{\sim}{e}^{P}\right|\right| \tag{3-19}$$

so that the shear response is completely autonomous and independent of the hydrostatic deformation.

In reality the above idealizations are only approximately true. For instance. it is found that in the case of metals. the shear stress response is affected somewhat by the presence of a compressive hydrostatic stress in the sense that the yield stress in shear is raised []. In endochronic plasticity terms the implication is that the entire monotonic shear stress-strain curve is "elevated". On the other hand. we have found F_s to be a slowly varying function of z. Under monotonic loading conditions the curvature and shape of the shear (or axial) stress-strain curve are almost entirely due to the form of the kernel function $\rho(z)$. and are affected to a lesser degree by the hardening function F_s. The conclusion is that under <u>monotonic</u> loading conditions one may. <u>as a first approximation</u>. consider F_s to be independent of z.

3.2.2 An Illustrative Example:　Pure Shear.

In view of the above observation for metals. let us apply Eqs. (3-12) - (3-16) to the case of monotonic loading in pure shear under a constant compressive stress. Thus we consider the shear response of a metal in the presence of constant σ and set:

$$F_s = F_s(\sigma) \tag{3-20}$$

In this case

$$d\underset{\sim}{e}^{P} = \begin{bmatrix} 0 & d\gamma^{P}/2 & 0 \\ d\gamma^{P}/2 & 0 & 0 \\ 0 & 0 & 0 \end{bmatrix} \tag{3-21}$$

Thus, in view of Eq. (3-15), it follows that

$$dz = \sqrt{\frac{1}{2}}\, d\gamma^P \quad . \tag{3-22}$$

Also the stress tensor $\underset{\approx}{s}$ is

$$\underset{\approx}{s} = \begin{bmatrix} 0 & \tau & 0 \\ \tau & 0 & 0 \\ 0 & 0 & 0 \end{bmatrix} , \tag{3-23}$$

so that, in view of Eq. (3-12) and (3-21), we find

$$\tau = \frac{1}{2} \int_0^{z_s} \rho(z_s - z')\frac{d\gamma^P}{dz'}\, dz' \quad . \tag{3-24}$$

Hence, the use of Eq. (3-16) and Eq. (3-22) in Eq. (3-24) leads to the result:

$$\tau = \sqrt{\frac{1}{2}} \int_0^{z_s} \rho(z_s - z')dz' \tag{3-25}$$

Let $M(z_s)$ be given by the expression:

$$M(z_s) = \int_0^{z_s} \rho(z')dz' \quad . \tag{3-26}$$

Then a simple change of variable in Eq. (3-25) gives

$$\tau = \sqrt{\frac{1}{2}}\, F_s M(z_s) , \tag{3-27}$$

where in view of Eqs. (3-16) and (3-22)

3-6

$$z_s = \sqrt{\frac{1}{2}} \frac{\gamma^p}{F_s} \quad . \tag{3-28}$$

By combining Eqs. (3-27) and (3-28), we find

$$\tau = \sqrt{\frac{1}{2}} F_s \, M\left(\frac{\sqrt{\frac{1}{2}} \gamma^p}{F_s}\right) \quad . \tag{3-29}$$

Equation (3-29) illustrates the way in which the hydrostatic stress affects the shear response through the fur tion F_s. Specifically, in the particular case where τ tends to a constant τ_∞ as γ tends to infinity, it follows from Eq. (3-29) that

$$\tau_\infty = \sqrt{\frac{1}{2}} F_s \, M_\infty \quad . \tag{3-30}$$

Equation (3-30) demonstrates how the functional form of $F_s(\sigma)$ may be determined from shear stress-strain tests which reveal the manner in which τ_∞ varies with σ.

Equation (3-29) provides an illustration of the way in which the endochronic theory predicts the form of the monotonic shear stress-plastic strain curve. For instance let $F_s = 1$ at some reference value of the hydrostatic stress. Then Eq. (3-29) becomes

$$\tau = \sqrt{\frac{1}{2}} M\left(\sqrt{\frac{1}{2}} \gamma^p\right) \quad . \tag{3-31}$$

The function M describes the form of the stress-strain curve in a general way which does not pre-empt the existence or otherwise of a yield point. We note, in regard to Eq. (3-26), that a yield point (or surface) will exist if $\rho(z)$ contains a delta function, as discussed earlier in Chapter 2 (see Eq. (2-101)). Thus while the theory does not depend on the yield point or, more generally, on the yield surface for its existence it can accommodate such material models without difficulty.

3.2.3 Cautionary Comments.

The above derivation leading to Eq. (3-31) is predicated on two conditions which we wish to discuss. The first has already been discussed and has to do with taking F_s to be independent of z. This is an approximation that has been used only for the

sole purpose of obtaining a closed form solution to a specific example. F_s is a slowly varying function but its role is essential and becomes more so under cyclic conditions leading to large values of z. For instance cross-hardening, which is defined as hardening in shear due to previously applied plastic tensile strain (or vice versa) is due to the dependence of F_s on z.

The second condition has to do with material prehistory, i.e., the strain history to which the material has been subjected prior to its present state. If the material prehistory is null then one is justified in setting z equal to zero at the initiation of the deformation and the above analysis is valid. If not, the prehistory must be known otherwise the integral on the right-hand side of Eq. (3-26) cannot be evaluated. These questions will be addressed in greater detail later in Chapter 5, where history-induced anisotropy is discussed.

3.2.4 The Kernel Function $\rho(z)$.

At this stage the reader may be wondering how one can determine the form of M or, in a more basic sense the form of $\rho(z)$. Again this question will be answered in its generality in Section 3.3. However, to satisfy the reader's curiosity at this stage we note, that when the above conditions do apply, Eq. (3-26) may be used to determine the kernel function $\rho(z)$ by simple differentiation. To this end we set $z_s = z$ when $F_s = 1$. Then it follows from Eq. (3-26) that

$$\rho(z) = \frac{dM}{dz} \; . \tag{3-32}$$

In a monotonic pure shear experiment $\tau(\gamma^p)$ is determined and known. Thus $d\tau/d\gamma^p$ is also a known function of γ^p, say $R(\gamma^p)$. If we now make use of Eqs. (3-22) and (3-27), it follows that

$$\frac{dM}{dz} = \frac{1}{2} R(\gamma^p) \tag{3-33}$$

or

$$\frac{dM}{dz} = \frac{1}{2} R(\sqrt{2} \, z)$$

Thus, upon use of Eq. (3-32):

$$\rho(z) = \frac{1}{2} R\left(\sqrt{2}\ z\right)$$

(3-34)

3.2.5 Special Form of $\rho(z)$: The Ramberg-Osgood Relation.

The stress-plastic strain curve of <u>annealed</u> metals (be it shear or axial) has been observed (Ramberg-Osgood) to obey a power law which, though empirical, seems to be valid over a substantial range of strain, the actual domain of plastic strain being a function of the particular metal at hand. Thus with specific reference to the case of shear, the reaction between τ and γ^p is of the form:

$$\tau = \tau_o \left(\gamma^p\right)^{1-\alpha},$$

(3-35)

where τ_o and α are material constants. Moreover α is always less than unity (to satisfy convexity) and equal to about 0.85 for most metals.

It is easy to demonstrate that Eq. (3-35) is a consequence of a special form of $\rho(z_s)$, given in Chapter 2, obtained from Eq. (2-111) by setting $r_o = 0$. This form is given by Eq. (3-26):

$$\rho\left(z_s\right) = \rho_o z_s^{-\alpha} \ ; \quad o < \alpha < 1$$

(3-36)

Thus, using Eqs. (3-26) to (3-28)

$$M\left(z_s\right) = \frac{\rho_o}{1-\alpha}\ z_s^{1-\alpha}$$

(3-37)

and

$$\tau = \left(\frac{1}{2}\right)^{1-\alpha/2} \frac{\rho_o}{1-\alpha}\ F_s^\alpha \left(\gamma^p\right)^{1-\alpha}$$

(3-38)

which is, of course, the Ramberg-Osgood relation where

$$\tau_o = \left(\frac{1}{2}\right)^{1-\alpha/2} \frac{\rho_o}{1-\alpha}\ F_s^\alpha \ .$$

(3-39)

In the above derivation σ was assumed constant and F_s was taken to be independent of z which is a reasonable approximation over the range of validity of the Ramberg-Osgood relation.

We point out that Eq. (3-35) cannot be true of metals which exhibit an ultimate stress as γ^p becomes large since

$$\lim_{\gamma^p \to \infty} \left(\gamma^p\right)^{1-\alpha} = \infty \; . \tag{3-40}$$

The basic question of materials which exhibit an ultimate stress (or ultimate surface) is taken up in the next subsection.

3.2.6 Materials with Ultimate Stress.

The question of ultimate stress will be examined first in the context of a one-dimensional stress response in the presence of <u>constant</u> hydrostatic stress. In the case of metals the effect of the hydrostatic stress on the response is really a moot one for moderate σ, since this effect is weak. In any event, we shall set $F_s = F_s(z)$ in which case

$$z_s = \int_0^{z_s} \frac{dz'}{F_s(z')} \; . \tag{3-41}$$

With specific reference to shear response, the constitutive equation of interest is Eq. (3-24). Under monotonic loading conditions equations (3-24) and (3-41) combine to give

$$\tau = \sqrt{\frac{1}{2}} \int_0^{z_s} \rho\left(z_s - z'\right) F_s^*(z') dz' \tag{3-42}$$

since now

$$F_s(z) = F_s\left[z\left(z_s\right)\right] = F_s^*\left(z_s\right) \tag{3-43}$$

In view of Eq. (3-42) the existence of an ultimate stress depends upon whether or not the integral on the right-hand side of Eq. (3-42) approaches a limit as $z_s \to \infty$. Here we shall consider hardening functions that have an upper bound in the sense that

3-10

$$\lim_{z_s \to \infty} F_s^* = F_\infty \quad . \tag{3-44}$$

Although this is a mathematical limitation on F_s, it is one which is justified on the basis of the physics of hardening in metals. Hardening is directly related to the density of dislocations and to the effect of the activation energies of the motion of these. Since the saturation density of dislocations is finite and the activation energies associated with their motion are also finite the saturation value of the hardening function must also be finite.

Regarding the kernel $\rho(z_s)$, we have already imposed the condition that $\rho(z_s)$ be integrable for all finite z_s to ensure boundedness of the stress response for finite strains, i.e.,

$$\int_0^{z_s} \rho(z') dz' < \infty \quad ; \quad z_s < \infty \tag{3-45}$$

Returning to Eq. (3-42), and in view of the fact that $\rho(z_s)$ is a positive integrable function and F_s is positive and bounded from above, it follows that

$$\tau \leq \sqrt{\frac{1}{2}} F_\infty \int_0^{z_s} \rho(z') dz' \tag{3-46}$$

where the relation

$$\int_0^{z_s} \rho(z_s - z') dz' = \int_0^{z_s} \rho(z') dz' \tag{3-47}$$

was used. It follows, therefore, from Eq. (3-45) that the existence of an ultimate stress τ_∞, where

$$\tau_\infty = \lim_{z_s \to \infty} \tau(z_s) \quad , \tag{3-48}$$

requires that

$$\lim_{z_s \to \infty} \int_0^{z_s} \rho(z')dz' < \infty \quad . \tag{3-49}$$

Note that the form given by Eq. (3-46) does **not** satisfy this condition! However the form of ρ given by Eq. (2-111) of Chapter 2 <u>does</u>. To wit, the form:

$$\rho = \rho_0 e^{-k_0 z_s} z_s^{-\alpha} \quad , \tag{3-50}$$

where ρ_0, k_0 and α are material functions, gives rise to an ultimate stress, since

$$\int_0^\infty \rho(z')dz' = \int_0^\infty \rho_0 e^{-k_0 z'} (z')^{-\alpha} dz = \rho_0 \frac{\Gamma(1-\alpha)}{k_0^{1-\alpha}} \tag{3-51}$$

where Γ is the complete Gamma function. Thus in view of Eq. (3-46):

$$\tau_\infty \leq \sqrt{\frac{1}{2}} F_\infty \rho_0 \frac{\Gamma(1-\alpha)}{k_0^{1-\alpha}} \tag{3-52}$$

and an ultimate stress exists. In fact one can show that

$$\tau_\infty = \sqrt{\frac{1}{2}} F_\infty \rho_0 \frac{\Gamma(1-\alpha)}{k_0^{1-\alpha}} \quad . \tag{3-53}$$

3.2.7 Constitutive Equation for Uniaxial Loading.

Under conditions of uniaxial loading, the stress and plastic strain tensors are given by the following expressions:

$$\sigma = \begin{bmatrix} \sigma_1 & 0 & 0 \\ 0 & 0 & 0 \\ 0 & 0 & 0 \end{bmatrix} \quad , \quad \underset{\sim}{\epsilon} = \begin{bmatrix} \epsilon_1^p & 0 & 0 \\ 0 & \epsilon_2^p & 0 \\ 0 & 0 & \epsilon_2^p \end{bmatrix} \tag{3-54a,b}$$

where the condition of isotropy has been used to define the plastic strain field in Eq. (3-54b). Furthermore the condition of plastic incompressibility must be satisfied. so that

$$\epsilon_1^p + 2\epsilon_2^p = 0 \quad . \tag{3-55}$$

The deviatoric stress and the deviatoric plastic strain tensors are. therefore. given by the following expressions:

$$\underset{\approx}{s} = \begin{pmatrix} \dfrac{2\sigma_1}{3} & & \\ & -\dfrac{\sigma_1}{3} & \\ & & -\dfrac{\sigma_1}{3} \end{pmatrix} \tag{3-56}$$

$$\underset{\approx}{e}^p = \begin{pmatrix} \epsilon_1^p & & \\ & -\dfrac{\epsilon_1^p}{2} & \\ & & -\dfrac{\epsilon_1^p}{2} \end{pmatrix} \quad . \tag{3-57}$$

Use of Eqs. (3-56) and (3-57) in Eq. (3-12) gives the following "uniaxial" constitutive equation:

$$\sigma_1 = \int_0^{z_s} E(z_s - z') \frac{d\epsilon_1^p}{dz'} \, dz' \tag{3-58}$$

where

$$E(z_s) = \frac{3}{2} \rho(z_s) \tag{3-59}$$

and dz and dz_s by virtue of Eqs. (3-15) and (3-16) are given by Eqs. (3-60) and (3-61). respectively.

$$dz = \sqrt{\frac{3}{2}} \left| d\epsilon_1^p \right| \tag{3-60}$$

$$dz_s = \frac{dz}{F_s(z)} \tag{3-61}$$

Thus in the case of incompressible plastic solids, knowledge of the shear response (kernel function $\rho(z_s)$ and hardening function $F_s(z)$) is sufficient to determine the constitutive response under conditions of axial stress.

3.3 Uniaxial Constitutive Response to Complex Strain Histories.

3.3.1 Simple Unloading.

In classical plasticity theories the problem of unloading requires special attention. Though more will be said about this later in the book, we deal with the problem briefly in this section so that the reader can appreciate the basic differences between the endochronic theory without a yield surface, and classical plasticity which is founded on the notion of a yield surface.

Let a yield surface be given by Eq. (3-62) in the six-dimensional stress space $\underset{\sim}{\sigma}$ for fixed values of $\underset{\sim}{g}$ and k:

$$f\left(\underset{\sim}{\sigma}, \underset{\sim}{g}, k\right) = 0 \tag{3-62}$$

where $\underset{\sim}{g}$ and k are internal structure parameters, i.e., internal variables. The outward normal $\underset{\sim}{n}$ to the yield surface is given by the expression:

$$\underset{\sim}{n} = \frac{\dfrac{\partial f}{\partial \underset{\sim}{\sigma}}}{\left\| \dfrac{\partial f}{\partial \underset{\sim}{\sigma}} \right\|} \tag{3-63}$$

An increment in stress $d\underset{\sim}{\sigma}$ is said to constitute "loading", in the sense of producing a plastic strain increment $d\underset{\sim}{\epsilon}^p$, if

$$\underset{\sim}{n} \cdot d\underset{\sim}{\sigma} > 0 \quad . \tag{3-64}$$

Conversely, the response is said to be elastic if

$$\underline{n} \cdot d\underline{\sigma} \leq 0 \quad . \tag{3-65}$$

In colloquial geometric language, loading takes place when the stress increment vector points outwards relative to the yield surface, while unloading occurs when $d\underline{\sigma}$ points inward. Neutral action -- but still elastic response* -- occurs when $d\underline{\sigma}$ is in the tangent plane passing through the point of origin of $d\underline{\sigma}$.

In endochronic plasticity without a yield surface,** such rules are unnecessary. In the case of one dimension, which is of interest in this section, two possibilities exist: either $d\epsilon_1^P$ is positive or negative. Using Eq. (3-60) we find that in the former case $d\epsilon_1^P/dz = +\sqrt{2/3}$ while in the latter case $d\epsilon_1^P/dz = -\sqrt{2/3}$. However, $d\epsilon_1$ and $d\epsilon_1^P$ have the same sign. Thus we have the following conditions:

$$d\epsilon_1 > 0 \; ; \; \frac{d\epsilon_1^P}{dz} = + \sqrt{\frac{2}{3}}$$

$$\tag{3-66a,b}$$

$$d\epsilon_1 < 0 \; ; \; \frac{d\epsilon_1^P}{dz} = - \sqrt{\frac{2}{3}} \quad .$$

To fix ideas consider the case of uniaxial loading in which the strain is increased from zero to a positive value ϵ_1^A and subsequently decreased continuously to its current value ϵ_1. Simultaneously the plastic strain is increased from zero to a value ϵ^{PA} and subsequently decreased to its current value ϵ_1^P. To keep the analysis simple we set $F_s = 1$, so that $z_s = z$. Then, using Eq. (3-58) and Eqs. (3-66a,b), we obtain the following result.

---

* An exception is the perfectly plastic body with a stationary yield surface. In this case neutral loading produces changes in the plastic strain tensor.

** A version of the theory <u>with</u> a yield surface is admissible and will be discussed later in Section 3.6.

$$\sigma_1 = \sqrt{\frac{2}{3}} \int_0^{z_A} E(z - z') dz' - \sqrt{\frac{2}{3}} \int_{z_A}^{z} E(z - z') dz' \qquad . \tag{3-67}$$

At this point we recall Eqs. (3-26) and (3-59) whereby

$$\int_0^z E(z') dz' = \frac{3}{2} M(z) \tag{3-68}$$

Use of Eq. (3-68) in Eq. (3-67) gives the following explicit relation for σ_1:

$$\sigma_1 = \sqrt{\frac{3}{2}} \left\{ M(z) - 2M(z - z_A) \right\} \quad . \tag{3-69}$$

At this juncture it is instructive to give the relation between ϵ_1 and z. This is obtained simply by integrating Eqs. (3-66a,b). In the range: $0 \leq \epsilon_1^p \leq \epsilon_1^{pA}$: $d\epsilon_1^p/dz = + ve$ and ϵ_1^p is given by the expression:

$$\epsilon_1^p = \sqrt{\frac{2}{3}} z \tag{3-70}$$

while in the range: $\epsilon_1^p \leq \epsilon^{pA}$: $d\epsilon_1^p/dz = - ve$, and ϵ_1^p is given by the expression

$$\epsilon_1^p - \epsilon_1^{pA} = 1 \sqrt{\frac{2}{3}} (z - z_A) \tag{3-71}$$

where

$$\epsilon_1^{pA} = \sqrt{\frac{2}{3}} z_A \qquad . \tag{3-72}$$

The range of interest here is the one governed by Eq. (3-71).

Thus using Eqs. (3-71) and (3-72) in Eq. (3-69) we find the following relation between σ_1 and ϵ_1^p:

3-16

$$\sigma_1 = \sqrt{\frac{3}{2}} \left\{ M\left[\sqrt{\frac{3}{2}} \left(2\epsilon_1^{pA} - \epsilon_1^p\right)\right] - 2M\left[\sqrt{\frac{3}{2}}\left(\epsilon_1^{pA} - \epsilon_1^p\right)\right]\right\} \qquad (3\text{-}73)$$

More simply, if we set $\bar{\sigma} \equiv \sqrt{2/3}\ \sigma_1$, $\bar{\epsilon}^p \equiv \sqrt{3/2}\ \epsilon_1^p$, then Eq. (3-73) becomes the simple relation:

$$\bar{\sigma} = M\left(2\bar{\epsilon}_p^A - \bar{\epsilon}_p\right) - 2M\left(\bar{\epsilon}^A - \bar{\epsilon}_p\right) \quad . \qquad (3\text{-}74)$$

A plot of $\sqrt{3/2}\ \epsilon_1^p$ versus z is shown in Figure 3.1 and correspondingly a plot of $\sqrt{2/3}\ \sigma_1$ versus $\sqrt{3/2}\ \epsilon_1^p$ is shown in Figure 3.2 for the case in which

$$E(z) = \frac{E_o}{z^\alpha} \ ; \quad \alpha = 0.864 \ ; \quad E_o = 260 \text{ ksi} \quad . \qquad (3\text{-}75)$$

Experimental data by Halford and Morrow [3.1] are also shown for comparison.

Of particular interest is the case when $\bar{\sigma}^A$ is so large that $M(\bar{\epsilon}_p^A)$ is virtually saturated and equal to M_∞. In this case $M(2\bar{\epsilon}_p^A - \bar{\epsilon}_p^A)$ remains practically constant during unloading and subsequent compression and almost equal to M_∞. Under these conditions Eq. (3-74) becomes

$$\bar{\sigma} = M_\infty - 2M\left(\bar{\epsilon}_p^A - \bar{\epsilon}^p\right) \quad . \qquad (3\text{-}76a)$$

Specifically if one regards point A as the new origin, and σ^* and ϵ_*^p are values of stress and plastic strain measured from A, then

$$\sigma^* = 2M\left(\epsilon_*^p\right) \qquad (3\text{-}77)$$

i.e., for a certain strain measured from A, the stress measured from A is equal to twice the stress obtained during the monotonic testing for the same value of the strain. This is an important feature of the theory.
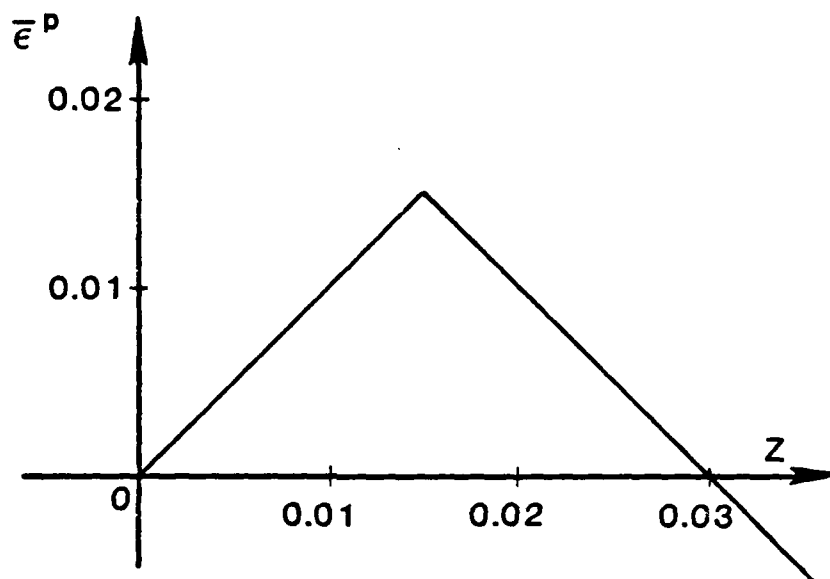
Figure 3.1. Plot of $\bar{\epsilon}^p$ versus z.
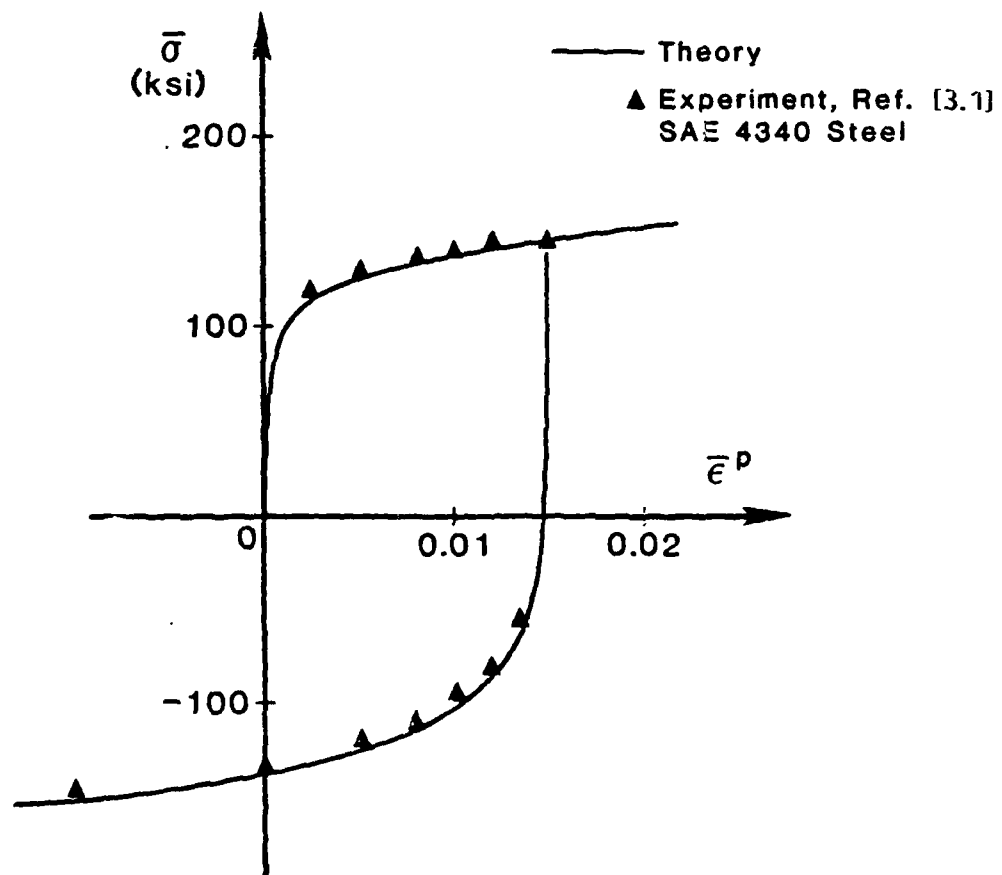
Figure 3.2.   Loading-unloading stress-plastic strain curve.

3.3.2 General Uniaxial Histories.

The most general uniaxial history consists of a set of unloadings and reloadings *ad infinitum*. The time interval $[0.z)$ consists of subintervals $[0.z_1)$. $\bullet\bullet\bullet[z_{r-1}.z_r)$ $\bullet\bullet\bullet.[z_n.z)$. If the initial loading is tensile then

$$\frac{d\bar{\epsilon}^p}{dz} = +1 \; ; \; 0 \leq z < z_1$$

and, in general, we can write

$$\frac{d\bar{\epsilon}^p}{dz} = -1 \; ; \; z_{r-1} \leq z < z_r \; , \; r \text{ even}$$

$$\frac{d\bar{\epsilon}^p}{dz} = +1 \; ; \; z_{r-1} \leq z < z_r, \; r \text{ odd} \qquad .$$

Thus, in a generic interval $z_{r-1} \leq z < z_r$ the following relation will always apply

$$\bar{\epsilon}^p - \bar{\epsilon}^p_{r-1} = \text{signum}\left(\frac{d\bar{\epsilon}^p}{dz}\right)(z - z_{r-1}) \qquad . \qquad (3\text{-}78)$$

Again, if $F_s = 1$ (no hardening), one uses Eqs. (3-58) and (3-78) to obtain the following relation between $\bar{\sigma}$ and the history of $\bar{\epsilon}^p$:

$$\bar{\sigma} = M(z) - 2M(z - z_1) + 2M(z - z_2) - \bullet\bullet\bullet$$

$$\bullet\bullet\bullet + \begin{cases} + 2M(z - z_n), & n \text{ odd} \\ \\ - 2M(z - z_n), & n \text{ even} \end{cases} \qquad (3\text{-}79)$$

3.3.3 Stress Response to Uniaxial Cyclic Histories.

In recent years, **cyclic plasticity**, which deals with the rate-independent inelastic response of materials (metals) to cyclic stress or strain histories, has become an important subject of research in applied mechanics and engineering design. Past experimental work, theoretical studies, and engineering analysis are well documented in the literature. For details see, typically, references [3.1] to [3.6].

On the basis of existing experimental results, one concludes that generally, when subjected to symmetric stress or strain cycles, annealed or soft materials will harden and will tend to a stable response, while cold-worked or hard materials will soften. When a stable response is reached, hysteresis loops in the stress-strain space become stable, closed, and symmetric. This has led to the definition of a cyclic stress-strain curve which is the locus of the tips of stable hysteresis loops.

Also, in the presence of a history of unsymmetric stress cycles, the material response involves a progressive increase of plastic strain, the direction of which is determined by the algebraic sign of the mean stress. This phenomenon is called cyclic "ratcheting". On the other hand, a history of symmetric cyclic straining relative to a nonzero mean strain will result in "cyclic relaxation" toward zero mean stress. Both phenomena occur whether or not the material response has been stabilized prior to these specific tests[3.7].

Under variable amplitude cycling, metals have a strong memory of their most recent point of load reversal. As the number of cycles increases, effects of prior plastic history tend to disappear. More precisely a material has a "fading" memory, in terms of the intrinsic time scale z, of the history of plastic deformation that preceded the cyclic history [3.8], as the latter progresses.

In this section we shall show that the endochronic theory predicts the above response characteristics in a simple and consistent fashion. The theory will also be validated in a broader sense by means of demonstrated agreement with the observed cyclic response of (i) normalized mild steel to **variable** uniaxial strain amplitude histories, and (ii) Grade 60 steel to a random strain history.

Analysis.

We begin with Eq. (3-58), i.e.,

$$\sigma_1 = \int_0^z E(z - z') \frac{d\epsilon_1^p}{dz'} dz' \qquad (3-80)$$

3-21

where in the remainder of this section we will substitute z for z_s and ς for z to simplify the notation. Recall that

$$dz = \frac{d\varsigma}{F_s(z)} \quad ; \quad d\varsigma = \sqrt{\frac{3}{2}} \left| d\epsilon_1^p \right| \ . \qquad (3\text{-}81a,b)$$

Before proceeding with the application of Eq. (3-80) to the histories of interest. we make certain general observations which have particular application to metals such as mild-steel.

There are basically two items of concern: (i) the prehistory, i.e., the strain history to which the specimen has been subjected prior to the uniaxial test and (ii) the hardening function $F_s(z)$. Item (i) is unknown and item (ii) can be determined experimentally as discussed in Section 3.4.2. The histories of interest are: the prehistory H_o. the cyclic strain history H_1 (at constant amplitude and zero mean strain). and the post-cyclic history H_2 (following a saturated response). In general the prehistory H_o is not known but this is one case where it can be treated rigorously. Thus we write Eq. (3-80) in the form:

$$\sigma_1 = \int_0^{z_o} E(z - z') \frac{d\epsilon_1^p}{dz'} dz' + \int_{z_o}^{z_1} E(z - z') \frac{d\epsilon_1^p}{dz'} dz' + \int_{z_1}^{z} E(z - z') \frac{d\epsilon_1^p}{dz'} dz'$$

$$(3\text{-}82)$$

where $z = 0$ is the temporal origin of the prehistory. z_o is the "time" of initiation of the uniaxial test and z_1 is the time of termination of the cyclic test at which steady-state response has been observed. Of course $\epsilon_1^p(z)$ in the interval $0 \leq z \leq z_o$. is not known. Also not known is whether F_s has reached saturation at or before z_o. or not at all. For this reason we define an intrinsic time z^* at which F_s becomes essentially constant. i.e..

$$F_s(z) \doteq F_s(z^*) \qquad (3\text{-}83)$$

for all $z \geq z^*$. Equation (3-83) can now be written in the form

$$\sigma_1 = \int_0^{z*} E(z - z')\frac{d\epsilon_1^p}{dz'}\, dz' + \int_{z*}^{z_1} E(z - z')\frac{d\epsilon_1^p}{dz'}\, dz' + \int_{z_1}^{z} E(z - z')\frac{d\epsilon_1^p}{dz'}\, dz \qquad (3-84)$$

We emphasize that $F_s = \text{constant} = 1$ (say) for $z \geq z*$.

Consider now the first integral on the right-hand side of Eq. (3-84), and let

$$I_o = \int_0^{z*} E(z - z')\, \frac{d\epsilon_1^p}{dz'}\, dz' \qquad . \qquad (3-85)$$

Evidently since F_s is monotonically increasing

$$I_o < F_s(z*) \int_0^{z*} E(z - z')\left|\frac{d\epsilon_1^p}{dz'}\right| dz' \qquad (3-86)$$

But since $F_s(z*) = 1$ and $|d\epsilon_1^p/dz'| = \sqrt{2/3}$, it follows that

$$I_o < \sqrt{\frac{2}{3}} \int_0^{z*} E(z - z')\, dz' \qquad (3-87)$$

or, recalling Eq. (3-68),

$$I_o < \sqrt{\frac{3}{2}}[M(z) - M(z - z*)] \qquad (3-88)$$

It will be shown later in Section 3.4.1 that because $M(z)$ is convex (see Eq. (3-149)):

$$\lim_{z \to \infty} \{M(z) - M(z - z*)\} = 0 \qquad . \qquad (3-89)$$

We presume that z_1 must be very large for the response to reach steady state and since $z > z_1$ the contribution of I_o to σ_1 can be ignored. In fact, Eq. (3-89) is the mathematical statement of "<u>fading memory</u>" in the sense that the effect of the

3-23

prehistory "fades" with time and asymptotically vanishes. thus having negligible effect on the steady response.

Thus. Eq. (3-84) becomes

$$\sigma_1 = \int_{z*}^{z_1} E(z - z')\frac{d\epsilon_1^p}{dz'}\,dz' + \int_{z_1}^{z} E(z - z')\frac{d\epsilon_1^p}{dz'}\,dz' \qquad (3-90)$$

where now

$$F_s = 1 \; ; \; dz = d\varsigma = \sqrt{\frac{3}{2}}\,\left|d\epsilon_1^p\right| \; . \qquad (3-91)$$

Moreover because of Eq. (3-91) the origin of the time scale can be shifted at will. so that we may take $z* = 0$. in which event

$$\sigma_1 = \int_{o}^{z_1} E(z - z')\frac{d\epsilon_1^p}{dz'}\,dz' + \int_{z_1}^{z} E(z - z')\frac{d\epsilon_1^p}{dz'}\,dz' \; . \qquad (3-92)$$

The time of initiation of the post-cyclic history is the time z_1 above. which is always assumed to be sufficiently large for a steady response to have been reached.

Uniaxial Cyclic Strain History at Constant Amplitude.

Let us now consider the class of metals whose asymptotic stress response to sustained cyclic strain histories at constant strain amplitude $\Delta\epsilon_1$ is a periodic stress history with constant amplitude $\Delta\sigma_1$. In other words. there exists a z_∞ and characteristic values z_r of z such that

$$\sigma_1\left(z_r + 2\sqrt{\frac{3}{2}}\,\Delta\epsilon_1\right) = \sigma_1\left(z_r\right) \qquad (3-93)$$

for all $z_r > z_\infty$. Thus in a uniaxial test of this type. and for $z > z_\infty$. the axial plastic strain amplitude $\Delta\epsilon_1^p$ is also constant and given by the following equation:

$$\Delta\epsilon_1^p = \Delta\epsilon_1 - \frac{\Delta\sigma_1}{E} \qquad (3-94)$$

3-24

where E is the elastic Young's modulus. This observation is central in calculating the asymptotic stress response to cyclic strain histories at constant amplitude. In consequence, we may regard the post-cyclic history in Eq. (3-92) as a cyclic history with <u>constant plastic strain amplitude</u> and thus set $z_1 = z_\infty$. We now observe that the first integral on the right-hand side of this equation has the same properties as the integral I_0 in Eq. (3-85). Thus following the same procedure we find

$$\int_0^{z_\infty} E(z - z') \frac{d\epsilon_1^p}{dz'} dz' < \left[\sqrt{\frac{2}{3}} \Big[M(z) - M(z - z_\infty) \Big] \right] \qquad (3\text{-}95)$$

Hence we utilize Eq. (3-89) and observe that the integral on the left-hand side of Eq. (3-95) goes to zero as z tends to infinity. Thus for $z \gg z_\infty$ (i.e., in an asymptotic sense)

$$\sigma_1 = \int_{z_\infty}^{z} E(z - z') \frac{d\epsilon_1^p}{dz'} dz' \qquad (3\text{-}96)$$

with the important qualification that the history in the above equation is one in which the <u>plastic</u> strain amplitude is <u>constant</u>. Again since $F_s = 1$ we may reset the origin of integration to zero so that

$$\lim_{z \to \infty} \sigma_1 = \int_0^{z} E(z - z') \frac{d\epsilon_1^p}{dz'} dz' \qquad (3\text{-}97)$$

where $\Delta\epsilon_1^p$ is constant and given by Eq. (3-94).

The following relation is obtained by virtue of Eqs. (3-78) and (3-97)

$$\sigma_1 = \lim_{n \to \infty} \left[\sum_{i=1}^{n} \int_{z_{i-1}}^{z_i} (-1)^{i-1} \sqrt{\frac{2}{3}} \, E(z - z') \, dz' \right.$$

(3-98)

$$\left. + (-1)^n \int_{z_n}^{z} \sqrt{\frac{2}{3}} \, E(z - z') \, dz' \right]$$

where $z_0 = 0$.

Application to Normalized Mild Steel.

It was found that in the case of normalized mild steel, the appropriate form of the kernel $E(z)$ is:

$$E(z) = E_0 \, z^{-\alpha} \qquad .$$

(3-99)

The manner in which E_0 and α were determined will be discussed in that which follows. In view of Eq. (3-99), Eq. (3-98) becomes

$$\sigma_1 = \lim_{z_n \to \infty} \sqrt{\frac{2}{3}} \, \frac{E_0}{1-\alpha} \left[z^{1-\alpha} + 2 \sum_{i=1}^{n} (-1)^i \left(z - z_i \right)^{1-\alpha} \right]$$

(3-100)

Use of Eq. (3-78) together with the fact that $z = \varsigma$ leads to the following expression for z:

$$z = \sqrt{\frac{3}{2}} \left[2n\Delta\epsilon_1^p \pm \epsilon_1^p \right] ,$$

(3-101)

where the minus sign is used for n odd and the plus sign for n even. In particular,

$$z_n = \sqrt{\frac{3}{2}} \, (2n - 1) \, \Delta\epsilon_1^p$$

(3-102)

At this point we use Eqs. (3-100), (3-101) and (3-102) to find the following closed form solution for σ_1:

3-26

$$\sigma_1 = \lim_{n \to \infty} \left(\frac{2}{3}\right)^{\alpha/2} \frac{E_o}{1-\alpha} \left[\Delta\epsilon_1^p\right]^{1-\alpha} F_n(\alpha, x) \qquad (3\text{-}103)$$

where:

$$x = \frac{\epsilon_1^p}{\Delta\epsilon_1^p} \qquad (3\text{-}104)$$

and

$$F_n(\alpha, x) = (2n \pm x)^{1-\alpha} + 2\sum_{i=1}^{n} (-1)^i (2n - 2i + 1 \pm x)^{1-\alpha} \qquad (3\text{-}105)$$

where, as above, the minus sign applies to n odd and the plus sign to n even.

The algebraic value $\Delta\sigma_1$ of the peak stress is found by setting $x = 1$ for n odd or $x = -1$ for n even in Eq. (3-105), and letting $n \to \infty$. Thus:

$$\Delta\sigma_1 = \left(\frac{2}{3}\right)^{\alpha/2} \frac{E_o}{1-\alpha} \left[\Delta\epsilon_1^p\right]^{1-\alpha} F_\infty(\alpha) \qquad (3\text{-}106)$$

where

$$F_\infty(\alpha) = \lim_{n \to \infty} F_n(\alpha) \qquad (3\text{-}107)$$

It can be shown [3.8] that $F_n(\alpha)$ tends to a constant $F_\infty(\alpha)$ as n tends to infinity, the constant depending on the value of α. Eq. (3-106) is the theoretical form of the "cyclic" stress-plastic strain curve which is basically a plot of the asymptotic peak stress $\Delta\sigma_1$ versus the amplitude of plastic strain $\Delta\epsilon_1^p$.

At this point we test the theory vis-á-vis experimental data on normalized mild steel [3.7]. In reference [3.7], a set of stable uniaxial hysteresis loops corresponding to various constant strain amplitudes was presented in the uniaxial stress-strain space. These data appear in Figure 3.3 where triangles denote experimental points. *A propos* of the ensuing theoretical predictions we note that the *geometric shape* of the loops is given by Eq. (3-103), whereas the peak stresses are given by Eq. (3-106). We also note that there are only two undetermined parameters in these equations: α and E_o.
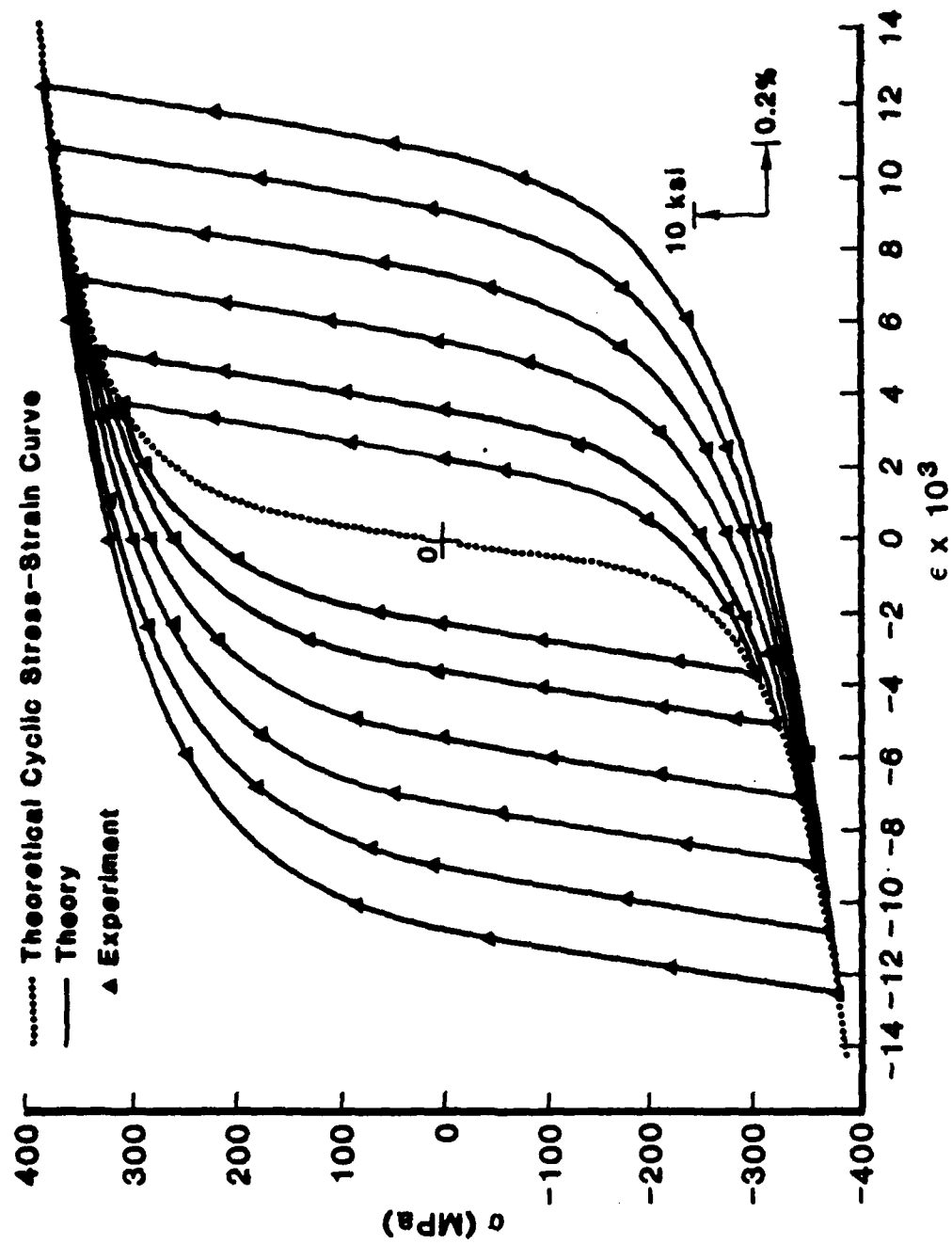
Figure 3.3 Steady hysteresis loops of normalized mild steel.

The form of Eq. (3-106) is corroborated by means of a plot of the experimental values of $\log \Delta\sigma_1$ versus $\log \Delta\epsilon_1^p$. This plot gives rise to a straight line as shown in Figure 3.4 and thereby determines the constants a and E_o which were found to be 0.864 and 107.6 MPa (15.61 ksi), respectively.

These values were then used in Eq. (3-103) to give the shape of the stable hysteresis loops for large n (say n > 25). Agreement between theory and experiment is shown in Figure 3.3 for all experimental amplitudes $\Delta\epsilon_1$. One observed that the agreement between theory and experiment is remarkable.

Regarding these results, we will note that <u>two</u> constants are sufficient to determine the cyclic stress-(plastic) strain response <u>as well as</u> the hysteretic cyclic behavior of normalized mild steel. It is also pertinent to mention that the analytical expressions involved, Eqs. (3-103) and (3-106), are closed-form solutions derived from a general constitutive equation pertaining to three-dimensional histories. Also of importance is that the prediction of unloading and reloading behavior did not necessitate special memory or loading-unloading rules but was dealt with routinely, as part of the total experimental history of interest. Specifically, the celebrated Bauschinger effect is predicted quantitatively and correctly from one and the same constitutive equation.

We make, in passing, an observation of historical interest. Equation (3-106) agrees with the following empirical relationship proposed by Landgraf [3.9] for steels, i.e.

$$\Delta\sigma \sim \left(\Delta\epsilon^p\right)^{1-a} \quad , \tag{3-108}$$

where $1-a$ ranges from 0.12 to 0.17. In the case of normalized mild steel, $1-a = 0.136$.

3.3.4 Variable Uniaxial Strain Amplitudes.

To extend the experimentally verified domain of validity of the theory, we test it under conditions of variable uniaxial strain amplitude histories. These histories fall into two distinct types. The first type is one where the specimen is subjected to a
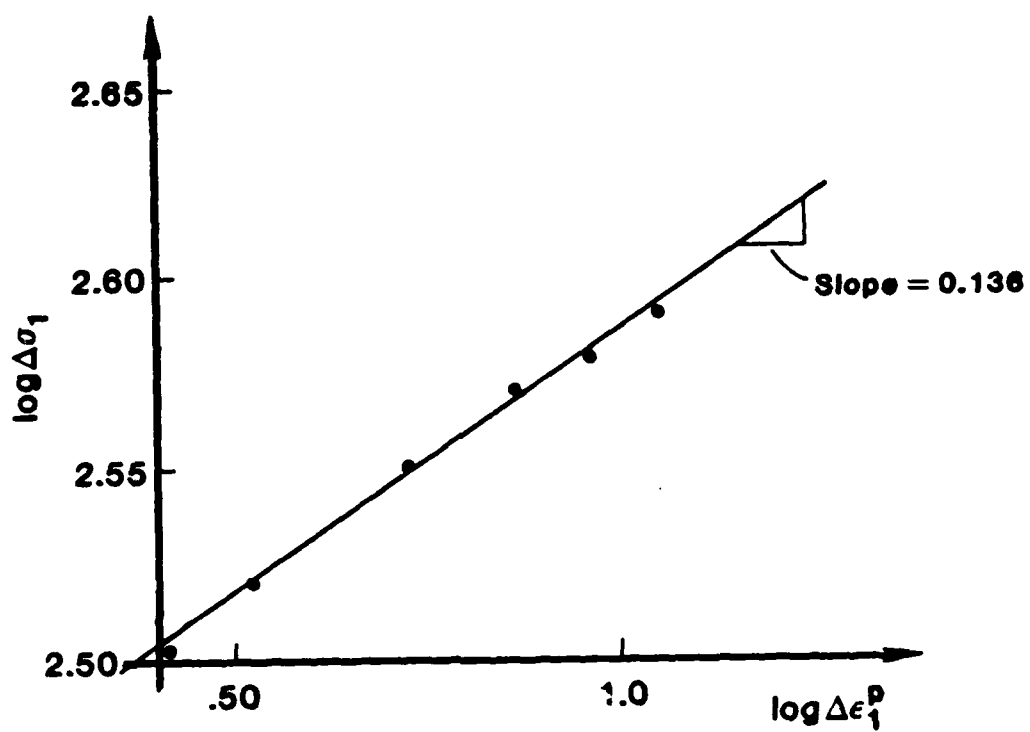
Figure 3.4. Determination of α and E_o.

constant strain amplitude history (until a periodic response is attained) which is then followed by another (different) type of history. The material that we will consider is *normalized mild steel* and the experiments were reported in Ref. [3.7]. The second type is a random uniaxial strain history [3.10] and the material is Grade 60 steel.

Histories of the First Type.

The appropriate equation for this case is Eq. (3-92) where the first integral on the right-hand side is used for the cyclic history and the second for the post-cyclic history Recall that $F_s = 1$ in both integrals. Three histories are treated and these are shown in Figures 3.5, 3.6 and 3.7. The corresponding experimental results are also shown by triangles. Equation (3-92) was integrated numerically using precisely the same values of the constants for normalized mild steel as found previously. The theoretical predictions are shown in the figures by the solid lines. The agreement between theory and experiment is again remarkable.

History of the Second Type.

This is a random uniaxial strain history and is shown in Figure 3.8. The experimental results reported by Dafalias and Popov in Ref. [3.10] are also shown by means of triangles. squares and circles. Here we faced the difficulty that if a prehistory existed it could not be treated rigorously. hence we assumed that it was null. Also we set $F_s = 1$ *because the method* used to calculated it gave that value within experimental error. (See Eq. (3-183).) Equation (3-79) was then used to predict the stress response analytically (since the plastic strain could be calculated directly from the experimental data) and is shown in Figure 3.8 by a continuous black line. The material parameters E_o and α were determined by using the procedure in Section 3.4. (See Eq. (3-136) and Figure 3.9). We found that $F_s = 1$. $E_o = 264.2$ MPa and $\alpha = 0.882$. Considering the complexity of the history the agreement between theory and experiment. shown in Figure 3.8. is indeed again close.

It is worthy of note that predicted values of the slopes of the stress-strain curve at the onset of loading and reloading are always equal to Young's modulus $(2.06 \times 10^5$ MPa). However. in Reference[3.10] those slopes were assigned a smaller value $(1.64 \times 10^5$ MPa) than the Young's modulus to account for "softening". This has not been necessary in the present case.
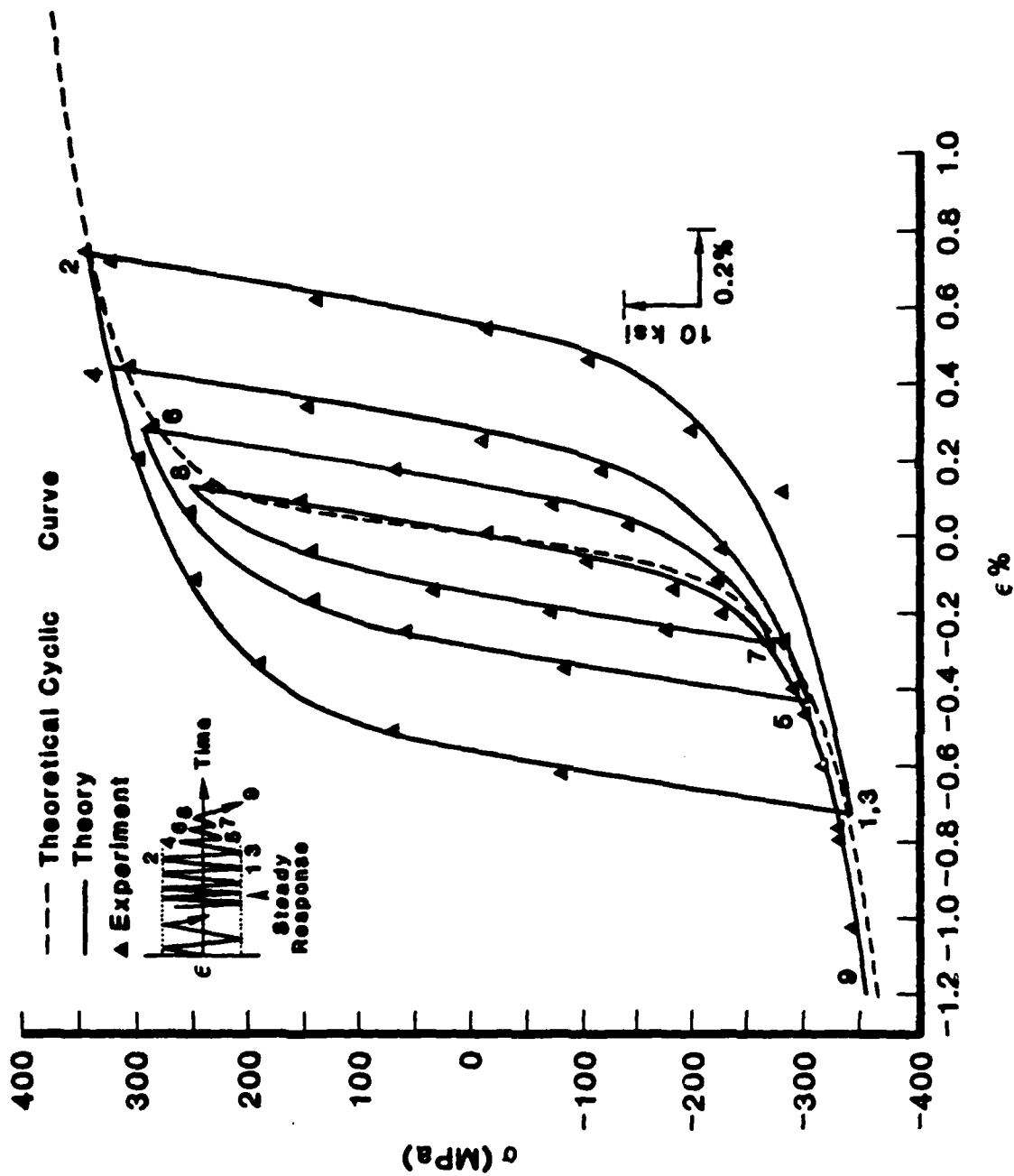
Figure 3.5   Uniaxial stress response of normalized mild steel under variable strain amplitudes.
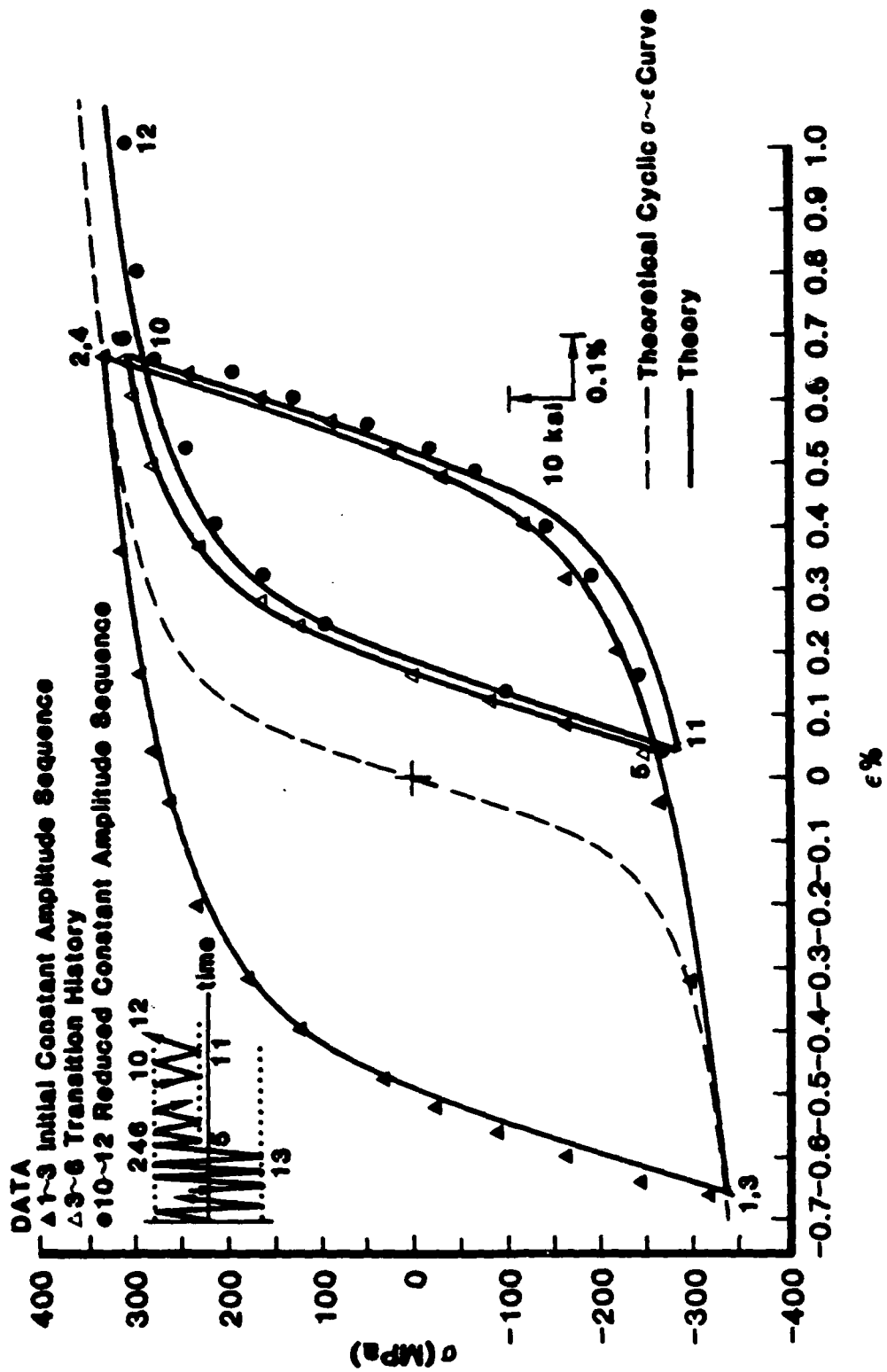
Figure 3.6   Uniaxial stress response of normalized mild steel under complex histories.

3-33
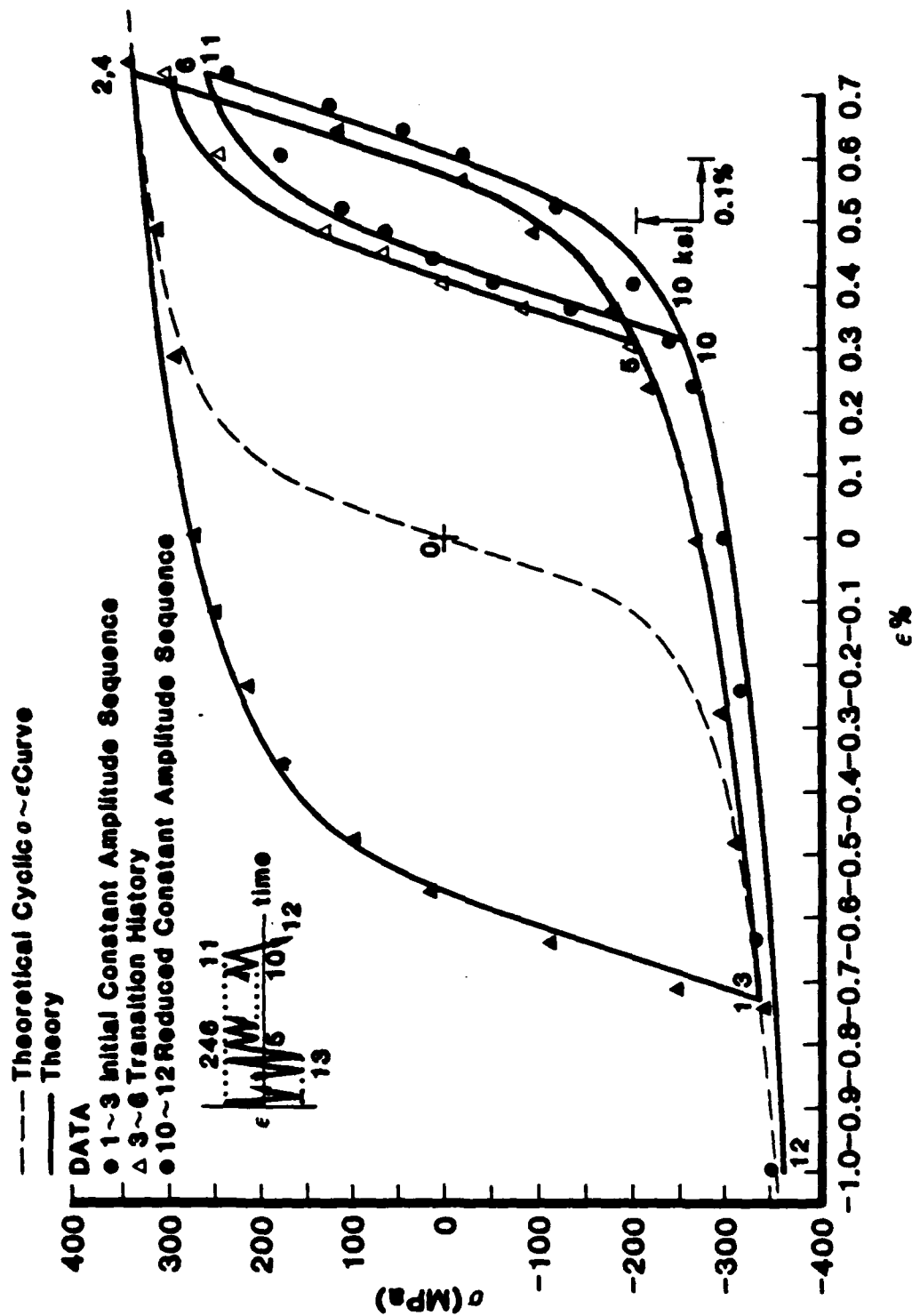
Figure 3.7   Uniaxial stress response of normalized mild steel under complex histories.

3-34

3.3.5 Cyclic Relaxation.

As a final example we consider the case where the uniaxial plastic strain is increased monotonically to a value ϵ_+^p, and is followed by a cyclic uniaxial strain history with amplitude $\Delta\epsilon^p$ about a mean value ϵ_o^p.

To calculate the stress response to this specific class of histories we use Eq. (3-79). The cyclic strain history is shown in Figure 3.10. With reference to this figure, we make the following definitions:

$$\epsilon_+^p = \epsilon_o^p + \Delta\epsilon^p \qquad (3-109)$$

$$\epsilon_-^p = \epsilon_o^p - \Delta\epsilon^p \qquad (3-110)$$

The value z_i of z at the i<u>th</u> reversal, is found from Eq. (3-81b). Thus

$$z_i = \sqrt{\frac{3}{2}} \left[\epsilon_o^p + (2i - 1)\ \Delta\epsilon^p\right] \ , \quad i = 1,\ 2,\ \ldots\ \infty. \qquad (3-111)$$

After n reversals have been completed, the value of z at the current strain ϵ^p is

$$z = \sqrt{\frac{3}{2}} \left[2n\ \Delta\epsilon^p + \epsilon_o^p + \bar{\epsilon}^p\right] \qquad (3-112)$$

where

$$\bar{\epsilon}^p = \epsilon^p - \epsilon_o^p \qquad (3-113)$$

and the minus and plus signs correspond to n odd and even, respectively. The stress response after n reversals is found upon using Eqs. (3-58), (3-111) and (3-112). Specifically, we find that

$$\sigma = \left(\frac{2}{3}\right)^{\alpha/2} \frac{E_o}{1 - \alpha} \left(\Delta\epsilon^p\right)^{1-\alpha} F_n\left(\alpha, x_o, x\right) \qquad (3-114)$$

3-35
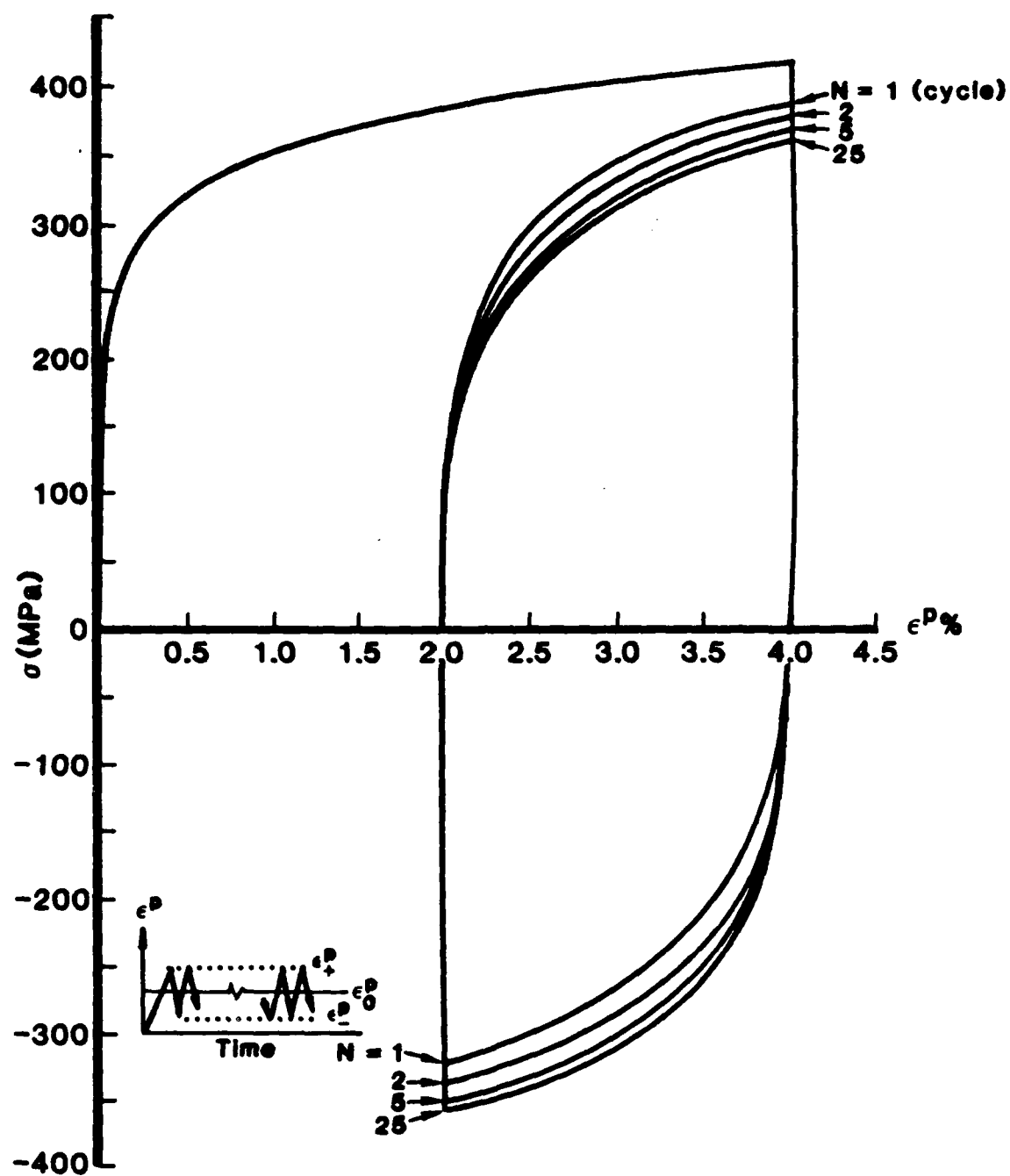
Figure 3.10.   Uniaxial cyclic relaxation of normalized mild steel.

where

$$F_n(\alpha, x_o, x) = (2n + x_o + x)^{1-\alpha}$$

$$+ 2 \sum_{i=1}^{n} (-1)^i (2n - 2i + 1 + x)^{1-\alpha} \qquad (3\text{-}115)$$

and

$$x_o = \frac{\epsilon_o^p}{\Delta \epsilon^p} \qquad (3\text{-}116)$$

$$x = \frac{\bar{\epsilon}^p}{\Delta \epsilon^p} \qquad (3\text{-}117)$$

If n is odd. x varies from 1 to -1. while if n is even. x varies from -1 to 1. It is x_o which allows cyclic relaxation to take place even though the material is stable. since $f(\varsigma) = 1$. The results are shown in Figure 3.10 where the same material constants. found previously. were used. We notice that as n becomes very large. the effect of x_o in Eq. (3-114) disappears as a result of the relation $\lim_{n \to \infty} F_n(\alpha. x_o. x) = F_\infty(\alpha. x)$. The hysteresis loops then become stable and symmetric with respect to ϵ_o^p and are of exactly the same form as those with zero mean uniaxial strain.

3.4 Method of Determination of the Material Functions $\rho(z)$ and $F_s(z)$.

As may be seen from Eqs. (3-12) through (3-16) <u>two</u> elastic constants. μ_o and K_o. and the two material functions. $\rho(z)$ and $F_s(z)$. completely determine the constitutive response of plastically incompressible metals. within the assumptions already discussed in the previous sections. Of these. $2\mu_o$ is the initial slope of a monotonic pure shear stress-(tensorial) strain curve and K_o is the elastic bulk modulus. The determination of the functions $\rho(z)$ and $F_s(z)$ is more complex. Just as in viscoelasticity. where there is no unique experimental technique for determining the (relaxation or creep) kernel in a constitutive functional. so it is in the endochronic theory. However a standard test does exist for this purpose although other "equivalent" tests may prove experimentally suitable and theoretically satisfactory.

The most convenient test (in the sense of being easy to perform experimentally) is the uniaxial cyclic shear-strain test under constant strain amplitude conditions. In the course of such a test with constant strain amplitude $\Delta\epsilon_1$, the material will normally harden (though materials with an initial state of large prestrain may soften) and the stress σ_1 corresponding to the maximum strain $\Delta\epsilon_1$ will increase with the number of cycles until the material reaches a steady state. When this happens, the hysteresis loops generated during the remainder of the test will essentially retrace themselves and an asymptotic steady cyclic hysteresis loop will prevail.

The above test, although easy to perform experimentally does not lend itself easily to rigorous analysis. A similar test, which however may be more difficult to perform experimentally, but not too much so, given the presently available experimental equipment, is the constant plastic strain test. This test is shown schematically in Figure 3.11.

Note that once steady state conditions have been reached, the constant plastic strain amplitude test performed at $\epsilon^p_{1,max} = \Delta/2 = OA = OB$ (in the notation of Figure 3.11) is equivalent to the constant strain amplitude test at $\epsilon_{1,max} = \Delta\epsilon_1 = OA' = OB'$. Thus under steady state conditions the two tests lead to identical experimental results, in terms of the steady hysteresis loops such as ADBC.

In this section we shall use the constant plastic strain amplitude test to discuss the determination of the function $\rho(z)$ because this test does in fact lend itself to rigorous theoretical treatment. Specifically, it will be shown that the steady-state hysteresis loop determines the function $\rho(z)$.

3.4.1 The Kernel Function $\rho(z)$.

Let us begin with the analytical foundations for the determination of the function $\rho(z)$. To this end we recall Eq. (3-12). Then, under uniaxial stress conditions and in view of the assumption of plastic incompressibility, we can write

$$dz = \sqrt{\frac{3}{2}} \left| d\epsilon^p_1 \right| , \qquad (3-118)$$

where ϵ^p_1 is the axial plastic strain corresponding to the axial stress σ_1. However because the unit of intrinsic time is arbitrary (and therefore adjustable) and strictly for the purposes of illustrating how ρ and F_s are determined from experiment we set

3-38
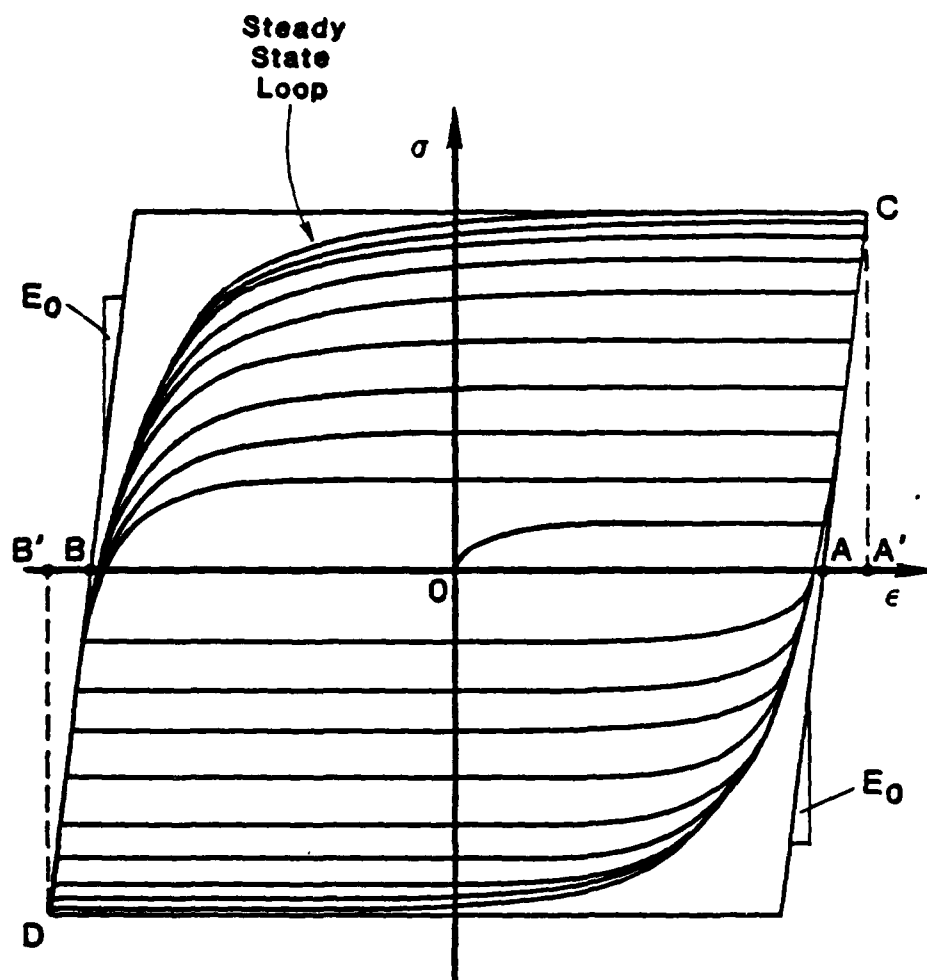
Figure 3.11 Constant plastic strain amplitude test.

$$d\zeta = \left| d\epsilon_1^p \right| \tag{3-119}$$

which is tantamount to setting

$$d\zeta = \sqrt{\frac{2}{3}} \left| \left| d\underset{\sim}{\epsilon}^p \right| \right| \tag{3-120}$$

We recall Eq. (3-80):

$$\sigma_1 = \int_o^z E(z - z') \frac{d\epsilon_1^p}{dz'} \, dz' \tag{3-121}$$

where

$$2E(z) = 3\rho(z) \tag{3-122}$$

The function F_s increases monotonically for continuously hardening materials until it reaches a constant value $F_{s.max}$ leading to steady state conditions. A constant F_s is necessary for a steady state response as has been shown analytically. For the purposes of analysis we set $F_{s.max} = 1$ for $z \geq z_o$. Under these conditions the history of ϵ_1^p versus z is shown in Figure 3.12. for the case of a cyclic test from z_o to z_n followed continuously by a monotonic test from z_n on z in the notation of this figure.

We note that in such a test and given that $F_s = 1$, the value of $d\epsilon_1^p/dz$ is either $+1$ or -1 depending on whether ϵ_1^p is increasing or decreasing with z. We write Eq. (3-121) in the form

$$\sigma_1 = \int_o^{z_o} E(z - z) \frac{d\epsilon_1^p}{dz'} \, dz' + \int_{z_o}^z E(z - z') \frac{d\epsilon_1^p}{dz'} \, dz' \tag{3-123}$$

or

$$\sigma_1 = R(z) + \int_{z_o}^z E(z - z') \frac{d\epsilon_1^p}{dz'} \, dz' \tag{3-124}$$
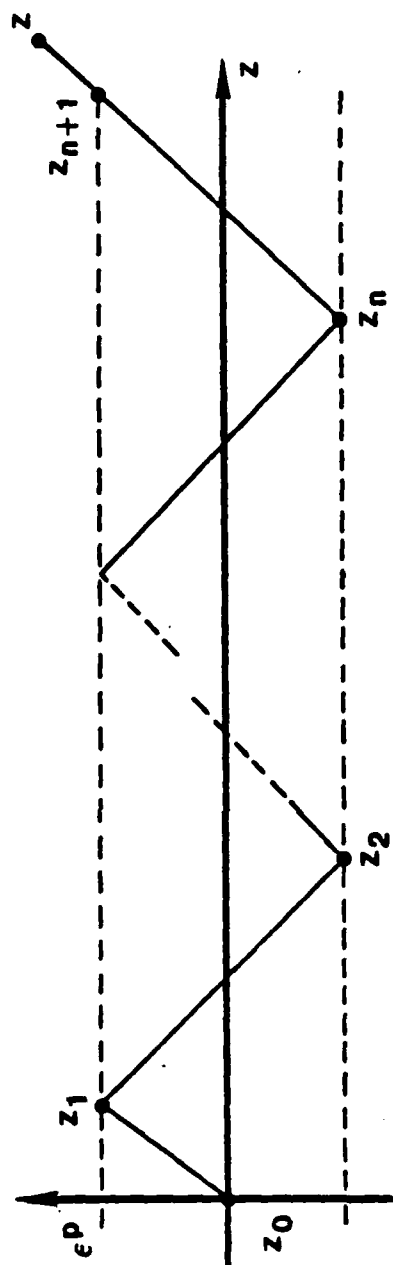
Figure 3.12   History of ϵ for a cyclic test from z_0 to z_n followed by a monotonic test from z_n to z.

where

$$R(z) = \int_0^{z_o} E(z - z')\, \frac{d\epsilon_1^p}{dz'}\, dz' \quad . \tag{3-125}$$

The function $R(z)$ enjoys the important property

$$\lim_{z \to \infty} R(z) = 0 \quad , \tag{3-126}$$

as will be shown later in this section.

The integral on the right-hand side of Eq.(3-124) may now be evaluated exactly so that

$$\sigma(z) = R(z) + M\left(z - z_o\right) - 2M\left(z - z_1\right) + 2M\left(z - z_2\right) \cdots$$

$$\cdots + 2M\left(z - z_n\right) \tag{3-127}$$

(n even)

where

$$M(z) = \int_0^z E(z')\, dz' \tag{3-128}$$

The stress response to this type of history is shown schematically in Figure 3.11.

We note for reference that

$$z_n = (n - 1)\Delta + \frac{\Delta}{2} + z_o \quad . \tag{3-129}$$

With this in mind, one may show by straightforward analysis, using Eq. (3-127) that

3-42

$$\sigma_{(z)} + \sigma_{(z+\Delta)} = 2M\left(z - z_n\right) + \hat{R} \tag{3-130}$$

where

$$\hat{R} = 2R(z) + M\left(z - z_o\right) - 2M\left(z - z_o + \frac{\Delta}{2}\right) + M\left(z - z_o\right) + \Delta \tag{3-131}$$

and

$$\lim_{z \to \infty} \hat{R}(z) = 0 \tag{3-132}$$

as will be shown presently. Thus in a steady-state cyclic test $(z \to \infty)$. it follows fro. Eq. (3-130) that

$$2M\left(z - z_n\right) = \sigma(z) + \sigma(z + \Delta) \tag{3-133}$$

The meaning of $\sigma(z)$ and $\sigma(z + \Delta)$ is shown in Figure 3.13. In view of the geometry of this figure it follows that if we set

$$z - z_n = \int_{z_n}^{z} d\epsilon^p \overset{\text{def}}{=} x \tag{3-134}$$

than

$$2M(x) = \sigma(x) + \sigma(x + \Delta) \tag{3-135}$$

Upon recalling the definition of $M(x)$ from Eq. (3-128). we infer from Eq. (3-135) that

$$2E(x) = \frac{d\sigma(x)}{dx} + \frac{d\sigma(x+\Delta)}{dx} \tag{3-136}$$

The geometric meaning of this equation is shown in Figure 3.13.

Thus the axia! cyclic strain test at constant plastic strain amplitude (or total strain amplitude. for that matter) provides a means of direct determination of the memory kernel $E(z)$ (and thus $\rho(z)$) - once steady state conditions have been reached. Of course the cyclic shear strain test will do just as well.
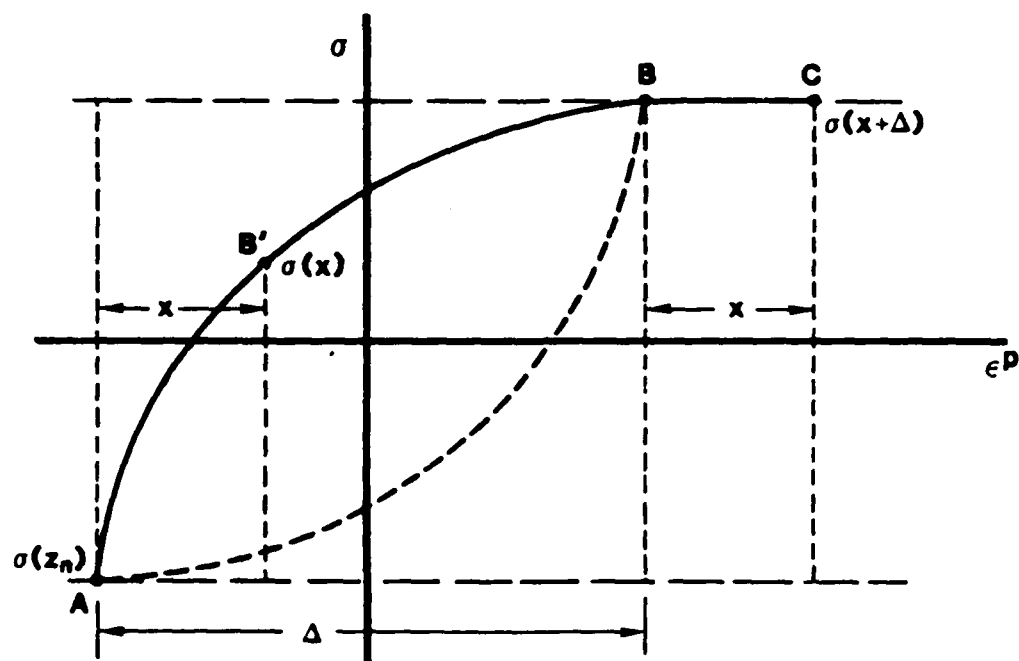
Figure 3.13   Stress-plastic strain relation in a steady-state cyclic test.

Shown in Figure 3.11 is the steady state hysteresis loop AB´BA and its extension BC generated by the plastic strain path from z_{n+1} to z. as shown in Figure 3.12. According to Eq. (3-136) the kernel function $E(x)$ is determined by the average of the slopes of the steady state hysteresis loop at B´ and C. Since the maximum range of x is Δ. $E(x)$ is determined for values of its argument x between zero and Δ.

Periodicity and Symmetry Characteristics of the Steady Response.

Of interest is the fact that if we set $z = z_n$ in Eq. (3-133) we obtain the important result

$$\sigma\left(z_n\right) = - \sigma\left(z_n + \Delta\right) \tag{3-137}$$

or. in the notation of Figure 3.12

$$\sigma_A = - \sigma_B \tag{3-138}$$

i.e.. steady state conditions prevail and the maximum value of the stress in tension is equal to that in compression. The more general periodicity condition

$$\sigma_n(x) = \sigma_{n+2}(x) \tag{3-139}$$

expressed in our present notation. can also be shown to hold as follows. In the limit of infinitely large z and as a result of Eqs. (3-127) and (3-129) one finds that

$$\sigma_n(z) = M\left[x + (n - 1)\Delta + \frac{\Delta}{2}\right] - 2M\left[(n - 1)\Delta + x\right]$$

$$\tag{3-140}$$

$$+ 2M[(n - 2) \Delta + x] - \ldots - 2M(x + \Delta) + 2M(x) .$$

Thus.

$$\sigma(x)_{n+2} - \sigma_n(x) = R_{n,n+2} \tag{3-141}$$

3-45

where

$$R_{n,n+2} = -2\{M[(n\Delta + x) + \Delta] - M(n\Delta + x)\}$$

$$+ M\left[\left(x + n\Delta + \frac{\Delta}{2}\right) - M\left[\left(x + n\Delta + \frac{\Delta}{2}\right) - \Delta\right]\right] \quad .$$

(3-142)

As we shall show presently

$$\lim_{n \to \infty} R_{n,n+2} = 0$$

(3-143)

and hence. Eq. (3-139) is valid.

Thus in the limit of large n the theory does indeed predict observed periodic steady state hysteresis loops with the attendant symmetry properties pertaining to tension and compression.

Convexity of M(z): Limit Properties of Series (3-127) and Related Series.

The function M(z) is convex in the sense that

$$M(z + a) - M(z) < aE(z)$$

(3-144)

for all positive finite a and all positive z. As is easily shown upon use of Eq. (3-128). this is a consequence of the fact that E(z). which is the slope of M(z). has the property

$$E(z + a) < E(z)$$

(3-145)

Specifically. it follows from the definition of M(z) that

$$M(z + a) - M(z) = \int_{z}^{z+a} E(z')dz'$$

(3-146)

However

$$\int_{z}^{z+a} E(z')dz' < aE(z)$$

(3-147)

3-46

as a result of Eq. (3-145). Hence condition (3-144) follows. The function $E(z)$ also enjoys the property

$$\lim_{z \to \infty} E(z) = 0 \qquad (3\text{-}148)$$

It now follows from Ineq. (3-144) that

$$\lim_{z \to \infty} \{M(z + a) - M(z)\} = 0 \qquad (3\text{-}149)$$

Conditions (3-145) to (3-149) will prove extremely useful in the subsequent analysis. For instance Eq. (3-133) is predicated on the validity of Eq. (3-132). To prove this relation we first show that

$$\lim_{z \to \infty} R(z) = 0 \qquad (3\text{-}150)$$

In view of Eq. (3-125)

$$R(z) \leq \int_0^{z_0} E(z - z') f(z') \left| \frac{d\epsilon^p}{dz'} \right| dz \qquad (3\text{-}151)$$

or

$$R(z) \leq F_s(z_0) \int_0^{z_0} E(z - z') dz' \quad , \qquad (3\text{-}152)$$

since $|d\epsilon^p/dz'| = 1$ and $F_s(z)$ is a monotonically increasing function up to $z - z_0$ and $F_s(z) = F_s(z_0)$: $z \geq z_0$. Thus, in view of Eq. (3-152)

$$R(z) \leq F_s(z_0)\left\{M(z) - M(z - z_0)\right\} \qquad (3\text{-}153)$$

where use was made of Eq. (3-128). We now set $z - z_0 = y$ and note that y tends to infinity as z tends to infinity. It follows from Eq. (3-153) that

3-47

$$R(z) \leq F_s(z_o)\{M(y + a) - M(y)\} \tag{3-154}$$

Hence, in view of Eq. (3-149)

$$\lim_{z \to \infty} R(z) = 0 \tag{3-155}$$

If we now write $\hat{R}$ in the form

$$\hat{R} = 2R + \left\{M\left(z - z_o + \Delta\right) - M\left[\left(z - z_o + \Delta\right) - \frac{\Delta}{2}\right]\right\} \tag{3-156}$$

$$- \left\{M\left(z - z_o + \frac{\Delta}{2}\right) - M\left(z - z_o - \frac{\Delta}{2}\right)\right\}$$

it follows from Eqs. (3-149) and (3-155) that

$$\lim_{z \to \infty} \hat{R} = 0 \tag{3-157}$$

Thus Eq. (3-133) has been validated.

A similar argument shows that Eq. (3-143) is also true and hence the periodicity condition (3-139), which establishes the existence of a steady (periodic) response for infinitely large z, has also been proved.

We pointed out earlier in this section that the constant cyclic strain amplitude test and the constant plastic strain amplitude test are equivalent. In the steady-state, either of these tests is a suitable (standard) test for the determination of the kernel function $\rho(z)$.

3.4.2 The Hardening Function $F_s(z)$.

Here we give a rigorous method for determining the material function $F_s(\varsigma)$ from experimental data when $F_s(\varsigma)$ is a slowly varying function in a sense to be defined subsequently. Consider, specifically .the uniaxial test with a loading-unloading history. The test is illustrated schematically in Figure 3.14 where the axial stress σ_1 is plotted versus the axial strain ϵ. The stress σ_1 is given by the relation
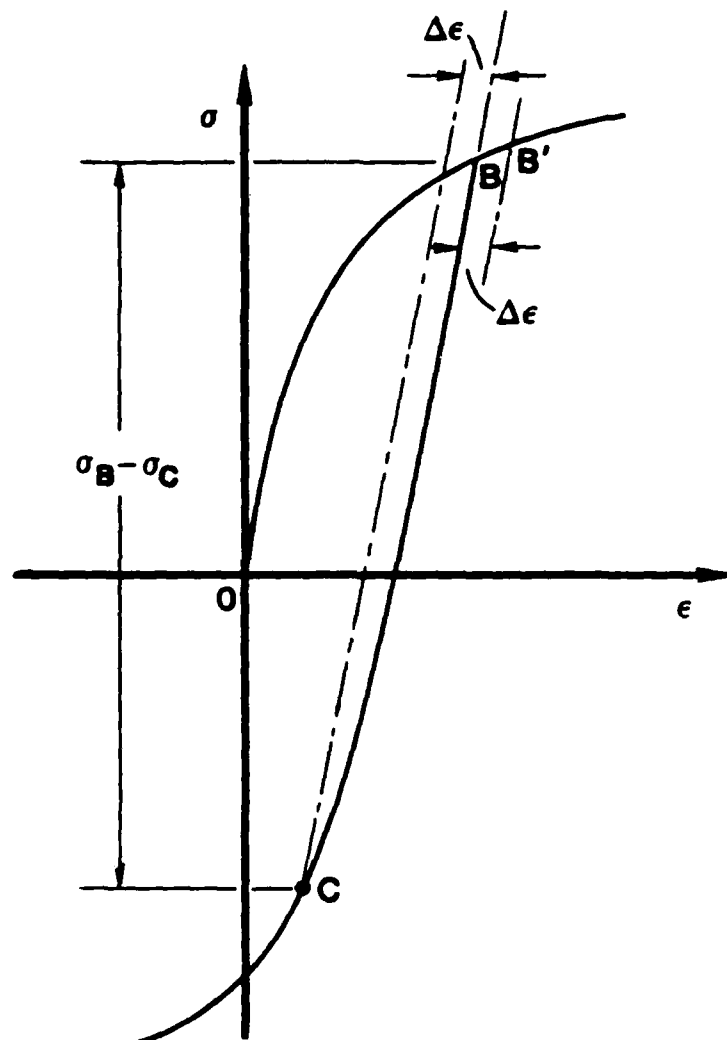
Figure 3.14   Determination of $F_s(z)$.

$$\sigma_1 = \int_0^z E(z - z')\frac{d\epsilon_1^p}{dz'}\, dz' \tag{3-158}$$

where

$$2E(z) = 3\rho(z) \tag{3-159}$$

$$d\varsigma = \left|d\epsilon^p\right| \tag{3-160}$$

$$dz = \frac{d\varsigma}{F_s(\varsigma)} \tag{3-161}$$

We wish to calculate the stress at points B and C where $\Delta\epsilon_1^p$ is an increment, not necessarily infinitesimal, in the plastic strain. Then in view of Eqs. (3-158), (3-160) and (3-161),

$$\sigma_{1B} = \int_0^{z_B} E(z_B - z')F_s^*(z')dz' \tag{3-162}$$

where z_B is the value of z at point B and

$$F_s^*(z) = F_s(\varsigma(z)) \tag{3-163}$$

The stress σ_1 at C is calculated using again Eqs. (3-158), (3-160), (3-161). Thus

$$\sigma_{1C} = \int_0^{z_B} E(z_B + \Delta z_B - z')\frac{d\epsilon^p}{dz'}\, dz'$$

$$+ \int_{z_B}^{z_B + \Delta z_B} E(z_B + \Delta z_B - z')\frac{d\epsilon^p}{dz'}dz' \ , \tag{3-164}$$

where use was made of the relation $z_C = z_B + \Delta z_B$. Note that in the interval $0 < z' < z_B$, $d\epsilon^p/dz' = +1$, whereas in the interval $z_B < z' < z_C$, $d\epsilon^p/dz' = -1$. It follows that

$$\sigma_{1C} = \int_0^{z_B} E(z_B + \Delta z_B - z') \, F_s^*(z') \, dz'$$

$$- \int_{z_B}^{z_B + \Delta z_B} E(z_B + \Delta z_B - z') F_s^*(z') \, dz' \quad .$$

(3-165)

In regard to the second term on the right-hand side of Eq. (3-164), note that in view of the mean value theorem we can write

$$\int_{z_B}^{z_B + \Delta z_B} E(z_B + \Delta z_B - z') F_s^*(z') \, dz' = F_s^*(\bar{z}_B) M(\Delta z_B)$$

(3-166)

where the function $M(z)$ is defined by the integral (see Eq. (3-128)),

$$M(z) = \int_0^z E(z - z') \, dz = \int_0^z E(z') \, dz'$$

(3-167)

and $z_B \leq \bar{z}_B \leq z_C$.

Let us now evaluate the first term on the right-hand side of Eq. (3-165). First we note that

$$\int_0^{z_B} E(z_B + \Delta z_B - z')F_s^*(z')dz'$$

$$= \int_0^{z_B + \Delta z_B} E(z_B + \Delta z_B - z')F_s^*(z')dz' \qquad (3\text{-}168)$$

$$- \int_{z_B}^{z_B + \Delta z_B} E(z_B + \Delta z_B - z')F_s^*(z')dz'$$

or

$$\int_0^{z_B} E(z_B + \Delta z_b - z)F_s^*(z')dz' = \sigma_B' - F_s^*(\bar{z}_B)M(\Delta z_B) \ , \qquad (3\text{-}169)$$

where the physical meaning of σ_B' is illustrated in Figure 3.14. In view of Eqs. (3-164), (3-165), and (3-169)

$$\sigma_{1C} = \sigma_{1B}' - 2F_s^*(\bar{z}_B)M(\Delta z_B) \ . \qquad (3\text{-}170)$$

Hence:

$$F_s^*(\bar{z}_B) = \frac{\sigma_{1B}' - \sigma_1}{2M(\Delta z_B)} \qquad (3\text{-}171)$$

We remark that this is an exact result irrespective of the magnitude of Δz_B. <u>A generalization of Eq. (3-153) applicable to any reversal point is given below without proof, which we leave to the reader.</u>

$$F_s^*(\bar{z}_B) = \frac{|\sigma_{1B}' - \sigma_1|}{2M(\Delta z_B)} \qquad (3\text{-}172)$$

We wish to use the preceding equation for the experimental determination of $F_s^*(z_B)$. If we let Δz_B be infinitesimal and if $F_s(z)$ is a slowly varying function (see discussion below) then

3-52

$$F_s^*(\bar{z}_B) \overset{\bullet}{=} F_s^*(z_B) \quad , \tag{3-173}$$

$$M(\Delta z_B) \overset{\bullet}{=} M\left(\left|\Delta\epsilon^P\right|/F_s^*(z_B)\right) \quad , \tag{3-174}$$

$$\sigma_{1B}' \overset{\bullet}{=} \sigma_{1B} \quad , \tag{3-175}$$

so that Eq. (3-172) becomes

$$F_s^*(z_B) \overset{\bullet}{=} \frac{\sigma_{1B} - \sigma_{1C}}{2M\left(\dfrac{\left|\Delta\epsilon^P\right|}{F_s^*(z_B)}\right)} \tag{3-176}$$

Furthermore since $F_s^*(z_B) = F_s(\varsigma_B)$. Eq. (3-176) determines the value of the function $F_s(\varsigma)$ at the point B. i.e., at $\varsigma = \varsigma_B$. The error associated with these approximations will be discussed below.

To solve for $F_s^*(z_B)$ it is necessary to know the functional form of $M(z)$. We shall demonstrate the procedure for determining of the form of the function $M(z)$ in the vicinity of $z = 0$. using the experimental data shown in Figure 3.8, observed by Dafalias and Popov [3.10] on grade 60 steel. In Figure 3.15 we show a plot. shown in open circles, of $\log\left|\sigma_{1b} - \sigma_{1c}\right|$ versus $\log\left|\Delta\epsilon^P\right|$ for point 1 of Figure 3.8. It shows a linear relation between the respective quantities. Such a relation is typical of reversal points.

On the basis of this finding. $M(z)$ must be a power function of its argument of the form

$$M(z) = M_o z^\beta \tag{3-177}$$

in the vicinity of $z = 0$. This conclusion follows directly from Eq. (3-176). which leads to the logarithmic relation

$$\log\left(\sigma_{1b} - \sigma_{1c}\right) = \log\left(2F_s^B\right) + \log\left[M\left(\left|\Delta\epsilon^P\right|/F_s^B\right)\right] \tag{3-177a}$$
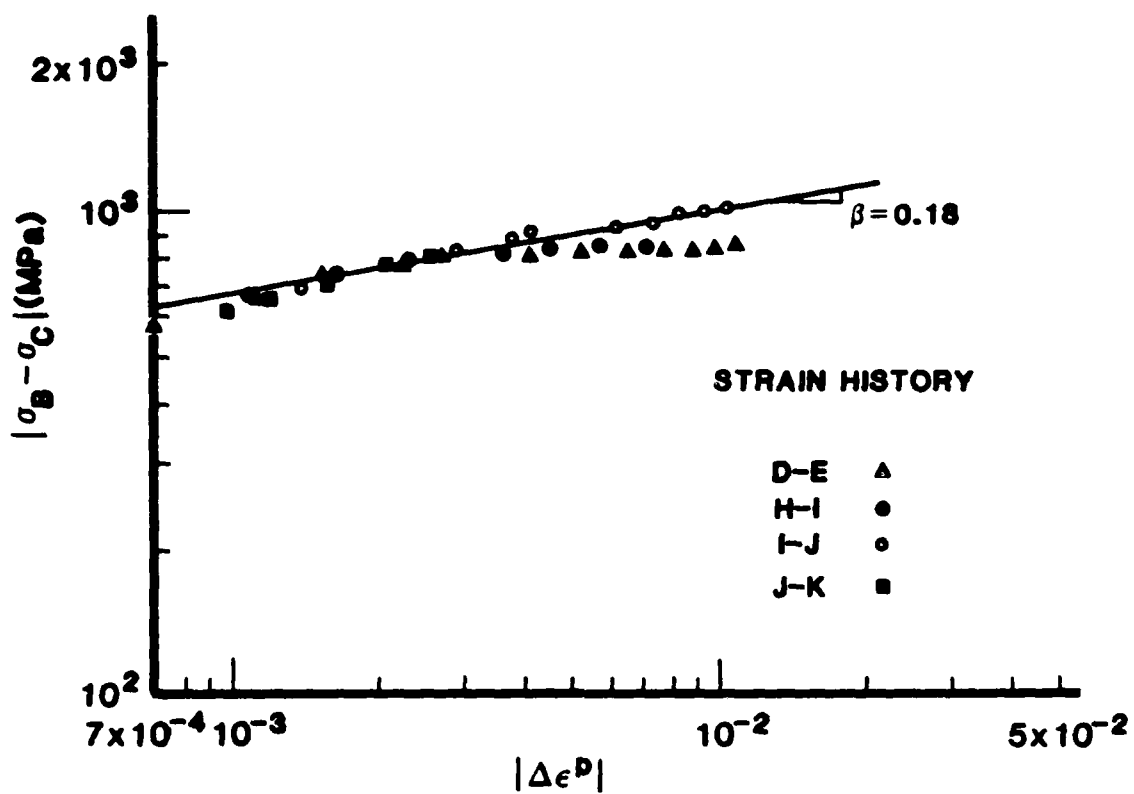
Figure 3.15   Plot of $\log|\sigma_b - \sigma_c|$ versus $\log|\Delta\epsilon^P|$ for Grade 60 steel.

where F_s^B is identically equal to $F_s^B = F_s(z_B)$. Evidently, if the relation between $\log(\sigma_{1b} - \sigma_{1c})$ and $\log|\Delta\epsilon^P|$ is linear, M must be a power function of $|\Delta\epsilon^P|/F_s^B$. Furthermore, since the value of the latter lies in the vicinity of zero, M is thereby determined for values of its argument in the vicinity of zero.

In consequence, and as a result of Eq. (3-167), E(z) is also a power function. Specifically

$$E(z) = E_o z^{-\alpha} \quad , \tag{3-178}$$

where $\alpha = 1 - \beta$ and $E_0 = (1 - \alpha)M_o$.

Discussion of Solution of Equation (3-176).

We discuss the solution of Eq. (3-176) in the vicinity of $z = o$ when the material function E(z) is given by the relation $E(z) = E_o/z^\alpha$. In this case, following Eq. (3-172), (in the vicinity of $z = o$)

$$M(z) = \frac{E_o}{1 - \alpha} z^{1-\alpha} \quad . \tag{3-179}$$

Using this expression, Eq. (3-176) may be solved explicitly for $F_s^*(z_B)$ to give

$$F_{sB} = F_s^*(z_B) = F_s(S_B) = \left\{ \frac{|\sigma_{1B} - \sigma_{1C}|}{2M\left(\left|\Delta\epsilon_1^P\right|\right)} \right\}^{1/\alpha} \tag{3-180}$$

More specifically using Eq. (3-177)

$$F_{sB}^\alpha = \frac{|\sigma_{1B} - \sigma_{1C}|}{\left(\dfrac{2E_o}{1 - \alpha}\right)\left|\Delta\epsilon_1^P\right|^{1-\alpha}} \quad . \tag{3-181}$$

The logarithmic form of the above equation, given below,

$$\log|\sigma_{1B} - \sigma_{1C}| = \log\left(\frac{2E_o}{1 - \alpha}F_{sB}^\alpha\right) + (1 - \alpha)\log\left|\Delta\epsilon_1^P\right| \quad , \tag{3-182}$$

3-55

is useful in determining both the parameter α and the function of F_{sB} to within a multiplicative constant. In effect, a plot of log $|\sigma_{1B} - \sigma_{1C}|$ versus $\log|\Delta\epsilon_1^P|$ gives a straight line with slope $(1 - \alpha)$ and intercept log $(2E_o/1 - \alpha)$ at $|\Delta\epsilon^P| = 1$. Such a plot is shown in Figure 3.15 for various reversal points in the case of Grade 60 steel. Although not shown, there is a great deal of scatter for $|\Delta\epsilon^P| < 7 \times 10^{-4}$. However, in the range $7 \times 10^{-4} < |\Delta\epsilon^P| < 10^{-2}$, the experimental points lie consistently close to a straight line with a slope $\beta = 0.18$. The fact that all points lie virtually on the same line implies that F_s is a constant in the range of z covered by the experiment.

We finally make a crucial observation. If the same value of $\Delta\epsilon_1^P$ is used at <u>all</u> reversal points chosen for the determination of F_s, then the denominator in Eq. (3-181) is a constant. Thus if $\Delta\sigma_1$ is the stress drop at <u>any</u> reversal point following the construction in Figure 3.14, then in view of Eq. (3-181)

$$F_s(z) = F_{so}\left\{\Delta\sigma_1(z)\right\}^{1/\alpha} , \qquad (3\text{-}183)$$

where F_{so} is a normalization constant to be chosen at one's convenience. Equation (3-183) gives a simple and powerful result for determining the function $F_s(z)$.

Error Associated with Equation (3-176).

Here we give an estimate of the error associated with Eq. (3-176) when M(z) is given by Eq. (3-177). The calculation is lengthy but straightforward. Basically the relation

$$F_s^*(z') = F_{sB}^* + \hat{F}_{sB}^*(z' - z_B) + 0\left[(z' - z)\right]^2 \qquad (3\text{-}184)$$

in the range $z_B < z' < z_B + \Delta z_B$, and the integral form of Eq. (3-8a) wherein

$$\varsigma = \int_o^z F_s^*(z')dz' , \qquad (3\text{-}185)$$

3-56

are used in Eq. (3-166) where

$$\hat{F}_{sB} = \frac{dF_s^*(z)}{dz}\bigg|_{z=z_B} \tag{3-186}$$

The resulting relation for the error ϵ is

$$(1 + \epsilon)F_{sB}^* = \frac{|\sigma_{1B} - \sigma_{1C}|}{2M\left(\frac{|\Delta\epsilon_1^p|}{F_{sB}^*}\right)} \quad , \tag{3-187}$$

where

$$\epsilon = \frac{\alpha(3 - \alpha)\Delta F_{sB}^*}{2(2 - \alpha)F_{sB}^*} + O\left(\frac{\Delta F_{sB}^*}{F_{sB}^*}\right)^2 \tag{3-188}$$

Thus ϵ is at most of $O(\Delta F_{sB}^*/F_{sB}^*)$.

3.5 Comparison Between Theory and Experiment for Multi-Dimensional Cases.

3.5.1 A Copper Plate with Two Edge Cracks.

The Experiment.

The truly predictive capability of the theory was put to the test by means of an experiment which was described in Refs. [3.11] and [3.12]. but which we shall discuss here. because of its importance in establishing the theory as a predictive instrument in the mechanical response of metals at room temperature.

The experiment consisted of subjecting a rectangular copper plate with two symmetrically placed edge cracks to reversed loading in a manner shown in Figure 3.16. The plate was machined from 2.54 cm thick OFHC copper (8.12 cm x 9.14 cm). Basically two tests were performed. In Test 1 strain gauges were attached to the specimen in the manner shown in Figure(3.17a) and the strain ϵ_y (in the direction of the applied load) was measured at the indicated stations along the notch line. The applied (tensile) stress was increased from zero to 36.8 MPa. at which point strain measurements were made. The stress was then
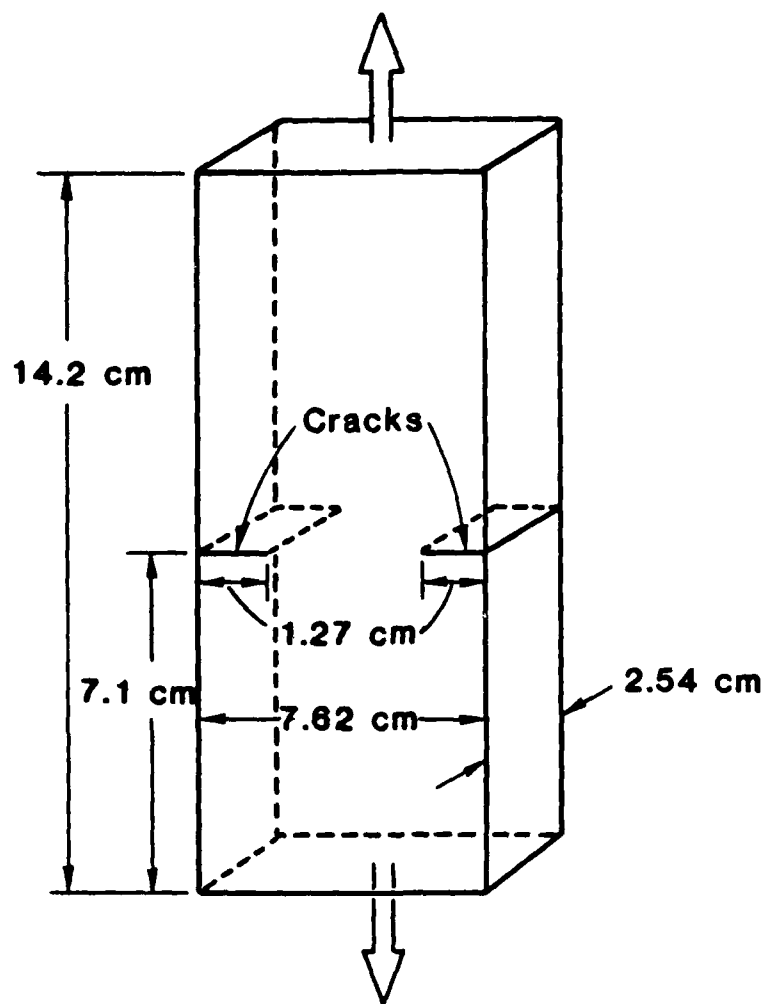
Figure 3.16. Description of copper plate used in experiments.
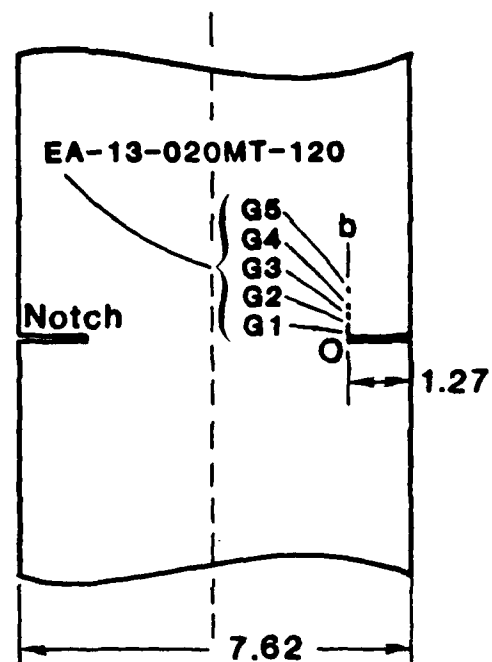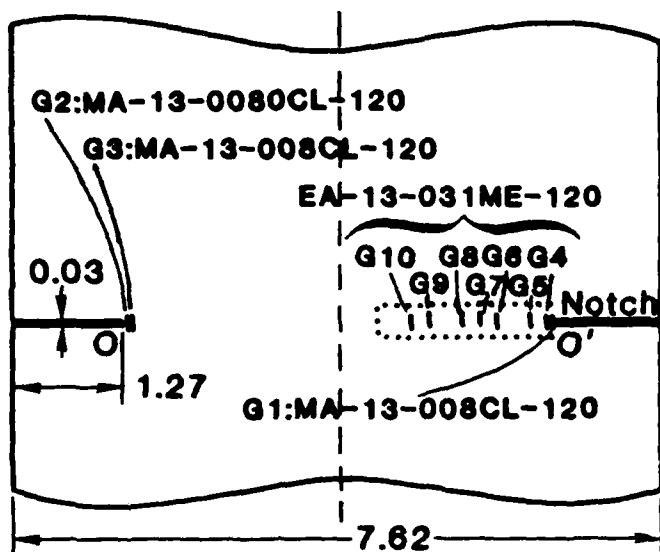
(a) Horizontally oriented gages

(b) Vertically oriented gages.

Figure 3.17. Location of strain gages.

decreased to zero where strains at this value of applied stress were also measured. At this point a compressive stress was applied, increasing from zero to a value of 36.8 MPa. Strain measurements were also made at this value of the applied stress. In Test 2 the strain gauges were mounted in the manner shown in Figure(3.17b). In this case the applied (tensile) stress was increased from zero to 23 MPa, where strain measurements were made. The applied stress was then decreased to zero. At this point a compressive stress was applied, increasing from zero to a value of 23 MPa where strain measurements were again made. The applied compressive stress was then decreased to zero, whereupon a tensile stress was applied, increasing from zero to a value of 23 MPa where again strain measurements were made. Details of the experimental procedure are given in Refs. [3.11] and [3.12].

Analysis.

Strains at the points of measurement were calculated using Eq. (3-12) to Eq. (3-16) in conjunction with a finite element program which we proceed to outline very briefly.

Equations (3-12) to (3-16) lend themselves to a differential relation between stress and strain. Specifically in the case where the infinitely large value $\rho(0)$ is approximated by a suitably large value, as is done in this analysis, one may differentiate Eq. (3-12) to obtain the following differential form of the constitutive equation:

$$d\underset{\sim}{s} = 2\rho(0)d\underset{\sim}{e}^{p} + 2\underset{\sim}{h}(z)dz \tag{3-189}$$

Equation (3-189), in conjunction with Eqs. (3-12) to (3-14) then gives the following equations, suitable for a finite element program:

$$d\underset{\sim}{s} = 2\hat{\mu}\ d\underset{\sim}{e} + \frac{\underset{\sim}{h}(z)}{\rho(0)}\ dz \tag{3-190}$$

$$d\underset{\sim}{\sigma} = 3K\ d\epsilon_{KK}\ \underset{\sim}{\ell} + 2\hat{\mu}\ d\underset{\sim}{e} + \frac{2\hat{\mu}}{\rho(0)}\ \underset{\sim}{h}\ dz \tag{3-191}$$

where

$$\hat{\mu} = \mu/\left(1 + \frac{\mu}{\rho(0)}\right) \tag{3-192}$$

Consider a material domain which is suitably divided into m elements (microdomains) giving rise to n nodes. The deformation field is thus described by 3n displacements and the stress field by 3n forces. The strain field in each element is assumed uniform, and so is the stress field.

Equation (3-191) may be written for any one particular element in vector form as follows:

$$d\{\sigma\} = [k]d\{\epsilon\} + \frac{2\hat{\mu}}{\rho(0)} \{h\}\, dz \tag{3-193}$$

Following Ref. [3.13], the statically equivalent forces $d\{p\}$ at the nodes of the element are related to $d\{\sigma\}$ by the relation:

$$d\{p\} = [b]^T d\{\sigma\} . \tag{3-194}$$

while the strains $d\{\epsilon\}$ in the element are related to the displacements $d\{u\}$ at the nodes of the element by the relation:

$$d\{\epsilon\} = [b]d\{u\} \tag{3-195}$$

It follows from Eqs. (3-193) to (3-195) that:

$$d\{p\} = [K]_\Delta\, d\{u\} + H_\Delta\, dz \tag{3-196}$$

where

$$[K]_\Delta = [b]^T\, [k][b] \tag{3-197}$$

and

$$[H]_\Delta = \frac{2\hat{\mu}}{\rho(0)}\, [b]^T\{h\} \tag{3-198}$$

Here, the suffix Δ specifies a particular microdomain. In the case at hand the microdomains are triangles.

If we now sum Eq. (3-196) over all elements, the following global relation is obtained:

$$d\{p\} = [K]\, d\{q\} + [H]d\{z\} . \tag{3-199}$$

3-61

where $\{p\}$ are the loads applied to the nodes of the material domain. $\{q\}$ are the corresponding displacements at the nodes. and $d\{z\}$ is the vector of intrinsic time increments. each pertaining to the appropriate microdomain in a three-dimensional domain. $[K]$ has dimensions $(3n \times 3n)$ but $[H]$ has dimensions $(3n \times m)$. Thus dz plays the role of a plasticity induced body force. In a two-dimensional domain of interest here. $[K]$ has dimensions $(2n \times 2n)$ but $[H]$ has dimensions $(2n \times m)$.

Solution of Eq. (3-199).

The difficulty in solving Eq. (3-199) lies in the fact that at each step in the incremental process the vector $d\{z\}$ is not known. Equation (3-199) is thus solved through iteration by initially setting $d\{z\}_n = d\{z\}_{n-1}$. Equation (3-199)is now solved in principle by simple inversion of the matrix $[K]$. or in practice. by solving the set of linear simultaneous equations in $d\{q\}$. giving the first approximation to $d\{q\}$. Thus $d\{u\}$ are now known and thus $d\{\epsilon\}$ and hence $d\underset{\sim}{\epsilon}$ may now be found using Eq. (3-195). Also $d\{\sigma\}$ and hence $d\underset{\sim}{s}$ may be found using Eq. (3-193). Thus $d\underset{\sim}{\epsilon}^p$ is now known in view of Eq. (3-194) and thus the "new" dz for each microdomain may be calculated using Eq. (3-15) and (3-14). The "new" values of $d\{z\}$ are then used in Eq. (3-199) to determine the second approximation to $d\{q\}$ by solving Eq. (3-199) anew. The procedure is continued until two successive approximations to $d\{q\}$ differ by an acceptable margin. Exceptions are points of unloading (in the sense of the externally applied stress) when the initial values of $d\{z\}$ are taken to be equal to zero.

Comparison Between Theory and Experiment.

A comparison between the measured and calculated values of the strains is given in Figures 3.18 to 3.23. Given the complexity of the experiment and of the inherent constitutive response and the fact that the material functions $\rho(z)$ and $f(\varsigma)$ were measured by an independent experiment in a round rod. the agreement between theory and experiment is truly remarkable.

3.5.2   **A Brass Tube Subjected to a Homogeneous Two-Dimensional, Non-Proportional Stress Field.   The Ohashi Experiments.**

The Experiment.

In a series of studies. Ohashi [3.14-3.16] and his collaborators investigated the stress response of brass to non-proportional strain paths in the deviatoric strain space $\underset{\sim}{e}$. In Figure 3.19 we illustrate a group of experiments which are performed along strain paths in the $(2e_{12}/\sqrt{3}.e_{11})$ space. The generic history consists of extending a thin tube in the axial direction until a certain value of e_{11} is reached. With e_{11} held constant at this value the tube was then twisted until a certain value of the shear strain e_{12} was reached. With e_{12} held constant at this value the tube was then either extended further. or the existing axial strain was reduced to zero.

The stress state along these paths was expressed in terms of a path length ℓ where:

$$d\ell^2 = \frac{2}{3} d\underset{\sim}{e} \cdot d\underset{\sim}{e} \tag{3-200}$$

Precise measurements showed that the stress response has a strong dependence on the history of the previous plastic deformation. Specifically. in reference to the paths D-G. it was found that there is a decrease of the equivalent stress $(\underset{\sim}{s} \cdot \underset{\sim}{s})^{1/2}$ with respect to the length ℓ. brought about by a rapid decrease of the axial stress while the tube was twisting under constant axial strain.

Ohashi and his associates regarded this phenomenon as a manifestation of some sort of inherent instability. In our terminology this is stress relaxation with respect to the intrinsic time ς. It means that elastoplastic materials. during specific strain histories. evince stress relaxation with respect to ς in very much the same fashion as viscoelastic materials do with respect to Newtonian time.

We shall show that the constitutive equation of the functional type proposed in Section 2.2.4 is appropriate for describing material behavior in the presence of complex strain paths that cause strong history effects. The phenomenon of fading memory discussed in previous references (see for instance. Ref. [2.19]) is evident in Figure 3.20 where the axial stress response curves converge asymptotically to a single curve which is independent of the intervening torsional strain history. Quantitatively the degree of fading memory is determined by the rate of decay of the kernel function $\rho(z)$.
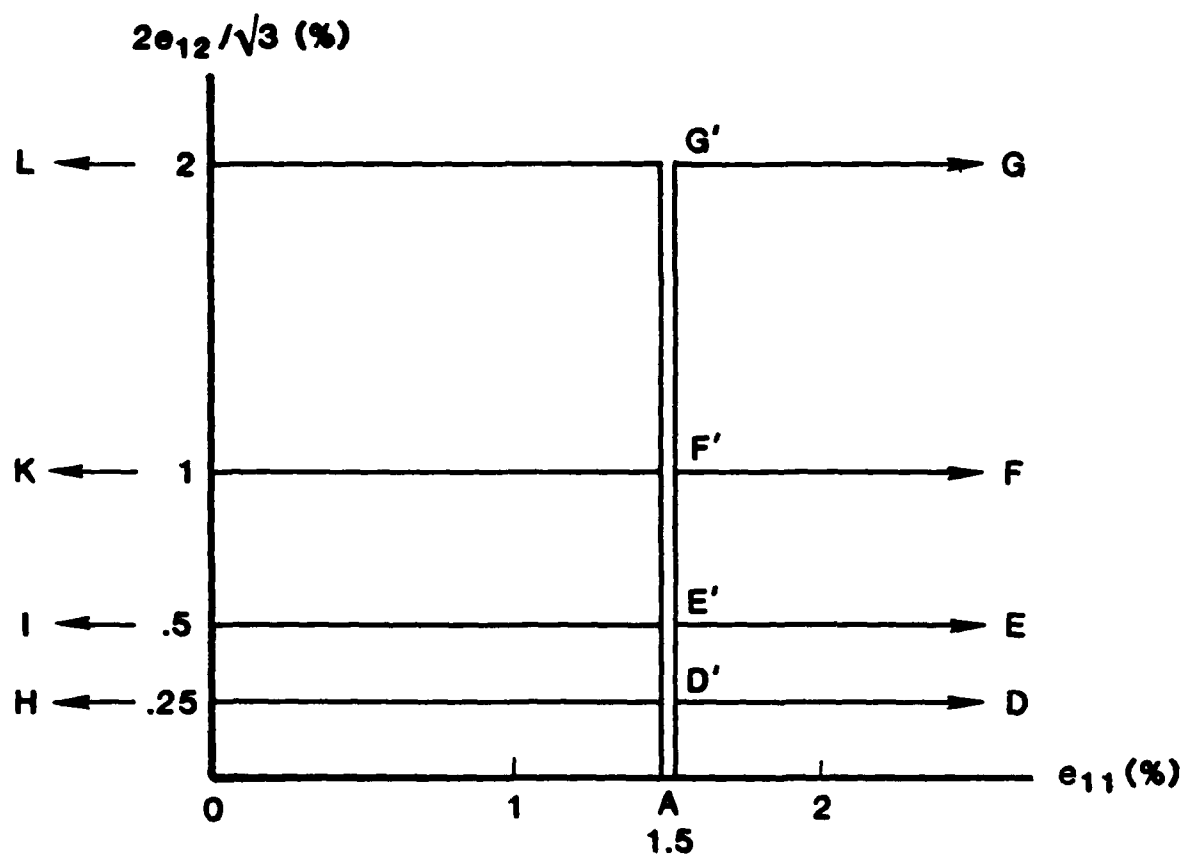
Figure 3.19.   Map of experimental strain paths.
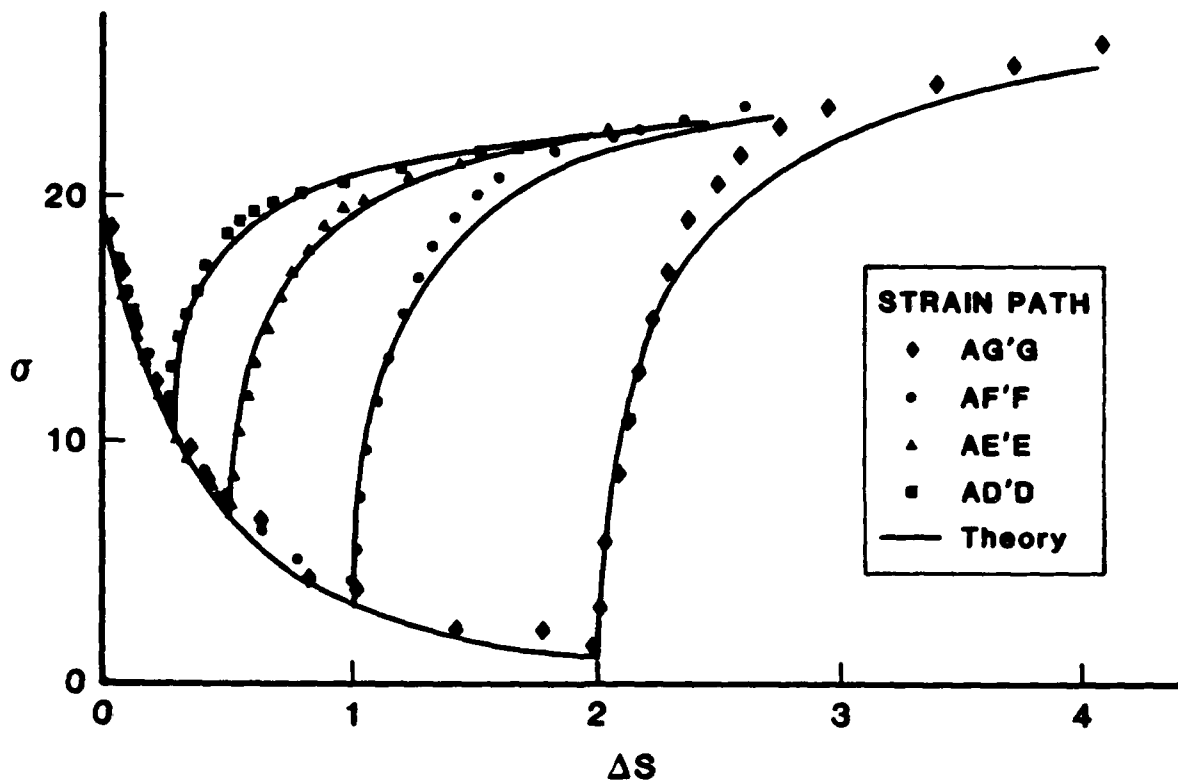
Figure 3.20   Axial stress response corresponding to the strain path indicated.
                Type: tension-shear-increased tension.

Because the appropriate cyclic experiment for the determination of the functions $\rho(z)$ and $f(\varsigma)$ was not performed by Ohashi, these functions were determined from the data by an iterative, laborious process which we will not describe here. Suffice it to say that the functions so found are of the form:

$$f(\varsigma) = \left[1 + c_o \varsigma\right]^{d_o} \tag{3-201}$$

$$\rho(z) = \rho_o \frac{e^{-kz}}{z^\alpha} \tag{3-202}$$

where

$$\rho_o = 15 \frac{kg}{mm^2} \ , \quad \alpha = 0.70, \ k = 180$$

$$c_o = 90 \ , \ d_o = 0.26 \quad .$$

Discussion of the Comparison Between Theory and Experiment.

(a) Paths, D, E, F, and G.

Figures 3.20 and 3.21 show, respectively, how the axial stress σ and the shear stress $\sqrt{3} \, S_{12}$ vary with the path length ℓ, following the first corner of a strain path. Points signify experimental data while solid lines depict calculated results based upon the endochronic model. Excellent representation of the material response is demonstrated. The axial stress relaxation following shearing at constant axial strain is predicted with remarkable accuracy.

(b) Paths H, I, K and L.

Figures 3.22 and 3.23 show relations corresponding to the paths H through L. In these figures, the points correspond to Ohashi's data and the solid lines to calculated results based on the endochronic model. In Figure 3.22 the calculated stresses are in conformity with experimental observations. In Figure 3.23 corresponding relations are shown for the shear stress response. Agreement is again good except that the calculated stresses relax faster than their experimentally observed
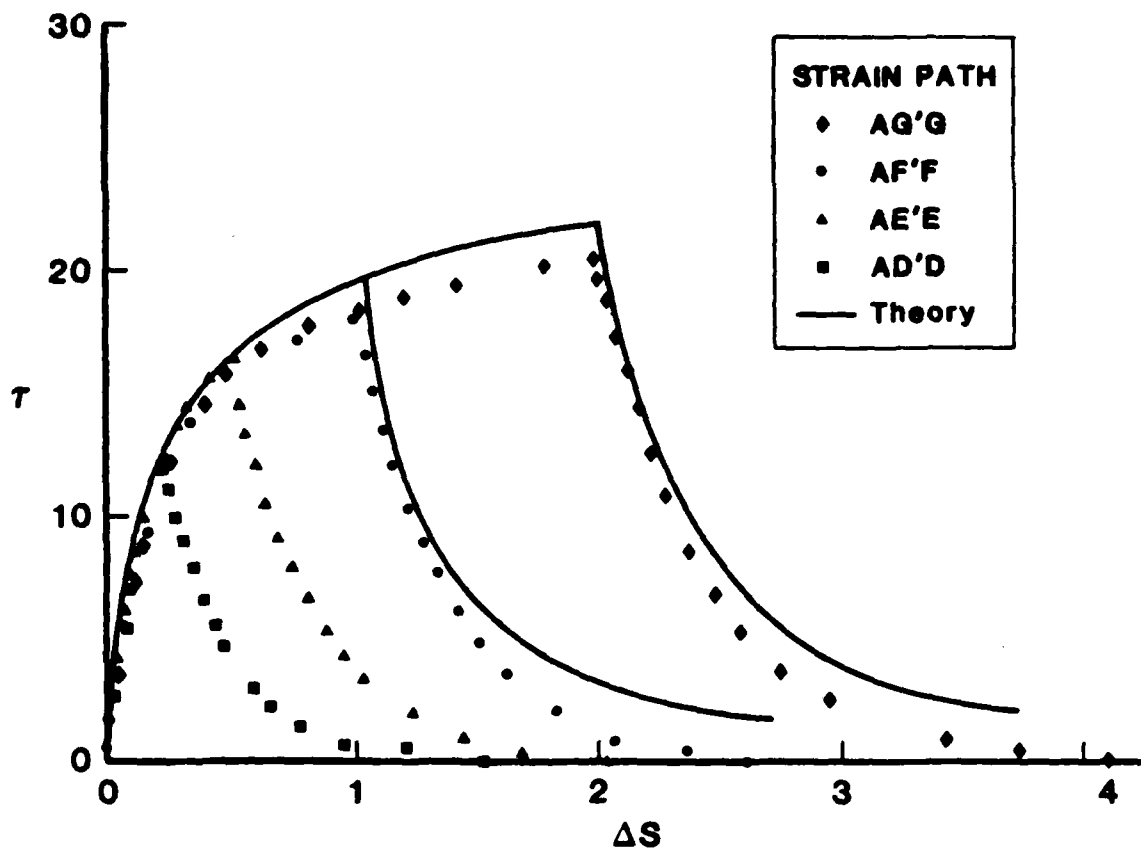
Figure 3.21.   Shear stress response corresponding to the strain path indicated.
Type: tension-shear-increased tension.
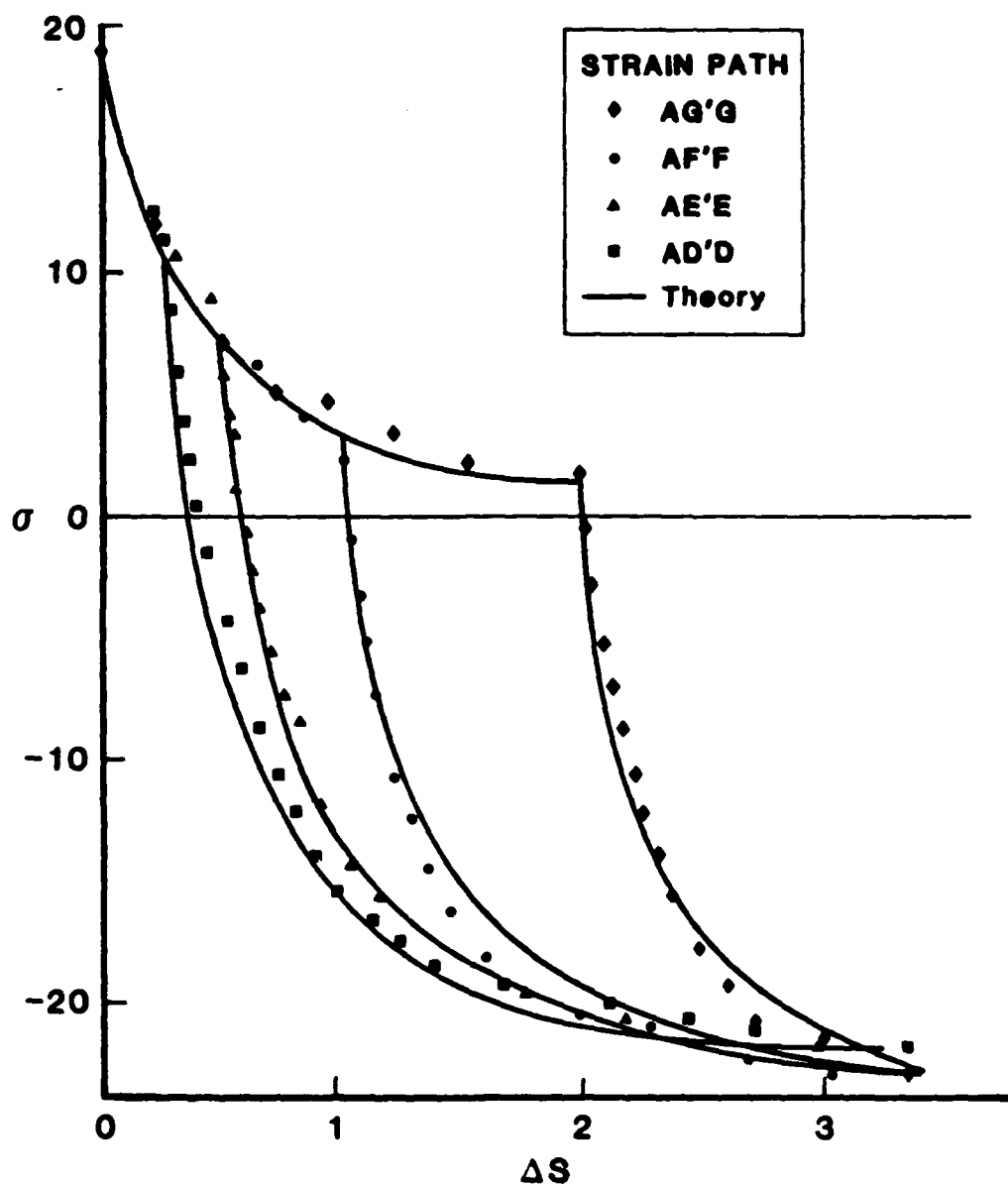
Figure 3.22. Axial stress corresponding to the strain path indicated. Type: tension-shear-reduced tension.
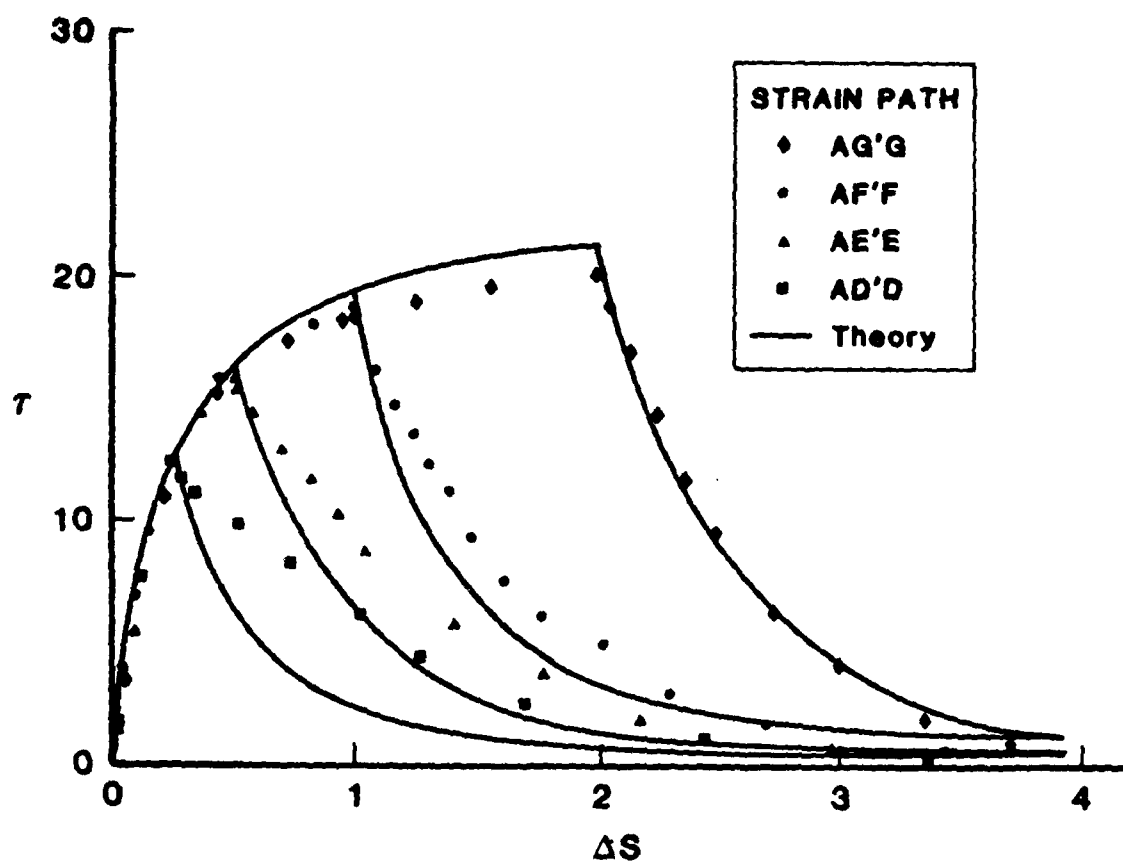
Figure 3.23. Shear stress response corresponding to the strain path indicated. Type: tension-shear-reduced tension.

counterparts at low values of the stresses. At higher stresses the agreement between observed and calculated values is again excellent. We suspect that the discrepancies are due to the presence of initial shear strain. However. this hypothesis needs to be investigated further.

3.6 Endochronic Plasticity with a Yield Surface.

3.6.1 General Considerations.

In Chapter 2 we dealt with the case of constitutive equations which have their basis in irreversible thermodynamics with a finite number of internal variables. Specifically. insofar as the deviatoric response is concerned. the resulting constitutive relation was given by Eq. (2-80). It was pointed out at the end of that section that this equation is. in fact. a special case of the more general equation:

$$\underset{\sim}{s} = \int_0^{z_s} \rho(z_s - z') \frac{d\underset{\sim}{e}}{dz'} dz' , \qquad (3\text{-}203)$$

where ρ is of the form

$$\rho = s_0 \delta(z_s) + \rho_1(z_s) \qquad (3\text{-}204)$$

and $\rho_1(0)$ is finite. This result was derived rigorously in Ref. [2.14]. where it was shown that Eq. (3-203) gives rise to a theory of plasticity with a yield surface. In addition it gives. as corollary. the constitutive equation that governs the motion of the center of the yield surface or. in other words. it gives a law for the evolution of the back stress. In this section we shall derive these results beginning with Eq. (2-80) which is repeated below for completeness:

$$\underset{\sim}{s} = s_0 \frac{d\underset{\sim}{e}^p}{dz_s} + \int_0^{z_s} \rho_1(z_s - z') \frac{d\underset{\sim}{e}^p}{dz'} dz' . \qquad (3\text{-}205)$$

Let us also recall the pertinent relations that apply to plastically incompressible solids:

$$d\varsigma = \left|\left|d\underset{\sim}{e}^{p}\right|\right|$$

(3-206)

$$dz_s = d\varsigma/F_s(\varsigma)$$

(3-207)

At this point let the tensor $\underset{\sim}{a}$ denote the integral on the right-hand side of Eq. (3-205), i.e., let

$$\underset{\sim}{a} = \int_0^{z_s} \rho_1(z_s - z')\frac{d\underset{\sim}{e}^p}{dz'}\, dz' \quad .$$

(3-208)

Then Eq. (3-205) becomes simply

$$\underset{\sim}{s} - \underset{\sim}{a} = s_o \frac{d\underset{\sim}{e}^p}{d\varsigma} F_s \, ,$$

(3-209)

where use was made of Eq. (3-207). Upon taking norms of both sides of Eq. (3-208) and using Eq. (3-206), it follows that:

$$\left|\left|\underset{\sim}{s} - \underset{\sim}{a}\right|\right| = s_o F_s(\varsigma) \quad .$$

(3-210)

The geometric interpretation of Eq. (3-209) in the five-dimensional space of $\underset{\sim}{s}$ is a hypersphere with center $\underset{\sim}{a}$ and radius $s_o F_s$: the equation itself is the algebraic statement of isotropic-cum-kinematic hardening of classical plasticity. In the three-dimensional space of the principal components of $\underset{\sim}{g}$ this equation is the algebraic representation of a cylinder normal to the π-plane i.e., with an axis of symmetry in the direction of the hydrostatic axis. In this regard the evolution of $\underset{\sim}{a}$ with plastic deformation represents kinematic hardening, in general non-linear, while the growth of F_s with plastic deformation, through ς, represents isotropic hardening. A geometric illustration of Eq. (3-209) in the π-plane is given in Figure 3.24. Note that the increment in the plastic strain vector is normal to the yield surface, in view of Eq. (3-209).

Thus, endochronic plasticity contains classical Von Mises plasticity as a special case when the kernel function ρ contains a delta-function in the sense of Eq. (3-204).
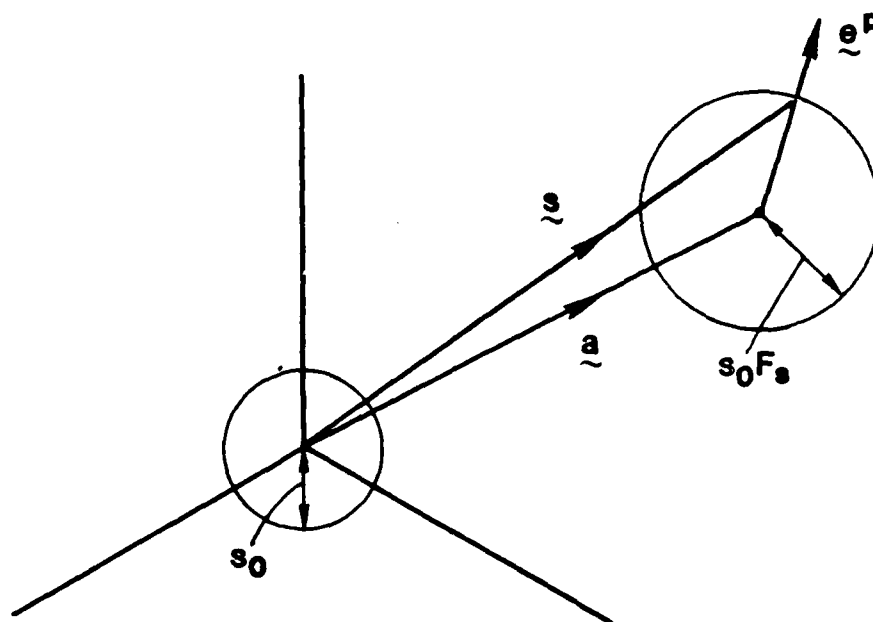
Figure 3.24   A geometric illustration of Eq. (3-209) in the π-plane.

However, there is more to these developments. One of the most difficult and basically unsolved problems of classical plasticity is the determination of the evolution equation that governs the back stress, i.e., the migration of the center of the yield surface in stress space, particularly since every material has its own characteristic evolution equation. Prager's rule of kinematic hardening, given by the expression

$$d\underset{\sim}{a} = C\ d\underset{\sim}{e}^p, \tag{3-211}$$

where C is a constant, gives a <u>linear</u> form of kinematic hardening which is not characteristic of metals and is at best a very crude approximation of experimentally observed behavior. In fact Mroz's theory of multiple yield surfaces [3.17] is a commendable effort to generalize Prager's linear kinematic hardening theory and is tantamount to a <u>piece-wise linear</u> kinematic hardening. It can be readily demonstrated by using Eq. (3-69) that this is achieved by approximating ρ_1 by a piece-wise constant function of z_s. However there is no particular virtue in this approximation and the (thermodynamic) representation of ρ_1 by a series of positive exponential terms is, numerically, a much better alternative as we show later in the book.

We close this sub-section with a cautionary comment. The curvature of the stress-strain curve in simple tension, say, is due mainly to kinematic hardening, i.e., the form of the kernel $\rho_1(z_s)$. Attempts to model the curvature by manipulating the isotropic hardening function may give good results in simple loading but will fail badly when unloading or other, more complex, paths are involved.

3.6.2 The Question of Unloading.

In endochronic plasticity the question of unloading reduces to the determination of $d\zeta$ given a strain increment $d\underset{\sim}{e}$ or a stress increment $d\underset{\sim}{s}$. We shall show how this is done in the following analysis.

We recall Eq. (3-209) which we write in the form

$$d\underset{\sim}{e}^p = \frac{d\zeta}{s_o F_s}\left(\underset{\sim}{s} - \underset{\sim}{a}\right) \ . \tag{3-212}$$

In view of Eq. (3-206) it follows from Eq. (3-212). or Eq. (3-209). that.

$$\left(\underset{\sim}{s} - \underset{\sim}{a}\right) \cdot \left(\underset{\sim}{s} - \underset{\sim}{a}\right) = s_o^2 F_s^2 \tag{3-213}$$

Thus. during a plastic deformation process. Eq. (3-213) must always be satisfied.

A simple differentiation of Eq. (3-213) leads to the expression:

$$\left(\underset{\sim}{s} - \underset{\sim}{a}\right) \cdot d\underset{\sim}{s} - \left(\underset{\sim}{s} - \underset{\sim}{a}\right) \cdot d\underset{\sim}{a} = s_o^2 F_s dF_s \quad . \tag{3-214}$$

At this point we use Eq. (3-209) to substitute for $\underset{\sim}{s} - \underset{\sim}{a}$ in the second term on the right-hand side of Eq. (3-214). and thus obtain

$$\left(\underset{\sim}{s} - \underset{\sim}{a}\right) \cdot d\underset{\sim}{s} = s_o \, F_s \, \frac{d\underset{\sim}{e}^p}{d\varsigma} \cdot d\underset{\sim}{a} + s_o^2 \, F_s \, dF_s \tag{3-215}$$

However $\underset{\sim}{a}$ is given by Eq. (3-208). Thus. upon differentiating this equation. we find

$$d\underset{\sim}{a} = \rho_1(0) d\underset{\sim}{e}^p + \underset{\sim}{h} \, \frac{d\varsigma}{F_s} \quad , \tag{3-216}$$

where use was made of Eq. (3-207). and the relations:

$$\underset{\sim}{h} = \int_o^{z_s} \rho_1'\left(z_s - z'\right) \frac{d\underset{\sim}{e}^p}{dz'} \, dz' \tag{3-217}$$

$$\rho_1' = \frac{d\rho_1}{dz_s} \quad . \tag{3-218}$$

A straightforward analysis using of Eqs. (3-215) and (3-216) leads to the expression:

$$\frac{(\underset{\sim}{s} - \underset{\sim}{a})}{s_o \, F_s} \cdot d\underset{\sim}{s} = H \, d\varsigma \quad , \tag{3-219}$$

where

$$H = \rho_1(0) + s_o F_s' + \frac{(\underset{\sim}{s} - \underset{\sim}{a}) \cdot \underset{\sim}{h}}{s_o \, F_s^2} \quad . \tag{3-220}$$

Note that H depends on the history of $\underset{\sim}{e}^p$ up to the present time ς but not on $d\varsigma$. We shall prove that H is always positive if $F_s' \geq 0$.

<u>Discussion of Eq. (3-219)</u>.

Given a deviatoric stress increment $d\underset{\sim}{s}$ from a point $\underset{\sim}{s}$ on the yield surface, we observe that, relative to the yield surface, either $d\underset{\sim}{s}$ is pointing outwards, is tangent to, or pointing inward. Thus

$$\left(\underset{\sim}{s} - \underset{\sim}{a}\right) \cdot d\underset{\sim}{s} = \begin{cases} +ve \\ 0 \\ -ve \end{cases} , \tag{3-221}$$

depending on the respective circumstance. <u>However $d\varsigma$ cannot be negative</u>. Thus, presuming that $H > 0$ (this will be shown later in this Section), either

$$\left(\underset{\sim}{s} - \underset{\sim}{a}\right) \cdot d\underset{\sim}{s} > 0 \tag{3-222}$$

and $d\varsigma$ is positive and is given by Eq. (3-219) or

$$\left(\underset{\sim}{s} - \underset{\sim}{a}\right) \cdot d\underset{\sim}{s} \leq 0 \tag{3-223}$$

in which case $d\varsigma = 0$, and the deformation is purely <u>elastic</u>.

This result again agrees with classical plasticity in the sense that the above rules also apply. A further result moreover is of interest. If Eq. (3-209) is used in Ineq. (3-222), it follows that whenever $d\underset{\sim}{s}$ gives rise to a plastic strain increment $d\underset{\sim}{e}^p$:

3-75

$$s_o \, F_s \, \frac{d\underset{\sim}{e}^p}{d\varsigma} \cdot d\underset{\sim}{s} > 0 \tag{3-224}$$

or

$$d\underset{\sim}{e}^p \cdot d\underset{\sim}{s} > 0 \quad , \tag{3-225}$$

since s_o, F_s and $d\varsigma$ are all positive. Thus the theory satisfies the Drucker stability postulate [3.18] provided that $H > 0$.

Recapitulation.

(i) **The necessary and sufficient conditions for plastic deformation are:**

$$||\underset{\sim}{s} - \underset{\sim}{a}|| = s_o \, F_s \tag{3-226}$$

and

$$\left(\underset{\sim}{s} - \underset{\sim}{a}\right) \cdot d\underset{\sim}{s} > 0 \tag{3-227}$$

(ii) **The necessary and sufficient conditions for elastic deformation are:**

$$||\underset{\sim}{s} - \underset{\sim}{a}|| < s_o \, F_s \tag{3-228}$$

or

$$||\underset{\sim}{s} - \underset{\sim}{a}|| = s_o \, F_s \tag{3-229a}$$

$$\left(\underset{\sim}{s} - \underset{\sim}{a}\right) \cdot d\underset{\sim}{s} \leq 0 \tag{3-229b}$$

Calculation of $d\underset{\sim}{e}^p$ for prescribed $d\underset{\sim}{e}$.

Let Eqs. (3-226) and (3-227) be satisfied. Then $d\varsigma$ is found from Eq. (3-219). i.e..

$$d\varsigma = \frac{\left(\underset{\sim}{s} - \underset{\sim}{a}\right) \cdot d\underset{\sim}{s}}{s_o \, F_s \, H} \tag{3-230}$$

3-76

The increment in plastic strain may now be found upon use of Eq. (3-212) or upon use of Eqs. (3-230) and (3-212) whereby

$$d\underset{\sim}{e}^P = \frac{1}{\left(s_o F_s\right)^2 H} \left(\underset{\sim}{s} - \underset{\sim}{a}\right) \times \left(\underset{\sim}{s} - \underset{\sim}{a}\right) \cdot d\underset{\sim}{s} \tag{3-231}$$

where the symbol x represents an outer product. In indicial notation:

$$de^P_{ij} = \frac{1}{\left(s_o F_s\right)^2 H} \left(s_{ij} - a_{ij}\right)\left(s_{k\ell} - a_{k\ell}\right) ds_{k\ell} \tag{3-232}$$

In fact Eq. (3-232) may be written in terms of a tangent modulus $C^P_{ijk\ell}$, i.e..

$$de^P_{ij} = C^P_{ijk\ell} ds_{k\ell} \tag{3-233}$$

where

$$C^P_{ijk\ell} = \frac{1}{\left(s_o F_s\right)^2 H} \left(s_{ij} - a_{ij}\right)\left(s_{k\ell} - a_{k\ell}\right) \tag{3-234}$$

Note that $C^P_{ijk\ell}$ is positive semi-definite and symmetric. Thus given any arbitrary tensor ξ_{ij} such that $\|\xi_{ij}\| \neq 0$. then

$$C^P_{ijk\ell} \xi_{ij}\xi_{k\ell} = \frac{1}{\left(s_o F_s\right)^2 H} \left[\left(s_{ij} - a_{ij}\right) \cdot \xi_{ij}\right]^2 \tag{3-235}$$

It then follows that

$$C^P_{ijk\ell} \xi_{ij}\xi_{k\ell} \geq 0 \quad . \tag{3-236}$$

This result will be central in proving uniqueness of the initial value and boundary value problems later in Section 5.5.

Calculation of $d\underset{\sim}{e}^P$ for Prescribed $d\underset{\sim}{\epsilon}$.

In finite element codes the driving input is generally the increment in strain $d\underset{\sim}{\epsilon}$. It is important. therefore. to give a means of calculating $d\underset{\sim}{e}^P$ given $d\underset{\sim}{\epsilon}$. Again let conditions (3-226) and (3-227) be satisfied. Then $d\varsigma$ is given by Eq. (3-230). However. now we may use the relation

$$d\underline{s} = 2\mu \, d\underline{\varepsilon}^e = 2\mu_o\left(d\underline{\varepsilon} - d\underline{\varepsilon}^P\right) \tag{3-237}$$

which may be substituted into Eq. (3-230) to give the following relation:

$$d\varsigma = \frac{2\mu_o}{\rho_o F_s H} \left(\underline{s} - \underline{a}\right) \cdot \left(d\underline{\varepsilon} - d\underline{\varepsilon}^P\right) \tag{3-238}$$

At this point we use Eq. (3-212), substitute for $d\underline{\varepsilon}^P$ in Eq. (3-238) and rearrange terms to obtain the following equation for $d\varsigma$:

$$d\varsigma = \frac{2\mu_o}{s_o F_s (H + 2\mu_o)} \cdot \left(\underline{s} - \underline{a}\right) \cdot d\underline{\varepsilon} \quad . \tag{3-239}$$

Thus, given $d\underline{\varepsilon}$, $d\varsigma$ may be calculated from the above expression.

Recapitulation

We now have the following necessary and sufficient conditions for the occurence of plastic or elastic deformation, given the deviatoric strain increment tensor $d\underline{\varepsilon}$:

(i) Necessary and sufficient conditions for plastic deformation:

$$||\underline{s} - \underline{a}|| = s_o F_s \tag{3-240}$$

and

$$\left(\underline{s} - \underline{a}\right) \cdot d\underline{\varepsilon} > 0 \quad . \tag{3-241}$$

(ii) Necessary and sufficient conditions for elastic deformation:

$$||\underline{s} - \underline{a}|| < s_o F_s \tag{3-242}$$

or

$$\|\underset{\sim}{s} - \underset{\sim}{a}\| = s_o F_s \tag{3-243a}$$

$$(\underset{\sim}{s} - \underset{\sim}{a}) \cdot d\underset{\sim}{e} \le 0 \qquad . \tag{3-243b}$$

3.6.5 The Sign of H.

It is clear from Eq. (3-220) that the sign of H depends, in part, on the sign of F_s' i.e., $dF_s/d\varsigma$. It is also clear from Eq. (3-210) that if $F_s' > 0$ the yield surface continues to expand and the material (plastically incompressible in this case) undergoes isotropic hardening, in addition to kinematic hardening which is inherent in the kernel $\rho(z_s)$. On the other hand, if $F_s' < 0$, isotropic softening takes place, and if $F_s' = 0$, hardening is only of kinematic character since the radius of the yield surface is constant in this case.

With the above in mind we first examine the magnitude of the last term on the right-hand side of Eq. (3-220) and show that

$$\frac{(\underset{\sim}{s} - \underset{\sim}{a}) \cdot \underset{\sim}{h}}{s_o F_s^2} \ge \rho(z_s) - \rho(0) \qquad . \tag{3-244}$$

The proof is given below.

It follows from Eqs. (3-209), (3-217), and (3-220) that

$$\left| \frac{(\underset{\sim}{s} - \underset{\sim}{a}) \cdot \underset{\sim}{h}}{s_o F_s^2} \right| = \frac{1}{F_s} \left| \frac{d\underset{\sim}{e}^p}{d\varsigma} \int_0^{z_s} \rho_1'(z_s' - z') \frac{d\underset{\sim}{e}^p}{dz'} dz' \right| \tag{3-245}$$

We note the following: Because F_s is monotonically increasing, $F_s(z) \le F_s|_{max}$. Also,

$$\left| \frac{d\underset{\sim}{e}^p}{d\varsigma} \int_0^{z_s} \rho_1'(z_s - z') \frac{d\underset{\sim}{e}^p}{dz'} dz' \right| \le$$

$$\int_0^{z_s} |\rho_1'(z_s - z')| \left| \frac{d\underset{\sim}{e}^p(\varsigma)}{d\varsigma} \cdot \frac{d\underset{\sim}{e}^p(z')}{dz'} \right| dz' \le$$

3-79

$$F_s\bigg|_{max} \int_0^{z_s} |\rho'(z_s - z')| \left| \frac{d\underset{\sim}{e}^p(\varsigma)}{d\varsigma} \frac{d\underset{\sim}{e}^p(\varsigma')}{d\varsigma'} \right| dz' \tag{3-246}$$

But

$$\frac{d\underset{\sim}{e}^p}{d\varsigma} \cdot \frac{d\underset{\sim}{e}^p}{d\varsigma'} \leq 1 \tag{3-247}$$

since $d\underset{\sim}{e}^p/d\varsigma$ is a unit tensor. In view of the above and Eq. (3-245), it follows that

$$\left| \frac{(\underset{\sim}{s} - \underset{\sim}{a}) \cdot \underset{\sim}{h}}{s_o F_s^2} \right| \leq \int_0^{z_s} |\rho_1'(z_s - z')| \, dz' \quad , \tag{3-248}$$

where use was made of Eq. (3-247) to observe that

$$\int_0^{z_s} |\rho_1'(z_s - z')| \left| \frac{d\underset{\sim}{e}^p}{d\varsigma} \cdot \frac{d\underset{\sim}{e}^p}{d\varsigma'} \right| dz' \leq$$

$$\int_0^{z_s} |\rho_1(z_s - z')| \, dz' \quad . \tag{3-249}$$

However $\rho_1'(z_s)$ is a negative monotonically increasing function. Thus

$$\int_0^{z_s} |\rho_1'(z_s - z')| \, dz' = \left| \int_0^{z_s} \rho_1'(z_s - z') \, dz' \right| \quad . \tag{3-250}$$

Equations (3-248) and (3-250) now combine to give the following result:

$$\left| \frac{(\underset{\sim}{s} - \underset{\sim}{a}) \cdot \underset{\sim}{h}}{s_o F_s^2} \right| \leq \left| \int_0^{z_s} \rho_1'(z_s - z') \, dz' \right| \quad . \tag{3-251}$$

However,

$$\left| \int_0^{z_s} \rho_1'(z_s - z') dz' \right| = |\rho_1(z_s) - \rho_1(0)| \qquad (3\text{-}252)$$

and hence

$$\left| \frac{(\underline{s} - \underline{a}) \cdot \underline{h}}{s_o F_s^2} \right| \leq |\rho_1(z_s) - \rho_1(0)| \quad . \qquad (3\text{-}253)$$

Thus at worst $(\underline{s}-\underline{a}) \cdot \underline{h}/s_o F_s^2$ cannot attain a value smaller than $\rho_1(z_s) - \rho_1(0)$. Making use of this result in Eq. (3-220) we find that

$$H \geq \rho_1(z_s) + s_o F_s' \quad . \qquad (3\text{-}254)$$

Hence H is always positive for finite values of z_s so long as $F_s' \geq 0$.

3.6.6 Determination of the Constant s_o and the Kernel $\rho_1(z_s)$.

As discussed previously, the form of $\rho(z_s)$ given in Eq. (3-204) and repeated below:

$$\rho(z_s) = s_o \delta(z_s) + \rho_1(z_s) \qquad (3\text{-}255)$$

is really a degenerate form of the function $\rho(z_s)$ whose actual form has been found invariably to be of the type

$$\rho(z_s) = \frac{1}{z_s^\alpha} \sum_r R_r e^{-k_r z_s} \quad , \qquad (3\text{-}256)$$

where one term in the summed series usually suffices, and $0 < \alpha < 1$, $k_r \geq 0$, $R_r > 0$. We remind the reader that $\rho(0) = \infty$ and that in the vicinity of $z = 0$,

$$\rho(z_s) \sim \frac{\rho_o}{z^\alpha} \qquad (3\text{-}257)$$

Suppose that we want to approximate $\rho(z_s)$ by a series of finite exponential terms in the sense that

$$\rho(z_s) \sim \sum_{r=1}^{n} A_r e^{-\beta_r z_s} \tag{3-258}$$

where n is finite. We realize immediately that such a representation cannot be valid near, or at the origin where $\sum_{r=1} A_r < \infty$, in disagreement with the value of $\rho(z_s)$ at $z_s = 0$. However we can approximate $\rho(z_s)$ as close to the origin as we wish by taking a sufficiently large number of exponential terms, or by using the approach described in Chapter 7. This may be proved rigorously, in view of Eq. (3-256) but we omit the proof since it is not of direct consequence in what follows. Thus let us say that the function $\rho_1(z_s)$, where

$$\rho_1(z_s) \stackrel{\text{def}}{=} \sum_{r=1}^{n} A_r e^{-\beta_r z_s} \tag{3-259}$$

is very close to $\rho(z_s)$ in the range $\delta \leq z < \infty$ but differs substantially from $\rho(z_s)$ in the range $0 \leq z < \delta$, where δ is a suitably small number (say 10^{-6}, or the smallest measurable strain).

Thus we may write

$$\rho(z_s) = \epsilon(z_s) + \rho_1(z_s) \tag{3-260}$$

where the "error" $\epsilon(z_s)$ is essentially zero outside the range $0 \leq z < \delta$. Consider now the following expression for the deviatoric stress tensor $\underset{\sim}{s}$:

$$\underset{\sim}{s} = \int_0^{z_s} \rho(z - z') \frac{d\underset{\sim}{e}^p}{dz'} dz' \tag{3-261}$$

Note that in view of Eq. (3-260), Eq. (3-261) becomes:

$$\underset{\sim}{s} = \int_0^{z_s} \rho_1(z_s - z') \frac{d\underset{\sim}{e}^p}{dz'} dz' + \int_0^{z_s} \epsilon(z_s - z') \frac{d\underset{\sim}{e}^p}{dz'} dz' \tag{3-262}$$

3-82

However, because of the fact that $\epsilon(z_s)$ vanishes outside the interval $0 \leq z < \delta$, Eq. (3-262) becomes:

$$\underset{\sim}{s} = \int_0^{z_s} \rho_1(z_s - z') \frac{d\underset{\sim}{\epsilon}^p}{dz'} \, dz' + \int_{z_s-\delta}^{z_s} \epsilon(z_s - z') \frac{d\underset{\sim}{\epsilon}^p}{dz'} \, dz' \, , \qquad (3\text{-}263)$$

but the interval $[\delta\ ]$ is sufficiently small to render the tangent $d\underset{\sim}{\epsilon}^p/d\varsigma$ to the plastic strain path constant in this interval. Thus

$$\int_{z_s-\delta}^{z_s} \epsilon(z_s - z') \frac{d\underset{\sim}{\epsilon}^p}{dz'} \, dz' \overset{\bullet}{=} F_s(z_s) \frac{d\underset{\sim}{\epsilon}^p}{d\varsigma} \int_{z_s-\delta}^{z_s} \epsilon(z_s - z) \, dz'$$

$$= F_s(z_s) \frac{d\underset{\sim}{\epsilon}^p}{d\varsigma} \int_0^{\delta} \epsilon(z') \, dz' \qquad (3\text{-}264)$$

To evaluate the right-hand side of Eq. (3-264) we note that in the interval δ and in view of Eq. (3-257) and (3-259)

$$\epsilon(z_s) = \frac{\rho_0}{z_s^a} - \rho_1(z_s) \qquad (3\text{-}265)$$

Thus:

$$\int_0^{\delta} \epsilon(z') \, dz' \overset{\bullet}{=} \frac{\rho_0}{1-a} \delta^{1-a} - \rho_1(\delta)\delta \qquad (3\text{-}266)$$

But at $z_s = \delta$, $\rho_1(\delta) = \rho(\delta)$ by assumption, and therefore

3-83

$$\int_0^\delta \epsilon(z')dz' \doteq \frac{\rho_o}{1-\alpha}\delta^{1-\alpha} - \frac{\rho_o}{\delta^\alpha} \cdot \delta = \frac{\alpha}{1-\alpha}\rho_o\delta^{1-\alpha} \tag{3-267}$$

In view. therefore of Eqs. (3-263). (3-264) and (3-267). it follows that

$$\underset{\sim}{s} = \int_0^{z_s} \rho_1(z_s - z')\frac{d\underset{\sim}{e}^p}{dz'}dz' + s_o\frac{d\underset{\sim}{e}^p}{dz_s} \tag{3-268}$$

where

$$s_o = \frac{\alpha}{1-\alpha}\rho_o\delta^{1-\alpha} \tag{3-269}$$

Thus the problem of the representation of the kernel $\rho(z_s)$ by the approximate form (3-255) is now solved. But the reader must not fail to note that in the representation of $\rho_1(z_s)$ given by Eq. (3-258). the constants A_r and β_r are functions of δ.

3-84

REFERENCES FOR CHAPTER 3

3.1   Morrow, J., and G. R. Halford, "Low Cycle Fatigue in Torsion," *Proc. Amer. Soc. Testing Mats.*, **62**, 695 (1962).

3.2   Wadsworth, N. J., "Work Hardening of Copper Crystals Under Cyclic Straining," *Acta Metallurgica*, **11** (1963).

3.3   Benham, P. P., and H. Ford, "Low Endurance Fatigue of a Mild Steel and an Aluminum Alloy," *J. Mech. Eng. Science*, **119** (1961).

3.4   Coffin, L. F., and J. F. Tavernelli, "The Cyclic Straining and Fatigue of Metals," *Transactions, Metallurgical Soc., Am. Inst. Mining, Metallurgical and Petr. Eng.*, **215**, 794 (1959).

3.5   Manson, S. S., and M. H. Hirchberg, "Fatigue Behavior in Strain Cycling in the Low and Intermediate Cycle Range," *Proc. 10th Sagamore Army Materials Research Conf.*, Sagamore, NY, pp. 13-16 (1963).

3.6   Valanis, K. C., "Effect of Prior Deformation on the Cyclic Response of Metals," *J. App. Mech.*, **41**, 441 (1974).

3.7   Jhansale, H. R., and T. H. Topper, "Engineering Analysis of the Inelastic Stress Response of a Structural Metal Under Variable Cyclic Strains," *ASTM, STP*, **519**, 246 (1973).

3.8   Valanis, K. C., and C. F. Lee, "Endochronic Theory of Cyclic Plasticity with Applications," *J. App. Mech.*, **51**, 367 (1984).

3.9   Landgraf, R. W., "The Resistance of Metals to Cyclic Deformation," *ASTM, STP*, **467**, 3 (1970).

3.10   Dafalias, Y. F., and E. P. Popov, "Plastic Internal Variables Formalism of Cyclic Plasticity," *J. App. Mech., J. App. Mech.*, **43**, 645 (1976).

3.11   Valanis, K. C., and J. Fan, "A Numerical Algorithm for Endochronic Plasticity and Comparison with Experiment," *Int. J. Comput. and Struct.*, **19**, 717 (1984).

3.12   Valanis, K. C., and J. Fan, "Experimental Verification of Endochronic Plasticity in Spatially Varying Strain Fields," PLASTICITY TODAY, Chapter 9, Ed. A. Sawzcuk and G. Bianchi, Elsevier Publishing Co. (1984).

3.13   Argyris, J. H., "Energy Theorems and Structural Analysis," *Aircraft Eng.*, October 1954, p. 347 - May 1955, p. 158.

3.14   Ohashi. Y.. *et al.*. "Stress-Strain Relation of the Integral Type for Deformation of Brass Along Strain Trajectories Consisting of Three Normal Straight Branches." *Arch. Mech..* **32**. 125 (1980).

3.15   Ohashi. Y.. *et al.*. "Stress-Strain Relation of Brass for the Plastic Deformation Along Bilinear Strain Trajectories with Various Corner Angles." *Proceedings. ICUTAM.* Toronto (1980).

3.16   Ohashi. Y.. *et al.*. "Precise Experimental Results on Behavior of Brass Under Complex Loading." *Bull. JSME.* **43**. 3732 (1977).

3.17   Mroz. Z.. "On the Description of Anisotropic Hardening." *J. Mech. Phys. Solids.* **15**. 163 (1967).

3.18   Drucker. D.C.. "A More Fundamental Approach to Plastic Stress-Strain Relations." *Proc. First U.S. National Congress of Applied Mechanics.* 487 (1951).

4. THEORY OF COMPRESSIBLE PLASTIC ISOTROPIC SOLIDS

4.1 Introduction.

The application of endochronic plasticity to metals. discussed in the preceding chapter. is facilitated by three assumptions which are quite realistic:

(1)   Under moderate hydrostatic stress.[*]   the hydrostatic response is elastic.

(2)   A constant moderate hydrostatic stress does not affect the mechanical response in shear.

(3)   Shearing at constant hydrostatic stress does not induce a change in the hydrostatic strain.

In the case of compressible plastic solids. such as soils. plain concrete and rock for example. the above assumptions are not realistic.

In regard to item (1) above. the typical hydrostatic behavior of concrete. rock and porous rock in compression is illustrated in Figure 4.1.   The pressure-volumetric strain curve is initially convex. becoming concave and asymptotically elastic.   Upon unloading at A to a point B a significant amount of plastic strain. ϵ_B. results.   There is obviously a great deal of hardening taking place. which affects dramatically the subsequent loading-unloading-reloading behavior as illustrate in the figure.   While. for metals. hardening. in general. is the result of multiplication of dislocations. in concrete and soils it is very much a function of compaction.   In both cases however the sources of hardening are the resistance coefficients "b^r" and in this particular instance. b_c^r (see Eq. (2-50b).   Thus while for metals one achieves hardening by letting b_1^r be an increasing function of z. in concrete and soils to account for the compaction effect on the hydrostatic. we set

$$b_0^r = b_{00}^r \, F_H\left(\epsilon^p\right) \tag{4-1}$$

where F_H is a monotonically increasing function of ϵ^p.

---

[*]   Of the order of the yield stress in tension.
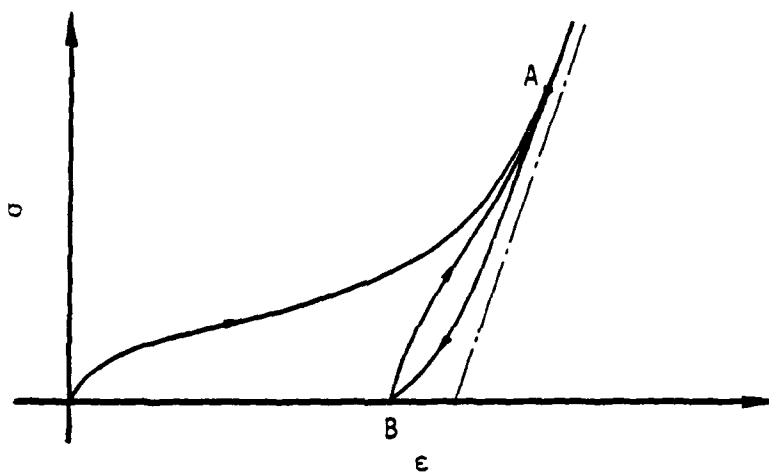
Figure 4.1 Typical response of plain concrete soils and porous rock to pure hydrostatic compression.

$$\sigma_3 \, \sigma_2 > \sigma_1$$
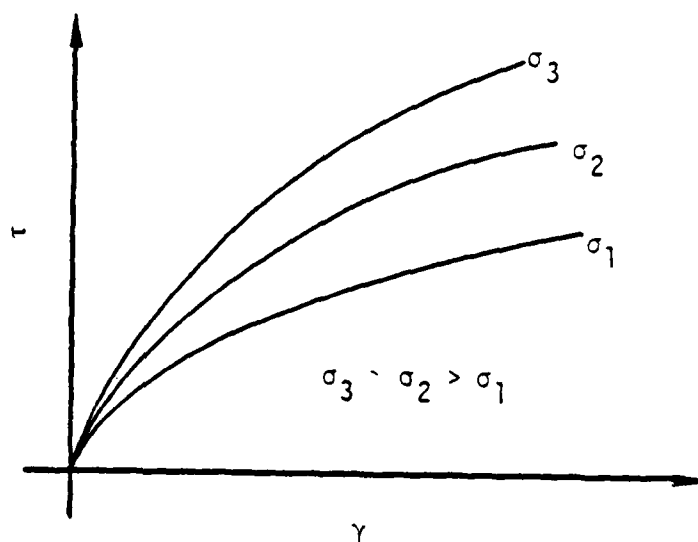
Figure 4.2 Typical shear response of plain concrete, soil and porous rock as a function of hydrostatic compression.

In reference to item (2), the shear response depends strongly upon the existing level of hydrostatic stress. This effect is illustrated schematically in Figure 4.2 where the shear stress is plotted versus the shear strain under monotonic loading conditions and at various levels of constant hydrostatic stress. To account for this effect, the deviatoric resistance coefficients, b_1^r have all been set proportional to a function F_s of the existing hydrostatic stress. Thus

$$b_1^r = b_{10}^r F_s(\sigma) \quad , \qquad (4\text{-}2)$$

according to Eq. (2-50a).

It is important to note, however, that in the case of cyclic histories where the value z becomes large, then F_s can also be expected to depend on z. The physical reason for this is that, in the case of soils, for example, the resistance coefficients depend on the particle arrangement in the material. Since the particle arrangement varies directly with the cumulative plastic strain, represented by z_1, F_s will also depend on z. Thus in general

$$F_s = F_s(\sigma, z) \qquad (4\text{-}3)$$

However for histories that are not repetitive, the dependence on z can be ignored as a first approximation.

In regard to item 3, the mechanical responses of concrete, soil and porous rock show strong shear-hydrostatic interaction in that shearing at constant hydrostatic stress produces a significant change in the hydrostatic strain and vice versa. As will be shown subsequently, endochronic plasticity accounts for this effect through the intrinsic time and specifically by virtue of the coupling constant k which appears in Eq. (3.1.7). note that in materials which are plastically incompressible, $d\epsilon^p = 0$. In such materials shear-hydrostatic interaction is absent.

The constitutive equations that pertain to the mechanical behavior of compressible plastic solids, such as soils, porous rock and concrete, were derived in Chapter 2 and summarized at the beginning of Chapter 3. They are given, again, here for reference.

$$\underset{\approx}{s} = \int_0^{z_s} \rho\left(z_s - z'\right)\frac{d\underset{\approx}{e}^p}{dz'}\, dz' \qquad (4\text{-}4)$$

4-3

$$\sigma = \int_0^{z_H} \phi(z_H - z') \, \frac{d\epsilon^p}{dz'} \, dz' \qquad (4\text{-}5)$$

$$\rho(0) = \phi(0) = \infty \qquad (4\text{-}6)$$

$$d\underset{\sim}{e}^p = d\underset{\sim}{e} - d\underset{\sim}{s}/2\mu_o \qquad (4\text{-}7)$$

$$\epsilon^p = d\epsilon - d\sigma/K_o \qquad (4\text{-}8)$$

$$dz^2 = \left|\left|d\underset{\sim}{e}^p\right|\right|^2 + k^2 |d\epsilon^p|^2 \qquad (4\text{-}9)$$

$$dz_s = dz/F_s \, , \qquad dz_H = dz/kF_H \qquad (4\text{-}10a,b)$$

For soil, porous rock and concrete, F_s can be represented quite accurately over a moderately wide range of σ by the linear expression:

$$F_s = c_o + \phi_o\sigma \, . \qquad (4\text{-}11)$$

where c_o and ϕ_o denote positive material constants. In addition, the function F_H is very closely given for these materials by an exponential function of the form

$$F_H = F_H^\bullet \, e^{\beta\epsilon^p} \qquad (4\text{-}12)$$

where, for convenience, we may normalize F_H to unity at $\epsilon^p = 0$, without loss of generality, and therefore take $F_H^\bullet = 1$.

We note at this point that the above equations have the property that the application of shear stress produces a change in the plastic volumetric strain, i.e., there is shear-volumetric coupling. however, as we shall show below, the shear-volumetric coupling is limited to densification. i.e., $\dot{\epsilon}^p > 0$. To show this, let us invert Eq. (4-5), that is, we express ϵ^p in terms of the history of σ to obtain

4-4

$$\epsilon^p = \int_0^{z_H} L(z_H - z')\frac{d\sigma}{dz'}\, dz' \quad , \tag{4-13}$$

where the kernel L is related to ϕ by the integral equation

$$\int_0^{z_H} \phi(z_H - z')\frac{dL}{dz'}\, dz' = H(z_H) \quad , \tag{4-14}$$

and H(z) denotes the Heaviside step function. If we let $z_H = z_H^1$ at the termination of the pure hydrostatic compression phase $(\sigma = \sigma_1)$, then in view of Eq. (4-13) we can write

$$\epsilon^p(z_H) = \int_0^{z_H^1} L(z_H - z')\frac{d\sigma}{dz'}\, dz' \quad , \tag{4-15}$$

since $d\sigma/dz_H = 0$ for $z_H > z_H^1$.

The application of shear will lead to a change in z, by virtue of Eq. (4-9), and therefore a change in z_H because of Eq. (4-10b). As a result, the integral on the right-hand side of Eq. (4-15) will change due to shearing and, hence, so will ϵ^p. Consequently, in the presence of hydrostatic stress, dz is given by Eq. (4-9) which depends upon the value of k. Finally, we note that, since the integral on the right-hand side of Eq. (4-15) is positive, Eq. (4-15) always predicts compaction ($\overset{\bullet}{\epsilon}{}^p > 0$) during shearing at fixed hydrostatic stress.

To account for dilatancy, the hydrostatic constitutive Eq. (4-5) must be modified. This has been done in a recent work by Valanis and Peters [4.1] in which the hydrostatic and deviatoric evolution equations are coupled. Two different modes of coupling have given rise to two different hydrostatic constitutive equations, which are given below without derivation:

$$\sigma = \int_0^{z_H} \phi(z_H - z')\frac{d\epsilon^p}{dz'}\, dz' + \int_0^{z_H} \Gamma(z_H - z')\frac{||\underset{\sim}{s}||^2}{F_s}\, dz' \tag{4-16}$$

and

$$\sigma = \int_0^{z_H} \phi(z_H - z')\frac{d\epsilon^P}{dz'}\, dz' + \int_0^{z_H} \Gamma(z_H - z')\ \underset{\sim}{s} \cdot \frac{d\underset{\sim}{\epsilon}^P}{dz'}\, dz' \qquad (4\text{-}17)$$

where $\Gamma(z_H)$ is termed the "dilatancy kernel".

From some initial applications to unsaturated soils, it appears that Eq. (4-17) is preferable. This subject will not be pursued in the present volume as it will be taken up in greater detail in a forthcoming second volume on Endochronic Plasticity by the authors. We add parenthetically that Eq. (4-17) was reported by Valanis in Ref.[4.2].

4.2 Hydrostatic Behavior.

In the preceding section, some of the general features of the hydrostatic behavior of compressible plastic solids, such as soils, concrete and porous rock, were described. In this section, several simple hydrostatic models which follow from the basic Eqs. (4-5), (4-6), (4-8), (4-9) and (4-10b) and which exhibit the basic features depicted in Figure 4.1 are developed. In addition, analytical methods are given for determining $\phi(z_H)$ and $F_H(\epsilon^P)$ from experimental data. For further details on the representation of hydrostatic stress, see Ref. [4.3].

4.2.1 Some Simple Hydrostatic Models.

Consider, first of all, the case in which the hydrostatic stress σ lies on the concave portion of the virgin hydrostat (see Figure 4.3). In this instance, the kernel $\phi(z_H)$ can be represented by a Dirac delta-function, i.e.,

$$\phi(z_H) = \phi_o \delta(z_H) \qquad (4\text{-}18)$$

where ϕ_o is a positive constant. Substitution of this expression into Eq. (4-5) leads to the result

$$\sigma = \phi_o \frac{d\epsilon^P}{dz_H} \qquad (4\text{-}19)$$
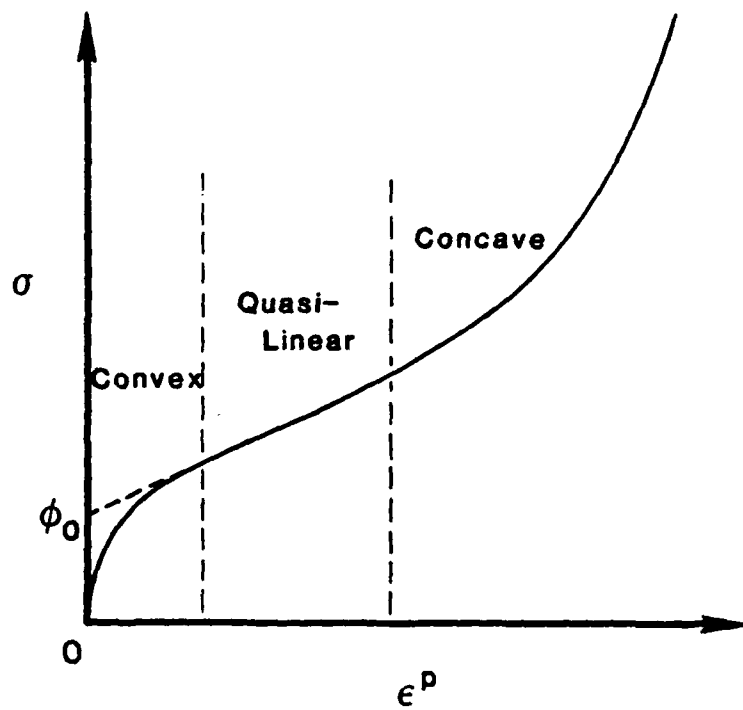
Figure 4.3 σ versus ϵ^p for virgin hydrostatic compression, showing various regions of response.

In a purely hydrostatic deformation, Eq. (4-9) gives the relation

$$dz = k |d\epsilon^p| \quad , \tag{4-20}$$

which for monotonic loading reduces to the expression

$$dz = k \, d\epsilon^p \tag{4-21}$$

Upon combining Eqs. (4-10b), (4-21), (4-19) and (4-12), we obtain the equation

$$\sigma = \phi_o e^{\beta \epsilon^p} \quad , \tag{4-22}$$

which is exactly the form adopted in the critical state theory of soils [4.4]. Note that ϕ_o is defined by the intersection of the extrapolated concave portion of the virgin hydrostat with the σ-axis, as shown in Figure 4.3.

Another way of modeling the hydrostatic response is to represent $\phi(z)$ by a single exponential term, i.e.,

$$\phi = \phi_o e^{-\alpha z_H} \tag{4-23}$$

If one uses Eqs. (4-5), (4-21), (4-23) and (4-12), the following relation for σ is obtained:

$$\sigma = \int_0^{z_H} \phi_o e^{-\alpha (z_H - z')} e^{\beta \epsilon^p (z')} dz' \tag{4-24}$$

The integral on the right-hand side of Eq. (4-24) can be evaluated approximately, since the function $\phi(z_H)$ is close to a delta function. In effect, we can write

$$\sigma = \phi_o e^{\beta \epsilon^p} \frac{1}{\alpha} \left(1 - e^{-\alpha z_H} \right) \quad , \tag{4-25}$$

where

$$z_H = \frac{1}{\beta} \left(1 - {}^{-\beta \epsilon^p} \right) \quad , \tag{4-26}$$

4-8

in view of Eqs. (4-21) and (4-10b). Equations (4-25) and (4-26) give the observed convexity of the hydrostatic stress-strain curve at small values of plastic hydrostatic strain, and concavity for large values of ϵ^P. The reason for this is that at small values of ϵ^P, and in view of Eq. (4-26), we can write:

$$z_H \sim \epsilon^P \tag{4-27}$$

and

$$e^{\beta \epsilon^P} \sim 1 \quad , \tag{4-28}$$

so that Eq. (4-25) becomes

$$\sigma \sim \phi_o \frac{1}{\alpha} \left[1 - e^{-\alpha \epsilon^P} \right] \tag{4-29}$$

which exhibits convexity. For large values of ϵ^P, Eq. (4-26) gives the asymptotic value

$$z_H \sim \frac{1}{\beta} \tag{4-30}$$

Thus, in view of Eq. (4-25), we have

$$\sigma \sim \frac{\phi_o}{\alpha} \left[1 - e^{-\alpha/\beta} \right] e^{\beta \epsilon^P} \tag{4-31}$$

i.e., at large ϵ^P the hydrostatic response becomes exponential and therefore concave.

4.2.2 Determination of the Functions $\phi(z_H)$ and $F_H(\epsilon^P)$.

Consider the case of monotonic hydrostatic compression from the natural unstrained state. In this case, we have from Eqs. (4-9) and (4-10b)

$$dz_H = d\epsilon^P / F_H \quad . \tag{4-32}$$

so that Eq. (4-5) takes the form

$$\sigma = \int_o^{z_H} \phi(z_H - z') F_H(\epsilon^{P\prime}) dz' \quad . \tag{4-33}$$

This equation, together with Eq. (4-8), completely defines the monotonic hydrostatic response.

In addition to the bulk modulus, K, there are two material functions that are necessary to define the hydrostatic behavior: the kernel $\phi(z_H)$ and the hardening function $F_H(\epsilon^P)$.

Consider first the hardening function F_H, which is discussed most clearly with reference to a typical hydrostatic response curve for plain concrete, as depicted in Fig. 4.4. here, the stress σ is shown as a function of the plastic volumetric strain ϵ^P for the case of monotonic compression from the virgin state. The curve ON represents the response for $F_H = 1$. In the initial stage of loading ($0 \leq \epsilon^P \leq OA$), F_H is essentially linear. In the stage $OA < \epsilon^P \leq OB$, it is basically hyperbolic. In the final stage ($\epsilon^P > OB$), $\sigma \to \infty$ as $\epsilon^P \to \epsilon_c^P$, since there is a limiting material compaction beyond which the material cannot be compacted further, no matter how high a stress σ is applied. Thus, it is necessary that F_H satisfy the following limiting condition:

$$\lim_{\epsilon^P \to \epsilon_c^P} F_H = \infty \qquad (4\text{-}34)$$

However, the exponential form of F_H, given in Eq. (4-12) is satisfactory over a substantial range of ϵ^P (say 0.05). Therefore the determination of F_H reduces to the determination of the constant β. Furthermore, the fact that the integral of the kernel ϕ_H saturates while F_H is still in the linear range, suggests that for $\epsilon^P < OA$

$$F_H = e^{\beta \epsilon^P} \sim 1 + \beta \epsilon^P + 0(\epsilon^P)^2 \qquad (4\text{-}35)$$

Thus, if our attention is restricted to the initial stage of response ($0 \leq \epsilon^P \leq OA$), we can write

$$F_H = 1 + \beta \epsilon^P \quad . \qquad (4\text{-}36)$$

where β is a positive constant. The linear representation of F_H inherent in Eq. (4-36) affords an explicit method for determining the value of β and the kernel $\phi(z_H)$, as we will show below.

With F_H given by Eq. (4-36), and for monotonic hydrostatic compression, it follows from Eqs. (4-9) and (4-10b) that,

4-10
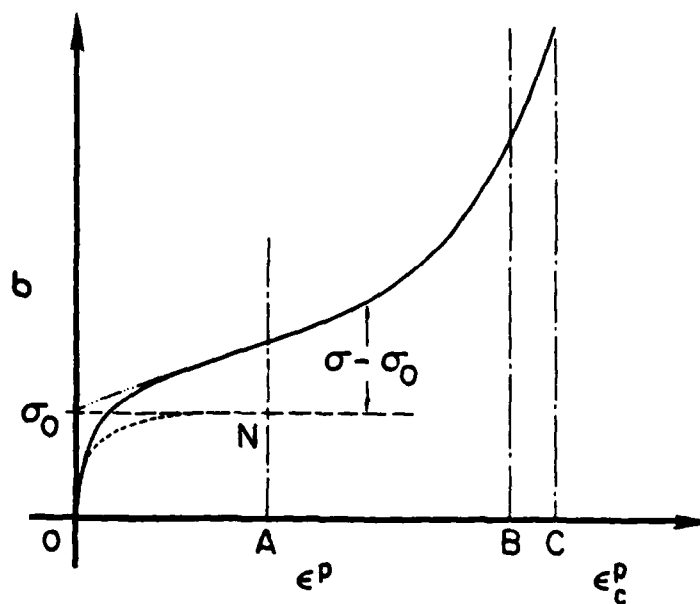
Figure 4.4   Pressure versus plastic volumetric strain for virgin hydrostatic compression.
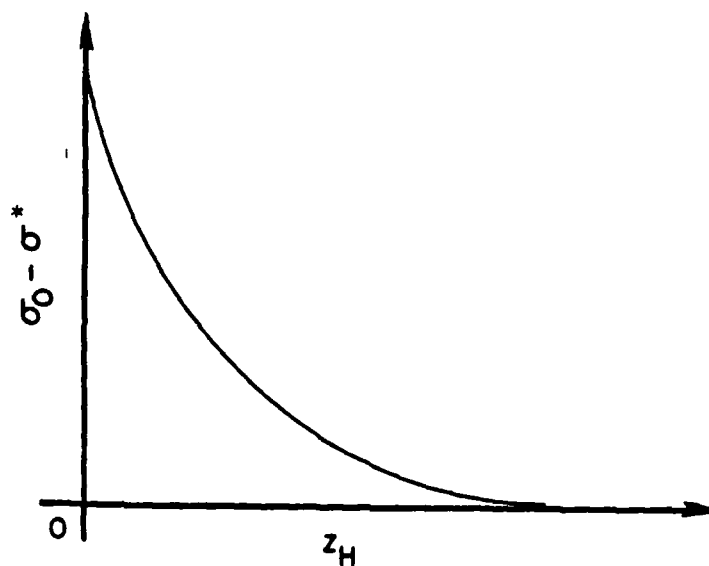
Figure 4.5   General form of the relationship between $\sigma_o - \sigma^*$ and z_H.

$$dz_H = d\epsilon^p/(1 + \beta\epsilon_p). \tag{4-37}$$

Hence

$$\epsilon^p = (1/\beta)\left[e^{\beta z_H} - 1\right], \tag{4-38}$$

so that

$$F_H = e^{\beta z_H}. \tag{4-39}$$

To determine $\phi(z_H)$ we resort to its (approximate) representation by a finite Dirichlet series as given below

$$\phi(z_H) = \sum_{r=1}^{n} B_r e^{-\beta_r z_H}, \tag{4-40}$$

where the constants B_r and β_r are positive and finite.

Therefore, upon substituting from Eqs. (4-39) and (4-40) into Eq. (4-33), we find

$$\sigma = \sum_r \int_o^{z_H} B_r e^{-\beta_r(z_H - z')} e^{\beta z'} dz', \tag{4-41}$$

which can be integrated to give

$$\sigma = \sum_r B_r e^{-\beta_r z_H} \left[\frac{1}{\beta_r + \beta}\right]\left[e^{(\beta_r + \beta)z_H} - 1\right]. \tag{4-42}$$

Upon defining a stress σ^* such that

$$\sigma^* = \frac{\sigma}{F_H} = \frac{\sigma}{1 + \beta\epsilon^p}, \tag{4-43}$$

4-12

Eq. (4-42) can be rewritten in the following form:

$$\sigma^* = \sum_r \frac{B_r}{\beta + \beta_r} \left[1 - e^{-(\beta + \beta_r) z_H} \right] \quad . \tag{4-44}$$

To determine the constants B_r, β_r, and β, we proceed as follows. The constant β is found from the straight line portion of the hydrostat which is given by the relation

$$\sigma = \sigma_o \left(1 + \beta \epsilon^p \right) \quad , \tag{4-45}$$

where σ_o is the intercept shown in Fig. 4.4. The remaining constants are found by plotting $\sigma_o - \sigma^*$ versus z_H, wherein z_H is obtained from Eq. (4-38) as

$$z_H = \frac{1}{\beta} \log \left(1 + \beta \epsilon^p \right) \quad . \tag{4-46}$$

A typical plot is shown in Fig. 4.5. It follows by virtue of Eq. (4-44) that

$$\sigma_o - \sigma^* = \sum_r \frac{B_r}{\beta + \beta_r} e^{-(\beta + \beta_r) z_H} \quad . \tag{4-47}$$

Hence, a Dirichlet series representation of the curve $\sigma_o - \sigma^*$ versus z_H gives $B_r/(\beta + \beta_r)$ and $\beta + \beta_r$. Since β is already known. B_r and β_r. and thus $\phi(z_H)$. are also known.

4.3 Shear at Constant Hydrostatic Stress.

In this section. the case of shear in the presence of a constant hydrostatic stress is considered in detail. This case occupies a particularly important place within the endochronic framework because it allows the analytic determination of F_s. ρ and k when F_s does not depend upon z_s.

4.3.1 General Considerations.

The loading history of interest in this section consists first of a pure hydrostatic compression some arbitrary level. say $\sigma = \sigma_1$. after which σ is held fixed at σ_1 and a

shear stress τ is applied. While τ is being applied, the total stress tensor $\underset{\sim}{\sigma}$ is of the form:

$$\underset{\sim}{\sigma} = \begin{bmatrix} \sigma_1 & \tau & 0 \\ \tau & \sigma_1 & 0 \\ 0 & 0 & \sigma_1 \end{bmatrix} \tag{4-48}$$

It will be assumed in the sequel that the fixed hydrostatic stress σ_1 is of sufficient magnitude to lie on the concave portion of the virgin hydrostat. This is important because it permits the hydrostatic kernel ϕ in Eq. (4-5)) to be represented by a Dirac δ function, which leads to considerable analytic simplification, as we will show.

There are two basic forms of F_s which do not exhibit a dependence on z_s for shear at constant hydrostatic stress, namely, the form in which F_s does not depend upon z_s *per se* and the form in which F_s depends upon z_s in general but, in the case of shear at constant hydrostatic stress, the dependence vanishes. As an example of the latter, we note the large class of materials that includes soils, concretes and rocks for which F_s depends on the hydrostatic stress σ and on the third invariant of the deviatoric stress tensor, J_3. For this class of materials,

$$F_s = F_s(\sigma, J_3) \tag{4-49}$$

In the case of shear at constant hydrostatic stress, σ is fixed at some value, say σ_1, and J_3 remains fixed during the shearing process, since the shear path is a radial line in the π-plane emanating from the origin. In this case, F_s does not depend upon z_s and, in fact, is a constant.

In that which follows, the governing equations for shear at a constant hydrostatic stress σ_1 are derived from the general system of endochronic equations given by Eqs. (4-4) to (4-10a,b) for the case in which F_s does not depend upon z_s. The equations become amenable to analysis if it is assumed that σ_1 lies on either the quasi-linear or the concave portions of the hydrostat (see Fig. 4.3), and this assumption will be adopted below. Procedures for utilizing the resulting equations in conjunction with experimental data to determine F_s, p and k are given.

It is convenient at this point to introduce the following notation:

$$d\varsigma_s = \left\|\left|d\underset{\approx}{e}^P\right|\right\| \quad , \quad d\varsigma_H = \left|d\epsilon^P\right| \tag{4-50a,b}$$

Equation (4-9) can therefore be written as

$$dz^2 = d\varsigma_s^2 + k^2 \, d\varsigma_H^2 \tag{4-51}$$

Since it is assumed that σ_1 lies on the concave part of the hydrostat, Eq. (4-19) applies and, in view of Eq. (4-50b), can be written in the form:

$$\sigma = \sigma_o k \, F_H \frac{d\varsigma_H}{dz} \, , \tag{4-52}$$

from which it follows that

$$d\varsigma_H = \frac{\sigma}{\sigma_o k F_H} \, dz \tag{4-53}$$

Combining Eqs. (4-51) and (4-53) leads to the expression

$$d\varsigma_s = \left[1 - \left(\frac{\sigma}{\sigma_o \, F_H}\right)^2\right]^{1/2} dz \tag{4-54}$$

which, upon substituting from Eq. (4-10a), yields

$$dz_s = \frac{\left[1 - \left(\frac{\sigma}{\sigma_o \, F_H}\right)^2\right]^{-1/2}}{F_s} \, d\varsigma_s \tag{4-55}$$

In order to proceed further, it becomes necessary at this point to select a specific form for F_H. In the following sections, the two forms for F_H given by Eqs. (4-12) and (4-36) are considered for this purpose.

4-15

4.3.2 The Case in Which $F_H = e^{\beta \epsilon}$.

Let us decompose the total plastic volumetric strain during shear at fixed σ into two components ς_H^H and ς_H^s such that

$$\epsilon^P = \varsigma_H^H + \varsigma_H^s \quad , \tag{4-56}$$

where the superscripts H and s refer, respectively, to hydrostatic and shear. Then, when

$$F_H = e^{\beta \epsilon^P} \quad , \tag{4-57}$$

the fixed hydrostatic stress σ_1 at the end of the pure hydrostatic compression phase is, from Eqs. (4-22), given by

$$\sigma_1 = \phi_o e^{-\beta \varsigma_H^H} \quad . \tag{4-58}$$

It therefore follows from Eqs. (4-56) and (4-58) that, during shearing,

$$\phi_o F_H = \phi_o e^{\beta \epsilon^P} = \sigma_1 e^{\beta \varsigma_H^s} \tag{4-59}$$

By combining Eqs. (4-54) and (4-59), and setting $\sigma = \sigma_1$, we obtain

$$d\varsigma_s = \left[1 - e^{-2\beta \varsigma_H^s} \right]^{1/2} dz \quad . \tag{4-60}$$

Setting

$$x \equiv e^{\beta \varsigma_H^s} \quad , \tag{4-61}$$

we can rewrite Eq. (4-60) as

$$d\varsigma_s = \left[1 - \left[\left(\frac{1}{x}\right)^2\right]\right]^{1/2} dz \quad . \tag{4-62}$$

Equations (4-52) and (4-57) can be combined to give

$$\sigma_1 = k\phi_o e^{\beta\varsigma_H} \frac{d\varsigma_H}{dz} \quad , \tag{4-63}$$

where we have set $\sigma = \sigma_1$. Upon using Eq. (4-56). Eq. (4-63) can be rewritten as

$$dz = ke^{\beta\varsigma_H^s} d\varsigma_H^s \quad . \tag{4-64}$$

We now introduce the change of variable

$$y = z - z^1. \tag{4-65}$$

where z^1 denotes *the value of z at the termination of the pure hydrostatic phase.* Equation (4-64) then takes the form

$$dy = \frac{k}{\beta} dx \quad , \tag{4-66}$$

where Eq. (4-61) has been used. Upon integrating this expression, we find

$$y = \left(\frac{k}{\beta}\right)(x - 1) \tag{4-67}$$

or

$$x = 1 + \left(\frac{\beta}{k}\right)y \tag{4-68}$$

Now let

$$a \equiv \frac{\beta}{k} \tag{4-69}$$

Then Eq. (4-68) reads

$$x = 1 + ay .$$ (4-70)

which can be combined with Eq. (4-62) to give

$$\frac{d\varsigma_s}{dz} = \frac{\sqrt{2ay + a^2 y^2}}{(1 + ay)} .$$ (4-71)

In view of Eq. (4-65). this equation becomes

$$\frac{d\varsigma_s}{dz} = \frac{\left[2a\left(z - z^1\right) + a^2\left(z - z^1\right)^2\right]^{1/2}}{\left[1 + a\left(z - z^1\right)\right]} .$$ (4-72)

Since

$$dz_s = \frac{dz}{F_s} ,$$ (4-73)

Eq. (4-72) can be rewritten as

$$\frac{d\varsigma_s}{dw} = F_s \frac{\left[2aF_s w + a^2 F_s^2 w^2\right]^{1/2}}{(1 + aF_s w)} ,$$ (4-74)

where we have set

$$w = z_s - z_s^1 .$$ (4-75)

Here. z_s^1 denotes the value of z_s at the termination of the pure hydrostatic phase.

After the pure hydrostatic compression phase has been completed and shearing begins at $\sigma = \sigma_1$. we can write from Eq. (4-53) that

$$d\epsilon_p^s = \frac{\sigma_1}{\phi_o} e^{-\beta\left(\epsilon_p^H + \epsilon_p^s\right)} \frac{dz}{k} ,$$ (4-76)

4-18

where ϵ_p^H and ϵ_p^s denote, respectively, the plastic volumetric strains at the end of the pure hydrostatic compression phase and during shearing.

For monotonic hydrostatic compression to σ_1, we have

$$\sigma_1 = \phi_o e^{\beta \epsilon_p^H} \ . \tag{4-77}$$

It then follows from Eqs. (4-76) and (4-77) that

$$d\epsilon_p^s = e^{-\beta \epsilon_p^s} \frac{dz}{k} \ , \tag{4-78}$$

which shows that $d\epsilon_p^s$ is always positive, thereby indicating that this model exhibits only compaction when there is shear in the presence of a fixed hydrostatic stress.

The deviatoric plastic strain increment tensor corresponding to Eq. (4-48) is of the form

$$d\underset{\sim}{e}^p = \begin{bmatrix} 0 & d\gamma^p & 0 \\ d\gamma^p & 0 & 0 \\ 0 & 0 & 0 \end{bmatrix} \ , \tag{4-79}$$

so that

$$\left|\left| d\underset{\sim}{e}^p \right|\right| = \sqrt{2}\ d\gamma^p \ . \tag{4-80}$$

Introducing this expression into Eq. (4-9), and setting $d\epsilon_p = d\epsilon_p^s$, gives

$$dz^2 = 2\left(d\gamma^p\right)^2 + k\left(d\epsilon_p^s\right)^2 \ . \tag{4-81}$$

Equation (4-78) may be solved for dz and the result combined with Eq. (4-81) to yield the expression

4-19

$$k \, d\epsilon_p^s \left[e^{2\beta\epsilon_p^s} - 1 \right]^{1/2} = \sqrt{2} \, d\gamma^p \ . \tag{4-82}$$

Recalling the change of variable given in Eq. (4-61), and with $\varsigma_H^s = \epsilon_p^s$, we can rewrite Eq. (4-82) in the form

$$\frac{k\left(x^2 - 1\right)^{1/2}}{\beta x} \, dx = \sqrt{2} \, d\gamma^p \ , \tag{4-83}$$

which can be integrated to give

$$\sqrt{x^2 - 1} - \cos^{-1}\left|\frac{1}{x}\right| = \frac{\sqrt{2}\beta}{k} \, \gamma^p \ , \tag{4-84}$$

where

$$x \equiv e^{\beta\epsilon_p^s} \ , \tag{4-85}$$

and the vertical bars enclosing a symbol denote its absolute value. Equation (4-84) therefore provides a closed-form theoretical solution for the shear-volumetric coupling during shear at a constant hydrostatic stress. The interesting feature of this equation is that the functional dependence of ϵ_p^s on γ^p is independent of the hydrostatic stress σ, provided that the fixed hydrostatic stress σ_1 is on the concave part of the hydrostatic curve. This important prediction, which results from the model, has been verified recently for a soil with weak cohesion by the authors. Since β is known from the hydrostatic test, k can be found by fitting Eq. (4-84) to the experimentally obtained curve of the function $\epsilon_p^s(\gamma^p)$.

We now return to the question of the shear stress response to increasing shear strain in the presence of constant σ. In view of Eq. (4-4), we can write

$$\tau = \int_0^{z_s} \rho\left(z_s - z'\right)\frac{d\gamma^p}{dz'} \, dz' \ . \tag{4-86}$$

4-20

However, $\gamma^p = 0$ during the pure hydrostatic compression phase, i.e., for z_s in the range $0 \leq z_s \leq z_s^1$. Therefore, if we set

$$w = z_s - z_s^1 \tag{4-87}$$

and recall Eq. (4-86), it follows that

$$\tau = \int_o^w \rho(w - w')\frac{d\gamma^p}{dw'} \, dw' \quad . \tag{4-88}$$

We note that

$$\frac{d\gamma^p}{dw} = \frac{d\gamma^p}{dz} \frac{dz}{dw} \tag{4-89}$$

and

$$\frac{dz}{dw} = \frac{dz}{dz_s} = F_s \quad . \tag{4-90}$$

Consequently,

$$\frac{d\gamma^p}{dw} = F_s \frac{d\gamma^p}{dz} \quad . \tag{4-91}$$

Let us now integrate Eq. (4-64), with $\varsigma_H^s = \epsilon_p^s$, during the shearing process; this leads to the expression

$$z - z^1 = \frac{k}{\beta}\left(e^{\beta\epsilon_p^s} - 1\right) \quad . \tag{4-92}$$

Setting

$$y \equiv z - z^1 \tag{4-93}$$

and recalling Eq. (4-61), we may write

4-21

$$x = 1 + \frac{\beta}{k} y \quad . \tag{4-94}$$

In view of Eqs. (4-81) and (4-93), it follows that

$$dz^2 = dy^2 = 2\left(d\gamma^p\right)^2 + k^2\left(d\epsilon_p^2\right) \quad . \tag{4-95}$$

Equation (4-94) may be differentiated to give

$$dx = \left(\frac{\beta}{k}\right)dy \tag{4-96}$$

which, in view of Eq. (4-61), may be written as

$$\beta e^{\beta \epsilon_p^s} d\epsilon_p^s = \frac{\beta}{k} dy \tag{4-97}$$

or, in view of Eq. (4-85),

$$\beta x \, d\epsilon_p^s = dx \quad . \tag{4-98}$$

We now introduce Eqs. (4-96) and (4-98) into Eq. (4-95); this gives

$$\frac{k^2}{\beta^2}\left(1 - \frac{1}{x^2}\right)dx^2 = 2\left(d\gamma^p\right)^2 \quad , \tag{4-99}$$

and upon taking the root we obtain

$$\frac{k}{\beta}\left(1 - \frac{1}{x^2}\right)^{1/2}dx = \sqrt{2} \, d\gamma^p \quad . \tag{4-100}$$

Returning to Eq. (4-91), we note that

$$\frac{d\gamma^p}{dz} = \frac{d\gamma^p}{dx} \frac{dx}{dz} = \frac{d\gamma^p}{dx} \frac{dx}{dy} \frac{dy}{dz} \quad . \tag{4-101}$$

Since $dy/dz = 1$ from Eq. (4-93) and

$$\frac{dx}{dy} = \frac{\beta}{k} \; , \tag{4-102}$$

it follows from Eq. (4-101) that

$$\frac{d\gamma^P}{dz} = \frac{\beta}{k} \frac{d\gamma^P}{dx} \quad . \tag{4-103}$$

Upon combining Eqs. (4-100) and (4-103), we find

$$\frac{d\gamma^P}{dz} = \frac{1}{\sqrt{2}} \left(1 - \frac{1}{x^2} \right)^{1/2} \tag{4-104}$$

which, when used in conjunction with Eq. (4-91), leads to the expression

$$\frac{d\gamma^P}{dw} = \frac{F_s}{\sqrt{2}} \left(1 - \frac{1}{x^2} \right)^{1/2} \quad . \tag{4-105}$$

If F_s does not depend upon z, we can integrate Eq. (4-90) to obtain

$$z_s - z_s^1 = \frac{1}{F_s} \left(z - z^1 \right) \quad . \tag{4-106}$$

Therefore, on the basis of Eqs. (4-93), (4-94), and (4-106), it follows that

$$x = 1 + \frac{\beta}{k} F_s \, w \; . \tag{4-107}$$

Equations (4-104) and (4-107) can be combined to give

$$\frac{d\gamma^P}{dw} = F_s \, G(w) \tag{4-108}$$

4-23

where we have set

$$G(w) \equiv \frac{\left[2a\, F_s w + a^2 F_s^2 w^2\right]^{1/2}}{\left(1 + a\, F_s w\right)} \tag{4-109}$$

and

$$a \equiv \frac{\beta}{k} \quad .$$

In view of Eq. (4-108). Eq. (4-88) may be written as

$$\tau(w) = \frac{1}{\sqrt{2}} \int_0^w \rho(w - w')\, G(w')\, dw' \quad . \tag{4-110}$$

An inspection of Eq. (4-109) reveals that the function $G(w)$ satisfies the basic requirements stipulated later in Section 4.3.4. Therefore, on the basis of the proof presented therein, we can write

$$\lim_{z_s \to \infty} \int_0^{z_s} \rho\!\left(z_s - z'\right) G(z')\, dz' = M_\infty \tag{4-111}$$

where

$$M_\infty = \int_0^\infty \rho(z')\, dz' \tag{4-112}$$

and $M_\infty < \infty$. Therefore, if we denote the limiting value of the shear stress by τ_∞, it follows from Eqs. (4-109) and (4-110) that

$$\tau_\infty = \frac{F_s}{\sqrt{2}}\, M_\infty \quad . \tag{4-113}$$

Without loss of generality, F_s may be normalized to unity at some arbitrary reference hydrostatic stress σ_R. When this is done, Eq. (4-113) becomes

$$\tau_\infty(\sigma_R) = \frac{M_\infty}{\sqrt{2}} , \qquad (4\text{-}114)$$

which may be combined with Eq. (4-113) to give, at an arbitrary σ,

$$\frac{\tau_\infty(\sigma)}{\tau_\infty(\sigma_R)} = F_s . \qquad (4\text{-}115)$$

This expression therefore shows that, when F_s is independent of z_s, the function F_s can be determined from experimental data obtained from the shearing phase of the test. By performing the shear at different values of θ in the π-plane, the dependence of F_s on θ (or J_3) can be determined.

Let us consider now the determination of the kernel function $\rho(z_s)$. From experimental data, one obtains the τ versus γ relationship, which is reducible to a function of the plastic shear strain, γ^p. For monotonic shearing at a fixed hydrostatic stress, and in view of Eq. (4-50a), we can write

$$d\varsigma_s = \sqrt{2}\, d\gamma^p . \qquad (4\text{-}116)$$

Furthermore, at the initiation of shear $\varsigma_s = 0$, so that

$$\varsigma_s = \sqrt{2}\, \gamma^p . \qquad (4\text{-}117)$$

This expression may be combined with Eq. (4-74) to give a relation between $d\gamma^p$ and dw, which can be numerically integrated to give γ^p as a function of w. The function $\tau(w)$ can therefore be found. When $\tau(w)$ is known, Eq. (4-110) is a Volterra integral equation of the first kind which can be solved numerically to obtain $\rho(w)$, once F_s is given. A numerical procedure designed for this purpose is described in Chapter 10.

4.3.3 The Case in Which $F_H = 1 + \beta \epsilon^p$.

As noted in Section 4.2.2. this case applies when the constant hydrostatic stress σ_1 at which the shearing occurs is located on the quasi-linear part of the concave portion of the virgin hydrostat. With

$$F_H = 1 + \beta \epsilon^p \quad , \tag{4-118}$$

Eq. (4-52) takes the form

$$\sigma = \phi_o k \left(1 + \beta \epsilon^p\right) \frac{d\varsigma_H}{dz} \quad , \tag{4-119}$$

which may be combined with Eq. (4-51) to give the following expression:

$$d\varsigma_s = \left\{ 1 - \left[\frac{\sigma_1}{\phi_o \left(1 + \beta \varsigma_H\right)} \right]^2 \right\}^{1/2} dz \quad . \tag{4-120}$$

Here, for monotonic loading. $\epsilon^p = \varsigma_H$ and σ_1. as before. denotes the fixed hydrostatic stress on the quasi-linear portion of the virgin hydrostat.

We decompose ς_H into two components. as in Eq. (4-56). and write:

$$\phi_o \left(1 + \beta \varsigma_H\right) = \phi_o \left(1 + \beta \varsigma_H^H\right) + \phi_o \left(\beta \varsigma_H^s\right) \tag{4-121}$$

where ς_H^H is the value of ς_H at the termination of the pure hydrostatic compression phase. while ς_H^s is the component due to the shear. For pure hydrostatic compression up to $\sigma = \sigma_1$. it follows from Eqs. (4-106). (4-19) and (4-118) that

$$\sigma_1 = \phi_o \left(1 + \beta \varsigma_H^H\right) \quad . \tag{4-122}$$

Hence. Eq. (4-121) can be rewritten as

$$\sigma_o\left(1 + \beta\varsigma_H\right) = \sigma_1 + \phi_o\beta\varsigma_H^s , \tag{4-123}$$

which can be combined with Eq. (4-120) to give the expression:

$$\frac{d\varsigma_s}{dz} = \left[1 - \left[1 + \frac{\phi_o\beta}{\sigma_1}\varsigma_H^s\right]^{-2}\right]^{1/2} \tag{4-124}$$

For shearing at $\sigma = \sigma_1$, it follows from Eq. (4-119) that

$$\sigma_1 = \phi_o k\left[1 + \beta\varsigma_H^H + \beta\varsigma_H^s\right]\frac{d\varsigma_H^s}{dz} . \tag{4-125}$$

Equation (4-122) may be used together with Eq. (4-125) to obtain the result:

$$dz = k\left[1 + \frac{\phi_o\beta}{\sigma_1}\varsigma_H^s\right]d\varsigma_H^s . \tag{4-126}$$

If we now set

$$y \equiv z - z^1 \tag{4-127}$$

$$x \equiv 1 + \beta\frac{\phi_o}{\sigma_1}\varsigma_H^s , \tag{4-128}$$

where z^1 denotes the value of z at which shearing begins. Eq. (4-126) can be written in the form:

$$dy = \left(\frac{k\sigma_1}{\beta\phi_o}\right)x \, dx . \tag{4-129}$$

Integrating this expression yields

$$y = \frac{1}{2a}\left(x^2 - 1\right) , \tag{4-130}$$

where we have set

$$a \equiv \frac{\beta\phi_o}{k\sigma_1} \quad . \tag{4-131}$$

From Eqs. (4-124) and (4-128), it follows that

$$\frac{d\varsigma_s}{dz} = \left[1 - \left(\frac{1}{x}\right)^2\right]^{1/2} \quad . \tag{4-132}$$

Equation (4-131) may be used to express Eq. (4-129) in the form:

$$dz = \frac{x \, dx}{a} \quad , \tag{4-133}$$

since $dy = dz$. We may now combine Eqs. (4-132) and (4-133) to give the expression:

$$d\varsigma_s = \frac{1}{a}\left(x^2 - 1\right)^{1/2} dx \tag{4-134}$$

which, upon integration, leads to the result:

$$\varsigma_s = \frac{1}{2a} \left\{ x\sqrt{x^2 - 1} - \log\left| x + \sqrt{x^2 - 1} \right| \right\} \quad . \tag{4-135}$$

Since $\varsigma_s = \gamma^p$ and $x = \beta\sigma_o/\sigma_1 \; \epsilon_p^s$, Eq. (4-135) is of the form:

$$\gamma^p = \gamma^p\left(\epsilon_p^s\right) \quad , \tag{4-136}$$

which provides a closed-form theoretical solution for the change in the plastic volumetric strain during shear at a constant hydrostatic stress σ_1, when σ_1 is located on the quasi-linear portion of a virgin hydrostat. In this case, it is interesting that the shear-volumetric coupling depends upon σ_1, through the dependence of both a and x on σ_1. This is in contrast to Eq. (4-84)[1] given earlier for the case $F_H = e^{\beta\epsilon}$, where the shear-volumetric coupling is independent of σ_1. Finally, since ϕ_o and β are

known from the virgin hydrostat. k can be found by fitting Eq. (4-136) to the experimentally determined curve of the function $\gamma^p = \gamma^p(\epsilon_p^s)$.

To develop a relation between γ^p and z_s at a reference hydrostatic stress σ_R, we return to Eq. (4-130) and write

$$x^2 = 1 + 2 \, ay \quad . \tag{4-137}$$

At a reference stress σ_R we may set $F_s = 1$ without loss of generality. As a result, $y = z_s$ so that Eq. (4-137) takes the form:

$$x^2 = 1 + 2a \, z_s \quad . \tag{4-138}$$

Therefore, upon combining Eqs. (4-135) and (4-138), the following expression results:

$$\varsigma_s = \frac{1}{2a} \left\{ \sqrt{2az_s} \, \sqrt{1 + 2az_s} - \log \left| \sqrt{2az_s} + \sqrt{1 + 2az_s} \right| \right\} \quad . \tag{4-139}$$

For shear at fixed σ, we have from Eq. (4-79) that

$$\varsigma_s = \sqrt{2} \, \gamma^p \quad . \tag{4-140}$$

Thus, Eqs. (4-139) and (4-140) provide a relation between γ^p and z_s during shear at fixed reference stress σ_R.

To determine the shear response to increasing shear strain in the presence of fixed σ, we recall Eqs. (4-88) and (4-91), which are repeated below:

$$\tau = \int_0^w \rho(w - w') \frac{d\gamma^p}{dw'} \, dw' \quad . \tag{4-141}$$

$$\frac{d\gamma^p}{dw} = F_s \frac{d\gamma^p}{dz} \tag{4-142}$$

where

$$w = z_s - z_s^1 \quad .$$ (4-143)

Since $\varsigma_s = \sqrt{2}\, \gamma^p$, we can write

$$\frac{d\gamma^p}{dw} = \frac{d\gamma^p}{d\varsigma_s}\, \frac{d\varsigma_s}{dw} = \frac{1}{\sqrt{2}}\, \frac{d\varsigma_s}{dw} \quad .$$ (4-144)

Equations (4-132) and (4-137) can be combined to give

$$\frac{d\varsigma_s}{dy} = \left(\frac{2ay}{1 + 2ay}\right)^{1/2} ,$$ (4-145)

where we have set $dy = dz$ on the basis of Eq. (4-127). Inasmuch as F_s is assumed to be independent of z during the shearing process, it follows that

$$z_s - z_s^1 = \frac{1}{F_s}\left(z - z^1\right)$$ (4-146)

or, equivalently,

$$w = \frac{y}{F_s} \quad .$$ (4-147)

Upon using this equation in Eq. (4-145), we can write

$$\frac{d\varsigma_s}{dw} = F_s\left(\frac{2a\, F_s w}{1 + 2a\, F_s w}\right)^{1/2} ,$$ (4-148)

which can be combined with Eqs. (4-141) and (4-144) to give the following expression for τ:

$$\tau = \frac{F_s}{\sqrt{2}} \int_0^w \rho(w - w')G(w')dw'$$ (4-149)

where

$$G(w) = \left[\frac{2a\,F_s w}{1 + 2a\,F_s w}\right]^{1/2} \quad .$$

(4-150)

An inspection of Eq. (4-150) reveals that the function $G(w)$ satisfies the basic requirements stipulated in Section 4.3.4. Therefore, on the basis of the proof presented there, we can write

$$\lim_{z_s \to \infty} \int_0^{z_s} \rho\left(z_s - z'\right) G(z')\,dz' = M_\infty$$

(4-151)

where M_∞ is defined according to Eq. (4-112). If we denote by τ_∞ the limiting value of τ as $z_s \to \infty$, is follows from Eqs. (4-149) and (4-151) that

$$\tau_\infty = \frac{F_s}{\sqrt{2}} M_\infty \quad .$$

(4-152)

Again, without loss of generality, we may normalize F_s to unity at some arbitrary reference hydrostatic stress σ_R. When this is done, Eq. (4-152) reads

$$\tau_\infty\left(\sigma_R\right) = \frac{M_\infty}{\sqrt{2}} \quad .$$

(4-153)

This result may be combined with Eq. (4-152) to yield the expression

$$\frac{\tau_\infty(\sigma)}{\tau_\infty\left(\sigma_R\right)} = F_s \quad .$$

(4-154)

Therefore, for the case in which F_s is independent of z_s, the function F_s can be determined from experimental data obtained during the shear phase of the test. By

4-31

keeping σ constant and performing the shear at different values of θ in the π-plane, the dependence of F_s on θ (or J_3) can be determined.

The procedure for determining the kernel function $\rho(z_s)$ in this case is the same as that described earlier in Section 4.3.2 and consequently will not be repeated.

4.3.4 A Proof of Equations (4-111) and (4-151).

Consider the equation

$$\tau(z) = \int_0^z \rho(z - z')G(z')dz' \tag{4-155}$$

where $\rho(z)$ is a weakly singular, positive, and monotonically decreasing function of z in the domain $o < z < \infty$, and

$$\lim_{z \to \infty} \rho(z) = 0 \quad . \tag{4-156}$$

In this section, we establish the basic requirements that the function $G(z)$ must satisfy in order for the following limiting condition to hold:

$$\lim_{z \to \infty} \int_0^z \rho(z - z')G(z')dz' = M_\infty \tag{4-157}$$

where

$$M(z) = \int_0^z \rho(z')dz' \tag{4-158}$$

and $M_\infty = M(\infty) < \infty$ \hfill (4-159)

First, we note that $M(z)$ is positive, monotonically increasing and convex in the sense that

$$M(z) - M(z - a) < a \left. \frac{dM}{dz} \right|_{z-a} \quad . \tag{4-160}$$

Therefore, in view of Eqs. (4-158) and (4-160)

$$M(z) - M(z - a) < a \, \rho(z - a) \quad , \tag{4-161}$$

so that from Eqs. (4-156) and (4-161) it follows that

$$\lim_{z \to \infty} \left\{ M(z) - M(z - a) \right\} = 0 \quad . \tag{4-162}$$

To prove the validity of Eq. (4-157) for certain functions $G(z)$, we first prove the following theorem.

Theorem: Let $R(z)$ be a positive monotonically decreasing function, bounded from above and below in the sense that

$$0 < R(z) \leq R(0) \tag{4-163}$$

and

$$\lim_{z \to \infty} R(z) = 0 \quad . \tag{4-164}$$

The operational definition of Eq. (4-164) is as follows: Given an ϵ, however small, there exists a $z < \infty$ such that

$$R(z) < \epsilon \quad . \tag{3.121}$$

Then, the following is true:

$$\lim_{z \to \infty} \int_0^z \rho(z - z')R(z')dz' = 0 \quad . \tag{4-165}$$

4-33

Proof: The integral I on the left-hand side of Eq. (4-166) may be written in the form:

$$I = \int_0^{z_0} \rho(z - z')R(z')dz' + \int_{z_0}^{z} \rho(z - z')R(z')dz' \qquad (4\text{-}167)$$

where $0 < z_0 < z$. Because of the properties of $R(z)$, it follows that

$$\int_0^{z_0} \rho(z - z')R(z')dz' < R(0) \int_0^{z_0} \rho(z - z')dz' \qquad (4\text{-}168)$$

or, in view of Eq. (4-158), we may write this as

$$\int_0^{z_0} \rho(z - z')R(z')dz' < R(0) \left\{ M(z) - M(z - z_0) \right\} \quad . \qquad (4\text{-}169)$$

Therefore, as a result of Eq. (4-162)

$$\lim_{z \to \infty} \int_0^{z_0} \rho(z - z')R(z')dz' = 0 \quad . \qquad (4\text{-}170)$$

Following the same reasoning as above, it can be shown that

$$\int_{z_0}^{z} \rho(z - z')R(z')dz' < R(z_0)M(z - z_0) \quad . \qquad (4\text{-}171)$$

Hence:

$$\lim_{z \to \infty} \int_{z_0}^{z} \rho(z - z')R(z')dz' < M_\infty R(z_0) \quad . \qquad (4\text{-}172)$$

4-34

Because of the properties of R(z) defined by Eqs. (4-165) and (4-166), the right-hand side of Eq. (4-172) can be made as small as one pleases, in the sense that given an ϵ however small there exists a z_o such that

$$M \, R\left(z_o\right) < \epsilon \quad . \tag{4-173}$$

Since z_o may be any large finite number, $M_\infty R(z_o)$ may differ from zero by an amount which can be made as small as one pleases. Therefore, in view of Eqs. (4-170) and (4-173), Eq. (4-166) is true and the theorem is proved.

Returning now to Eq. (4-166), we note that whenever the function $1 - G(z)$ has the properties of R(z), it follows that

$$\lim_{z \to \infty} \int_0^z \rho(z - z')\left\{1 - G(z')\right\}dz' = 0 \tag{4-174}$$

and hence Eq. (4-166) is proved.

REFERENCES FOR CHAPTER 4.

4.1   Valanis, K. C., and J. Peters, "A Constitutive Theory of Soils with Dilatant Capability." WES Report ---, Vicksburg, MS (1987).

4.2   Valanis, K. C., "Endochronic Theory of Soils and Concrete." *Proc. Constitutive Laws for Engineering Materials, Theory and Applications,* Vol. I, p. 247 (1987). Ed. C. S. Desai *et al.,* Elsevier.

4.3   Valanis, K. C., and H. E. Read, "An Endochronic Plasticity Theory of Concrete." *Mech. of Materials,* 5, 277 (1986).

4.4   Schofield, A. J., and C. P. Wroth, "Critical State Soil Mechanics." McGraw Hill, London, 1968.

5. GENERAL TOPICS

In this chapter we deal with certain specific aspects of endochronic plasticity which, however, have wider implications in the general subject of constitutive theory. In Section 5.1 we deal with the topic of history-induced anisotropy in materials that are isotropic in their initial state. In Section 5.2 we discuss Drucker's and Il'iushin's postulates and address the problem of closure of hysteresis loops in one-dimensional stress- strain space. We also touch upon some of the thermodynamic implications which do not appear to be well understood in the literature. In Section 5.3 we also discuss Drucker's and Il'iushin's postulates as they relate to irreversible thermodynamics and more specifically to endochronic plasticity, insofar as the Il'iushin postulate is concerned, and finally in Section 5.4 we discuss questions of uniqueness of boundary and initial value problems for inelastic solids and deal with these more specifically in the context of endochronic plasticity.

5.1 Isotropy and History-Induced Anisotropy.

Because this is not a text book on continuum mechanics we do not intend to devote an inordinate amount of space to the details of this topic which can be found elsewhere. In simple materials -- in the sense of Noll [5.1], where the stress is determined by a functional of the deformation gradient -- objectivity is satisfied by formulating a constitutive equation in the material frame of reference (Lagrangian formulation). The result is a general statement of the fact that the Piola stress tensor $\underset{\sim}{\tau}$ is a function of the history of the right Cauchy-Green deformation tensor $\underset{\sim}{C}$ or, equivalently, of the Green strain tensor $\underset{\sim}{E}$ where

$$\underset{\sim}{E} = \frac{1}{2}\left(\underset{\sim}{C} - \underset{\sim}{\delta}\right) \tag{5-1}$$

Thus in mathematical terms

$$\underset{\sim}{\tau} = \underset{\sim}{F}[\underset{\sim}{E}] \quad , \tag{5-2}$$

the functional $\underset{\sim}{F}$ being defined with respect to a time scale which, for the moment we leave unspecified.

In small deformation problems the Piola stress tensor $\underset{\sim}{\tau}$ is approximately equal to the Cauchy stress $\underset{\sim}{\sigma}$ and the Green strain tensor $\underset{\sim}{E}$ is also approximately equal to the small strain tensor $\underset{\sim}{\epsilon}$ so in a first order of approximation of the displacement gradient norm $||\nabla u||$ one writes

$$\underset{\sim}{g} = F[\underset{\sim}{\varepsilon}] + O\|\nabla u\|^2 \quad, \tag{5-3}$$

and no distinction is made between $\underset{\sim}{g}$ and $\underset{\sim}{\tau}$. Furthermore objectivity, in regard to Eq. (5-3), is now satisfied (only) approximately provided that strains and rotations are small.

The fact is, however, that strictly the correct formulation is

$$\underset{\sim}{\tau} = \underset{\sim}{F}[\underset{\sim}{\varepsilon}] \quad, \tag{5-4}$$

even though the measurement of $\underset{\sim}{\tau}$ is approximate in the sense that it is measured relative to the spatial (laboratory) frame of reference. However in that which follows we shall make no further distinction between $\underset{\sim}{\tau}$ and $\underset{\sim}{g}$.

5.1.1 Definition of Material Symmetries.

Let x_i denote a Cartesian <u>material</u> frame of reference which, insofar as small deformation fields are concerned, may be approximately represented by a <u>stationary</u> laboratory frame. Also let R represent all transformations

$$\bar{x} = Rx \tag{5-5}$$

or

$$\bar{x}_i = R_{ij}x_j \quad, \tag{5-6}$$

such that

$$\left|\bar{x}_i\right| = \left|x_i\right| \quad, \tag{5-7}$$

where single bars denote the norm of a vector. Evidently transformations R leave all material vectors unstretched. Also they are divisible into two irreducible classes R_- and R_+. The former involves reflection of the coordinate system about the origin (and is the only member of its class) while the latter involve rotation without reflection. All other R's can be obtained by successive application of R_+ and R_-. We note that

5-2

$$Det\left(R_-\right) = -1, \quad Det\left(R_+\right) = +1 \qquad (5\text{-}8a,b)$$

Definition

A material is said to possess symmetry with respect to a group G of transformations R if the functional F is form invariant with respect to transformations of this group. Thus in matrix notation

$$R\, F[\epsilon]R^T = F[R\epsilon R^T] \qquad (5\text{-}9)$$

5.1.2 Experimental Justification.

Condition (5-9) is appreciated most readily by considering the following experiment. Let a homogeneous strain history ϵ be applied to a specimen in a coordinate system x, and let the stress response be σ in accordance with the relation

$$\sigma = F[\epsilon] \qquad (5\text{-}10)$$

Let now another strain history $\bar{\epsilon}$ be applied to the same specimen in the same coordinate system, where $\bar{\epsilon}$ is related to the previous strain history ϵ by a transformation R of the symmetry group G. i.e.,

$$\bar{\epsilon} = R\, \epsilon R^T \qquad (5\text{-}11)$$

A material will have symmetry with respect to R if the new observed stress response $\bar{\sigma}$ is related to σ by the same transformation. i.e.,

$$\bar{\sigma} = R\, \sigma\, R^T \qquad (5\text{-}12)$$

Since the material has not changed. and the coordinate system has not changed. the function F has not changed either. Thus

$$\bar{\sigma} = F[\bar{\epsilon}] \qquad (5\text{-}13)$$

Now using Eqs. (5-11) and (5-12) in Eq. (5-13) we obtain Eq. (5-9).

Remark

Simple materials are centrosymmetric. This is evident since

$$R_- = -\delta \tag{5-14}$$

where δ is the unit matrix. Therefore condition (5-9) is satisfied for all F.

5.1.3 Definition of Isotropy.

A material is said to be isotropic if and only if constraint (5-9) is satisfied for all R_+ and, therefore, all R, in view of the above remark. The group that contains all R^+ is called the maximal group G_{max}.

Example

Equations (3-1) and (3-2) are constitutive equations of an isotropic material. To demonstrate this we note that for any R in G_{max} the response $\bar{s}$ to the strain history $\bar{\varepsilon}^p$ where

$$\bar{\varepsilon}^p = R\,\varepsilon^p R^T \tag{5-15}$$

and

$$\bar{s} = R\,s R^T \tag{5-16}$$

is given by the expression:

$$\bar{s} = \int_0^{\bar{z}_s} \rho\left(\bar{z}_s - z'\right)\frac{d\bar{\varepsilon}^p}{dz'}\,dz' \tag{5-17}$$

However, in view of Eqs. (3-7) and (3-8a), we have

$$\bar{z}_s = z_s \tag{5-18}$$

Thus

5-4

$$\bar{\underset{\sim}{s}} = \int_0^{z_s} \rho\left(z_s - z'\right)\frac{d\bar{\underset{\sim}{e}}^p}{dz'}\ dz'\ ,$$ (5-19)

and it follows that

$$R\int_0^{z_s} \rho\left(z_s - z'\right)\frac{d\underset{\sim}{e}^p}{dz'}\ dz' \qquad R^T = \int_0^{z_s} \rho\left(z_s - z'\right)\frac{d\bar{\underset{\sim}{e}}^p}{dz'}\ dz'$$ (5-20)

Hence Condition (5-9) is satisfied for all R in G_{max} insofar as the deviatoric response is concerned. The proof for the hydrostatic response follows similar lines. Thus the material is isotropic.

5.1.2 History-Induced Anisotropy.

There is a great deal of ill-defined terminology which attempts to describe perceived anisotropy by virtue of application of a history of strain or stress. Such phrases as "strain-induced" and "stress-induced" anisotropy abound. Here, we shall proceed very carefully to define the meaning of "history-induced" anisotropy.

Let a material element be isotropic in its reference state. A pre-history is a strain history of this material element, at the conclusion of which the stress tensor in the element is zero. In colloquial language such a history must involve "loading" and "unloading" since during the initial part of the history a stress is induced which must be subsequently removed. For the sake of easy reference we call that new stress-free state of the element the "subsequent" state.

It is an experimental fact that in metals which have undergone plastic deformation, the condition of isotropy. i.e.. Eq. (5-9) is violated when applied to the "subsequent" state. We show this below by recourse to Eq. (3-1) for materials that are plastically incompressible.

To this end consider the case where the material element is in its _virgin_ state i.e., _in a state prior_ to the application of the pre-history as defined above. Consider now a history $\underset{\sim}{e}^{p(1)}$ where

$$\underset{\sim}{e}^{p(1)} = \begin{pmatrix} e^p & & \\ & -\dfrac{e^p}{2} & \\ & & -\dfrac{e^p}{2} \end{pmatrix} \qquad (5\text{-}21)$$

In this case and as a result of Eq. (3-1), we can write:

$$\underset{\sim}{s}^{(1)} = \begin{pmatrix} s & & \\ & -\dfrac{s}{2} & \\ & & -\dfrac{s}{2} \end{pmatrix} \qquad , \qquad (5\text{-}22)$$

where

$$s = \int_0^z \rho(z - z') \frac{de^p}{dz'} \, dz' \quad , \qquad (5\text{-}23)$$

and for easy reference we have set $z_s \equiv z$.

This stress field is due to simple tension in direction x_1.

Consider now a history $\underset{\sim}{e}^{p(2)}$ where

$$\underset{\sim}{e}^{p(2)} = \begin{pmatrix} -\dfrac{e^p}{2} & & \\ & e^p & \\ & & -\dfrac{e^p}{2} \end{pmatrix} \qquad (5\text{-}24)$$

5-6

In this case

$$
\underset{\sim}{s}^{(2)} = \begin{bmatrix} -\dfrac{s}{2} & & \\ & s & \\ & & -\dfrac{s}{2} \end{bmatrix} \quad , \tag{5-25}
$$

which is simple tension in direction x_2.

It follows from Eqs. (5-22) and (5-25) that the stress response in the first experiment -- simple tension in direction x_1 -- is exactly the same as the stress response in the second experiment, which is again simple tension in direction x_2. This is one example where in colloquial terms the stress response is independent of the strain field orientation relative to the material. More precisely, rotation of the strain field relative to the material gives rise to the <u>same</u> rotation of the stress field relative to the material. In isotropic materials this is true of all rotations.

Consider now the case where the history $\underset{\sim}{\varepsilon}^{p(1)}$, given by Eq. (5-21), is applied to the material <u>after</u> a history $\overline{\underset{\sim}{\varepsilon}}^{p}$ has been applied, where

$$
\overline{\underset{\sim}{\varepsilon}}^{p} = \begin{bmatrix} \overline{e}^{p} & & \\ & -\dfrac{1}{2}\,\overline{e}^{p} & \\ & & -\dfrac{1}{2}\,\overline{e}^{p} \end{bmatrix} \quad , \tag{5-26}
$$

so that at the terminal point of this history (which qualifies as a prehistory) the stress $\underset{\sim}{s}$ is zero, i.e.,

$$
\underset{\sim}{s} = \overline{\underset{\sim}{s}} = \begin{bmatrix} 0 & & \\ & 0 & \\ & & 0 \end{bmatrix} \tag{5-27}
$$

Thus setting $z_s \equiv z$ for easy reference, then at $z = z_1$ (the terminal point of the prehistory) we have

$$\bar{s} = \int_0^{z_1} \rho(z_1 - z') \frac{d\bar{e}^p}{dz'} dz' = 0 \tag{5-28}$$

Note that the history $e^{p(1)}$ is again being applied to an initially stress free material which, however, now has a pre-history $\bar{e}^p$ which consists of loading and unloading in simple tension in direction x_1.

We note that now $s_1^{(1)}$, which is the deviatoric component of stress in direction x_1 after the application of the history e^p, is given by the expression:

$$s_1^{(1)} = \int_0^{z_1} \rho(z - z') d\bar{e}^p + \int_{z_1}^{z} \rho(z - z') de^p \quad , \tag{5-29}$$

where

$$\int_0^{z_1} \rho(z - z') d\bar{e}^p \begin{cases} = 0 \ , & z = z_1 \\ \neq 0 \ , & z \neq z_1 \end{cases} \tag{5-30}$$

On the other hand when history $e^{p(2)}$, given by Eq. (5-24), is now applied following the prehistory $\bar{e}^p$, it follows that

$$s_2^{(2)} = -\frac{1}{2} \int_0^{z_1} \rho(z - z') d\bar{e}^p + \int_{z_1}^{z} \rho(z - z') de^p \quad , \tag{5-31}$$

in view of Eq. (5-26).

Clearly $s_1^{(1)} \neq s_2^{(2)}$, so that rotation of the strain field in a plastically deformed metal (a material with plastic prehistory) no longer produces a mere rotation of the

5-8

stress field.   Thus the material is <u>no longer isotropic if the state with a prehistory is regarded as the initial state</u>.   Note however that the material is isotropic when referred to its virgin state.

The problem may be considered in more general terms.   From Eq. (3-1) we can write

$$\mathbf{s} = \int_0^{z_1} \rho(z - z') \, d\bar{\mathbf{e}}^P + \int_{z_1}^{z} \rho(z - z') d\mathbf{e}^P \, , \tag{5-32}$$

where $\bar{\mathbf{e}}^P$ is a pre-history in the sense that

$$\int_0^{z_1} \rho\left(z_1 - z'\right) \, d\bar{\mathbf{e}}^P = \mathbf{0} \tag{5-33}$$

With an appropriate change of variable, $z^* = z - z_1$, and noting that prior to $z = 0$ there was no prehistory, we can write:

$$\mathbf{s} = \int_{-\infty}^{0} \rho(z - z') d\bar{\mathbf{e}}^P + \int_{0}^{z} \rho(z - z') d\mathbf{e}^P \, , \tag{5-34}$$

where the star has been dropped on z^* and

$$\int_{-\infty}^{0} \rho(z - z') d\bar{\mathbf{e}}^P = 0 \tag{5-35}$$

One may write Eq. (5-34) in the form

$$\mathbf{s} = \mathbf{s}^{0} + \int_{0}^{z} \rho(z - z') d\mathbf{e}^P \quad , \tag{5-36}$$

where $\underset{\sim}{s}(0) = \underset{\sim}{0}$ but not if $z > 0$.

It follows from the definition of isotropy (Eq. (5-9)) that if the material is to be isotropic in its new reference state then

$$R \underset{\sim}{s}^o R^T = \underset{\sim}{s}^o \tag{5-37}$$

But Eq. (5-37) is possible only if $\underset{\sim}{s}^o = \underset{\sim}{0}$. However $\underset{\sim}{s}^o$ is a deviatoric tensor so that the above condition is impossible to satisfy. Thus any plastic strain prehistory will always bring about induced anisotropy relative to the "subsequent" reference state.

5.2 The Postulates of Drucker and Il'iushin.

This section is devoted to a discussion of the postulates of Drucker [5.2] and Il'iushin [5.3]. It is shown that both postulates are satisfied in the small by the endochronic plasticity theory discussed herein. Contrary to popular opinion, it is proved that both postulate have a common origin and are, in fact, variants of one and the same thermodynamic postulate.

5.2.1 The Drucker Stability Postulate.

In 1959, Drucker [5.2] introduced a "stability" postulate on the basis of a work hypothesis. The postulate states specifically that if a material is in a stress state $\underset{\sim}{\sigma}_o$, then the work performed by the extra stress in plastically deforming the material in an isothermal cycle of "application" and "removal" of stress relative to the state $\underset{\sim}{\sigma}_o$ is always positive. Thus

$$\oint_\sigma \left(\underset{\sim}{\sigma} - \underset{\sim}{\sigma}_o \right) d\underset{\sim}{\varepsilon} > 0 \quad , \tag{5-38}$$

where the subscript σ to the integral signifies a cycle that is closed with respect to stress. If $\underset{\sim}{\sigma}$ is infinitesimally close to $\underset{\sim}{\sigma}_o$ then Ineq. (5-38) becomes

$$\oint_{\sigma_o} d\sigma \cdot d\varepsilon > 0 \quad , \tag{5-39}$$

which is a statement of positive work by an infinitesimal stress increment in an infinitesimal closed <u>stress</u> cycle (in the sense that upon completion of the cycle the stress state is σ_o).

Evidently this postulate cannot admit softening materials since a closed stress cycle in such materials cannot be performed. However in the case of hardening materials with a yield surface, the above postulate gives rise to some definitive results as demonstrated in Ref. [5.3]. There, it is shown that the yield surface must be convex and that the plastic strain increment must be normal to the yield surface in stress space.

In Figure 5.1 we give the initial and subsequent yield surface (at its outermost point prior to unloading) in connection with a cyclic stress path that originates and terminates at the point O by means of "application" and "removal" of stresses in the sense of Drucker i.e., during application

$$\frac{\partial G}{\partial \sigma} \cdot d\sigma > 0 \quad , \tag{5-40}$$

while during removal

$$\frac{\partial G}{\partial \sigma} \cdot d\sigma \leq 0 \quad , \tag{5-41}$$

where

$$G\left(\sigma, g_r\right) = 0 \tag{5-42}$$

is the equation for the yield surface. g_r being structural parameters or internal variables. Thus the "removal of stress" designates a stress path which lies totally within the yield surface. We note that since O is <u>within</u> the subsequent yield surface (this is an important consideration), the work done in going from B to O is independent of the path. Thus
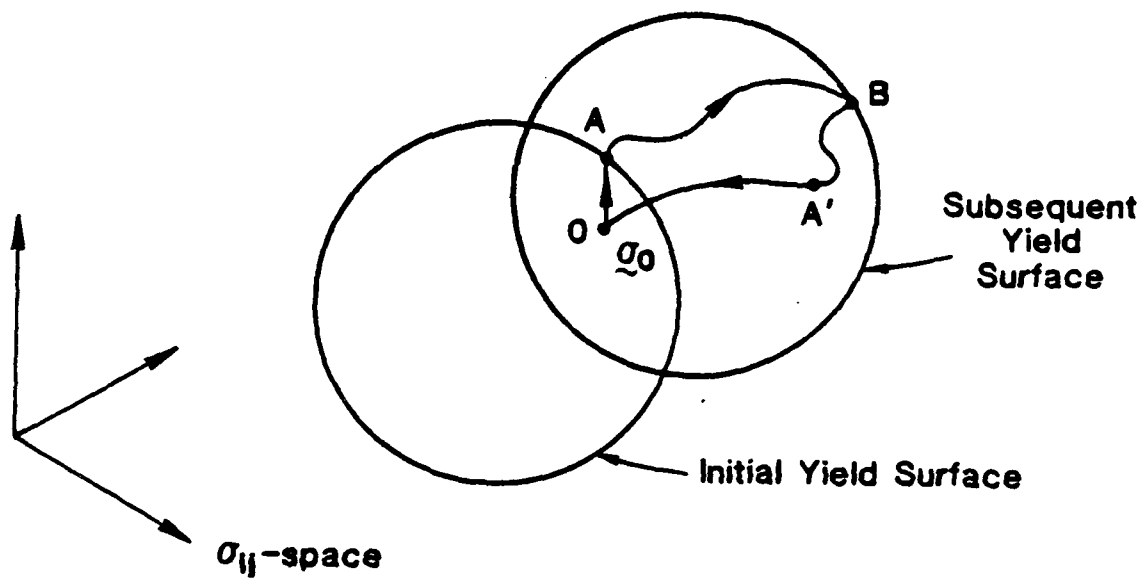
Figure 5.1. A closed cycle in stress space.
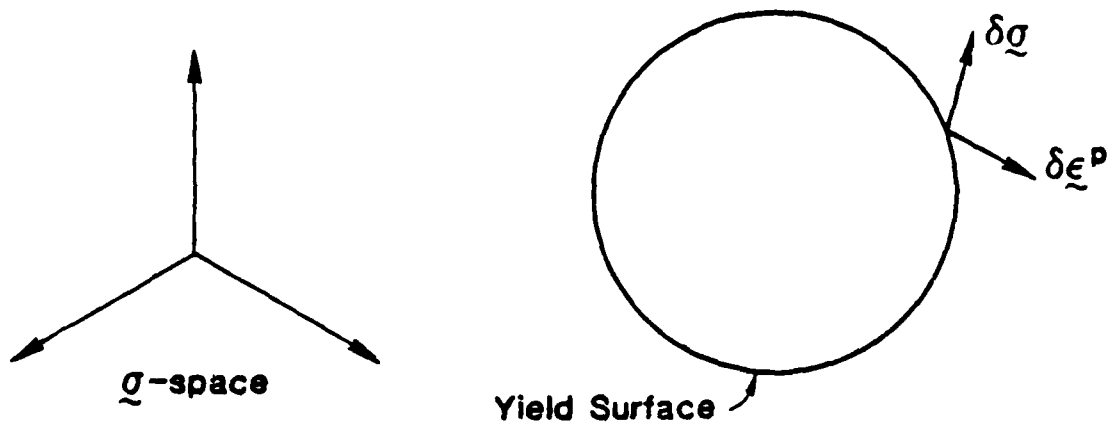
Figure 5.2. Violation of Ineq. (5-47).

$$\int_{BA'0} (\mathbf{g} - \mathbf{g}_o) \cdot d\mathbf{\xi} = \int_{BA0} (\mathbf{g} - \mathbf{g}_o) \cdot d\mathbf{\xi} \tag{5-43}$$

and

$$\oint_\sigma (\mathbf{g} - \mathbf{g}_o) \cdot d\mathbf{\xi} = \int_A^B (\mathbf{g} - \mathbf{g}_o) \cdot d\mathbf{\xi} + \int_B^A (\mathbf{g} - \mathbf{g}_o) \cdot d\mathbf{\xi} \tag{5-44}$$

But since the path BA is totally within the yield surface, $d\mathbf{\xi} = d\mathbf{\xi}^e$, and thus, using Eq. (5-44):

$$\oint_\sigma (\mathbf{g} - \mathbf{g}_o) \cdot d\mathbf{\xi} = \int_A^B (\mathbf{g} - \mathbf{g}_o) \cdot d\mathbf{\xi}^P \tag{5-45}$$

for any path AB such that O is within the subsequent yield surface. Thus the Drucker inequality requires that

$$\int_A^B (\mathbf{g} - \mathbf{g}_o) \, d\mathbf{\xi}^P > 0 \quad , \tag{5-46}$$

provided that the material possess a yield surface and the point of origin of the cycle lies within the subsequent yield surface.

Note that elastoplastic coupling is not admitted (in the sense of elastic properties being influenced by plastic deformation) otherwise on the return path BAO, the elastic work from A to O is not equal to its counterpart from O to A. However more will be said about this later. .

Drucker's argument of normality and convexity is two-fold. We repeat it here for the benefit of the reader. We shall limit ourselves to the associated flow rule, i.e., the case where the plastic potential and the yield function have the same form to within a constant of proportionality.

The fundamental hypothesis of classical plasticity is that the direction of the increment of plastic strain depends on the previous history of stress but is independent of the direction of the current stress increment.

With this in mind. we shall show that Eq. (5-46) is central to the geometric demonstration of convexity and normality.

(i)   To show normality. set $\sigma_o = \sigma_A$ and let σ be infinitesimally close to σ_A. Then Ineq. (5-46) becomes:

$$(\underline{\sigma} - \underline{\sigma}_A) \cdot \delta\underline{\varepsilon}^P > 0 \tag{5-47a}$$

or

$$\delta\underline{\sigma} \cdot \delta\underline{\varepsilon}^P > 0 \tag{5-47b}$$

Note that. for this form of the inequality. the question of elastoplastic coupling is irrelevant since the branch OA in Fig. (5.1) is missing and B is infinitesimally close to A so that the elastic properties are calculated at A.

With regard now to Fig. (5.2) it may be seen that if $\delta\underline{\varepsilon}^P$ is not normal to the surface. a stress increment $\delta\underline{\sigma}$ can always be found to violate Ineq. (5-47) since the direction of $\delta\underline{\varepsilon}^P$ is independent of the direction of $\delta\underline{\sigma}$. Thus $\delta\underline{\varepsilon}^P$ must be normal to the yield surface.

(ii) To show convexity. again recall Ineq. (5-46). and let B be infinitesimally close to A. It then follows (to a first order of magnitude) that

$$(\underline{\sigma}_A - \underline{\sigma}_o) \cdot \delta\underline{\varepsilon}^P > 0 \tag{5-48}$$

With regard to Fig. 5.3 it is evident that a yield surface cannot be concave since a stress vector $\underline{\sigma}_A - \underline{\sigma}_o$ can always be found which violates Ineq. (5-48).

Again. note that the question of elastoplastic coupling is irrelevant since B is infinitesimally close to A so that any change in elastic properties is of second order in $||\delta\underline{\varepsilon}^P||$ as opposed to the first order validity (in $||\delta\underline{\varepsilon}^P||$) of Ineq. (5-48).
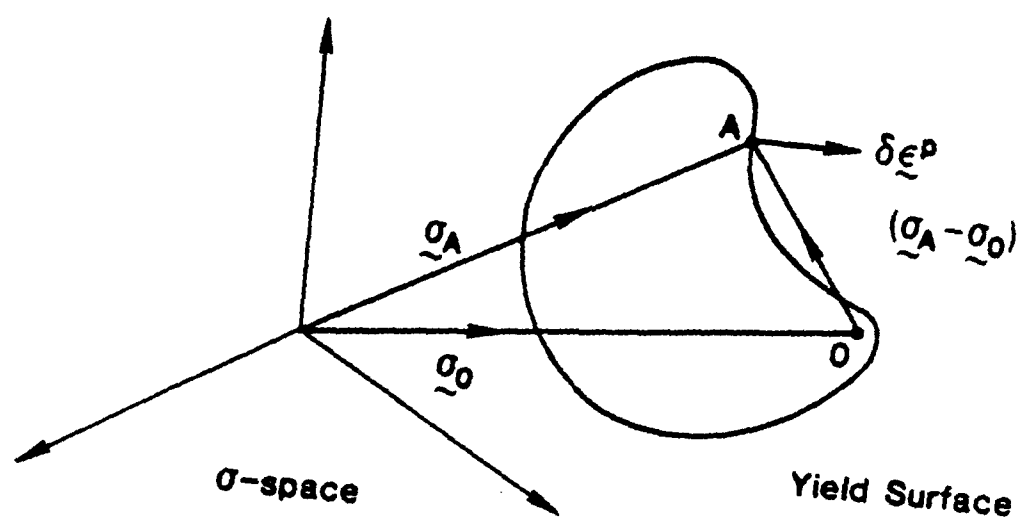
Figure 5.3. Violation of Ineq. (5-48).

5-15

5.2.2 Drucker's Postulate and Endochronic Plasticity.

In Chapters 2 and 3 we dealt with two constitutive equations of endochronic plasticity, one with a finite yield surface and one without. On the other hand, we showed in Chapter 3 that the latter model can be approximated to any desired degree of accuracy by an infinitesimal kinematic hardening surface. Thus it may be represented by a constitutive equation of the type

$$\underset{\sim}{s} = s_o \frac{d\underset{\sim}{e}^p}{dz} + \int_0^z \rho_1(z - z')\frac{d\underset{\sim}{e}^p}{dz'} dz' \quad , \tag{5-49}$$

where s_o is of infinitesimal magnitude and ρ_1 is well behaved at the origin, i.e., $\rho_1(o) < \infty$.

The response associated with Eq. (5-49) is discussed in Section 6 of Chapter 3, where it is shown (Eq. (3-219)) that given a stress increment $d\underset{\sim}{s}$ such that

$$\left(\underset{\sim}{s} - \underset{\sim}{a}\right) \cdot d\underset{\sim}{s} > 0 \quad , \tag{5-50}$$

where

$$\underset{\sim}{a} = \int_0^z \rho_1(z - z')\frac{d\underset{\sim}{e}^p}{dz'} dz' \quad . \tag{5-51}$$

The corresponding value of $d\varsigma$. (i.e., an increment $d\underset{\sim}{s}$ which constitutes loading), which is non-negative and positive when Eq. (5-50) applies, is given in Eq. (3-219) whereby

$$H d\varsigma = \frac{\left(\underset{\sim}{s} - \underset{\sim}{a}\right) \cdot d\underset{\sim}{s}}{s_o F_s} \quad , \tag{5-52}$$

s_o being the initial radius of the yield surface and F_s the deviatoric hardening junction. The function H is given by Eq. (3-220) i.e.,

$$H = \rho_1(0) + s_o F'_s + \frac{(\underset{\sim}{s} - \underset{\sim}{a}) \cdot \underset{\sim}{b}}{s_o F_s^2} \tag{5-53}$$

in the notation of Section 3.6, where it was shown that H is always positive provided that

$$F'_s = \frac{dF_s}{d\varsigma} \geq 0 \quad , \tag{5-54}$$

i.e., no softening is permitted to take place in the course of plastic deformation.

If, on the other hand,

$$(\underset{\sim}{s} - \underset{\sim}{a}) \cdot d\underset{\sim}{s} \leq 0 \quad , \tag{5-55}$$

it was shown in Section 3.6 that $d\varsigma = 0$ and the deformation is elastic. Thus Ineq. (5-50) is always satisfied in the course of plastic deformation. It was also shown (Eq. (3-212)) that

$$d\underset{\sim}{e}^p = \frac{d\varsigma}{s_o F_s} (\underset{\sim}{s} - \underset{\sim}{a}) \tag{5-56}$$

Thus in view of Ineq. (5-50), and Eq. (5-56), we can write:

$$d\underset{\sim}{e}^p \cdot d\underset{\sim}{s} = \frac{d\varsigma}{s_o F_s}(\underset{\sim}{s} - \underset{\sim}{a}) \cdot d\underset{\sim}{s} > 0 \tag{5-57}$$

Therefore, the local form of Drucker's inequality is satisfied.

5.2.3 Il'iushin's Postulate and Endochronic Plasticity.

This postulate [5.3] states that positive work is done in an isothermal closed cycle of strain, during which plastic strain takes place. Thus

$$W = \oint_\epsilon \underset{\sim}{\sigma} \cdot d\underset{\sim}{\epsilon} > 0 \tag{5-58}$$

Il'iushin demonstrated [5.3] that in the context of a plasticity theory where the yield surface is defined in strain space the postulate is sufficient to establish convexity of the surface and normality of the increment of plastic strain to the yield surface.

In this section we demonstrate that the endochronic theory of plastically incompressible solids satisfies the Il'iushin postulate when the stress and/or strain fields are one-dimensional. Specifically in Fig. 5.4, we show a plot of shear stress s versus shear strain e for a history of homogeneous deformation where the strain increases monotonically from zero to a value e_A at point A, decreases to a value e_B at point B and then increases again to its previous value e_A at point C. The Il'iushin postulate requires that according to Eq. (5-58):

$$\oint_e s\,de > 0 \tag{5-59}$$

In the case of a constant (positive) elastic shear modulus unaffected by plastic deformation, as is substantially the case in metals, we can write

$$\oint_e s\,de^e = \frac{1}{2\mu_0} \oint_e s\,ds , \tag{5-60}$$

where e^e is the elastic shear strain. Therefore, to satisfy the Il'iushin postulate it suffices to show that

$$\oint_e s\,de^p + \frac{1}{2\mu_0} \oint_e s\,ds > 0 \tag{5-61}$$

However we note that neither of the above integrals is closed with respect to itself, in the sense that

$$s_A \neq s_0 \quad ; \quad e_A^p \neq e_C^p , \tag{5-62}$$

a fact that makes the first integrqal in Ineq. (5-61) difficult to evaluate.
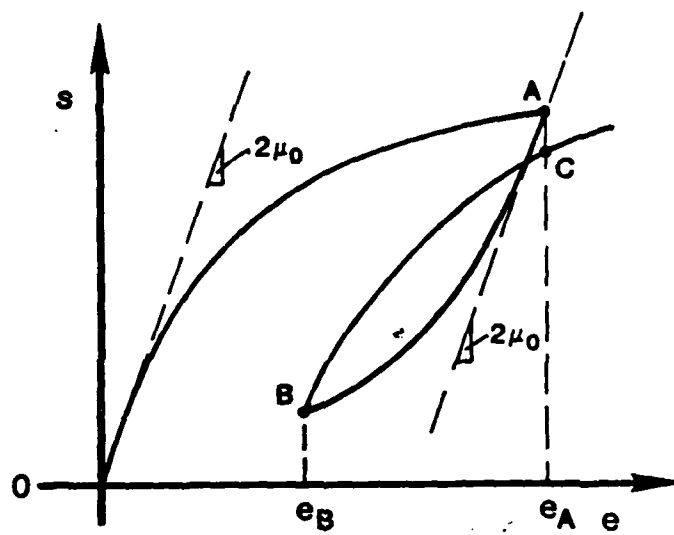
Figure 5.4. An Il'iushin cycle.

The difficulty is avoided by reference to Chapter 2 where it was demonstrated that the constitutive response of a plastic solid in shear consists of the series superposition of an elastic and a rigid plastic solid as illustrated in Fig. 2.1. Therefore insofar as the essential constitutive characteristics of the theory are concerned one need only apply the Il'iushin principle to the rigid plastic solid. i.e., the constitutive equation (2-87). whereby

$$s = \int_0^z \rho(z - z') \frac{de^p}{dz'} \, dz' \tag{5-63}$$

The intention, therefore, is to show that

$$\oint_{e^p} s \, de^p > 0 \quad , \tag{5-64}$$

in the presence of the constitutive Eq. (5-63). in accordance with Fig. 5.5 where e^p has been denoted by θ for convenience of notation.

Furthermore, in that which follows. we shall limit ourselves to the case where

$$F(z) = 1. \tag{5-65}$$

i.e., no hardening takes place during the deformation process.

Analytical Demonstration of Ineq.(5-64).

The history of θ versus z for the strain history shown in Fig. 5.5 is depicted in Fig. 5.6. where θ stands for e^p.

Loading takes place in the range $z \leq z \leq z_A$. while unloading in the range $z_A < z \leq z_B$. Reloading occurs in the range $z_B < z < \infty$. The end point of reloading is z_0. We consider each of the phases below in detail.
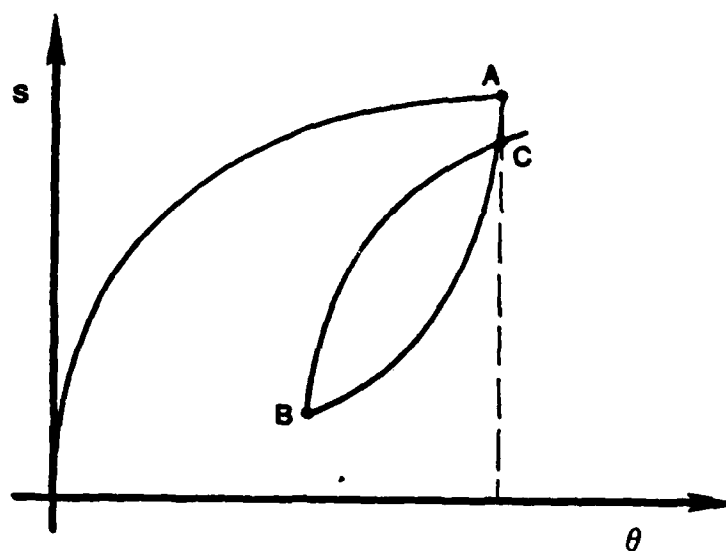
Figure 5.5.   A closed strain cycle.
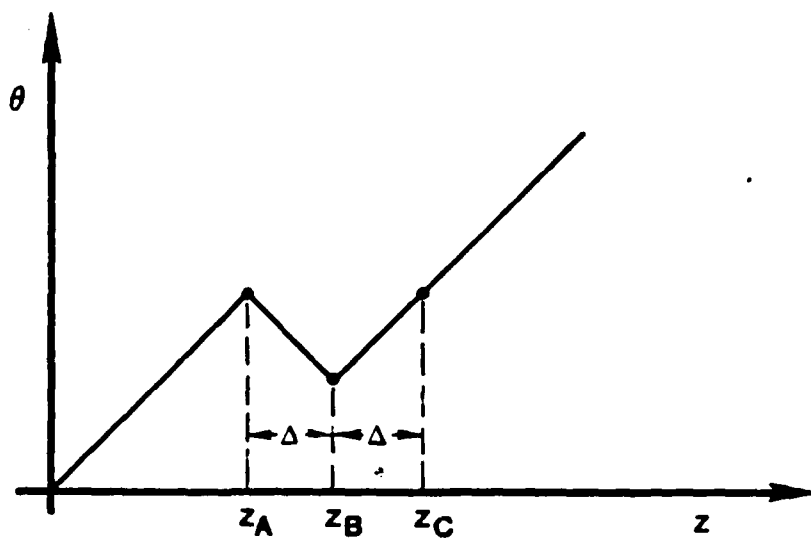
Figure 5.6.   History of θ versus z.

(i)   Loading: $d\theta/dz = 1, \; 0 \leq \; < \; \leq z_A$

In this case Eq. (5-63) gives the following relation for the shear stress:

$$s = M(z) = M(\theta): \; s_A = M(z_A) = M(\theta_A) \quad . \tag{5-66}$$

where in the notation of Chapter 3

$$M(z) = \int_0^z \rho(z')dz' \tag{5-67}$$

(ii)   Unloading: $\dfrac{d\theta}{dz} = 1, \; 0 \leq z \leq z_A, \quad \dfrac{d\theta}{dz} = -1 \; , \; z_A < z \leq z_B.$

Again, using Eq. (5-63)

$$s = M(z) - 2M(z - z_A) \quad , \tag{5-68}$$

where in view of Fig. 5.6

$$z = 2\theta_A - \theta. \quad z_A = \theta_A \tag{5-69}$$

Setting:

$$\theta_1 - \theta = x \quad . \tag{5-70}$$

it follows from Eq. (5-68) that

$$s_U = M(\theta_1 + x) - 2M(x) \; . \tag{5-71}$$

where the suffix U designates the functional dependence of s on x during unloading.

(iii)   Reloading:

$$\dfrac{d\theta}{dz} = 1 \; , \; 0 \leq z \leq z_A; \; z_B < z < \infty \; , \; \dfrac{d\theta}{dz} = -1 \; , \; z_A < z \leq z_B$$

Again. using Eq. (5-63) in conjunction with the above values of $d\theta/dz$ one finds that

$$s = M(z) - 2M(z - z_A) + 2M(z - z_B) \quad , \tag{5-72}$$

where

$$z_A = \theta_A \ ; \ z_B = 2\theta_A - \theta_B \ ; \tag{5-73}$$

$$z - z_A = \theta + \theta_A - 2\theta_B \ , z - z_B = \theta - \theta_B \tag{5-74}$$

Setting

$$y = \theta - \theta_B \ , \quad \Delta = \theta_B - \theta_A \quad \left(\theta \geq \theta_2\right) \quad , \tag{5-75}$$

one obtains the following expression for s

$$s_R = M\left(y + \Delta + \theta_A\right) - 2M\left(y + \Delta\right) + 2M(y) \quad , \tag{5-76}$$

where the suffix R designates the dependence of s on y during reloading.

We now note that

$$x + y = \Delta \tag{5-77}$$

Thus in terms of y

$$s_U = M(\theta_A + \Delta - y) - 2M(\Delta - y) \tag{5-78}$$

To prove that Eq. (5-63) satisfies the Il'iushin postulate it is necessary and sufficient to show that the integral I. where

$$I = \int_0^\Delta \left(s_R - s_U\right) dy \tag{5-79}$$

is positive for all $\Delta < \infty$, i.e.,

$$I = \int_0^\Delta \left(s_R - s_U\right) dy > 0 \tag{5-80}$$

To this end let x be a running variable and M^* the integral of $M(x)$. i.e..

$$M^*(\Delta) = \int_0^\Delta M(x)\,dx \qquad (5\text{-}81)$$

It then follows that. in view of Eq. (5-76)

$$\int_0^\Delta s_R\,dy = M^*\big(2\Delta + \theta_A\big) - M^*\big(\Delta + \theta_A\big)$$

$$- 2M^*(2\Delta) + 4M^*(\Delta) \qquad (5\text{-}82)$$

and

$$\int_0^\Delta s_U\,dy = M^*\big(\theta_A + \Delta\big) - M^*\big(\theta_A\big) - 2M^*(\Delta) \qquad (5\text{-}83)$$

Now since $I(0) = 0$. it follows that to prove that $I(\Delta)$ is positive for all $\Delta < \infty$. it is sufficient to show that

$$\frac{dI}{d\Delta} > 0 \quad , \quad \Delta < \infty , \qquad (5\text{-}84)$$

i.e.,

$$6M(\Delta) - 4M(2\Delta) +$$

$$+ M\big(2\Delta + \theta_A\big) - 2M\big(\Delta + \theta_A\big) + M\big(\theta_A\big) > 0 \qquad (5\text{-}85)$$

But $M(x)$ is a <u>convex function</u> in the sense that:

$$M(x - a) - M(x) > M(x) - M(x + a) \qquad (5\text{-}86)$$

for all $x \geq 0$, $a \leq x$. Therefore

$$M(x - a) - 2M(x) + M(x + a) > 0 \tag{5-87}$$

Thus letting $x = \Delta + \theta_A$; $a = \Delta$, it follows that

$$M(2\Delta + \theta_A) - 2M(\Delta + \theta_A) + M(\theta_A) > 0 \tag{5-88}$$

To prove Ineq. (5-85) it remains to show that

$$3M(\Delta) > 2M(2\Delta) \tag{5-89}$$

This of course is a constraint on the stress strain curve.

Specifically with reference to kernels of the type given by the following expression (which are valid near the origin and are therefore appropriate for infinitesimal cycles)

$$\rho(z) = \rho_o z^{-a} \tag{5-90}$$

one obtains

$$M(\Delta) = \frac{\rho_o}{\beta} \Delta^\beta \ , \quad \beta = 1 - a \tag{5-91}$$

Thus for such kernels, and in view of Ineq. (5-89), we have

$$2^\beta < \frac{3}{2} \tag{5-92}$$

or

$$\beta < 0.585; \ a > 0.415 \tag{5-93}$$

Note that for infinitesimal cycles this is a necessary and sufficient condition that the Il'iushin postulate is satisfied. Generally for metals, $0.8 < a < 0.9$ so that the above constraint is always satisfied.

5.2.4 Hysteresis Loop Closure.

Hysteresis loop closure in the context of a one-dimensional stress-strain response is the condition in which the reloading curve emanating from point B in Figure 5.5 lies above the unloading curve AB. Experimental observation indicates that this behavior is characteristic of dissipative, rate-insensitive solids. A perusal of Figure 5.5 shows that closure is a <u>necessary</u> condition for the satisfaction of Il'iushin's inequality. Thus, since we have already demonstrated that the endochronic theory satisfies Il'iushin's Postulate, in one dimension, we have also demonstrated that the model also exhibits closure of hysteresis loops in a one-dimensional stress-strain space.

5.3 The Thermodynamically Conjugate Postulates of Drucker and Il'iushin.

In this section, the thermodynamic conjugacy of the Drucker and Il'iushin postulates is demonstrated by showing that they can be derived from a single thermodynamic postulate which is stated below.

5.3.1 A Thermodynamic Postulate.

Consider the following thermodynamic postulate:

"The irreversible entropy production during an isothermal cycle, closed either with respect to stress or strain, is greater than the free energy released during the cycle."

Stated analytically, the above postulate is given by the expression:

$$\theta \Delta \gamma > - \Delta \text{ (Free energy)}, \tag{5-94}$$

where θ is the temperature, γ the irreversible entropy and Δ denotes the net change measured at the completion of the cycle.

It must be emphasized that Ineq. (5-94) is a postulate and not a fundamental thermodynamic requirement, insofar as we know at the present time.

<u>The Gibbs Formulation.</u>

In this case the independent variables are the stress and the internal variables q_r, and the free energy is the Gibbs free energy ϕ. Thus Ineq. (5-94) becomes

$$\theta \Delta \gamma \; > \; - \; \Delta \phi \qquad\qquad\qquad (5\text{-}95)$$

or

$$\theta \oint_\sigma d\gamma \; > \; - \; \oint_\sigma d\phi \quad , \qquad\qquad\qquad (5\text{-}96)$$

which may be written as

$$\theta \oint_\sigma d\gamma \; > \; - \; \oint_\sigma \left[\frac{\partial \phi}{\partial \sigma} \cdot d\sigma + \frac{\partial \phi}{\partial g_r} \cdot dg_r \right] \qquad\qquad (5\text{-}97)$$

But

$$- \frac{\partial \phi}{\partial g_r} \cdot dg_r \; = \; \theta \; d\gamma \qquad\qquad\qquad (5\text{-}98)$$

and

$$\xi \; = \; - \; \partial \phi / \partial \sigma \quad , \qquad\qquad\qquad (5\text{-}99)$$

so that Ineq. (5-98) reduces to the form

$$- \oint_\sigma \xi \cdot d\sigma \; > \; 0 \quad , \qquad\qquad\qquad (5\text{-}100)$$

which says that the net complementary work during a stress cycle must be negative. Or more generally

$$- \oint_\sigma \left(\xi - \xi_o \right) \cdot d\sigma \; > \; 0 \qquad\qquad\qquad (5\text{-}101)$$

for any $\underset{\sim}{\varepsilon}_0$ since $\int_\sigma d\underset{\sim}{\sigma} = 0$. Or more generally still

$$-\oint_\sigma \left(\underset{\sim}{\varepsilon} - \underset{\sim}{\varepsilon}_0\right) \bullet d\left(\underset{\sim}{\sigma} - \underset{\sim}{\sigma}_0\right) > 0 \qquad (5\text{-}102)$$

for any $\underset{\sim}{\sigma}_0$ which is constant and which here is the point of origin of the stress cycle.

We now integrate the lefthand side of Ineq. (5-102) by parts to obtain

$$\left(\underset{\sim}{\varepsilon} - \underset{\sim}{\varepsilon}_0\right) \bullet \left(\underset{\sim}{\sigma} - \underset{\sim}{\sigma}_0\right) \Bigg|_{\sigma_0}^{\sigma_0} + \oint_\sigma \left(\underset{\sim}{\sigma} - \underset{\sim}{\sigma}_0\right) \bullet d\left(\underset{\sim}{\varepsilon} - \underset{\sim}{\varepsilon}_0\right) > 0 \qquad (5\text{-}103)$$

Since the lefthand side is zero and $\underset{\sim}{\varepsilon}_0$ is constant, it follows that

$$\oint_\sigma \left(\underset{\sim}{\sigma} - \underset{\sim}{\sigma}_0\right) \bullet d\underset{\sim}{\varepsilon} > 0 \ , \qquad (5\text{-}104)$$

which is the Drucker postulate [5.2].

Thus, contrary to a number of previous statements, some by Drucker himself [5.2], the Drucker Postulate is, in fact, a consequence of a thermodynamic inequality which states that in the course of a thermodynamic cycle, isothermal and closed with respect to stress, the increment in dissipation is greater in value than the decrement in the Gibbs free energy.

The Helmholtz Formulation.

In this case, the independent variables are the strain and the internal variables g_r, and the free energy is the Helmholtz free energy ψ. Thus Eq. (5-94) becomes

$$\theta \, \Delta\phi > - \Delta\psi \qquad (5\text{-}105)$$

or

$$\theta \oint_{\underline{\xi}} d\gamma > - \oint_{\underline{\xi}} d\psi \quad , \tag{5-106}$$

which can be written in the form:

$$\theta \oint d\gamma > - \oint \left(\frac{\partial \psi}{\partial \underline{\xi}} \cdot d\underline{\xi} + \frac{\partial \psi}{\partial g_r} \cdot dg_r \right) \tag{5-107}$$

But

$$\theta \, d\gamma = - \frac{\partial \psi}{\partial g_r} \cdot dg_r \tag{5-108}$$

and

$$\underline{g} = \frac{\partial \psi}{\partial \underline{\xi}} \tag{5-109}$$

Thus Ineq. (5-107) becomes

$$\oint_{\underline{\xi}} \underline{g} \cdot d\underline{\xi} > 0 \tag{5-110}$$

which is the Il'iushin postulate [5.3]. Now since $\oint d\underline{\xi} = 0$, Eq. (5-110) can be re-expressed as the "modified" Il'iushin postulate in the form:

$$\oint_{\underline{\xi}} \left(\underline{g} - \underline{g}_o \right) \cdot d\underline{\xi} > 0 \tag{5-111}$$

Thus the "modified" Il'iushin postulate requires that the "work done by an external agency in the course of a closed <u>strain</u> cycle be positive.

5-30

Specifically if g_0 is close to g we have the following local. modified form of the Il'iushin postulate:

$$\oint_\epsilon \delta g \cdot \delta \xi > 0 ,$$ (5-112)

which is the "conjugate" of the Drucker postulate in its local form. given by Ineq. (5-47).

We illustrate the physical meaning of the above postulates in the following section by means of a stress-strain diagram in the case of a simple elastic-perfectly plastic solid. shown in Figure 5.7.

5.3.2 Thermodynamics of an Elastic-Perfectly Plastic Solid.

Let the spring stiffness be E and the frictional resistance of the block be b. The Helmholtz free energy is the strain energy stored in the spring so that

$$\psi = \frac{1}{2} E\left(\epsilon^e\right)^2 = \frac{1}{2} \frac{\sigma^2}{E}$$ (5-113)

or

$$\psi = \frac{1}{2} E(\epsilon - q)^2$$ (5-114)

The stress σ is given by the expression

$$\sigma = \frac{\partial \psi}{\partial \epsilon} = E(\epsilon - q)$$ (5-115)

which is of course as it should be since ϵ^e is equal to $\epsilon - q$.

The Gibbs free energy ϕ is related to ψ by the expression:

$$\phi = \psi - \sigma\epsilon$$ (5-116)

where ϕ is a function of σ and q. Thus using Eqs. (5-113) and (5-115) in Eq. (5-116). it follows that

5-31
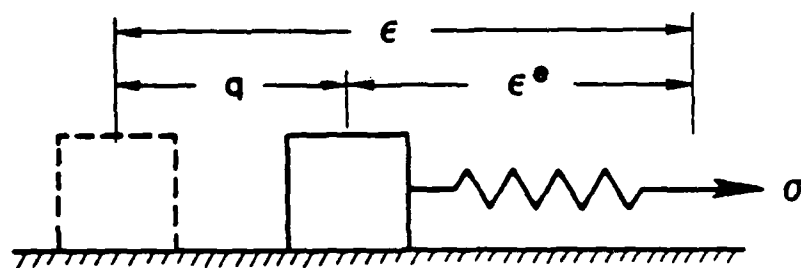
Figure 5.7. An elastic-perfectly plastic solid.

$$\phi = - \frac{1}{2} \frac{\sigma^2}{E} - \sigma q \qquad (5\text{-}117)$$

We may now use the thermodynamic equations associated with ϕ. i.e..

$$\epsilon = - \frac{\partial \phi}{\partial \sigma} \ , \quad \frac{\partial \phi}{\partial q} + b \frac{dq}{dz} = 0 \quad , \qquad (5\text{-}118a,b)$$

where

$$dz = \left| d\epsilon^p \right| \qquad (5\text{-}119)$$

$$d\epsilon^p = d\epsilon - d\epsilon^e = dq \qquad (5\text{-}120)$$

and use was made of Eq. (5-115) in Eq. (5-120). Thus

$$dz = |dq| \qquad (5\text{-}121)$$

In view of Eqs. (5-118a.b)

$$\epsilon = \frac{\sigma}{E} + q \qquad (5\text{-}122)$$

$$\sigma = b \frac{dq}{dz} \qquad (5\text{-}123)$$

Thus using Eqs. (5-120) and (5-123)

$$\sigma = b \frac{d\epsilon^p}{dz} \qquad (5\text{-}124)$$

Equation (5-124) is the endochronic constitutive equation of an elastic-perfectly plastic solid.

The Dissipation

We recall the relation

$$\theta d\gamma = - \frac{\partial \phi}{\partial q} dq , \qquad (5-125)$$

where $\theta d\gamma$ (the temperature multiplied by an increment in irreversible entropy) is equal to dD where D is the dissipation. Note that

$$dD = \theta d\gamma = \sigma dq = \sigma d\epsilon^p , \qquad (5-126)$$

by virtue of Eqs. (5-117). (5-120) and (5-125). Thus in this simple model the dissipation D is equal to the plastic work W^p, i.e.,

$$D = W^p = \int \sigma d\epsilon^p \qquad (5-127)$$

The Gibbs Type Postulate of Drucker.

We now return to the illustration of the postulates of the Gibbs type (to which the Drucker postulate belongs) by means of stress-strain diagram of the simple elastic-perfectly plastic solid. as shown in Figure 5.8.

Consider first the meaning of Ineq. (5-94). In view of Eq. (5-127) we note that $\theta \Delta \gamma$ is equal to the plastic work done during the cycle i.e.,

$$\theta \Delta \gamma = \text{Area } (B'BCC')$$
$$\qquad\qquad\qquad\qquad (5-128)$$
$$= \text{Area } (A'BCD')$$

On the other hand. we can write:

$$\Delta \phi = \phi_D - \phi_A = - \sigma \left(\epsilon_D^p - \epsilon_A^p \right) , \qquad (5-129)$$

in view of Eqs. (5-117) and (5-120).
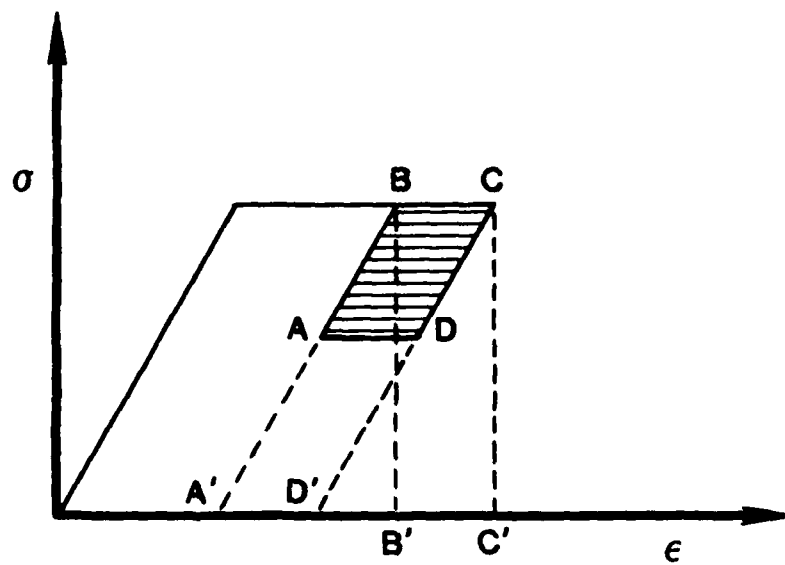
Figure 5.8.   A Drucker cycle, ABCD, for an elastic-perfectly plastic solid.

Thus

$$- \Delta\phi = \text{Area } (A'ADD')$$

Therefore. Ineq. (5-94) states that

$$\text{Area } (A'BCD') > \text{Area } A'ADD' . \tag{5-130}$$

or that

$$\text{Area } (ABCD) > 0 . \tag{5-131}$$

which is Drucker's postulate since

$$\text{Area } (ABCD) = \oint_\sigma (\sigma - \sigma_A) d\epsilon \tag{5-132}$$

The Helmholtz-Type Postulate of Il'iushin.

We now illustrate the postulates of the Helmholtz type (to which the Il'iushin postulate belongs) by means of a stress-strain diagram of the simple elastic-perfectly plastic solid. as shown in Figure 5.9. The thermodynamics. in this case. is simple. The free energy ψ is given by Eq. (5-114) and the stress σ by Eq. (5-115). The evolution equation for q is now

$$b \frac{dq}{dz} + \frac{\partial\psi}{\partial q} = 0 \tag{5-133}$$

Thus

$$\sigma = b \frac{dq}{dz} = b \frac{d\epsilon^P}{dz} \tag{5-134}$$

as before.

Also

$$\theta d\eta = dD = - \frac{\partial\psi}{\partial q} dq = \sigma dq = \sigma d\epsilon^P \tag{5-135}$$
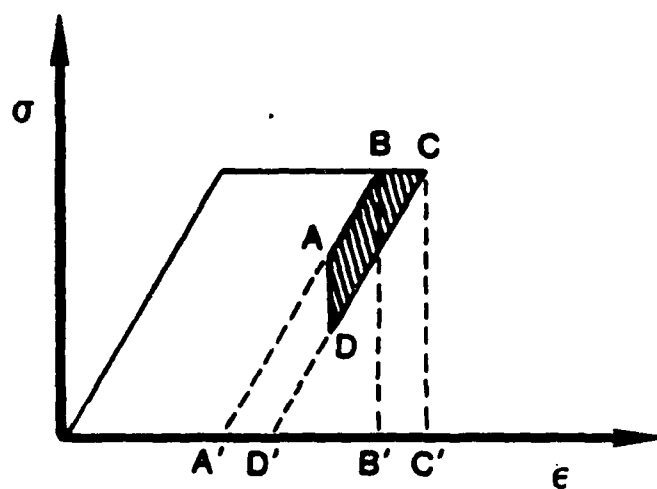
SCA-1696

Figure 5.9. An Il'iushin cycle, ABCD, for an elastic-perfectly plastic solid.

and thus:

$$dD = dW_p = \sigma d\epsilon^P \qquad (5\text{-}136)$$

as before.

We now return to Ineq. (5-105). Evidently

$$\theta \Delta \gamma = \Delta D = \text{Area } (B'BCC') = \text{Area } (A'BCD'), \qquad (5\text{-}137)$$

in view of Eq. (5-136). On the other hand, we have

$$\Delta \psi = \frac{1}{2E}\left[\sigma_D^2 - \sigma_A^2\right]$$

Thus by inspection:

$$\Delta D = \text{Area } (A'BCD') > -\Delta \psi = \text{Area } (A'ADD') \qquad (5\text{-}138)$$

or

$$\text{Area } (A'BCD') - \text{Area } (A'ADD') = \text{Area } (ABCD) > 0 \qquad (5\text{-}139)$$

which is the Il'iushin postulate.

We have thus proved and demonstrated by means of a simple example that the Il'iushin and Drucker postulates are conjugate versions of one and the same thermodynamic inequality, i.e., Ineq. (5-94).

5.4 The Question of Uniqueness.

The question of uniqueness of the solution to the initial and boundary value problems is always paramount in constitutive theories. Models that appear perfectly satisfactory in describing the stress response to homogeneous strain histories may give rise to ill-posed boundary and/or initial value problems. The question was discussed *in some detail by Valanis in Ref. [5.5], where the reader is referred.* In this reference, Valanis introduced the concept of a "positive material model". Uniqueness proofs relying on an inequality, such as that which chracterizes a positive material

model, have been given by other authors for the <u>static</u> boundary value problem. See, for instance, Refs. [5.6] and [5.7]. The importance of the concept lies in the fact that if a constitutive equation gives rise to a positive material model, then the boundary and initial value problems associated with the constitutive equation have unique solutions.

5.4.1 Definition of a Positive Material Model.

Let $\sigma_{ij}(x_k,t)$ be a stress field which is continuous and differentiable in x_k and t: also let $u_i(x_k,t)$ be a displacement field which is continuous and differentiable in x_k and twice differentiable in t. Furthermore let σ_{ij} and u_i satisfy Newton's law of motion. At this point we introduce the following notation:

$$\delta\sigma_{ij} \stackrel{\text{def}}{=} \sigma_{ij}(t + \delta t) - \sigma_{ij}(t)$$

$$\hspace{10cm} \text{(5-140)}$$

$$\delta u_i \stackrel{\text{def}}{=} u_i(t + \delta t) - u_i(t)$$

Now let $\sigma_{ij}^{(1)}$ and $\sigma_{ij}^{(2)}$ on one hand and $\epsilon_{ij}^{(1)}$ and $\epsilon_{ij}^{(2)}$ on the other, be two stress fields and two strain fields respectively that are solutions to the initial (or boundary) value problem. A material model is then said to be <u>positive</u> if

$$\left[\dot{\sigma}_{ij}^{(2)} - \dot{\sigma}_{ij}^{(1)}\right]\left[\dot{\epsilon}_{ij}^{(2)} - \dot{\epsilon}_{ij}^{(1)}\right] > 0 \quad , \hspace{3cm} \text{(5-141a)}$$

whenever $||\dot{\underset{\sim}{\sigma}}^{(2)} - \dot{\underset{\sim}{\sigma}}^{(1)}||$ and $||\dot{\underset{\sim}{\epsilon}}^{(2)} - \dot{\underset{\sim}{\epsilon}}^{(1)}||$ are different from zero, or <u>equivalently</u> if

$$\left[\delta\sigma_{ij}^{(2)} - \delta\sigma_{ij}^{(1)}\right]\left[\delta\epsilon_{ij}^{(2)} - \delta\epsilon_{ij}^{(1)}\right] > 0 \quad , \hspace{2.5cm} \text{(5-141b)}$$

whenever $||\delta\underset{\sim}{\sigma}^{(2)} - \delta\underset{\sim}{\sigma}^{(1)}||$ and $||\delta\underset{\sim}{\epsilon}^{(2)} - \delta\underset{\sim}{\epsilon}^{(1)}||$ are different from zero.

A few remarks are in order. It was shown in Ref.[5.5] that there are degrading materials which are unstable in the sense of Drucker and yet they are posit c in sense of Eq. (5-141) provided they are strain-rate dependent in a certain consti e sense discussed in the above reference. This is important because there has been no established proof of uniqueness for degrading rate-insensitive materials. to our knowledge.

5.4.2 Uniqueness in the Context of Endochronic Plasticity.

(i)   Endochronic plasticity with a yield surface.

We begin with relation (3-209). i.e..

$$\underset{\sim}{s} - \underset{\sim}{a} = s_o \frac{d\underset{\sim}{e}^p}{d\varsigma} F_s$$

and set

$$\dot{\sigma}_{ij}^{(2)} - \dot{\sigma}_{ij}^{(1)} = \Delta\dot{\sigma}_{ij} \quad ; \quad \dot{\epsilon}_{ij}^{(2)} - \dot{\epsilon}_{ij}^{(1)} = \Delta\dot{\epsilon}_{ij} \qquad (5\text{-}142)$$

Then in view of Ineq. (5-141) and the fact that the hydrostatic response is treated as elastic:

$$\Delta\dot{\underset{\sim}{s}} \cdot \Delta\dot{\underset{\sim}{e}}^p + \Delta\dot{\underset{\sim}{\alpha}} \cdot \Delta\dot{\underset{\sim}{e}}^e > 0 \qquad (5\text{-}143)$$

However

$$\Delta\dot{\underset{\sim}{\alpha}} \cdot \Delta\dot{\underset{\sim}{\xi}}^e = \Delta\dot{\underset{\sim}{\xi}}^e \cdot \underset{\sim}{C} \cdot \Delta\dot{\underset{\sim}{\xi}}^e \quad , \qquad (5\text{-}144)$$

and since the elastic stiffness $\underset{\sim}{C}$ (in this case isotropic) is positive definite it follows that to demonstrate that the model is positive we need only show that

$$\Delta\dot{\underset{\sim}{s}} \cdot \Delta\dot{\underset{\sim}{e}}^p > 0 \qquad (5\text{-}145)$$

whenever $||\Delta\dot{\underset{\sim}{e}}^p|| \neq 0$.

Evidently two possibilities exist. Either both stress increments $\delta \underset{\sim}{s}^{(2)}$ and $\delta \underset{\sim}{s}^{(1)}$ produce plastic strain increments $\delta \underset{\sim}{e}_p^{(2)}$ and $\delta \underset{\sim}{e}_p^{(1)}$ respectively. i.e..

$$\left[\underset{\sim}{s} - \underset{\sim}{a}\right] \cdot \dot{\underset{\sim}{s}}^{(1)} > 0, \quad \left[\underset{\sim}{s} - \underset{\sim}{a}\right] \cdot \dot{\underset{\sim}{s}}^{(2)} > 0 \quad , \tag{5-146a}$$

or one does but the other does not. i.e..

$$\left[\underset{\sim}{s} - \underset{\sim}{a}\right] \cdot \dot{\underset{\sim}{s}}^{(1)} > 0 \ , \quad \left[\underset{\sim}{s} - \underset{\sim}{a}\right] \cdot \dot{\underset{\sim}{s}}^{(2)} \leq 0 \quad . \tag{5-146b}$$

We begin with the possibility that both $\delta \underset{\sim}{s}^{(1)}$ and $\delta \underset{\sim}{s}^{(2)}$ give rise to plastic strain increments $(\delta \underset{\sim}{e}_p^{(1)}, \delta \underset{\sim}{e}_p^{(2)})$.

Now using Eq. (3-209) it follows that

$$\Delta \dot{\underset{\sim}{e}}^P = \left[\frac{\underset{\sim}{s} - \underset{\sim}{a}}{s_o F_s}\right] \Delta \dot{\zeta} \quad , \tag{5-147}$$

where

$$\Delta \dot{\zeta} = \dot{\zeta}^{(2)} - \dot{\zeta}^{(1)} \quad , \tag{5-148}$$

and thus

$$\Delta \dot{\underset{\sim}{s}} \cdot \Delta \dot{\underset{\sim}{e}}^P = \Delta \dot{\zeta} \left[\frac{1}{s_o F_s}\right] (\underset{\sim}{s} - \underset{\sim}{a}) \cdot \Delta \dot{\underset{\sim}{s}} \tag{5-149}$$

We now use Eq. (3-219) and note that it does not depend on $\dot{\underset{\sim}{e}}^P$ or $\dot{\underset{\sim}{s}}$. in view of Eq. (3-220). Thus

$$\frac{\underset{\sim}{s} - \underset{\sim}{a}}{s_o F_s} \Delta \dot{\underset{\sim}{s}} = H \Delta \dot{\zeta} \tag{5-150}$$

Hence using Eqs. (5-149) and (5-150)

$$\Delta\dot{\underset{\sim}{s}} \cdot \Delta\dot{\underset{\sim}{e}}^{p} = H(\Delta\dot{\zeta})^{2} \, , \tag{5-151}$$

and since H is always positive for hardening materials it follows that Ineq. (5-145) is satisfied and the constitutive Eq. (3-209) defines a positive material mode. Hence any well posed initial or boundary value problem associated with Eq. (3-209) will have a <u>unique</u> solution.

We now consider the second possibility whereby

$$\left(\underset{\sim}{s} - \underset{\sim}{a}\right) \cdot d\underset{\sim}{s}^{(2)} > 0 \, , \quad \left(\underset{\sim}{s} - \underset{\sim}{a}\right) \cdot d\underset{\sim}{s}^{(1)} \leq 0 \tag{5-152}$$

In this case $\delta\underset{\sim}{e}_{p}^{(1)} = 0$, the inequality to be proved is that

$$\left[\dot{\underset{\sim}{s}}^{(2)} - \dot{\underset{\sim}{s}}^{(1)}\right]\dot{\underset{\sim}{e}}_{p}^{(2)} > 0 \tag{5-153}$$

However,

$$\dot{\underset{\sim}{s}}^{(2)}\dot{\underset{\sim}{e}}_{p}^{(2)} > 0 \tag{5-154}$$

by virtue of Ineq. (5-153). Also

$$- \dot{\underset{\sim}{s}}^{(1)} \cdot \dot{\underset{\sim}{e}}_{p}^{(2)} = - \dot{\underset{\sim}{s}}^{(1)} \cdot \left(\underset{\sim}{s} - \underset{\sim}{a}\right) \frac{d\varsigma^{(2)}}{s_{o}F_{s}} \, , \tag{5-155}$$

as a result of Eq. (3-209). But the right-hand side of Eq. (5-155) is always positive by virtue of Ineq. (5-151). Therefore Ineq. (5-153) is also satisfied and the material model is positive in all eventualities.

(ii) <u>Endochronic Plasticity Without a Yield Surface.</u>

We now begin with Eq. (3-1), i.e.,

$$\underset{\sim}{s} = \int_{0-}^{z} \rho(z - z') \frac{d\underset{\sim}{e}^{p}}{dz'} dz' \quad , \tag{5-156}$$

where $\rho(z)$ is singular at the origin and has the following form in the neighborhood of $z = 0$:

$$\rho = \rho_o z^{-\alpha} \; : \; 0 < \alpha < 1 \tag{5-157}$$

In Eq. (5-156) we emphasized the fact that the lower limit of integration is o-, so that while $\|d\underset{\sim}{e}^{p}/dz|_{o}\| \neq 0$, $\|d\underset{\sim}{e}^{p}/dz|_{o-}\| = 0$. In view of this observation we may now differentiate Eq. (5-156) to obtain

$$\frac{d\underset{\sim}{s}}{dz} = \int_{0-}^{z} \rho(z - z') \frac{d^{2}\underset{\sim}{e}^{p}}{dz'^{2}} dz' \tag{5-158}$$

This is obtained by writing Eq. (5-156) in the equivalent form

$$\underset{\sim}{s} = \int_{0-}^{z} M(z - z') \frac{d^{2}\underset{\sim}{e}^{p}}{dz'^{2}} dz' \tag{5-159}$$

Equation (5-159) is obtained by integrating the right-hand side of Eq. (5-156) by parts and setting

$$M(z) = \int_{0-}^{z} \rho(z') dz' \quad , \quad \left. \frac{d\underset{\sim}{e}^{p}}{dz} \right|_{0-} = 0 \tag{5-157a,b}$$

and noting that $M(0) = M(0_-) = 0$. Thus, differentiating Eq. (5-159) leads to Eq. (5-158).

Before proceeding further we set the stage by stating, without proof, the flow rules for endochronic plasticity without a yield surface.[*] Let $\underset{\sim}{\ell}$ be the unit vector tangent to the plastic strain path at its terminal point. Let $\delta\underset{\sim}{s}_+$ be a stress increment such that $\underset{\sim}{\ell} \cdot \delta\underset{\sim}{s}_+ > 0$, then $\underset{\sim}{\ell}_+$, the direction of the resulting strain increment $\delta\underset{\sim}{e}^p_+$, is given the equation

$$\underset{\sim}{\ell}_+ = \underset{\sim}{\ell} \tag{5-158}$$

The magnitude $\delta\varsigma_+$ of the plastic strain increment $\delta\underset{\sim}{e}^p_+$ is as follows

$$\delta\varsigma_+ = \frac{||\delta\underset{\sim}{s}_+||}{||\underset{\sim}{m}||} F_s \quad , \tag{5-159}$$

where use was made of Eq. (5-158) and $\underset{\sim}{m}$ is defined by the expression:

$$\underset{\sim}{m} = \int_{0-}^{z} \rho(z - z') \frac{d^2 \underset{\sim}{e}^p}{dz'^2} dz' \tag{5-160}$$

Note that $\underset{\sim}{m}$ depends on the history of $\underset{\sim}{e}^p$ up to $z' = z$ but not on $d\underset{\sim}{e}^p_+$.

Now let $\delta\underset{\sim}{s}_-$ be a stress increment such that $\underset{\sim}{\ell} \cdot \delta\underset{\sim}{s}_- \leq 0$. In this case $\underset{\sim}{\ell}_-$, the direction of the resulting strain increment $\delta\underset{\sim}{e}^p_-$, is given by the expression

$$\underset{\sim}{\ell}_- - \underset{\sim}{\ell} = - 2\underset{\sim}{n}_s \left(\underset{\sim}{\ell} \cdot \underset{\sim}{n}_s \right) \quad , \tag{5-161}$$

---

where $\underset{\sim}{n}_s$ is the direction of $\delta\underset{\sim}{s}$. However in this case

$$\delta\varsigma_- = 0 \quad . \tag{5-162}$$

in the sense that

$$\lim_{||\delta\underset{\sim}{s}_-|| \to 0} \left(\frac{\delta\varsigma_-}{||\delta\underset{\sim}{s}||}\right) = 0 \tag{5-163}$$

Proof of Uniqueness.

As previously, to prove uniqueness we must show that the model satisfies the following inequality:

$$\Delta\dot{\underset{\sim}{s}} \cdot \Delta\dot{\underset{\sim}{e}}^P \geq 0 \tag{5-164}$$

Again we distinguish two cases: (a) when both $\delta\underset{\sim}{s}^{(2)}$ and $\delta\underset{\sim}{s}^{(1)}$ are of the $\delta\underset{\sim}{s}_+$ type; and (b) when $\delta\underset{\sim}{s}^{(2)}$ is of the $\delta\underset{\sim}{s}_+$ type and $\delta s^{(1)}$ is of the $\delta\underset{\sim}{s}_-$ type.

Case (a)

We utilize Eq. (5-158) to find that

$$\Delta\dot{\underset{\sim}{s}} = \underset{\sim}{m} \, \Delta\dot{z} = \underset{\sim}{m} \, F_s \Delta\dot{\varsigma} \tag{5-165}$$

Now we utilize Eq. (5-160) to show that

$$\Delta\dot{\underset{\sim}{e}}^P = \underset{\sim}{\ell} \, \Delta\dot{\varsigma} \tag{5-166}$$

At this point we combine Eqs. (5-165) and (5-166) to obtain the expression:

$$\Delta\dot{\underset{\sim}{s}} \cdot \Delta\dot{\underset{\sim}{e}}^P = F_s\left(\Delta\dot{\varsigma}\right)^2\left(\underset{\sim}{\ell} \cdot \underset{\sim}{m}\right) \tag{5-167}$$

Thus Ineq. (5-164) will be satisfied if $\underset{\sim}{\ell} \cdot \underset{\sim}{m} > 0$, or.

$$\underset{\sim}{\ell} \cdot \int_0^z \rho(z - z') \frac{d^2 \underset{\sim}{e}^p}{dz'^2} \, dz' > 0 \qquad (5\text{-}168)$$

To show this we write $\rho(z)$ in the form of a distribution. Specifically

$$\rho(z) = \lim_{R \to \infty} \int_0^R D(\alpha) e^{-\alpha z} d\alpha \qquad (5\text{-}169)$$

where the integral on the right-hand side of Eq. (5-169) converges uniformly to $\rho(z)$ as $R \to \infty$. In view of this we may substitute Eq. (5-169) in Eq. (5-168) and reverse the order of integration to obtain

$$\lim_{R \to \infty} \int_0^R D(\alpha) \left\{ \underset{\sim}{\ell} \cdot \int_{0-}^z e^{-\alpha(z-z')} \frac{d(F_s \underset{\sim}{\ell})}{dz'} \, dz' \right\} d\alpha > 0 \ , \qquad (5\text{-}170)$$

where use was made of the relation

$$\frac{d \underset{\sim}{e}^p}{dz'} = F_s \underset{\sim}{\ell}(z') \qquad (5\text{-}171)$$

If we now integrate by parts with respect to z and use the condition $\underset{\sim}{\ell}|_{0-} = 0$, we obtain

$$\underset{\sim}{\ell} \cdot \int_{0-}^z e^{-\alpha(z-z')} \frac{d(F_s \underset{\sim}{\ell})}{dz'} \, dz' = F_s - \alpha \underset{\sim}{\ell} \cdot \int_0^z e^{-\alpha(z-z')} F_s(z') \underset{\sim}{\ell}(z') dz' \qquad (5\text{-}172)$$

Now since

$$|\underset{\sim}{\ell}(z) \cdot \underset{\sim}{\ell}(z')| \leq 1 \qquad (5\text{-}173)$$

and $(F_s(z) \geq F_s(z'))$. since no softening is admitted. it follows that

$$\left| \underset{\sim}{\ell} \cdot \int_0^z e^{-\alpha(z-z')} F_s(z') \underset{\sim}{\ell}(z') dz \right| \leq F_s \int_0^z e^{-\alpha(z-z')} dz' \tag{5-174}$$

or

$$\left| \underset{\sim}{\ell} \cdot \int_0^z e^{-\alpha(z-z')} F_s(z') \underset{\sim}{\ell}(z') dz' \right| \leq \frac{F_s}{\alpha} \left(1 - e^{-\alpha z} \right) \tag{5-175}$$

Thus making use of Eq. (5-165) in Eq. (5-172) we establish the following inequality:

$$\underset{\sim}{\ell} \cdot \int_0^z e^{-\alpha(z-z')} \frac{d}{dz'} (F_s \underset{\sim}{\ell}) dz' > F_s e^{-\alpha z} \tag{5-176}$$

It follows therefore that

$$\lim_{R \to \infty} \int_0^R D(\alpha) \left[\underset{\sim}{\ell} \cdot \int_0^z e^{-\alpha(z-z')} \frac{d}{dz'} (F_s \underset{\sim}{\ell}) \right] d\alpha$$

$$= \lim_{R \to \infty} \int_0^R D(\alpha) F_s e^{-\alpha z} d\alpha \tag{5-177}$$

But the right-hand side of Eq. (5-177) is equal to $\rho(z)$ which is always positive and hence Ineq. (5-170) and hence Ineq. (5-168) are proved. Thus succinctly

$$\mathcal{L} \cdot \int_0^z \rho(z - z') \frac{d^2 \underset{\sim}{e}^p}{dz'^2} \, dz' > \rho(z) > 0 \qquad (5\text{-}178)$$

Therefore in view of Eq. (5-167)

$$\Delta \dot{\underset{\sim}{s}} \cdot \Delta \dot{\underset{\sim}{e}}^p > 0 \qquad (5\text{-}179)$$

and the material model is positive when $d\underset{\sim}{s} = d\underset{\sim}{s}_+$.

Case (b)

In this case the appropriate inequality which is to be proved is:

$$\left(\dot{\underset{\sim}{s}}_+ - \dot{\underset{\sim}{s}}_- \right) \cdot \left(\dot{\underset{\sim}{e}}^p_+ - \dot{\underset{\sim}{e}}^p_- \right) \geq 0 \qquad (5\text{-}180)$$

However, by virtue of Eq. (5-162):

$$\dot{\underset{\sim}{e}}^p_- = \underset{\sim}{\mathcal{L}}_- \dot{\underset{\sim}{s}}_- = 0 \qquad (5\text{-}181)$$

Thus Ineq. (5-180) reduces to:

$$\left(\dot{\underset{\sim}{s}}_+ - \dot{\underset{\sim}{s}}_- \right) \cdot \dot{\underset{\sim}{e}}^p_+ > 0 \qquad (5\text{-}182)$$

But

$$\dot{\underset{\sim}{s}}_+ \cdot \dot{\underset{\sim}{e}}^p_+ > 0 \qquad , \qquad (5\text{-}183)$$

as a result of Ineq. (5-179). Also

$$- \dot{\underset{\sim}{s}}_- \cdot \dot{\underset{\sim}{e}}^p_+ = \left(- \dot{\underset{\sim}{s}}_- \cdot \underset{\sim}{\mathcal{L}}_+ \right) \dot{\underset{\sim}{s}}_+ \qquad (5\text{-}184)$$

But in view of Eq. (5-158), $\underset{\sim}{\ell}_+ = \underset{\sim}{\ell}$ and thus

$$- \dot{\underset{\sim}{s}}_- \cdot \underset{\sim}{\ell}_+ = - \dot{\underset{\sim}{s}}_- \cdot \underset{\sim}{\ell} \geq 0 \tag{5-185}$$

by definition of case (b). Therefore, Ineq. (5-170) is validated.

Thus the material model is positive in all cases and the solution to the initial (or boundary) value problem is unique.

REFERENCES FOR CHAPTER 5

5.1 Noll, W., "On the Continuity of the Solid and Fluid States," *J. Rational Mechs. and Analyais*, Vol. 4, 3, (1955).

5.2 Drucker, D. C., "A Definition of Stable Inelastic Material," *J. App. Mech.*, 26, 101, (1959).

5.3 Il'iushin, A. A., "On the Postulate of Plasticity," *PMM*, 25, 503, (1961).

5.4 Drucker, D. C., "A More Fundamental Approach to Plastic Stress-Strain Relations," *Proc. 1st. U.S. Congress App. Mechs.*, ASME, pp. 487-491, (1951).

5.5 Valanis, K. C., "On Uniqueness of Solution of the Initial Value Problem in Softening Materials," *J. App. Mechs.*, 52, 649, (1985).

5.6 Hill, R., "The Mathematical Theory of Plasticity," Oxford Univ.; Press, 1950.

5.7 Drucker, D. C., "On the Uniqueness in the Theory of Plasticity," *O. App. Math.*, 14, 35, (1956).

6. FLOW RULES IN ENDOCHRONIC PLASTICITY
(Plastically Incompressible Solids)

In the parlance of classical plasticity the "Flow Rule" is a geometric or algebraic algorithm which answers the question:

> Given a stress increment $d\underset{\sim}{s}$ or alternatively a strain increment $d\underset{\sim}{e}$.
> what is the corresponding increment $d\underset{\sim}{e}^P$?

In classical plasticity the answer to the above question is complicated by the fact that, depending on the direction of the stress or strain increment, the plastic strain increment may or may not be zero. As part of the answer, therefore, there exists an "unloading rule" which determines the directions of $d\underset{\sim}{s}$ or $d\underset{\sim}{e}$ for which $d\underset{\sim}{e}^P$ is equal to zero.

In "endochronic plasticity", and specifically in the modern version as proposed by Valanis [6.1], such an unloading rule is not necessary because the increment in plastic strain is never exactly zero for any situation and can always be calculated directly from the constitutive equation, even though there are cases in which it's immeasurably small, as we shall show in Chapter 7. One suspects, however, that since endochronic plasticity may be regarded, in a limiting sense, as a plasticity theory with an infinitesimal yield surface, there must exist rules, which henceforth we shall refer to as the "Flow Rules", that give the magnitude and direction of the increment in plastic strain without the necessary computation.

Trangenstein and Read [6.2] were the first to address this question. Limiting themselves to the case of deviatoric plastic response, which we shall do here, they considered the case of an arbitrary change in the direction of a stress path which was previously smooth. Using specific asymptotic expansions, consistent with the properties of the weakly singular deviatoric memory kernel, they found that the increment in plastic strain is in the direction of the tangent of the previous stress path at the point of origin of the stress increment.

They also found that the incremental inelastic compliance C^P has the following properties:

$$C^P \equiv \frac{\left|\left|d\underset{\sim}{e}^P\right|\right|}{\left|\left|d\underset{\sim}{s}\right|\right|} = \begin{cases} k \cos \phi, & \underset{\sim}{t} \cdot d\underset{\sim}{s} > 0 \\ \\ 0, & \underset{\sim}{t} \cdot d\underset{\sim}{s} < 0 \end{cases} \tag{6-1}$$

where k is a constant. $\underset{\sim}{t}$ is the unit tangent vector at the end point of the smooth stress path (the point of initiation of the deviatoric stress increment $d\underset{\sim}{s}$) and ϕ is the angle between $\underset{\sim}{t}$ and $d\underset{\sim}{s}$. As pointed out by Murakami and Read [6.3], the above results were based on an assumed asymptotic expansion that forces $d\underset{\sim}{\varepsilon}^p$ to be in the direction $\underset{\sim}{t}$ and is valid only in the specific case where the smooth stress path is radial in the π-plane.

In a more recent paper, cited above, Murakami and Read reexamined the problem considered in Ref. [6.2], using a more general form of asymptotic expansion which does not place constraints on the direction of $d\underset{\sim}{\varepsilon}^p$. Though they did not determine, in their analysis, the direction of the resulting plastic strain increment $d\underset{\sim}{\varepsilon}^p$, they found the following result which, as we shall show in Chapter 8, is "operationally" valid for all stress paths in a sense given in our analysis.

Let θ be the angle between $d\underset{\sim}{s}$ and $d\underset{\sim}{\varepsilon}^p$. Then Murakami and Read found that

$$\left|\left|d\underset{\sim}{\varepsilon}^p\right|\right| = \begin{cases} \neq 0, & \cos\theta > 0 \\ \\ = 0, & \cos\theta < 0 \end{cases} \tag{6-2}$$

More specifically their general results are summarized in the following expression:

$$C^p = \left|\left|\frac{d\underset{\sim}{\varepsilon}^p}{d\underset{\sim}{s}}\right|\right| = \begin{cases} \dfrac{\cos\phi}{\gamma(z_o)}, & \phi < \dfrac{\pi}{2} \\ \\ 0, & \phi \geq \dfrac{\pi}{2} \end{cases} \tag{6-3}$$

where

$$\gamma(z_o) = \cos\theta \left|\left|\frac{d\underset{\sim}{s}}{dz}\right|\right|_{z_o}, \tag{6-4}$$

z_o being the value of z prior to the imposition of the stress increment $d\underset{\sim}{s}$. Also, using asymptotic methods, it was shown in Ref. [6.3] that, for large z and when the

stress state is close to the ultimate surface, the plastic deviatoric strain rate vector becomes coaxial with the deviatoric stress vector. For full details see Chapter 8.

In Chapter 7 we address the question of endochronic plastic flow rules in its entirety. i.e., we consider increments in stress $d\underset{\sim}{s}$ relative to arbitrary previous stress paths, or increments in strain $d\underset{\sim}{e}$ relative to arbitrary previous strain paths. As it turns out it is not the direction $\underset{\sim}{t}$ that determines the direction of the subsequent plastic strain increment $d\underset{\sim}{e}^p$ but $\underset{\sim}{\ell}$, <u>the direction of the tangent to the terminal point of the plastic strain path</u>, prior to the imposition of the stress increment $d\underset{\sim}{s}$ or the strain increment $d\underset{\sim}{e}$. Though the full results will be given in the analysis in Chapter 7, we give here the essential results for the benefit of the reader, first obtained by Valanis in Ref. [6.4].

Let $\underset{\sim}{\ell}$ be defined as above. Also let $d\underset{\sim}{s}$ be denoted by $d\underset{\sim}{s}_+$ when $\underset{\sim}{\ell} \cdot d\underset{\sim}{s} > 0$ and correspondingly by $d\underset{\sim}{s}_-$ when $\underset{\sim}{\ell} \cdot d\underset{\sim}{s} < 0$. It is then shown that in the limit of vanishingly small $||d\underset{\sim}{s}||$:

$$\underset{\sim}{\ell}_+ = \underset{\sim}{\ell} \tag{6-5}$$

But

$$\underset{\sim}{\ell}_- = \underset{\sim}{\ell} - 2\underset{\sim}{n}_s(\underset{\sim}{\ell} \cdot \underset{\sim}{n}_s) . \tag{6-6}$$

where $\underset{\sim}{n}_s$ is the direction of the appropriate stress increment. Note that

$$\underset{\sim}{\ell}_- = \underset{\sim}{\ell} \tag{6-7}$$

when $\underset{\sim}{\ell} \cdot d\underset{\sim}{s} = 0$. Also,

$$d\varsigma_+ = 0||d\underset{\sim}{s}_+|| \tag{6-8}$$

but

$$d\varsigma_- = 0||d\underset{\sim}{s}_-||^{1/1-\alpha} \tag{6-9}$$

Thus, if $||d\underset{\sim}{s}_+||$ is of the order of 10^{-3}, $d\varsigma_+$ is also of the same order. However if $||d\underset{\sim}{s}_-||$ is of this order, then given that for metals α is about 0.86, it follows that

$$d\varsigma_- = 0(10^{-21}) \tag{6-10}$$

which. of course. is not measurable. Thus from an operational viewpoint. $d\varsigma_{-} = 0$. In the special case where $\mathcal{L} \cdot d\underset{\sim}{\varepsilon} = 0$. $d\varsigma = 0$. Formulae for the calculation of $d\varsigma$ are given in Chapter 7.

It follows. therefore. that while $d\underset{\sim}{\varepsilon} = d\underset{\sim}{\varepsilon}_{+}$ the plastic strain path is continuous and has a continuous tangent. At points of reversal from $d\underset{\sim}{\varepsilon}_{+}$ to $d\underset{\sim}{\varepsilon}_{-}$. the tangent suffers a discontinuous change while the path remains continuous. The reader should also note that. in calculations subsequent to a reversal. it is $\underset{\sim}{\mathcal{L}}_{-}$ that should play the role of $\underset{\sim}{\mathcal{L}}$.

We close this chapter by pointing out that. obviously. the lower branch of equality (6-3) is in fact an approximation of Eq. (7-56) while the upper branch is an alternative form of Eq. (7-45). This is shown in Section 8.4. Of course this must be the case because Eqs. (7-45) and (7-56) were obtained for arbitrary stress histories while Eq. (6-3) was obtained under the assumption that the previous stress history was smooth. Thus Eqs. (7-45) and (7-56) must contain Eq. (6-3) as a special case.

REFERENCES FOR CHAPTER 6.

6.1   Valanis, K. C., "Endochronic Theory with Proper Hysteresis Loop Closure," S-CUBED. La Jolla, CA., Report No. SSS-R-80-4182, August 1979.

6.2   Trangenstein, J. A., and H. E. Read, "The Inelastic Response Characteristics of the New Endochronic Theory with Singular Kernel," *Intl. J. Solids and Structs.*, Vol.18(11) (1982), 947.

6.3   Murakami, H., and H. E. Read, "Endochronic Plasticity: Some Basic Properties of Plastic Flow and Failure," *Intl. J. Solids and Structs.*, Vol.23(1), (1987), 133.

6.4   Valanis, K. C., "Flow Rules in Endochronic Plasticity for Plastically Incompressible Solids," in preparation.

7. ANALYTIC DERIVATION OF THE FLOW RULES OF ENDOCHRONIC PLASTICITY FOR PLASTICALLY INCOMPRESSIBLE SOLIDS.

The plastic flow rules of the endochronic theory are derived in this chapter for the case of plastically incompressible solids. The versions of the endochronic theory with, and without, a yield surface are considered in detail. Finally, a computational scheme is given for calculating $d\varsigma$.

Before proceeding with the analysis, we note that in the case of classical plasticity, the plastic flow rule is well established and can be succintly described as follows: Let the end-point of the stress vector lie on the yield surface. Then if the end-point of the stress increment vector $d\underset{\sim}{s}$ lies outside the yield surface, plastic deformation will take place and the direction of the increment of the plastic strain vector $d\underset{\sim}{e}^p$ will be perpendicular to the yield surface at the point of emanation of $d\underset{\sim}{s}$. On the other hand, if the end-point of $d\underset{\sim}{s}$ lies inside or on the yield surface then the deformation will be elastic.

Against this background, we turn now to derive the plastic flow rules of the endochronic theory, considering, first, the version of the theory with a yield surface and later the version without a yield surface.

7.1 Endochronic Theory with a Yield Surface.

This case was discussed in its essential terms in Section 3.6 and in so far as the increment $d\underset{\sim}{s}$ is concerned the appropriate flow rule is the same as in classical plasticity. It is repeated here for completeness. Let

$$||\underset{\sim}{s} - \underset{\sim}{a}|| = s_o F_s \tag{7-1}$$

Condition (7-1) ensures that the end point of the stress vector lies on the yield surface. Then if

$$(\underset{\sim}{s} - \underset{\sim}{a}) \cdot d\underset{\sim}{s} > 0, \tag{7-2}$$

plastic deformation will take place. $d\varsigma$ will be given by Eq. (3-219). $d\underset{\sim}{e}^p$ will be given by Eq. (3-212) or Eq. (3-231) and will be perpendicular to the yield surface at the end point of $\underset{\sim}{s}$. However, if

$$(\underset{\sim}{s} - \underset{\sim}{a}).d\underset{\sim}{s} \leq 0 \quad . \tag{7-3}$$

then the ensuing deformation will be elastic. We note that the equality sign is valid only to a first order of approximation.

It is also of interest that endochronic plasticity affords an analysis which without further assumptions provides a flow rule when the increment of total strain $d\underset{\sim}{e}$ is given. The flow rule is obtained by virtue of Eq. (3-239) and is as follows:

Flow Rule:

> If $d\underset{\sim}{e}$ emanates from a point on the yield surface and its end point lies outside the yield surface then plastic deformation will take place, the increment of the plastic strain path $d\varsigma$ will be given by Eq. (3-239) and $d\underset{\sim}{e}^p$ by Eq. (3-212). On the other hand, if the end point of $d\underset{\sim}{e}$ lies inside the yield surface then the deformation will be elastic.

Thus, in analytic terms, if condition (7-1) applies and

$$(\underset{\sim}{s} - \underset{\sim}{a}).d\underset{\sim}{e} > 0 \quad . \tag{7-4}$$

plastic deformation will take place and $d\underset{\sim}{e}^p$ will be perpendicular to the yield surface at the end point of $\underset{\sim}{s}$ according to Eq. (3-212). However if

$$\left(\underset{\sim}{s} - \underset{\sim}{a}\right) \cdot d\underset{\sim}{e} \leq 0 \quad , \tag{7-5}$$

then the deformation will be elastic. Again the equality sign is valid only to a first order of approximation.

7.2 Endochronic Theory Without a Yield Surface.

This is by far the most difficult case and requires a careful analysis, which is based fundamentally on the treatment of endochronic plasticity with an infinitesimal yield surface, given in Section 3.6. We begin with Eq. (3-1), which is repeated below for convenience:

$$\underset{\sim}{s} = \int_0^{z_s} \rho(z_s - z') \frac{d\underset{\sim}{e}^p}{dz'} dz' \tag{3-1}$$

It follows that in terms of a __first order__ expansion:

$$\underset{\sim}{s} + d\underset{\sim}{s} = \int_0^{z_s} \rho(z_s + dz_s - z')\frac{d\underset{\sim}{e}^p}{dz'} dz' + M(dz_s)\frac{d\underset{\sim}{e}^p}{dz'}\bigg|_{z_s + dz_s}, \tag{7-6}$$

where use was made of Eq. (3-26). If we now set $dz_s = \delta$ in the nomenclature of Section 3.6 then Eq. (7-6) becomes:

$$\underset{\sim}{s} + d\underset{\sim}{s} = \int_0^{z_s} \rho(z_s + \delta - z')\frac{d\underset{\sim}{e}^p}{dz'} dz' + M(\delta)\frac{d\underset{\sim}{e}^p}{dz'}\bigg|_{z + \delta} \tag{7-7}$$

As stipulated in Section 3.6. the functions $\rho(z_s)$ and $\rho_1(z_s)$ coincide for all $z_s \geq \delta$ and therefore

$$\rho(z_s + \delta - z') = \rho_1(z_s + \delta - z') , \qquad 0 < z' < z_s \tag{7-8}$$

However in terms of a first order expansion in δ. the right-hand side of Eq. (7-8) is given by the expression

$$\rho_1(z_s + \delta - z') = \rho_1(z_s - z') + \delta \, \rho_1'(z_s - z'), \tag{7-9}$$

where ρ_1' is given by Eq. (3-218). In view of Eqs. (3-208). (7-8) and (7-9). Eq. (7-7) becomes:

$$\underset{\sim}{s} + d\underset{\sim}{s} = \underset{\sim}{a} + \delta \, \underset{\sim}{h} + M(\delta)\frac{d\underset{\sim}{e}^p}{dz'}\bigg|_{z_s + \delta} \tag{7-10}$$

where as previously (see Eq. (3-208):

7-3

$$\mathbf{\underline{z}} = \int_0^{z_s} \rho_1(z_s - z')\, \frac{d\underline{e}^p}{dz'}\, dz' \tag{7-11}$$

It follows that to within $0(\delta^2)$

$$d\underline{\underline{z}} = \rho_1(\delta)\, \frac{d\underline{e}^p}{dz'}\Bigg|_{z_s+\delta}\delta + \delta \int_0^{z_s} \rho_1'(z_s - z')\, \frac{d\underline{e}^p}{dz'}\, dz' \tag{7-12}$$

However, because $\rho_1(z_s)$ is well behaved at the origin, it follows that

$$\rho_1(\delta) = \rho_1(0) + 0(\delta) \tag{7-13}$$

See Fig. 7.1 where $\rho_1(z_s)$ is illustrated pictorially.

Thus ignoring terms of $0(\delta^2)$:

$$d\underline{\underline{z}} = \rho_1(0)\, \frac{d\underline{e}^p}{dz'}\Bigg|_{z_s+\delta}\delta + \underline{b}\,\delta \quad, \tag{7-14}$$

where Eq. (3-217) was used. We now make use of the following relations:

$$\rho_1(\delta) = \rho_o\, \delta^{-\alpha} \tag{7-15}$$

$$M(\delta) = \rho_o \delta^{1-\alpha}/1-\alpha \tag{7-16}$$

Equations (7-10), (7-14), (7-15), and (7-16) then combine to give the desired equation in terms of the infinitesimal yield surface s_o:

$$\underline{s} + d\underline{s} = \underline{\underline{z}} + d\underline{\underline{z}} + s_o\, \frac{d\underline{e}^p}{dz'}\Bigg|_{z_s+\delta} \tag{7-17}$$

$$\mathbf{\mathfrak{z}} = \int_0^{z_s} \rho_1\left(z_s - z'\right)\frac{d\mathbf{\mathfrak{z}}^\rho}{dz'}\, dz'$$

$$\mathbf{\mathfrak{h}} = \int_0^{z_s} \rho_1'\left(z_s - z'\right)\frac{d\mathbf{\mathfrak{z}}^\rho}{dz'}\, dz'$$
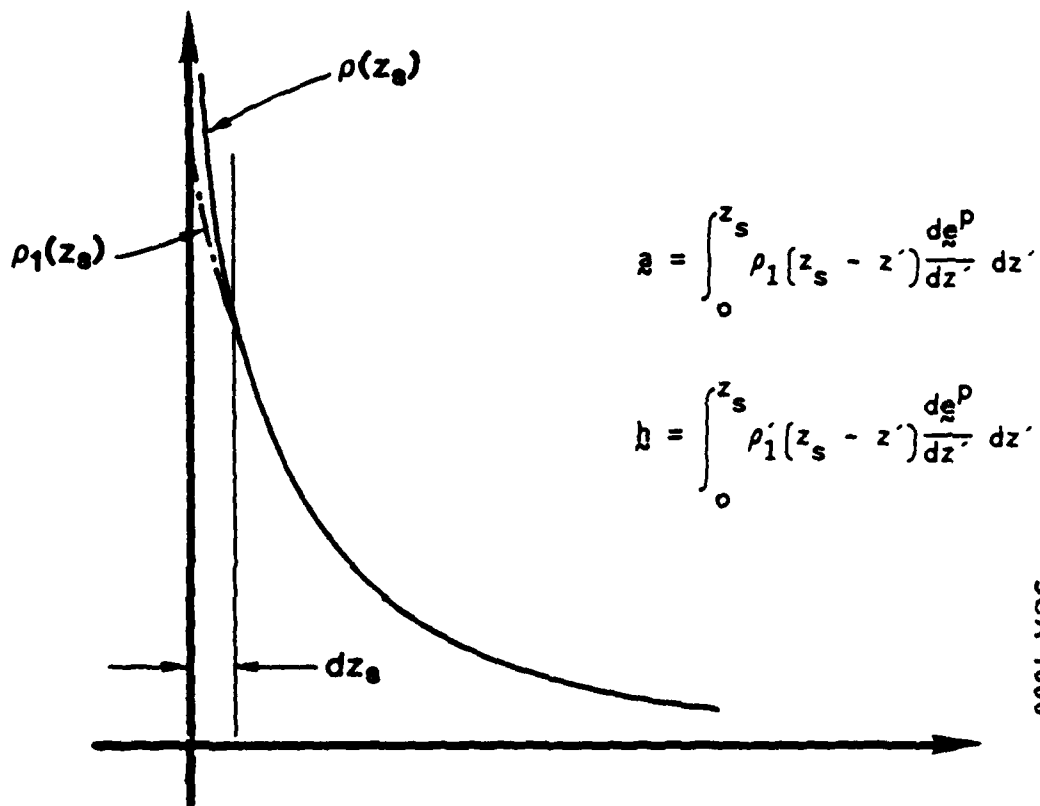
SCA-1666

Figure 7.1 Illustration of the functions $\rho(z_s)$, $\rho_1(z_s)$, $\mathbf{\mathfrak{z}}(z_s)$ and $\mathbf{\mathfrak{h}}(z_s)$.

where

$$s_o = \rho_o(\alpha/1-\alpha)\delta^{1-\alpha} \; , \tag{7-18}$$

in accordance with the value derived previously. See Eq. (3-269).

The above analysis shows the equivalence of Eqs. (3-1) and (3-268) to within an error which goes to zero in the limit of $\delta = 0$. This was already done in Section 3.6 and in that sense the foregoing analysis was repetitious. However it served another purpose in that it identified the meaning of δ, which as the reader will recall, was set equal to dz_s. Thus the above analysis also identified the tensor valued integrals $\underset{\sim}{a}$ and $\underset{\sim}{b}$ which, as is now apparent, depend directly on the value of δ. This dependence is shown pictorially in Fig. 7.1. Note that $\rho(z_s) = \rho_1(z_s)$, $dz_s \leq z_s$ and $\rho_1'(0) = \rho_1'(dz_s)+0(dz_s)$.

We state these results formally.

$$\lim_{\delta \to 0} \int_0^{z_s} \rho(z - z')\frac{d\underset{\sim}{e}^p}{dz'} \, dz' = \int_0^{z_s} \rho_1(z_s - z') \frac{d\underset{\sim}{e}^p}{dz'} \, dz' + s_o \frac{d\underset{\sim}{e}^p}{dz_s} \tag{7-19}$$

$$\lim_{\delta \to 0} s_o = \frac{\alpha}{1-\alpha} \rho_o \, \delta^{1-\alpha} \quad , \tag{7-20}$$

where

$$\rho_1(z_s) = \rho(z_s) \; , \quad \delta \leq z_s \; . \tag{7-21}$$

Thus, to summarize, in view of Eqs. (3-268), (7-19) and (7-20), we have

$$\lim_{\delta \to 0} \underset{\sim}{s} = \underset{\sim}{a} + s_o \frac{d\underset{\sim}{e}^p}{dz_s} \tag{7-22}$$

and in view of Eq. (7-17)

$$\underset{\sim}{s} + d\underset{\sim}{s} = \underset{\sim}{a} + d\underset{\sim}{a} + s_o \left. \frac{d\underset{\sim}{e}^p}{dz_s} \right|_{z_s + \delta} \qquad (7\text{-}23)$$
$$\lim \delta \to 0$$

In Figure 7.2 we show a plastic strain path (in plastic strain space) in the presence of three infinitesimal yield surfaces (circles) of different sizes (in stress-space). The equation of interest is

$$\underset{\sim}{s} = s_o \frac{d\underset{\sim}{e}^p}{dz_s} + \underset{\sim}{a} \quad , \qquad (7\text{-}24)$$

assuming that no elastic deformation has followed the last increment $d\underset{\sim}{a}$, or, if it has, $\underset{\sim}{s}$ has been restored to its value preceding elastic deformation. Of importance is the observation that the segment $\overline{AB}$, which is the difference between $\underset{\sim}{s}$ and $\underset{\sim}{a}$, is by virtue of Eq. (7-24) in the direction $d\underset{\sim}{e}^p/dz$, which is the tangent to the plastic strain path at its terminal point $\underset{\sim}{a}$. Thus all infinitesimal yield circles tangent at B, each depending on a different value of δ, must have their center on the segment AB. This, of course, is based on the fact that s_o in Eq. (7-24) is infinitesimal and the expectation that all three plastic strain paths which have evolved on the basis of Eq. (7-24), each corresponding to a different value of s_o, converge to the same plastic strain path as s_o tends to zero.

These circles are shown again in Fig. 7.3 for clarity. Consider now an increment of stress $d\underset{\sim}{s}_+$ as shown in this figure, such that

$$\left(\underset{\sim}{s} - \underset{\sim}{a} \right) \cdot d\underset{\sim}{s}_+ > 0 \qquad (7\text{-}25)$$

or, in view of the above discussion and following Fig. 7.2,

$$\left(\frac{d\underset{\sim}{e}^p}{dz} \right)_a \cdot d\underset{\sim}{s}_+ > 0 \qquad (7\text{-}26)$$

SCA-1663

$$\underset{\sim}{s} = s_0 \frac{d\underset{\sim}{e}^p}{dz} + \underset{\sim}{a}$$
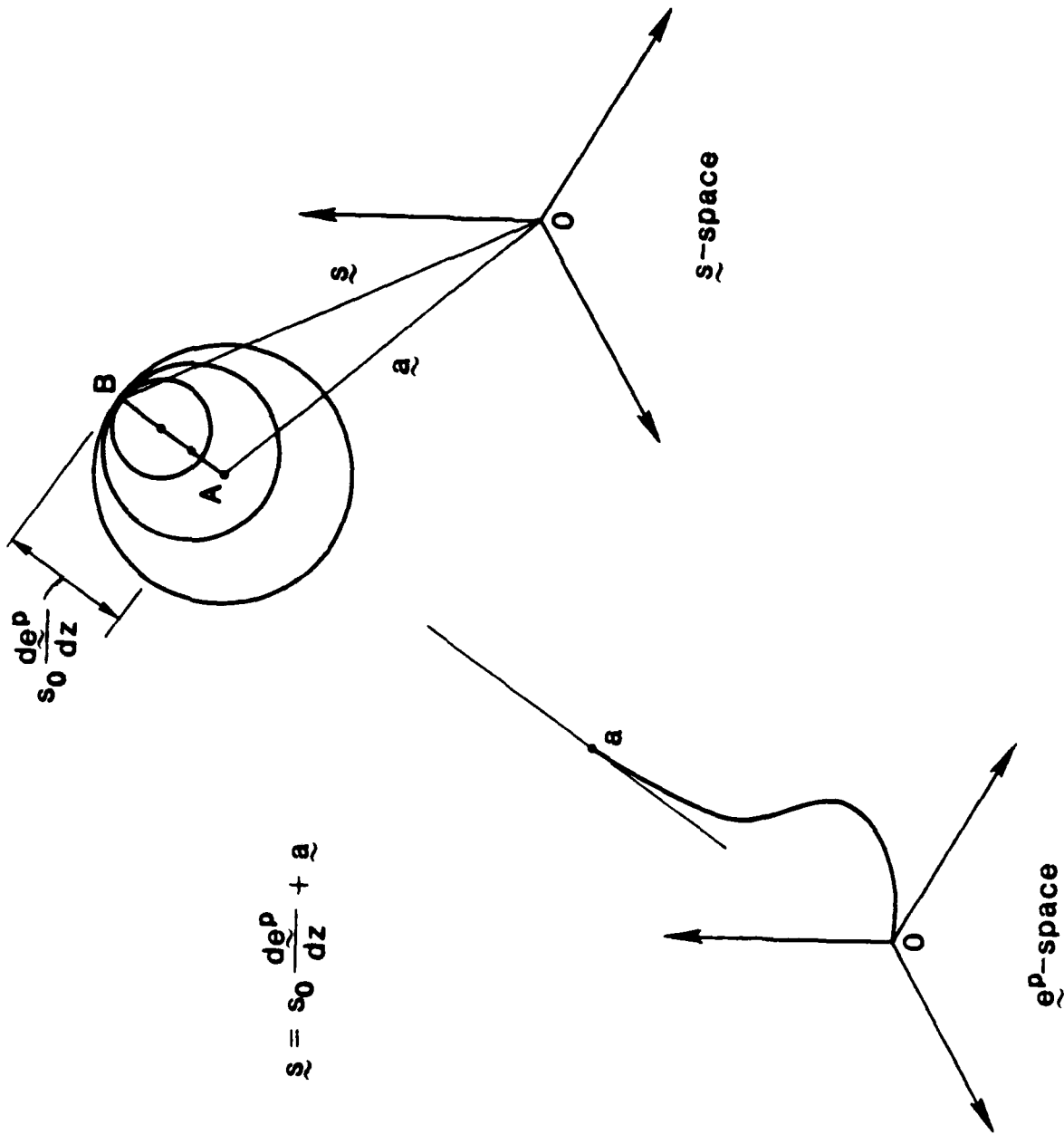
Figure 7.2   A plastic strain path in $\underset{\sim}{e}^p$-space in the presence of _infinitesimal_ yield surfaces of different sizes.
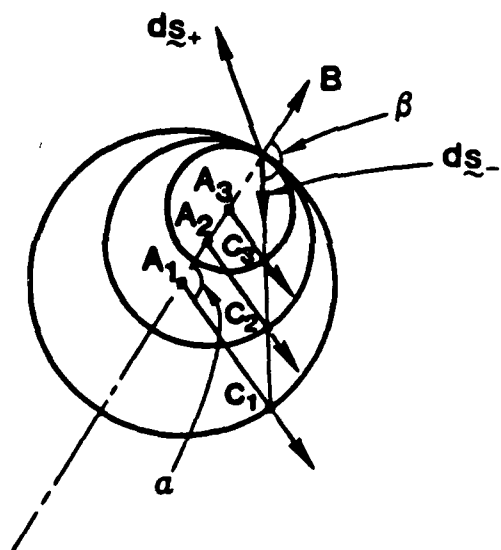
Figure 7.3   Three infinitesimal yield circles with different radii.

or, more simply

$$\underset{\sim}{\ell} \cdot d\underset{\sim}{s}_+ > 0 \quad , \tag{7-27}$$

where

$$\underset{\sim}{\ell} \equiv \left(\frac{d\underset{\sim}{\varepsilon}^p}{dz}\right)_a \tag{7-28}$$

We now let $\underset{\sim}{\ell}_+$ be equal to $\left.\dfrac{d\underset{\sim}{\varepsilon}^p}{dz}\right|_{z_s+\delta}$ and note from Eqs. (7-22) and (7-23) that:

$$s_o\underset{\sim}{\ell} \cdot \left.\frac{d\underset{\sim}{\varepsilon}^p}{dz_s}\right|_{z_s+\delta} = s_oF_s\,\underset{\sim}{\ell} \cdot \underset{\sim}{\ell}_+ + d\left(\underset{\sim}{s} - \underset{\sim}{a}\right) \cdot \underset{\sim}{\ell}$$

$$= s_oF_s + d\left(\underset{\sim}{s} - \underset{\sim}{a}\right) \cdot \underset{\sim}{\ell} \tag{7-29}$$

Also,

$$d\left(\underset{\sim}{s} - \underset{\sim}{a}\right) \cdot \underset{\sim}{\ell} = s_o\left(\frac{d^2\underset{\sim}{\varepsilon}^p}{dz_s^2} \cdot \underset{\sim}{\ell}\right)\delta + 0\left(\delta^2\right)$$

$$= s_oF_s'\,d\varsigma + 0\left(\delta^2\right) \quad , \tag{7-30}$$

since,

$$\frac{d^2\underset{\sim}{\varepsilon}^p}{dz_s^2} = s_oF_s'\,\frac{d\underset{\sim}{\varepsilon}^p}{d\varsigma}\,d\varsigma + s_oF_s\,\frac{d^2\underset{\sim}{\varepsilon}^p}{d\varsigma^2}\,d\varsigma \tag{7-31}$$

and

$$d\left(\frac{d\underset{\sim}{\varepsilon}^p}{d\varsigma} \cdot \frac{d\underset{\sim}{\varepsilon}^p}{d\varsigma}\right) = 2\,\underset{\sim}{\ell} \cdot \frac{d^2\underset{\sim}{\varepsilon}^p}{d\varsigma^2}\,d\varsigma = 0 \tag{7-32}$$

Thus combining Eq. (7-29) and (7-30) we find the following result:

$$\ell \cdot \ell_+ = 1 + s_o(F_s'/F_s)\delta + o(\delta^2) \quad . \tag{7-33}$$

Therefore, in the case where $\ell \cdot d\underset{\sim}{s} > 0$, i.e., $d\underset{\sim}{s} = d\underset{\sim}{s}_+$,

$$\ell_+ = \ell$$
$$\lim \delta = 0 \tag{7-34}$$

Thus the plastic strain path is continuous and has a continuous derivative for stress histories consisting of infinitesimal segments $d\underset{\sim}{s}_+$.

The situation where $d\varsigma$ is infinitesimal but different from zero is shown on a highly exaggerated scale in Fig. 7.4. Point A denotes the center of the infinitesimal yield surface when the plastic strain path terminates at a. In this case AB is parallel to the tangent to the path at a. The point A_1 is the center of the infinitesimal yield surface when the path terminates at a_1. In this case the segment A_1B_1 is parallel to the tangent to the path at a_1.

Consider now a stress increment $d\underset{\sim}{s}_-$ shown in Fig. 7.3, along the line BC_1 such that

$$\left(\underset{\sim}{s} - \underset{\sim}{a}\right) \cdot ds_- < 0 \tag{7-35}$$

or

$$\ell \cdot d\underset{\sim}{s}_- < 0 \tag{7-36}$$

In this case $d\varsigma = 0$ provided that

$$||d\underset{\sim}{s}_-|| \leq BC_r \quad (r = 1,2,3) \quad , \tag{7-37}$$

depending on which infinitesimal yield surface one wishes to consider. However, when

$$||d\underset{\sim}{s}_-|| > BC_r \quad (r = 1,2,3) \quad , \tag{7-38}$$
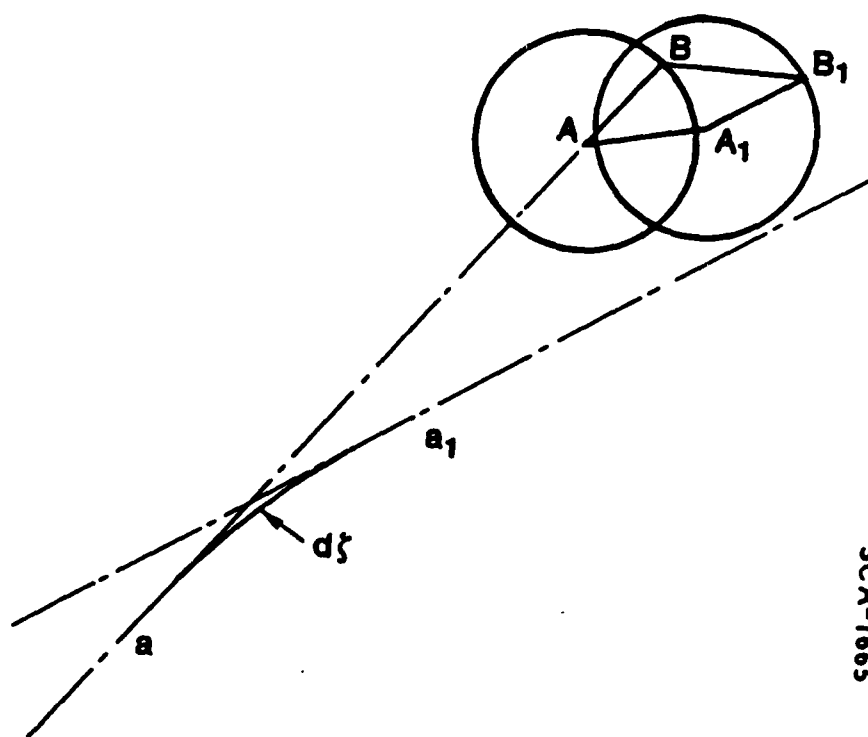
Figure 7.4   Infinitesimal yield surfaces corresponding to points a and a_1 on the plastic strain path.

then $d\varsigma \neq 0$ and $d\varepsilon^p/dz$ is along the line $A_r C_r$ $(r = 1,2,3)$. One can show by a simple geometric proof that all lines $A_r C_r$ $(r = 1,2,3)$ are parallel.

Hence when inequalities (7-36) and (7-38) apply $d\varepsilon^p/dz$ is in the direction $A_r C_r$ and this direction is also independent of the size of the yield surface. In this case the plastic strain path is continuous but its derivative is discontinuous!

To determine the direction C_r we let the angle between $A_r B$ and $B C_r$ be equal to β. Thus

$$\cos\beta = \underset{\sim}{\ell} \cdot \frac{d\underset{\sim}{s}_-}{||d\underset{\sim}{s}_-||} = \underset{\sim}{\ell} \cdot \underset{\sim}{n}_s \quad , \tag{7-39}$$

where $\underset{\sim}{n}_s$ is a generic symbol for the direction of $d\underset{\sim}{s}$, be it $d\underset{\sim}{s}_+$ or $d\underset{\sim}{s}_-$. Also let $\underset{\sim}{\ell}_-$ be the direction of the segment $A_r C_r$, this being the direction of the increment of plastic strain corresponding to an "unloading" stress increment that satisfies inequalities (7-36) and (7-38).

We note parenthetically that if α is the angle between the unit vectors $\underset{\sim}{\ell}$ and $\underset{\sim}{\ell}_-$ then,

$$\cos \alpha = \underset{\sim}{\ell} \cdot \underset{\sim}{\ell}_- \tag{7-40}$$

It follows from the diagram of Fig. 7.3 that

$$\left(A_r B\right)\underset{\sim}{\ell} + \left(B C_r\right)\underset{\sim}{n}_s = \left(A_r C_r\right)\underset{\sim}{\ell}_- \tag{7-41}$$

But

$$A_r B = A_r C_r \tag{7-42}$$

and

$$\frac{B C_r}{A_r B} = -2\cos\beta \tag{7-43}$$

Thus in view of Eqs. (7-41), (7-42) and (7-43) the following relation, which will be of central importance in unloading behavior in the context of endochronic plasticity, follows:

$$\underset{\sim}{\ell} - 2\underset{\sim}{n}_s \cos\beta = \underset{\sim}{\ell}_- \qquad (7\text{-}44)$$

Or, using Eq. (7-39)

$$\underset{\sim}{\ell} - 2\underset{\sim}{n}_s (\underset{\sim}{\ell} \cdot \underset{\sim}{n}_s) = \underset{\sim}{\ell}_- \qquad (7\text{-}45)$$

Equation (7-45) gives the direction $\underset{\sim}{\ell}_-$, i.e., the direction of the plastic strain increment following unloading, in terms of the known directions $\underset{\sim}{\ell}$ and $\underset{\sim}{n}_s$. Note that this equation is independent of the size of the yield surface!!

On the basis of the foregoing analysis we can now put forth the flow rule for endochronic plasticity without a yield surface. This rule is based on Eqs. (7-34) and (7-35) <u>whose validity is independent of the size of the yield surface</u>. <u>These equations, therefore, remain valid as the radius of the yield surface goes to zero</u>.

Flow Rule:

Let $\underset{\sim}{\ell}$ be the tangent vector to the terminal point of the plastic strain path in $\underset{\sim}{\varepsilon}^p$-space. Then if the stress increment $d\underset{\sim}{s}$ is such that

$$d\underset{\sim}{s} \cdot \underset{\sim}{\ell} > 0 . \qquad (7\text{-}46)$$

it is denoted by $d\underset{\sim}{s}_+$ and is in a "loading" direction, whereupon $\underset{\sim}{\ell}_+$, the direction of the resulting plastic strain increment, is in the direction of $\underset{\sim}{\ell}$ in the limit of $||d\underset{\sim}{s}|| = 0$. Thus

$$\underset{\sim}{\ell}_+ = \underset{\sim}{\ell}$$
$$\lim ||d\underset{\sim}{s}|| = 0 \qquad (7\text{-}47)$$

Therefore when the stress path is continuous -- even though its tangent may be discontinuous -- the plastic strain path is continuous and has a continuous derivative at every point.

On the other hand if the stress increment $d\underset{\sim}{s}$ is such that

$$d\underset{\sim}{s} \cdot \underset{\sim}{\ell} < 0 . \qquad (7\text{-}48)$$

it is denoted by $d\underset{\sim}{\varepsilon}_-$ and is in an "unloading" direction, whereupon $\underset{\sim}{\ell}_-$, the direction of the resulting strain increment, in the limit of $||d\underset{\sim}{\varepsilon}|| = 0$, is given by the expression:

$$\underset{\sim}{\ell}_- = \underset{\sim}{\ell} - 2\underset{\sim}{n}_s(\underset{\sim}{\ell} \cdot \underset{\sim}{n}_s)$$

$$\lim ||d\underset{\sim}{\varepsilon}|| = 0 \tag{7-49}$$

We note that in this case the plastic strain path is continuous but its derivative is discontinuous since now $\underset{\sim}{\ell}_- \neq \underset{\sim}{\ell}$.

The case when $d\underset{\sim}{\varepsilon}$ is perpendicular to the plastic strain path at its end point, i.e., when

$$d\underset{\sim}{\varepsilon} \cdot \underset{\sim}{\ell} = 0 \tag{7-50}$$

does not seemingly belong to either of the above two cases. However the direction $\underset{\sim}{\ell}$ when condition (7-50) applies can be obtained from considerations of continuity in the sense that in this event $\underset{\sim}{\ell}_+$ must be equal to $\underset{\sim}{\ell}_-$. But Eqs. (7-47) and (7-49) satisfy this condition in their present form and thus their range of validity extends to the case where condition (7-50) applies.

Recapitulation:

The flow rule of endochronic plasticity without a yield surface in the limit of $||d\underset{\sim}{\varepsilon}|| = 0$ is:

$$d\underset{\sim}{\varepsilon} \cdot \underset{\sim}{\ell} \geq 0 \quad : \quad \underset{\sim}{\ell}_+ = \underset{\sim}{\ell} \tag{7-51}$$

$$d\underset{\sim}{\varepsilon} \cdot \underset{\sim}{\ell} \leq 0 \quad : \quad \underset{\sim}{\ell}_- = \underset{\sim}{\ell} - 2\underset{\sim}{n}_s(\underset{\sim}{\ell} \cdot \underset{\sim}{n}_s) \tag{7-52}$$

7.3 The Value of $d\varsigma$.

<u>Case (a)</u> $d\underset{\sim}{\varepsilon} = d\underset{\sim}{\varepsilon}_+$

Combine Eqs. (7-23) and (7-24) to obtain:

$$s_o F_s \underset{\sim}{\ell} + d\underset{\sim}{\varepsilon} = d\underset{\sim}{a} + s_o F_s(\varsigma + d\varsigma)\underset{\sim}{\ell}_+$$

$$= d\underset{\sim}{a} + s_o(F_s + F_s' d\varsigma)\underset{\sim}{\ell}_+ \tag{7-53}$$

But in this case the plastic strain path is continuous and differentiable. Thus:

$$\underset{\sim}{\ell}_+ - \underset{\sim}{\ell} = \frac{d^2 \underset{\sim}{e}^p}{d\varsigma^2} \, d\varsigma \qquad (7\text{-}54)$$

Hence we use Eqs. (7-53) and (7-54) to arrive at the following result:

$$d\underset{\sim}{s} = d\underset{\sim}{a} + s_o F'_s \underset{\sim}{\ell} \, d\varsigma + s_o F_s \frac{d^2 \underset{\sim}{e}^p}{d\varsigma^2} \, d\varsigma + 0\left(\delta\varsigma^2\right) \qquad (7\text{-}55)$$

It follows, therefore, that

$$d\underset{\sim}{s} \cdot \underset{\sim}{\ell} = d\underset{\sim}{a} \cdot \underset{\sim}{\ell} + s_o F'_s d\varsigma \qquad (7\text{-}56)$$

since, as previously,

$$\underset{\sim}{\ell} \cdot \frac{d^2 \underset{\sim}{e}^p}{d\varsigma^2} = 0 \qquad (7\text{-}57)$$

Now use Eq. (3-216) to determine $d\varsigma$ in the form given below:

$$d\varsigma \, H = d\underset{\sim}{s}_+ \cdot \underset{\sim}{\ell} \quad , \qquad (7\text{-}58)$$

where

$$H = \rho_1(o) + s_o F'_s + \frac{\underset{\sim}{\ell} \cdot \underset{\sim}{h}}{F_s} \qquad (7\text{-}59)$$

This equation is reminiscent of Eq. (3-220) however now both s_o and $\underset{\sim}{h}$ are functions of $dz_s (= d\varsigma/F_s)$ and hence Eq. (7-59) must be solved iteratively. Nonetheless a conclusion which we will refer to later is that, in view of Eqs. (7-58) and (7-59), when $ds = ds_+$:

$$d\varsigma = 0\left(||d\underset{\sim}{s}||\right) \qquad (7\text{-}60)$$

Case (b) $d\underset{\sim}{s} = d\underset{\sim}{s}_{-}$

Again combine Eqs. (7-23) and (7-24) to obtain the expression:

$$s_o F_s \underset{\sim}{\ell} = d\underset{\sim}{s} = d\underset{\sim}{a} + s_o F_s (\varsigma + d\varsigma)\underset{\sim}{\ell}_{-} \tag{7-61}$$

In this case the plastic strain path is not differentiable in the sense that $\underset{\sim}{\ell}_{-} - \underset{\sim}{\ell}$ is finite i.e., the tangent to the path is discontinuous at ς. However $\underset{\sim}{\ell}_{-}$ is given by Eq. (7-44) which in combination with Eq. (7-61) gives:

$$s_o F_s + d\underset{\sim}{s} \cdot \underset{\sim}{\ell} = d\underset{\sim}{a} \cdot \underset{\sim}{\ell} + s_o F_s (\varsigma + d\varsigma) \left(1 - 2\cos^2\beta \right) \tag{7-62}$$

Note at this point that

$$d\underset{\sim}{s} \cdot \underset{\sim}{\ell} = ds \, \cos\beta \tag{7-63}$$

where $ds = \|d\underset{\sim}{s}\|$. Then following the analysis in case (a), Eq. (7-62) reduces to the following expression:

$$ds \, \cos\beta = \left[\rho_1(0) + \frac{\underset{\sim}{h} \cdot \underset{\sim}{\ell}}{F_s} \right] d\varsigma - \frac{2\alpha}{1-\alpha} \, \rho_o \, \cos^2\beta \left(\frac{1}{F_s} \right)^{1-\alpha} d\varsigma^{1-\alpha}$$

$$+ F_s' \left(1 - 2\cos^2\beta \right) \frac{2\alpha}{1-\alpha} \, \rho_o \left(\frac{1}{F_s} \right)^{1-\alpha} d\varsigma^{2-\alpha} \tag{7-64}$$

where Eq. (7-18) was used.

We wish to show that $d\varsigma$ is of higher order of smallness than $d\varsigma^{1-\alpha}$ whenever $0 < \alpha < 1$. Specifically we wish to prove the following lemma.

Lemma.

Given a positive α however small and a positive integer n then there exists a $d\varsigma$ such that

$$d\varsigma^{1-\alpha} = 10^n \, d\varsigma \tag{7-65}$$

Discussion. To fix ideas let $d\varsigma = 10^{-12}$, say, and $n = 6$. Then $d\varsigma^{1-a} = 10^{-6}$. Thus in this case

$$d\varsigma = 0\left(d\varsigma^{1-a}\right)^2 \tag{7-66}$$

Proof. The proof is elementary. Take logs of both sides of Eq. (7-65) to find that

$$d\varsigma = 10^{- n/a} \tag{7-67}$$

Thus given n and a, $d\varsigma$ is given by Eq. (7-67).

More simply, but in a less informative fashion:

$$\lim_{d\varsigma=0}\left(\frac{d\varsigma}{d\varsigma^{1-a}}\right) = \lim_{d\varsigma=0} d\varsigma^a = 0 \tag{7-68}$$

We shall consider two cases:

(i) $\beta = \frac{\pi}{2}$

(ii) $\beta = \frac{\pi}{2} + \beta_0$

where β_0 is <u>not</u> vanishingly small. In case (i), and in view of Eq. (7-64), $d\varsigma = 0$. In case (ii), and in view of the above theorem

$$\lim_{d\varsigma \to 0} ds \cos\beta = - \frac{2a}{1 - a} \rho_0 \cos^2\beta \left[\frac{d\varsigma}{F_s}\right]^{1-a} \tag{7-69}$$

Hence:

$$d\varsigma = F_s\left[\frac{ds}{\dfrac{2a}{1 - a} \rho_0 |\cos\beta|}\right]^{1/1-a} \tag{7-70}$$

Note that in real metals $\alpha \doteq 0.86$ in which case $1/1-\alpha \sim 7.0$. Thus

$$d\varsigma = 0(ds)^7. \tag{7-71}$$

Thus, $d\varsigma$ is __not__ measurable and, therefore, "zero" for small changes $d\underset{\sim}{s}$ in the deviatoric stress. However, it is not exactly zero.

In more rigorous terms, if $d\varsigma_+$ and $d\varsigma_-$ correspond to stress increments $d\underset{\sim}{s}_+$ and $d\underset{\sim}{s}_-$ such that $||d\underset{\sim}{s}_-|| = ||d\underset{\sim}{s}_+|| = ||d\underset{\sim}{s}||$, then:

$$\lim_{||d\underset{\sim}{s}||=0} \left(\frac{d\varsigma_-}{d\varsigma_+}\right) = 0 \quad . \tag{7-72}$$

Thus, in an operational sense, i.e., in terms of a measurable $d\varsigma$, given an increment of stress $d\underset{\sim}{s}-$, then $d\varsigma- = 0$.

7.4 A Computational Scheme for Calculating $d\varsigma$.

The underlying idea of the scheme is that given $\rho(z_s)$, weakly singular near the origin, we define a function $\rho_1(z_s)$ such that

$$\rho_1(z_s) = \rho(z_s) \quad , \quad z_s \geq \delta \tag{7-73}$$

but

$$\rho_1(z_s) = \text{finite function,} \quad z_s \leq \delta \quad , \tag{7-74}$$

where the finite function will be defined shortly and δ is a vanishingly small number. Of importance is the fact that in the interval $[\delta.z]$. $\rho_1(z_s)$ is finite and can therefore be approximated as closely as we please by a finite sum of exponential terms. i.e.,

$$\left| \rho_1(z_s) - \sum_{r=1}^{n} A_r e^{-a_r z_s} \right| < \epsilon \tag{7-75}$$

where ϵ is a "tolerance" error.

7-19

More precisely, given a positive number δ however small, an n can be found such that Eq. (7-75) applies for all $\delta \leq z_s$.

Thus we define the "finite function" in Eq. (7-74) by extending the representation (7-75) of $\rho_1(z_s)$ in the entire domain $0 \leq z_s$. Hence

$$\rho_1(z) = \sum_r A_r \, e^{-\alpha_r z_s} \tag{7-76}$$

for all z.

It was then shown in Section 3.6 that $\rho(z_s)$ can be represented in the <u>entire</u> interval $[0.z_s]$ by the expression:

$$\rho(z_s) = \rho_1(z_s) + s_o \delta(z_s) \quad, \tag{7-77}$$

where $\delta(z_s)$ is the Dirac delta function and

$$s_o = \frac{\alpha}{1 - \alpha} \, \rho_o \, \delta^{1-\alpha} \tag{7-78}$$

Basically, therefore, $s_o \delta(z_s)$ is a <u>correction</u> term associated with the representation of $\rho(z_s)$ by the Dirichlet series (7-75). As pointed out previously, the representation of ρ given by Eq. (7-77) introduces an infinitesimal yield surface, with all the implications associated with such a surface and which were already discussed in this section.

Now we recognize, however, that the strength s_o of the delta function is known by virtue of Eq. (7-78) and thus we can represent the δ-function itself to any degree of accuracy by a single exponential term. Specifically we set

$$\delta(z_s) \stackrel{\bullet}{=} \gamma \, e^{-\gamma z_s} \quad, \tag{7-79}$$

where γ is a suitably large number. Thus:

$$\rho(z) = \sum_{r=1}^{n} A_n \, e^{-\alpha_n z_s} + s_o \, \gamma e^{-\gamma z_s} \quad, \tag{7-80}$$

where $s_o \gamma e^{-\gamma z} s$ is the "correction term" to the representation of the singular kernel $\rho(z_s)$ by a Dirichlet series.

The computational significance of Eq. (7-80) will be appreciated better by virtue of the following example. In practical terms we wish to choose n as small as possible. In Fig. 7.5 we show a hypothetical example where n was set equal to 3. The desired error ϵ then determines δ, and δ determines s_o which is given by Eq. (7-78). The constant γ in Eq. (7-79) should be determined as follows.

Suppose we wish the approximate "Heaviside step function", associated with the approximate δ-function given by Eq. (7-79), to saturate within 1 percent of its value at $z_s = \delta$. Then

$$1 - e^{-\gamma \delta} = 0.99 \tag{7-81}$$

Thus, for $\delta = 0.001$

$$\gamma = \frac{4.605}{\delta} \sim 4.6 \times 10^3 \tag{7-82}$$

We may now use the standard formula for calculating dz given in Chapter 10, namely:

$$a dz^2 + b dz + c = 0 \tag{7-83}$$

where, in the case that the stress increment $\Delta \underset{\sim}{q}$ is prescribed, we have

$$a = 1 - \frac{||\bar{\underset{\sim}{q}}||^2}{\left(\bar{A} F_s\right)^2} \tag{7-84}$$

$$b = -2 \left[\bar{\underset{\sim}{q}} \cdot d\underset{\sim}{s}\right] \Big/ \bar{A}^2 F_s \tag{7-85}$$

$$c = - \left|\left|\frac{d\underset{\sim}{s}}{\bar{A}}\right|\right|^2 \tag{7-86}$$
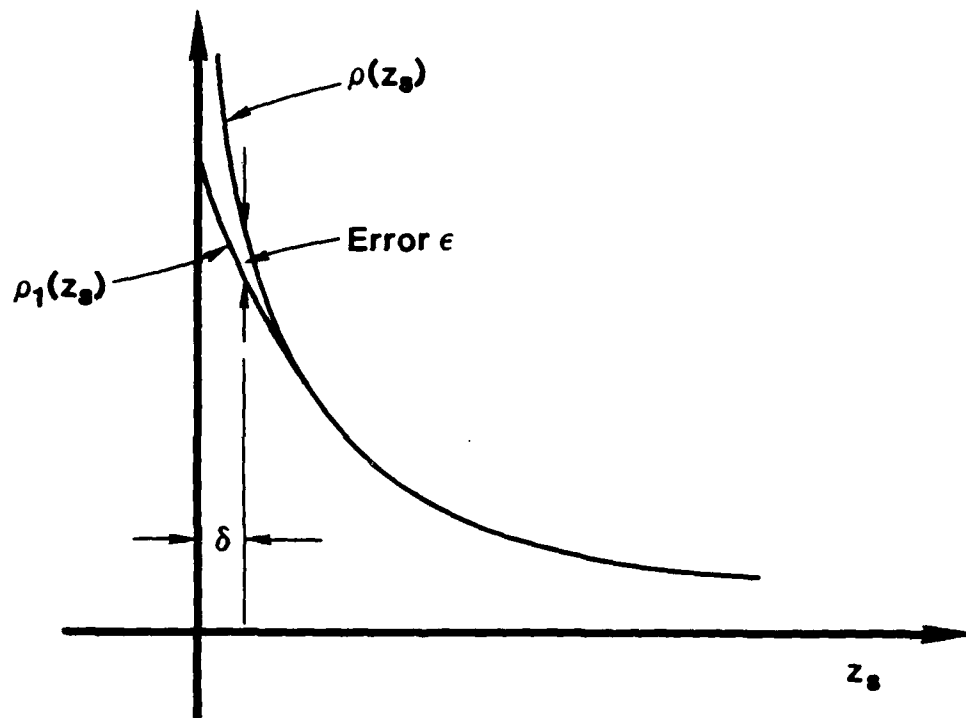
Figure 7.5 δ as a function of the error ϵ.

in the following notation:

$$\widetilde{A} = \sum_{r=1}^{n+1} A_r \tag{7-87}$$

$$\overline{Q} = \sum_{r=1}^{n+1} a_r Q_r \tag{7-88}$$

where

$$A_{n+1} = s_o \gamma \tag{7-89}$$

$$a_{n+1} = \gamma \quad . \tag{7-90}$$

8. PLASTIC FLOW CHARACTERISTICS OF PLASTICALLY INCOMPRESSIBLE SOLIDS

In Chapter 7, we gave an analytical derivation of the flow rules of endochronic plasticity for plastically incompressible solids. As pointed out in that chapter, these rules are valid for all continuous stress paths, irrespective of whether the paths are smooth (differentiable) or not. In this chapter, we give an analysis which addresses the flow rules from another perspective, namely, asymptotic expansions. The plastic flow characteristics are determined for the case of an abrupt change in loading direction in stress space from an otherwise smooth (differentiable) stress path. In addition, asymptotic methods are also used to explore the direction of the plastic strain increment vector when the stress state is near an ultimate surface.

The reader may well ask why the analytical techniques of Chapter 8 are different from those of Chapter 7. The reason is as follows. When the writing of the book began, all that was known about the flow rules of endochronic plasticity was given in the works of Trangenstein and Read [8.1] and Murakami and Read [8.2,8.3] and the material in this chapter is based substantially on those works, which treat the asymptotic cases of very small z and very large z near an ultimate surface, as well as the abrupt change in loading direction from a previously smooth stress path.

During the course of writing this book, Valanis developed the analysis of Chapter 7, from a geometric perspective, which gives the flow rules for general stress paths and for all z. Also given are explicit formulae for determining the direction of $d\underset{\sim}{\varepsilon}^P$ corresponding to a stress increment $d\underset{\sim}{s}$, which is not provided in the analysis of Chapter 8. Thus, the results in Chapter 8 are, in this regard, a special case of those given in Chapter 7.

We felt, however, that the analysis of Chapter 8 is valuable in that it corroborates the results of Chapter 7 and gives additional information regarding the flow rules not contained in Chapter 7. Also, it contains the results of numerical calculations of plastic strain paths corresponding to some complex stress paths, some of which have been investigated experimentally in the literature.

8.1. Basic Equations for Deviatoric Response

In this chapter, we consider the system of equations which govern the deviatoric behavior of a plastically incompressible endochronic solid. These equations were given earlier in Chapter 3 (see Eqs. (3-12) to (3-16)) but are repeated below for easy reference:

$$\mathbf{s} = \int_0^{z_s} \rho(z_s - z') \frac{d\mathbf{e}^p}{dz'} \, dz'$$ (8-1)

$$d\varsigma = \left\| d\mathbf{e}^p \right\|$$ (8-2)

$$dz_s = \frac{d\varsigma}{F_s}$$ (8-3)

$$d\mathbf{e}^p = d\mathbf{e} - \frac{d\mathbf{s}}{2G}$$ (8-4)

In addition, the following form of the weakly singular shear kernel given in Eq. (2-111) is adopted

$$\rho(z) = \rho_o \frac{e^{-\beta z}}{z^\alpha} \; ,$$ (8-5)

where β and ρ_o are positive material constants and $0 < \alpha < 1$. As shown in Section 3.2.6 (see Eq. (3-53)), this form of the kernel function leads to an ultimate (failure) surface. In the remainder of this chapter, the subscript s will be suppressed, and any reference to the intrinsic time z will be tacitly understood to refer to z_s.

The plastic flow properties of the model described by Eqs. (8-1) to (8-5) are explored first for the case in which there is no deviatoric hardening, i.e., $F_s = 1$; as shown in Section 3.2.6, this leads to an ultimate (failure) surface whose trace in the deviatoric (π) plane is a circle. Finally, the plastic flow properties of the model for the case in which F_s depends upon σ and J_3', the third invariant of the deviatoric stress tensor, are considered; such a form of F_s is characteristic of geomaterials, such as soils, rocks and concrete, and leads to an ultimate (failure) surface whose trace in the π-plane is non-circular.

8.2 Plastic Flow Properties in the Absence of Hardening ($F_s = 1$)

Consider the system of equations described above and set $F_s = 1$, which corresponds to no hardening. In this section, a number of features of plastic flow of this model are established. First, analytic solutions are obtained for two limiting cases of response to smooth stress paths. Next, the plastic response of the model to an arbitrary abrupt change is the loading direction in the π-plane on an otherwise smooth stress path is examined analytically and a theoretical solution is obtained, using asymptotic methods, for the plastic compliance as a function of the new loading direction. Finally, the response of the model to a variety of complex stress and complex strain paths is explored through the use of numerical methods.

Note that, for $F_s = 1$, Eq. (8-1) may be written as:

$$\underset{\sim}{s} = \int_0^z \rho(z - z') \underset{\sim}{\ell}(z') dz' \tag{8-6}$$

where $\underset{\sim}{\ell}$, a unit vector, was defined earlier in Eq. (7-28) as:

$$\underset{\sim}{\ell} \equiv \frac{d\underset{\sim}{e}^p}{d\zeta} \tag{8-7}$$

Also, by making the change of variable

$$y = z - z' , \tag{8-8}$$

and introducing the form of $\rho(z)$ given by Eq. (8-5), Eq. (8-6) becomes

$$\underset{\sim}{s} = \rho_0 \int_0^z \frac{e^{-\beta y}}{y^\alpha} \underset{\sim}{\ell}(z - y) dy , \tag{8-9}$$

which will be used in the sequel.

8.2.1 Small z Near the Origin of the Deviatoric Plane.

To explore the plastic flow properties of the above model for small z near the origin of deviatoric space, we begin by differentiating Eq. (8-6) as follows:

$$\frac{d\underset{\sim}{s}}{dz} = \rho(z)\underset{\sim}{\ell}(0) + \int_0^z \rho(y)\underset{\sim}{\ell}{'}(z - y)\,dy \quad , \tag{8-10}$$

where the superscripted prime denotes differentiation with respect to z. Assuming smooth strain paths, $\underset{\sim}{\ell}$ and $\underset{\sim}{\ell}{'}$ can be expanded in Taylor series as follows:

$$\underset{\sim}{\ell}(0) = \underset{\sim}{\ell}(z) - \sum_{n=1}^{\infty} \frac{1}{n!}\, z^n \underset{\sim}{\ell}{}^n(0)$$

$$\tag{8-11}$$

$$\underset{\sim}{\ell}{'}(z - y) = \sum_{n=0}^{\infty} \frac{(-1)^n}{n!}\, y^n \underset{\sim}{\ell}{}^{n+1}(z)$$

Substitution of Eqs. (8-11) into Eq. (8-10) leads to the expression:

$$\frac{d\underset{\sim}{s}}{dz} = \rho(z)\underset{\sim}{\ell}(z) - \sum_{n=1}^{\infty} \frac{1}{n!}\, z^n \rho(z)\underset{\sim}{\ell}{}^n(0) + \underset{\sim}{\ell}{'}(z) \int_0^z \rho(y)\,dy$$

$$\tag{8-12}$$

$$+ \sum_{n=1}^{\infty} \frac{(-1)^n}{n!}\, \underset{\sim}{\ell}{}^{n+1}(z) \int_0^z y^n \rho(y)\,dy$$

For small z, $\rho(z)$ varies as $z^{-\alpha}$; thus, we can write:

$$z^n \rho(z) = 0 \left(z^{n-\alpha}\right)$$

$$\int_0^z \rho(y)\,dy = 0\left(z^{1-\alpha}\right) \tag{8-13}$$

$$\int_0^z y^n \rho(y)\,dy = 0\left(z^{n+1-\alpha}\right)$$

Hence, Eq. (8-12) can be expressed in the form:

$$\frac{d\underset{\sim}{s}}{dz} = \rho(z)\underset{\sim}{\ell} + 0\left(z^{1-\alpha}\right) \quad , \tag{8-14}$$

which shows that for small z ($z << 1$), $d\underset{\sim}{s}/dz$ and $\underset{\sim}{\ell}$ are coaxial, since $0 < \alpha < 1$.

In view of Eq. (8-7), it therefore follows that $d\underset{\sim}{\varepsilon}^p$ and $d\underset{\sim}{s}$ are coaxial for small z. This result illustrates one of the unique features of the endochronic theory which sets it apart from classical plasticity, namely, that in the endochronic theory plastic flow develops immediately upon application of load, while in classical plasticity, plastic flow does not occur until after the stress state has reached the yield surface.

8.2.2. Large z Near an Ultimate Surface.

Let us consider a stress path which is arbitrary for $z < z_o$, but at z_o it monotonically approaches the ultimate surface. For $z > z_o$, the plastic strain path, and hence $\underset{\sim}{\ell}$, will be smooth and simple during the recent past $\{z - y | 0 \leq y \leq y_m\}$, where y_m is a characteristic of the material such that for $y \geq y_m$, $e^{-\beta y}$ is negligible. Under these conditions, we wish to consider the constitutive expression for $\underset{\sim}{s}$ given by Eq. (8-9), namely:

$$\mathfrak{s} = \rho_0 \int_0^z \frac{e^{-\beta y}}{y^\alpha} \, \mathfrak{l}(z - y) \, dy \tag{8-15}$$

For a large class of materials, including metals and geomaterials, it has been found through experience in applying the theory that $\beta \gg 1$ (typically on the order of 10^3 to 10^4). For such large β, the major contribution to the above integral occurs near $y = 0$. Because of the smoothness of the $\mathfrak{e}^P$-path for $z > z_0$, the function $\mathfrak{l}(z - y)$ can be expanded in a Taylor series about $y = 0$ to give:

$$\mathfrak{l}(z - y) = \mathfrak{l}(z) - y \, \mathfrak{l}'(z) + \frac{1}{2} y^2 \mathfrak{l}''(z) - \ldots \tag{8-16}$$

However, due to the large value of β, $\mathfrak{l}(z - y)$ can be represented by the first few terms of the above series over $\{0 \le y \le y_m\}$ where $e^{-\beta y}$ is not negligible. Therefore, Eq. (8-15) can be expressed as:

$$\mathfrak{s} = \rho_0 \int_0^z \frac{e^{-\beta y}}{y^\alpha} \left[\mathfrak{l}(z) - y \, \mathfrak{l}'(z) + \ldots \right] dy + 0\left(e^{-\beta z}\right) \tag{8-17}$$

Applying Watson's lemma* to the integral and performing the integration, one finds that

$$\mathfrak{s} = \rho_0 \left[\mathfrak{l}(z) \frac{\Gamma(1 - \alpha)}{\beta^{1-\alpha}} - \mathfrak{l}'(z) \frac{\Gamma(2 - \alpha)}{\beta^{2-\alpha}} + 0\left[\frac{1}{\beta^{3-\alpha}}\right] \right] + 0\left(e^{-\beta z}\right) , \tag{8-18}$$

where $\Gamma(\bullet\bullet\bullet)$ denotes the gamma function. Upon introducing Eq. (3-53), (with an appropriate change of notation), together with the relation $\Gamma(n+1) = n\Gamma(n)$, Eq. (8-18) can be rewritten in the form:

$$\mathfrak{s} = s_\infty \left[\mathfrak{l} - c\mathfrak{l}' + \frac{1}{2} c^2 \left[\frac{2 - \alpha}{1 + \alpha}\right] \mathfrak{l}'' - \frac{1}{6} c^3 \left[\frac{2 - \alpha}{1 - \alpha}\right] \left[\frac{3 - \alpha}{1 - \alpha}\right] \mathfrak{l}''' + \ldots \right] , \tag{8-19}$$

where

$$c \equiv \frac{1 - \alpha}{\beta} \tag{8-20}$$

---

* See, for instance, Reference [8.4].

Let us take the Euclidean norm of both sides of Eq. (8-19), and neglect terms of $0(\beta^{-2})$ and higher compared with unity; this results in the expression

$$\left|\left|\underset{\sim}{s}\right|\right| = s_\infty\left[1 - c^2\left\{1 + \frac{1}{2}\left[\frac{2 - \alpha}{1 - \alpha}\right]\right\}\left(\underset{\sim}{\ell'} \cdot \underset{\sim}{\ell'}\right)\right] \, , \tag{8-21}$$

where, since $\underset{\sim}{\ell}$ is a unit vector, we have that $\underset{\sim}{\ell} \cdot \underset{\sim}{\ell'} = 0$. Inasmuch as $||\underset{\sim}{s}|| \rightarrow s_\infty$ as the ultimate surface is approached, it follows from Eq. (8-21) that $\underset{\sim}{\ell'} \rightarrow 0$ also. Returning to Eq. (8-19), and neglecting terms of $0(\beta^{-2})$, we have:

$$\underset{\sim}{s} = s_\infty\left[\underset{\sim}{\ell} - c\underset{\sim}{\ell'}\right] \tag{8-22}$$

As the ultimate surface is approached, $\underset{\sim}{\ell'} \rightarrow 0$ as shown above, so that Eq. (8-22) reduces simply to

$$\underset{\sim}{s} = s_\infty \frac{d\underset{\sim}{\varepsilon}^p}{dz} \, , \tag{8-23}$$

where use has been made of Eq. (8-7). This expression shows that as the ultimate surface is approached, $d\underset{\sim}{\varepsilon}^p$ becomes coaxial with $\underset{\sim}{s}$. Therefore, since the ultimate surface of the model considered here cuts the π-plane in a circle, the vector $d\underset{\sim}{\varepsilon}^p$ becomes normal to this surface as $\underset{\sim}{s}$ approaches the surface. This feature of the theory is illustrated in Figure 8.1. Later, in Section 8.3, the plastic flow properties of the version of the model which exhibits a non-circular ultimate surface in the π-plane are explored.

To show the relationship to classical plasticity, let us rewrite Eq. (8-23) as

$$\underset{\sim}{\dot{\varepsilon}}^p = \left(\frac{\dot{z}}{s_\infty}\right)\underset{\sim}{s} \quad , \tag{8-24}$$

where the superposed dot denotes differentiation with respect to time. Upon recalling from Eqs. (8-2) and (8-3) that for $F_s = 1$:

$$dz = \left|\left|d\underset{\sim}{\varepsilon}^p\right|\right| \quad ,$$

when the stress state is very close to the ultimate surface, we can write:
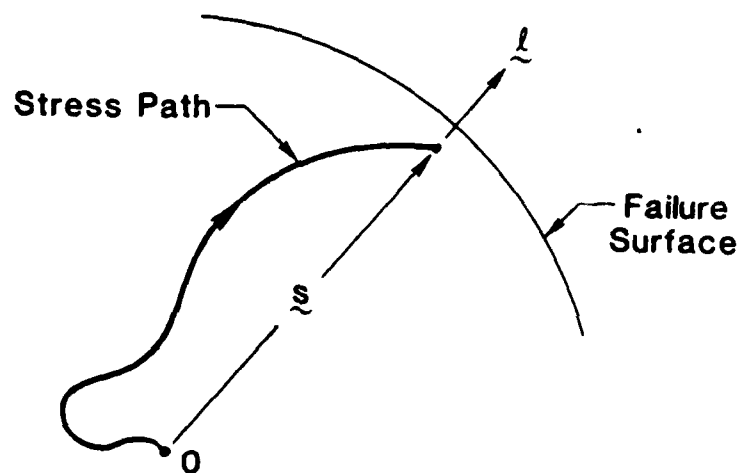
Figure 8.1   Stress path in the π-plane, showing $\underset{\sim}{\ell}$ becoming coaxial with $\underset{\sim}{s}$ as failure surface is approached.

$$s_\infty = \left|\left|\underset{\approx}{s}\right|\right| \quad , \qquad\qquad\qquad\qquad (8\text{-}25)$$

Eq. (8-24) can then be expressed in the form:

$$\overset{\bullet}{\underset{\approx}{e}}^P = \overset{\bullet}{\lambda}\underset{\approx}{s} \quad , \qquad\qquad\qquad\qquad (8\text{-}26)$$

where

$$\overset{\bullet}{\lambda} = \frac{\left|\left|\overset{\bullet}{\underset{\approx}{e}}^P\right|\right|}{\left|\left|\underset{\approx}{s}\right|\right|} \qquad\qquad\qquad\qquad (8\text{-}27)$$

Equation (8-26), with $\overset{\bullet}{\lambda}$ defined by Eq. (8-27), is the well-known Prandtl-Reuss equation of classical plasticity [8.5]. Therefore, for smooth limiting behavior in the neighborhood of an ultimate surface whose trace in the π-plane is a circle, we find that the endochronic theory leads to the same plastic behavior (or flow rule) as classical plasticity. In general, however, the plastic flow properties of the endochronic theory differ substantially from those of classical plasticity, as will be demonstrated in the following section and in Section 8.3.

8.2.3 Abrupt Change in the Loading Direction.

Important insight into the constitutive properties of complex nonlinear constitutive theories can often be obtained by examining their responses to abrupt changes in loading direction from an otherwise smooth loading path. In this section, the response of the endochronic model with $F_s = 1$ to an abrupt change in loading direction is analyzed, using asymptotic analytic methods.

Consider Figure 8.2, which depicts a stress path in the π-plane that is smooth up to some point P. At P, an abrupt change in the loading direction occurs for subsequent loading. In the following analysis, the tangent to the smooth stress path at P is denoted by $\underset{\sim}{t}$, and the arbitrary new loading direction is represented by $\underset{\sim}{b}$, where both $\underset{\sim}{t}$ and $\underset{\sim}{b}$ are unit vectors. The value of the intrinsic time at P will be denoted by z_o. The stress path is therefore smooth for $0 \leq z \leq z_o^-$ and, at $z = z_o$, it suddenly changes direction so that for $z \geq z_o^+$, the deviatoric stress increment $d\underset{\sim}{s}$ lies in the new direction $\underset{\sim}{b}$. Here, z_o^- and z_o^+ denote the left and right neighborhood values of z_o, respectively.
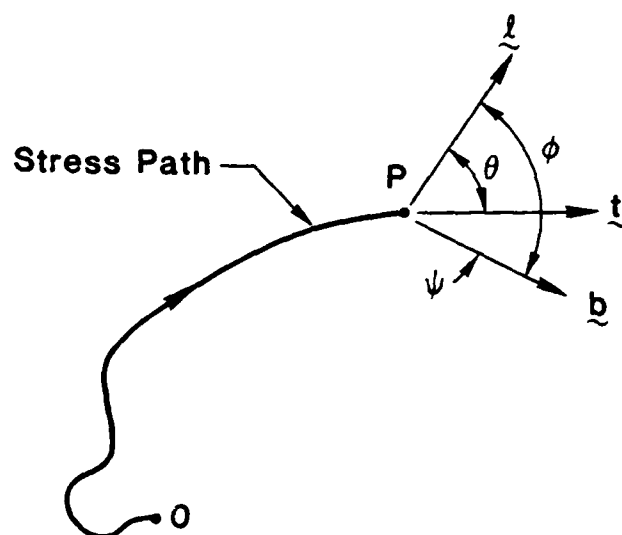
Figure 8.2.   Smooth stress path in the π-plane, showing the unit vectors $\underset{\sim}{\ell}$, $\underset{\sim}{b}$, and $\underset{\sim}{t}$ and the angles θ, ϕ and ψ.

Let us now introduce the notation

$$\Delta \underset{\sim}{s}(z_0) \equiv \underset{\sim}{s}(z_0 + \Delta z) - \underset{\sim}{s}(z_0) \tag{8-28}$$

Using Eq. (8-9) to evaluate the right-hand side of this expression, we obtain:

$$\Delta \underset{\sim}{s}(z_0) = \rho_0 \int_0^{\Delta z} \frac{e^{-\beta y}}{y^\alpha} \underset{\sim}{\ell}(z_0 + \Delta z - y)dy + \rho_0 \int_{\Delta z}^{z_0} \frac{e^{-\beta y}}{y^\alpha} [\underset{\sim}{\ell}(z_0 + \Delta z - y) - \underset{\sim}{\ell}(z_0 - y)]dy$$

$$\tag{8-29}$$

$$+ \rho_0 \int_{z_0}^{z_0 + \Delta z} \frac{e^{-\beta y}}{y^\alpha} \underset{\sim}{\ell}(z_0 + \Delta z - y)dy - \rho_0 \int_0^{\Delta z} \frac{e^{-\beta y}}{y^\alpha} \underset{\sim}{\ell}(z_0 - y)dy$$

Let us now consider the form that this equation takes as $\Delta z \to 0$. We first note that along the smooth portion of the stress path, Eq. (8-9) may be differentiated to give at $z = z_0^-$:

$$\frac{d\underset{\sim}{s}}{dz}\Bigg|_{z_0^-} = \rho_0 \frac{e^{-\beta z_0}}{z_0^\alpha} \underset{\sim}{\ell}(0) + \rho_0 \int_0^{z_0} \frac{e^{-\beta y}}{y^\alpha} \underset{\sim}{\ell}'(z_0 - y)dy \tag{8-30}$$

Also, since

$$\underset{\sim}{\ell}(z_0 + \Delta z - y) - \underset{\sim}{\ell}(z_0 - y) \doteq \underset{\sim}{\ell}'(z_0 - y)\Delta z \quad, \tag{8-31}$$

we can write

$$\int_{\Delta z}^{z_0} \frac{e^{-\beta y}}{y^\alpha} [\underset{\sim}{\ell}(z_0 + \Delta z - y) - \underset{\sim}{\ell}(z_0 - y)]dy \doteq \rho_0 \Delta z \frac{d\underset{\sim}{s}}{dz}\Bigg)_{z_0^-} \tag{8-32}$$

8-11

In addition, it follows that

$$
\int_{z_o}^{z_o+\Delta z} \frac{e^{-\beta z_o}}{y^\alpha} \underset{\approx}{\mathscr{L}}(z_o + \Delta z - y) = \rho_o \frac{e^{-\beta z_o}}{z_o^\alpha} \underset{\approx}{\mathscr{L}}(0)\Delta z \tag{8-33}
$$

Upon introducing Eqs. (8-32) and (8-33) into Eq. (8-29), the following expression results:

$$
\Delta\underset{\approx}{\mathbf{s}}(z_o) = \Delta z \left.\frac{d\underset{\approx}{\mathbf{s}}}{dz}\right]_{z_o^-} + \rho_o \int_0^{\Delta z} \frac{e^{-\beta y}}{y^\alpha} \left[\underset{\approx}{\mathscr{L}}(z_o + \Delta z - y) - \underset{\approx}{\mathscr{L}}(z_o - y)\right] dy \tag{8-34}
$$

Consider now an asymptotic expansion for $\underset{\approx}{\mathscr{L}}(z_o + \Delta z)$; this should be expressed in terms of two linearly independent vectors, one of which must be $\underset{\sim}{\mathbf{b}}$. For the other vector, $\underset{\sim}{\mathscr{L}}$ and $\underset{\sim}{\mathbf{t}}$ are available, since they are both linearly independent of $\underset{\sim}{\mathbf{b}}$. If $\underset{\sim}{\mathscr{L}}$ is selected for this purpose, as was done by Trangenstein and Read [8.1], $\underset{\sim}{\mathscr{L}}$ is restricted to be coaxial with $\underset{\sim}{\mathbf{t}}$, a condition which is not correct for stress states near the ultimate surface (see Section 8.2.2). Therefore, the appropriate vectors to use in the asymptotic expansion for $\underset{\approx}{\mathscr{L}}(z_o + \Delta z)$ evidently are $\underset{\sim}{\mathbf{b}}$ and $\underset{\sim}{\mathbf{t}}$.

On this basis, the following form for the asymptotic expansion of $\underset{\sim}{\mathscr{L}}$ is adopted:

$$
\underset{\approx}{\mathscr{L}}(z_o + \Delta z) - \underset{\approx}{\mathscr{L}}(z_o) = -\underset{\sim}{\mathbf{t}}\, a_1\Delta z^u + \underset{\sim}{\mathbf{b}}\left[\beta_o + \beta_1\Delta z^p\right] \tag{8-35}
$$

where a_1, β_o, u and p are constants. Furthermore, it will be assumed that

$$
\beta_o + \beta_1\Delta z^p > 0 \quad \text{for } \Delta z > 0 \tag{8-36}
$$

Upon substituting Eq. (8-35) into Eq. (8-34), and using the following expansions for the integrals:

$$\int_0^{\Delta z} \frac{e^{-\beta y}}{y^\alpha} (\Delta z - y)^u dy = \frac{\Gamma(1 - \alpha)\Gamma(1 + u)}{\Gamma(2 + u - \alpha)} \Delta z^{1+u-\alpha}$$

$$\int_0^{\Delta z} \frac{e^{-\beta y}}{y^\alpha} dy = \frac{1}{1 - \alpha} \Delta z^{1-\alpha} \tag{8-37}$$

$$\int_0^{\Delta z} \frac{e^{-\beta y}}{y^\alpha} (\Delta z - y)^p dy = \frac{\Gamma(1 - \alpha)\Gamma(1 + p)}{\Gamma(2 + p - \alpha)} \Delta z^{1+p-\alpha} \quad ,$$

it follows that:

$$\Delta \underset{\sim}{s}(z_0) = \underset{\sim}{t}\left\{ \Delta z \left|\left|\frac{d\underset{\sim}{s}}{dz}\right|\right|_{z_0^-} - \alpha_1 \rho_0 \frac{\Gamma(1 - \alpha)\Gamma(1 + u - \alpha)}{\Gamma(2 + u - \alpha)} \Delta z^{1+u-\alpha} \right\}$$

$$\tag{8-38}$$

$$+ \underset{\sim}{b}\left\{ \frac{\rho_0 \beta_0}{1 - \alpha} \Delta z^{1-\alpha} + \rho_0 \beta_1 \frac{\Gamma(1 - \alpha)\Gamma(1 + p)}{\Gamma(2 + p - \alpha)} \Delta z^{1+p-\alpha} \right\} \quad ,$$

where use has been made of the relationship

$$\frac{d\underset{\sim}{s}}{dz}\bigg)_{z_0^-} = \underset{\sim}{t}\left|\left|\frac{d\underset{\sim}{s}}{dz}\right|\right|_{z_0^-} \quad . \tag{8-39}$$

The new stress increment. $\Delta \underset{\sim}{s}$. at the point of the abrupt change in loading direction. is assumed to be in the arbitrary direction $\underset{\sim}{b}$. As a result. the coefficient of $\underset{\sim}{t}$ in Eq. (8-38) must vanish. which leads to the following conditions:

$$u = \alpha$$

$$a_1 = \left|\left|\frac{d\underset{\sim}{s}}{dz}\right|\right|_{z_o^-} \Gamma(2)/\left\{\rho_o \Gamma(1 - \alpha)\Gamma(1 + \alpha)\right\} \tag{8-40}$$

From Figure 8.2, we can write

$$\cos\theta = \underset{\sim}{\ell} \cdot \underset{\sim}{t}$$

$$\cos\phi = \underset{\sim}{\ell} \cdot \underset{\sim}{b} \tag{8-41}$$

$$\cos\psi = \underset{\sim}{b} \cdot \underset{\sim}{t}$$

Also, since $\underset{\sim}{\ell}$ is a unit vector, it follows that

$$\left|\left|\underset{\sim}{\ell}(z_o + \Delta z)\right|\right|^2 = 1 \tag{8-42}$$

Upon substituting Eqs. (8-35), (8-40) and (8-41) into Eq. (8-42), one obtains the result:

$$1 \overset{\bullet}{=} \left\{1 + \beta_o\big(\beta_o(\beta_o 2\cos\phi)\big)\right\} - 2\,a_1\big(\cos\theta + \beta_o\cos\psi\big)\Delta z^\alpha \tag{8-43}$$

$$+ 2\beta_1\big(\cos\phi + \beta_o\big)\Delta z^p + \beta_1^2 \Delta z^{2p} - 2a_1\beta_1\cos\psi\Delta z^{\alpha+p}.$$

Inasmuch as the direction $\underset{\sim}{b}$ is arbitrary with respect to $\underset{\sim}{\ell}(z_o)$, there are accordingly three ranges of ϕ that must be considered. But before doing this, let us note that for the case of no hardening ($F_s=1$) considered here, it follows that $dz = ||d\underset{\sim}{e}^P||$. Accordingly, we can write

$$\frac{d\underset{\sim}{s}}{dz}\bigg)_{z_o^+} \equiv \lim_{\Delta z \to 0} \frac{\Delta\underset{\sim}{s}(z_o)}{\Delta z} = \underset{\sim}{b}\left|\left|\frac{d\underset{\sim}{s}}{d\underset{\sim}{e}^P}\right|\right|_{z_o^+} \tag{8-44}$$

8-14

Consequently, a finite value of $d\underset{\sim}{\mathbf{s}}/dz$ at z_o^+ implies plastic response, while an infinite value indicates purely elastic response.

(i) $\cos\phi > 0$.

The zero order terms in Eq. (8-43), together with the non-negative condition from Eq. (8-36), require that

$$\beta_o = 0. \tag{8-45}$$

The next higher order terms in Eq. (8-43), together with Eq. (8-40a) imply that

$$p = u = \alpha$$

$$\beta_1 = \alpha_1 \cos\theta/\cos\phi. \tag{8-46}$$

Upon substituting Eqs. (8-45) and (8-46) into Eq. (8-38), we find that

$$\left. \frac{d\underset{\sim}{\mathbf{s}}}{dz} \right)_{z_o^+} = \underset{\sim}{\mathbf{b}} \, \frac{\cos\theta}{\cos\phi} \, \left| \left| \frac{d\underset{\sim}{\mathbf{s}}}{dz} \right| \right|_{z_o^-} \qquad . \tag{8-47}$$

The finite value of $d\underset{\sim}{\mathbf{s}}/dz$ at z_o^+ implies plastic response for this case.

(ii) $\cos\phi = 0$.

In this instance, the zero order terms in Eq. (8-42) must satisfy Eq. (8-45), while the next higher order terms require that

$$-2\alpha_1\cos\theta \, \Delta z^\alpha + \beta_1^2 \Delta z^{2p} = 0 \qquad . \tag{8-48}$$

As a result,

$$p = \frac{u}{2} = \frac{\alpha}{2} \tag{8-49}$$

$$\beta_1 = (2\alpha_1\cos\theta)^{1/2} \quad ,$$

8-15

which on substitution into Eq. (8-38) leads to the result

$$\left.\frac{d\underset{\sim}{s}}{dz}\right)_{z_o^+} \to \infty \quad , \tag{8-50}$$

implying that the response is purely elastic.

(iii) $\cos\phi < 0$.

The zero order terms in Eq. (8-43) must satisfy the condition

$$\beta_o = -2\cos\phi. \tag{8-51}$$

while the next higher order terms require that

$$p = \alpha. \tag{8-52}$$

Inasmuch as $\beta_o \neq 0$, we obtain in this case the condition (8-50), implying that the response is purely elastic.

The results from the three cases considered above can be conveniently expressed in terms of the incremental plastic compliance, C^p, as follows:

$$C^p \equiv \left|\left|\frac{d\underset{\sim}{e}^p}{d\underset{\sim}{s}}\right|\right| = \begin{cases} \dfrac{\cos\phi}{\gamma(z_o)} \quad , \quad \phi < \pi/2 \\[4mm] 0 \quad , \quad \phi \geq \pi/2 \end{cases} \tag{8-53}$$

where

$$\gamma(z_o) \equiv \cos\theta \left|\left|\frac{d\underset{\sim}{s}}{dz}\right|\right|_{z_o^-} . \tag{8-54}$$

Equation (8-54) reveals that C^p is a continuous function of the angle ϕ and is zero for all stress increments normal to $\underset{\sim}{\ell}$, as well as for those which have a negative component with respect to $\underset{\sim}{\ell}$ at z_o^-. This is illustrated in Figure 8.3, where the
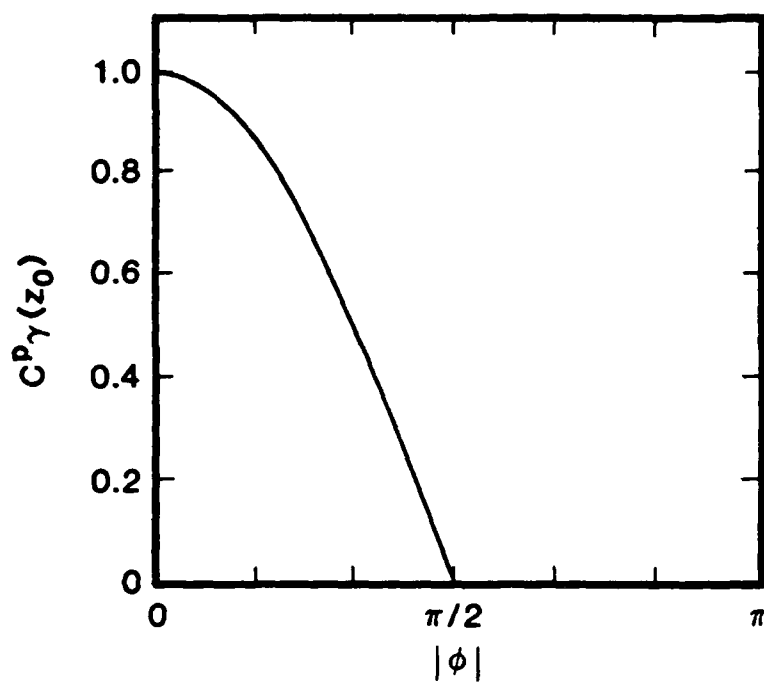
Figure 8.3.   Variation of incremental plastic compliance with angle ϕ.

variation of the dimensionless incremental plastic compliance, $C^P\gamma(z_o)$, with ϕ is shown. Note also that, through $\gamma(z_o)$, C^P depends upon the angle θ between the unit vectors $\underset{\sim}{\ell}$ and $\underset{\sim}{t}$ and that this angle depends upon the plastic strain history.

It is emphasized that Eq. (8-53) was derived on the basis of an assumed abrupt change in loading direction from an otherwise smooth stress path. To explicitly define C^P, one must know, at the point of abrupt change in loading direction, the angles ϕ and θ, as well as $||d\underset{\sim}{s}/dz||$ at z_o^-, all of which depend upon the plastic strain history. In general, to evaluate these quantities requires that the governing equations of the model be integrated along the stress path and, due to the nonlinear nature of the equations, this can be accomplished only through numerical methods, which are treated in the following section.

In the case of a smooth stress path, i.e., no abrupt change in loading direction, Eq. (8-53) furnishes no useful information. In this case, $\underset{\sim}{\ell}$ is coaxial with $\underset{\sim}{t}$ so that $\psi = 0$ and $\theta = \phi$. Upon introducing these conditions into Eq. (8-53), and recalling from Section 7.2 (Eq. (7-46)) that $\cos\theta \geq 0$ for loading, it follows that

$$C^P = \left|\left|\frac{d\underset{\sim}{e}^P}{d\underset{\sim}{s}}\right|\right| , \qquad (8\text{-}55)$$

which is simply the definition of C^P adopted in Eq. (8-53).

For proportional loading, $\underset{\sim}{\ell}$ is coaxial with $\underset{\sim}{t}$ so that $\psi = \phi$. In this case, it can be shown that Eq. (8-53) reduces to the expression for C^P given by Trangenstein and Read [8.1], who assumed a form of asymptotic expansion for $\underset{\sim}{\ell}(z_o + \Delta z)$ which inadvertently forced $\underset{\sim}{a}$ to be coaxial with $\underset{\sim}{t}$.

8.2.4 Complex Stress and Strain Paths.

The response characteristics of the endochronic model for a number of selected complex stress and strain paths in the π-plane are considered in this section. The selected paths provide insight into the plastic flow properties of the model for paths that lie between the two limiting cases treated analytically in Sections 8.2.1 and 8.2.2.

Because of the nonlinear nature of the governing equations, numerical methods are used to integrate the equations along these paths and, for this purpose, the incremental numerical method described in Chapter 10 was used.

The specific endochronic model adopted for the studies described in this section had the following material properties: The shear modulus was taken to be $G = 38.61$ MPa, while the kernel function $\rho(z)$ was described by three terms in the series (3-258), with the following values of α_r and R_r:

$$(\alpha_1, \alpha_2, \alpha_3) = (0.767, 1.15, 2.75) \times 10^4$$

$$(R_1, R_2, R_3) = (0.46, 2.2, 5.9) \times 10^2 \text{ GPa}$$

(8-56)

Let us consider, first, a complex <u>strain path</u> in the deviatoric plane which has the triangular form shown in Figure 8.4. The path starts at $\underset{\sim}{e} = \underset{\sim}{0}$, proceeds outward along the e_3-axis, and then turns abruptly to follow the triangular trajectory in a counterclockwise direction. The endochronic model described above was driven around this complex strain path and the corresponding stress history was predicted. Figure 8.4 shows the deviatoric stress vectors predicted by the model at selected points along the triangular path. Note that at the turning points where a sudden change in the direction of the strain increment $\Delta\underset{\sim}{e}$ occurs, the stress vector changes smoothly, gradually approaching coaxiality with the strain increment.

The response of a clay soil to a prescribed strain path qualitatively similar to that shown in Figure 8.4 has been studied by Pearce [8.6], using a true triaxial device. The results from this study are depicted in Figure 8.5, where the deviatoric stress vectors measured during the test at selected points along the strain path are shown. As a comparison of the two figures will reveal, the predicted and measured stress vectors at points along the prescribed strain paths are qualitatively very similar. It should also be noted that the response of a classical plasticity model with hardening to the complex strain path shown in Figure 8.4 was also studied numerically and produced a similar variation of the stress vectors along the path.

8-19

Figure 8.5. Measured stress response of a clay soil to a prescribed triangular strain path in the deviatoric strain plane (from Reference [8.6]).

Figure 8.4. Predicted stress response of an endochronic model to a prescribed triangular strain path in the deviatoric strain plane.

Substantial differences between endochronic theory and classical plasticity become apparent, however, when prescribed complex stress paths are considered. Figure 8.6, for example, shows four different circular stress paths which intersect the origin. The model was driven around each of these paths and the deviatoric plastic strain increment vectors $\Delta \varepsilon^P$ were calculated for specified increments of $||\Delta s_{\sim}/\sigma_{\infty}||$. The results are depicted in Figure 8.6, where the predicted vectors $\Delta \varepsilon^P$ are shown at selected points along the stress paths. Figure 8.6(a) shows two small circular stress paths that are close to the origin of the π-plane. For the path with the smaller radius, the vectors $\Delta \varepsilon^P$ and Δs are essentially coaxial, which is consistent with Eq. (8-14) given earlier. For the other path, $\Delta \varepsilon^P$ is coaxial with Δs near the origin, but increasingly becomes more radial in direction as failure is approached; this feature of the model is more clearly illustrated in Figure 8.6(b) by the stress path which intersects the failure surface. Here, we see that $\Delta \varepsilon^P$ is tangent to the stress path near the origin, but becomes increasingly radial in direction, and therefore approaches coaxiality with s as failure is approached. Also, as the stress state becomes increasingly closer to failure, $\Delta \varepsilon^P \to \infty$. The results described above, which were obtained with the incremental numerical procedure, are fully consistent with the two limiting cases treated in Sections 8.2.1 and 8.2.2.

Figure 8.7 shows several stress paths consisting of two linear segments in the π-plane. The paths begin at the origin of the π-plane, proceed outward along the s_3-axis and then turn abruptly to follow linear trajectories which make angles of 30 degrees, 60 degrees and 90 degrees with the s_3-axis. The only difference between the figures (a) and (b) is the location of the point on the s_3-axis where the paths veer away from this axis. In Figure 8.7(a), the second segment begins at $s_3 = \sigma_{\infty}/6$ while in Figure 8.7(b) the second segment begins at twice this distance from the origin, $s_3 = \sigma_{\infty}/3$. The vectors $\Delta \varepsilon^P$ predicted by the model are shown at selected locations along the second segment of each path. On the first segment, $\Delta \varepsilon^P$ is parallel to the s_3-axis and is not shown to avoid overcrowding the figure. A comparison between the vectors $\Delta \varepsilon^P$ shown in the two figures reveals that the effect of having the second segment begin closer to the failure surface is to increase the radial component of $\Delta \varepsilon^P$ along the initial portion of the paths. In Figure 8.7(a), the $\Delta \varepsilon^P$ vectors initially are almost tangent to the stress path while in Figure 8.7(b) they have a significant radial component. Ultimately, the vectors $\Delta \varepsilon^P$ tend toward coaxiality with the stress vector s as the failure surface is approached.
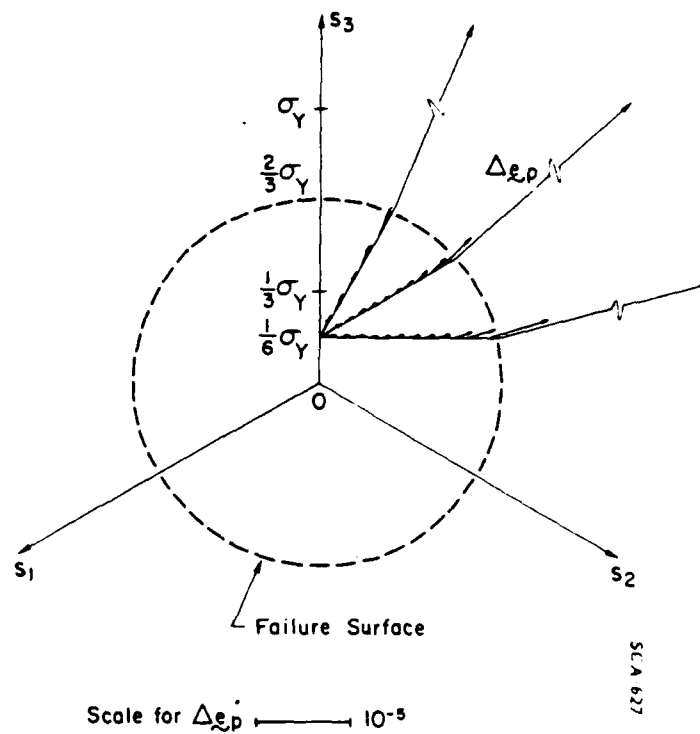
Scale for $\Delta \underset{\sim}{e}_p$ ⊢————⊣ 1.2×10^{-7}
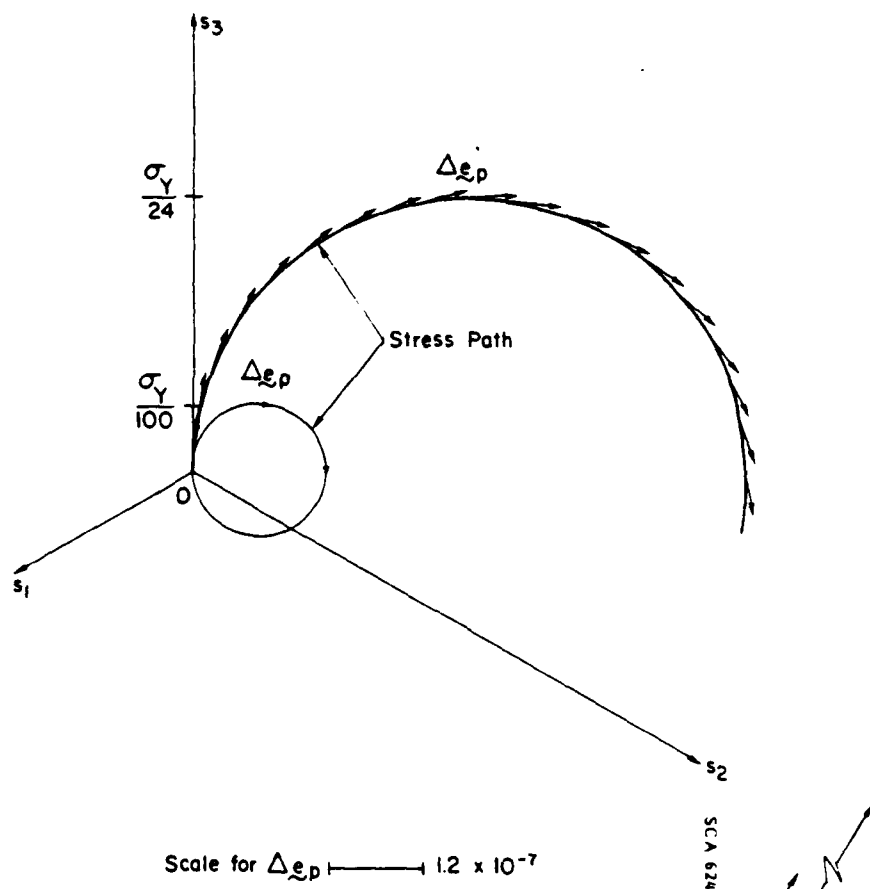
(a) Small radii paths near the origin.

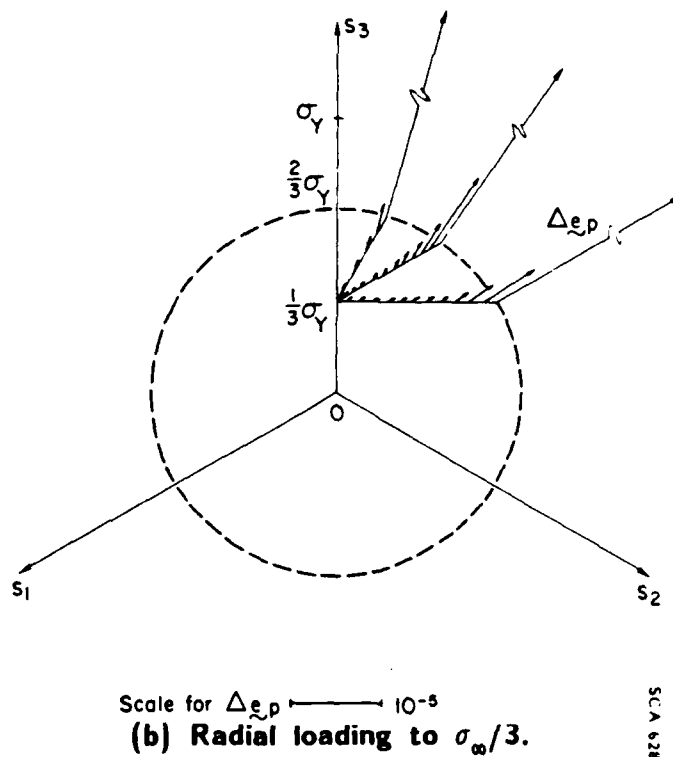Scale for $\Delta \underset{\sim}{e}_p$ ⊢——⊣ 10^{-6}
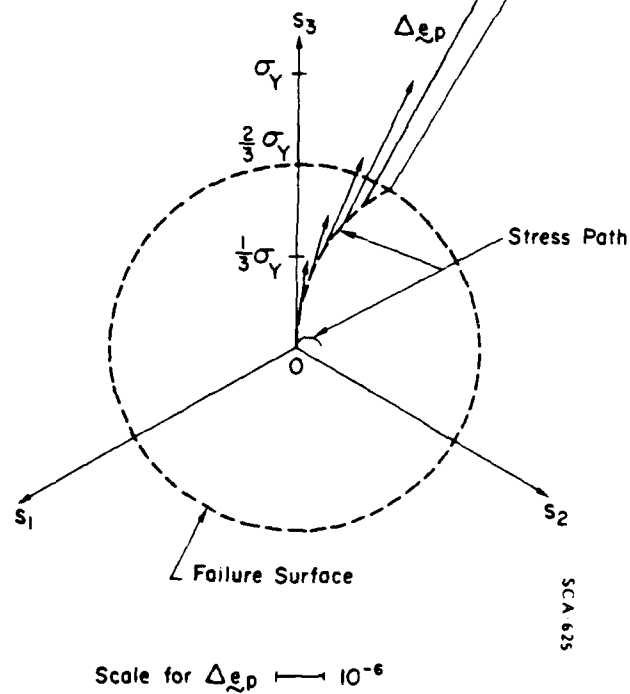
(b) Large radius path.

Figure 8.6.   Circular stress paths and corresponding plastic strain increment vectors predicted by the model.

(a) Radial loading to $\sigma_\infty/6$.

Scale for $\Delta \underset{\sim}{e}_p$ ⊢———⊣ 10^{-5}

SCA 627

Scale for $\Delta \underset{\sim}{e}_p$ ⊢———⊣ 10^{-5}

(b) Radial loading to $\sigma_\infty/3$.

SCA 628

Figure 8.7.   Bilinear stress paths with corresponding plastic strain increment vectors predicted by the model.

Next, let us consider the stress path shown in Figure 8.8, which has a circular segment which is near to, and concentric with, the failure surface. The stress path begins at the origin of the π-plane, proceeds upward along the s_3-axis and then follows the circular trajectory in a clockwise fashion. As before, the vectors $\Delta \underset{\sim}{\varepsilon}^P$ predicted by the model are shown at selected locations along the circular path. Note that these vectors are nearly perpendicular to the stress path and nearly coaxial with the stress vector, $\underset{\sim}{s}$. Again, these features of the model are in full agreement with the behavior predicted in Section 8.2.2 for the limiting case of response near a failure surface.

Finally, Figure 8.9 shows a complex stress path in the π-plane which consists first of radial loading along the s_3-axis, followed by a triangular trajectory that is traversed in a counterclockwise direction. Again, the vectors $\Delta \underset{\sim}{\varepsilon}^P$ predicted by the model at selected locations along the triangular portion of the stress path are shown. Note that after an abrupt change in the loading direction (at the corners of the triangle), the vectors $\Delta \underset{\sim}{\varepsilon}^P$ greatly diminish in magnitude, reflecting the unloading that is occurring. Also, as the stress path approaches the failure surface, the vector $\Delta \underset{\sim}{\varepsilon}^P$ becomes increasing coaxial with the vector $\underset{\sim}{s}$, in agreement with the analytic results presented earlier in Section 8.2.2.

8.3 PLASTIC FLOW PROPERTIES WITH HARDENING

In the preceding sections, we explored the plastic flow properties of the endochronic model for the case in which there was no shear hardening, i.e., $F_s = 1$. By virtue of the form adopted for the shear kernel $\rho(z_s)$ in Eq. (8-5), it was noted that when $F_s = 1$ the resulting model exhibits an ultimate surface which intersects the π-plane in the form of a circle. While such an ultimate surface provides a reasonable representation for a number of materials, there is also a large class of materials of considerable practical interest for which it is not appropriate; this includes rocks, soils and concretes, for example. For these materials, the ultimate surface depends upon the hydrostatic stress σ, and its trace in a π-plane is, in general, non-circular.

The shear hardening function F_s is responsible for defining the shape of the ultimate surface exhibited by the endochronic model. For the class of materials noted above, the ultimate surface depends on σ and on the third invariant of the deviatoric stress tensor, J_3. Therefore, to describe the behavior of these materials within the endochronic framework, F_s must have the general form:
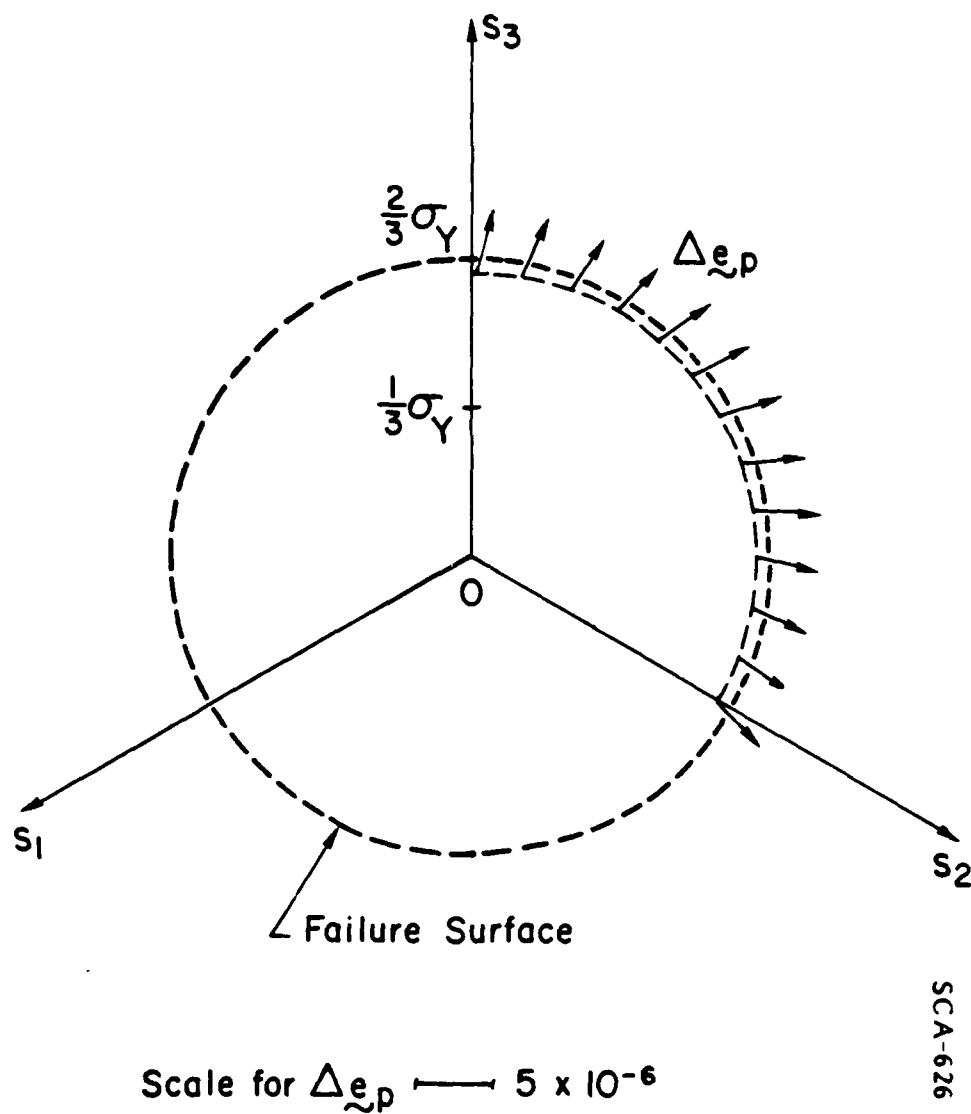
Figure 8.8.   Circular stress path near the failure surface and the corresponding plastic strain increment vectors predicted by the model.
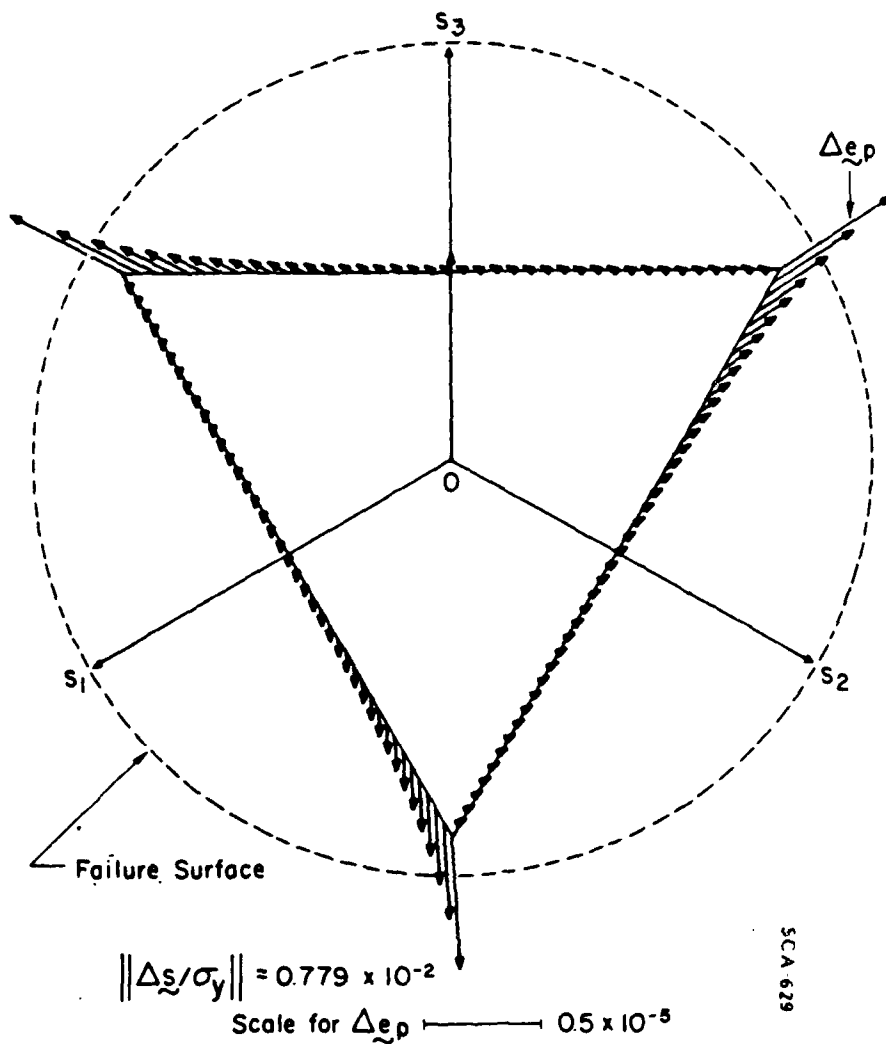
Figure 8.9. Triangular stress path with corresponding plastic strain increment vectors predicted by the model.

$$F_s = F_s\left(\sigma, J_3\right) , \qquad\qquad (8\text{-}57)$$

where

$$J_3 = \det(\underset{\sim}{s}) . \qquad\qquad (8\text{-}58)$$

The notation $\det(\underset{\sim}{s})$ refers to the determinant of the components of $\underset{\sim}{s}$.

In this section, the plastic flow properties of the endochronic model defined by Eqs. (8-1) to (8-5) are explored for the case in which the shear hardening function has the form of Eq. (8-57). As before, we will restrict attention for analytic convenience to the case in which deformation takes place at constant hydrostatic stress. i.e., $\sigma = \sigma_o$. The developments presented in this section are originally due to Murakami and Read [8.3].

The system of equations that we consider in this section consists of Eqs. (8-1) to (8-5) with the shear hardening function F_s having the form indicated by Eq. (8-57). Therefore, for deviatoric deformation at $\sigma = \sigma_o$. it follows from Eq. (8-2) that

$$\frac{d\underset{\sim}{e}^p}{dz} = \underset{\sim}{\ell}(z) \ F\left(\sigma_o, J_3\right) \qquad\qquad (8\text{-}59)$$

where, as before:

$$\underset{\sim}{\ell} \equiv \frac{d\underset{\sim}{e}^p}{d\varsigma} \qquad\qquad (8\text{-}60)$$

and the subscript s has been suppressed. Upon introducing Eq. (8-59) into Eq. (8-1) and using the kernel function defined by Eq. (8-5). one may write:

$$\underset{\sim}{s} = \rho_o \int_0^z \frac{e^{-\beta(z-z')}}{(z - z')} \ \underset{\sim}{\ell}(z) \ F\left[\sigma_o, J_3(z')\right] dz' \qquad\qquad (8\text{-}61)$$

This equation can be rewritten in the form:

$$\mathbf{\underset{\sim}{s}} = \rho_o \int_o^z \frac{e^{-\beta y}}{y^\alpha} \, \mathbf{\underset{\sim}{\ell}}(z - y) \, F[\sigma_o, J_3(z - y)] \, dy \tag{8-62}$$

by making the change of variable $y = z - z'$.

8.3.1 Small z Near the Origin of the Deviatoric Plane.

The analysis for this case proceeds in the same manner as that given earlier in Section 8.2.1 and, because of this, the details will not be repeated here. The final result is that the behavior has the same form as Eq. (8-14), namely:

$$\frac{d\mathbf{\underset{\sim}{s}}}{dz} = \rho(z)\mathbf{\underset{\sim}{\ell}} + 0\left(z^{1-\alpha}\right) \tag{8-63}$$

Therefore, as one might expect, the behavior at a considerable distance from the ultimate surface is independent of F_s. Equation (8-63) reveals that for small z ($z<<1$), $d\mathbf{\underset{\sim}{s}}/dz$ and $\mathbf{\underset{\sim}{\ell}}$ are coaxial, which implies that $d\mathbf{\underset{\sim}{s}}$ and $d\mathbf{\underset{\sim}{e}}^P$ are also coaxial.

8.3.2 Large z Near an Ultimate Surface.

Let us now explore the asymptotic form of Eq. (8-62) as the ultimate surface is approached, following the same procedure described earlier in Section 8.2.2. For this purpose, we consider a stress path which is arbitrary for $z < z_o$, but at z_o monotonically approaches the ultimate surface. For $z > z_o$, the plastic strain path and hence $\mathbf{\underset{\sim}{\ell}}$ will be smooth and simple during the recent past $\{z - y | 0 \leq y \leq y_m\}$, where y_m is a characteristic of the material such that, for $y \geq y_m$, $e^{-\beta y}$ is negligible. When $\beta >> 1$, which appears to be true for most materials, the major contribution to the integral in Eq. (8-62) occurs near $y = 0$. In view of the smoothness of the $\mathbf{\underset{\sim}{e}}^P$-path for $z > z_o$, we may expand the function $\mathbf{\underset{\sim}{a}}(z-y)F[\sigma_o, J_3(z - y)]$ in a Taylor series about $y = 0$ to give:

$$\mathfrak{L}(z - y)F[\sigma_0, J_3(z - y)] = \mathfrak{L}(z)F[\sigma_0, J_3(z)]$$

$$- y\left\{\mathfrak{L}'(z)F[\sigma_0, J_3(z)] + \mathfrak{L}(z)\frac{\partial F}{\partial J_3} \cdot \frac{\partial J_3}{\partial z}\right\} + \cdots \tag{8-64}$$

Because of the typically large value of β, only the first few terms of the above series are needed over $\{o \leq y \leq y_m\}$ where $e^{-\beta y}$ is not negligible. With this in mind, Eq. (8-62) can therefore be written as:

$$\mathfrak{s} = \rho_0 \int_0^\infty \frac{e^{-\beta y}}{y^\alpha} \left[\mathfrak{L}(z)F[\sigma_0, J_3(z)] - y\left\{\mathfrak{L}'(z)F[\sigma_0, J_3(z)]\right.\right.$$

$$\left.\left. + \mathfrak{L}(z)\frac{\partial F}{\partial J_3}\frac{\partial J_3}{\partial z}\right\} + \cdots\right]dy \tag{8-65}$$

Upon applying Watson's lemma (see Reference [8.4], for example) to the integral and performing the integration, it follows that

$$\mathfrak{s} = \rho_0 \mathfrak{L}(z)F[\sigma_0, J_3(z)]\frac{\Gamma(1 - \alpha)}{\beta^{1 - \alpha}} - \left\{\mathfrak{L}(z_s)F_s(z_s)\right\}'\frac{\Gamma(2-\alpha)}{\beta^{(2-\alpha)}}$$

$$+ O\left[\frac{1}{\beta^{(3-\alpha)}}\right]\right] + O\left(e^{-\beta z_s}\right) \tag{8-66}$$

Since we have found that for most materials $\beta \gg 1$, the first term on the right-hand side of the above equation dominates. In this case, it follows from Eq. (8-66) that, near the ultimate surface, $\mathfrak{s}$ is coaxial with $\mathfrak{L}$ and hence with $d\mathfrak{e}^P$. The model therefore exhibits a plastic flow rule near the ultimate surface that is of the Prandtl-Reuss type. Because of the assumed dependence of F on J_3, the ultimate surface does not, in general, cut the π-plane in a circle. As a result, the plastic strain increment $d\mathfrak{e}^P$ will not, in general, be normal to the ultimate surface, as shown in Figure 8.10. Near the ultimate surface, then, the model exhibits plastic behavior that is similar to what is termed <u>non-associated flow</u> in elastic-plastic theories.
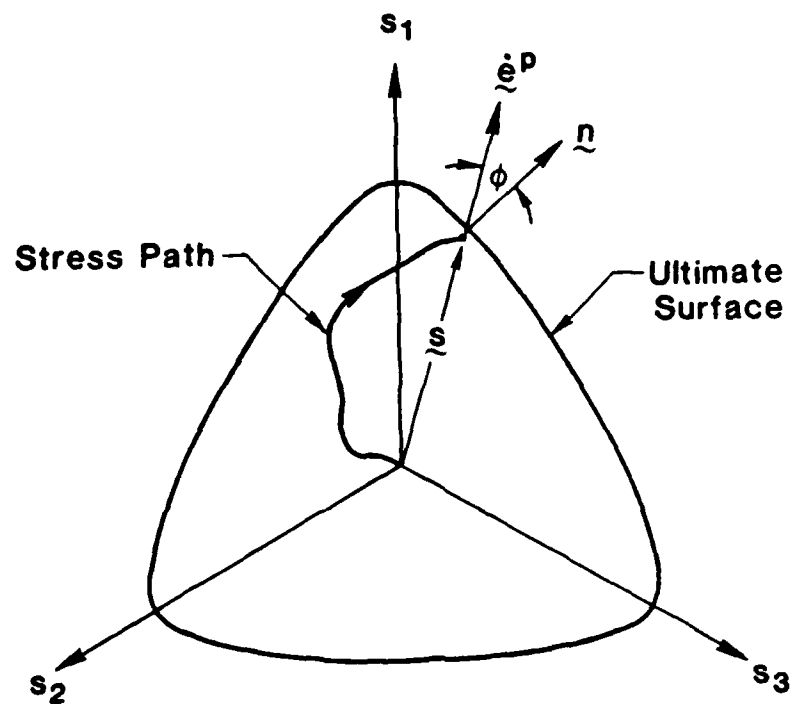
Figure 8.10   Trace of ultimate surface in the π-plane showing the orientation of the vectors $\dot{\underset{\sim}{e}}^p$ and $\underset{\sim}{n}$ for a stress state near the surface. Here $\underset{\sim}{n}$ is the normal to the ultimate surface in the neighborhood of $\underset{\sim}{s}$.

8.4 Consistency Between Eq. (8-53) and Eqs. (7-45), (7-57).

In this section, we wish to show that Eqs. (7-45) and (7-57) are, respectively, identical to the upper and lower branch of Eq. (8-53), as pointed out in Chapter 6. To show the upper branch we recall Eqs. (7-11) and (7-24) and set $F_s = 1$, to obtain the constitutive relation

$$\mathbf{\underset{\sim}{s}} = \mathbf{\underset{\sim}{s}}_o \frac{d\underset{\sim}{e}^p}{dz} + \int_o^z \rho_1(z - z') \frac{d\underset{\sim}{e}^p}{dz'} \, dz' \quad , \tag{8-67}$$

in view of the fact that in Chapter 8, $z \equiv \varsigma$.

We also note the condition

$$\left|\left|\frac{d\underset{\sim}{e}^p}{dz}\right|\right| = 1 \tag{8-68}$$

and the relation

$$\frac{d^2\underset{\sim}{e}^p}{dz^2} \cdot \frac{d\underset{\sim}{e}^p}{dz} = 0 \quad , \tag{8-69}$$

which is obtained by differentiating the relation (8-68). Thus differentiating Eq. (8-67) with respect to z, using Eq. (8-69) and noting Eq. (7-59) in the light of $F_s' = 0$, we find that

$$H = \frac{d\underset{\sim}{s}}{dz} \cdot \underset{\sim}{\ell} \quad , \tag{8-70}$$

where note is taken of the fact that $\underset{\sim}{\ell} = d\underset{\sim}{e}^p/dz$.

Thus

$$H = \underset{\sim}{t} \cdot \underset{\sim}{\ell} \left|\left|\frac{d\underset{\sim}{s}}{dz}\right|\right| \tag{8-71}$$

Therefore, if z_o is the terminal point of the plastic strain path prior to the imposition of the stress increment $d\underset{\sim}{s}_+$, then

$$H = \underset{\sim}{t} \cdot \underset{\sim}{\ell} \left|\left|\frac{d\underset{\sim}{s}}{dz}\right|\right|_{z_o} \tag{8-72}$$

$$H = \cos\theta \left|\left|\frac{d\underset{\sim}{s}}{dz}\right|\right|_{z_o} \tag{8-73}$$

Hence $H = \gamma$. We now recall Eq. (7-45) and note that

$$\frac{d\underset{\sim}{s}_+}{||d\underset{\sim}{s}_+||} = \underset{\sim}{b} \tag{8-74}$$

Thus Eq. (7-45) becomes:

$$dz\, H = ||d\underset{\sim}{s}_+||\; \underset{\sim}{b} \cdot \underset{\sim}{\ell} = ||d\underset{\sim}{s}_+||\, \cos\phi \tag{8-75}$$

Hence:

$$C^P = \frac{\left|\left|d\underset{\sim}{e}^P\right|\right|}{||d\underset{\sim}{s}_+||} = \frac{dz}{||d\underset{\sim}{s}_+||} = \frac{\cos\phi}{H_{z_o}} \tag{8-76}$$

so that

$$C^P = \frac{\cos\phi}{\gamma(z_o)} \tag{8-77}$$

which was the relation to be proved for the upper branch of Eq. (8-53). The lower branch is obvious.

REFERENCES FOR CHAPTER 8

8.1 Trangenstein, J. A., and H. E. Read. "The Inelastic Response Characteristics of the New Endochronic Theory with Singular kernel," *Intl. J. Solids and Structs.,* Vol. 18(11), (1982).

8.2 Murakami, H., and H. E. Read. "Endochronic Plasticity: Some Basic Properties of Plastic Flow and Failure," *Intl. J. Solids and Structs.,* Vol. 23(1), 1987, 133.

8.3 Murakami, H., and H. E. Read. "Plastic Flow Properties of an Endochronic Model with a Third-Invariant Ultimate Surface," to appear.

8.4 Carrier, G. F., M. Krook and C. E. Pearson. "Functions of a Complex Variable, Theory and Technique," McGraw-Hill, New York, 1966.

8.5 Hill, R., The Mathematical Theory of Plasticity, Oxford University Press, London, 1950.

8.6 Pearce, J. A., "The Behavior of Soft Clay in a New True Triaxial Apparatus," PhD. Dissertation, University of Cambridge, 1971.

9. PLAIN CONCRETE

Plain concrete, when subjected to general loading paths which drive it into the nonlinear inelastic regime, exhibits a rich variety of complex constitutive features which in the past have made it a very difficult material to model mathematically. Some of the salient and complex response features that are observed for this material include volume changes due to shear in the presence of a fixed hydrostatic pressure, influence of hydrostatic pressure on deviatoric behavior, hardening due to compaction, hysteresis and stress-path dependence. Furthermore, if the concrete experiences significant cracking in preferred directions, there is the added complexity of material anisotropy.

In recent years, a variety of nonlinear constitutive models have been proposed in the literature for plain concrete. Despite this, there is still no general constitutive model available which is capable of realistically describing the entire spectrum of concrete behavior, including both pre- and post-cracking response. In this chapter, we illustrate the application of the endochronic theory to plain concrete and show the remarkable capability that it has for predicting the observed behavior of this material for stress histories which do not produce significant cracking. The model has been calibrated to laboratory data for a medium strength plain concrete, and proof-tested against other data involving complex stress paths from the same laboratory investigation.

In the following sections of this chapter, details of the model are given and procedures for applying it to the data of Scavuzzo.et al. [9.1] are described. The results from numerous proof-tests conducted to explore the predictive capability of the model are shown to illustrate its ability to describe the observed behavior of plain concrete when driven around complex stress paths. The model discussed in this chapter was first introduced and applied to plain concrete by Valanis and Read [9.2].

9.1. The Model.

The basic equations of the endochronic model considered in this chapter were given earlier in Section 4.1 but are repeated below for convenience. Under the assumption of small strains and isothermal deformation, the governing equations for the model are as follows:

$$\underset{\sim}{s} = \int_0^{z_s} \rho\left(z_s - z'\right) \frac{d\underset{\sim}{e}^p}{dz'} \, dz' \tag{9-1}$$

9-1

$$\sigma = \int_{0}^{z_H} \phi(z_H - z') \frac{d\epsilon^p}{dz'} dz' \tag{9-2}$$

$$d\underset{\sim}{e}^p = d\underset{\sim}{e} - d\underset{\sim}{s}/2\mu \tag{9-3}$$

$$d\epsilon^p = d\epsilon - d\sigma/K \tag{9-4}$$

$$dz^2 = \left|\left| d\underset{\sim}{e}^p \right|\right|^2 + k^2 \left| d\epsilon^p \right|^2 \tag{9-5}$$

$$dz_s = \frac{dz}{F_s} \quad , \quad dz_H = \frac{dz}{kF_H} \tag{9-6}$$

where the notation has been defined earlier. Here, the kernel functions are taken in the form:

$$\rho(z_s) = \sum_r A_r e^{-\alpha_r z_s}, \tag{9-7}$$

$$\phi(z_H) = \sum_r B_r e^{-\beta_r z_H}, \tag{9-8}$$

where A_r, B_r, α_r and β_r are all positive and finite. In the present application of the model to plain concrete, we found that very satisfactory results can be obtained by taking only the first two terms in the above series.

The function F_H reflects the effect of compaction on hydrostatic behavior and, accordingly, is taken to depend on the plastic volumetric strain ϵ^p. The function F_s, on the other hand, accounts for the effect of the hydrostatic stress σ on shear behavior and failure. As a result, F_s is responsible for the form of the trace of the failure surface in the π-plane. For concrete materials, in general, the trace is nearly triangular at low pressures and becomes increasingly circular with increases in pressure. The function F_s, then, will in general depend upon both σ and the third invariant of the deviatoric stress tensor, J_3'.

In the application of the model to the data of Scavuzzo, *et al.* [9.1], the model predictions are not likely to be sensitive to the fine details of the failure surface, since the response regime of interest is not in the close proximity of the failure surface. Because of this, and to simplify the model, we will assume in that which follows that F_s depends only on σ. Later on, in Section 9.5, we will show how a third invariant failure surface can be easily incorporated in the endochronic model presented above; we will also calibrate the failure surface to failure data on plain concrete.

The model described above is rate-independent and isotropic in the sense discussed in Section 5.1. It portrays, as we shall show, the major features of the nonlinear, inelastic behavior exhibited by plain concrete over the stress range when significant cracking does not occur. These features include volume changes due to stress in the presence of a fixed hydrostatic stress, the effect of hydrostatic compression on deviatoric behavior, hydrostatic hardening due to compaction, hysteresis and stress-path dependence.

Finally, we note that the above model exhibits only compaction when there is shear in the presence of a fixed hydrostatic stress. This is consistent with the data of Scavuzzo, *et al.* [9.1], who found that the plain concrete they studied exhibited only compaction for all of the stress paths considered, none of which produced significant cracking. When cracking becomes significant, dilatancy can be expected to occur and it can be accounted for within the basic endochronic framework given above by introducing a more general form of Eq. (9-2), as described in Section 4.1 (see Eqs. (4-16) and (4-17).

9.2 Application to Plain Concrete Data.

To apply the model described above to plain concrete requires the determination of the functions $\rho(z_s)$, $\phi(z_H)$, $F_H(\epsilon^p)$, $F_s(\sigma)$, the shear-volumetric coupling parameter k, and the elastic moduli, K and μ. For this purpose, we rely heavily on the analytic developments given earlier in Sections 4.2 and 4.3. With these, the model can be fitted in a direct manner (without the need for iteration or optimization) by using only a small portion of the data presented by Scavuzzo, *et al.* [9.1]. The data used for this purpose include a virgin hydrostatic curve, shear responses at several different

fixed hydrostatic stresses, and a triaxial compression ailure envelope covering a range of confining pressures. The specific data from Reference [9.1] used to fit the model are shown in Figure 9.1. In this figure, as well as in the subsequent discussion, τ_o and σ_o denote, respectively, the octahedral shear stress and octahedral normal stress, while γ_o and ϵ_o are, respectively, the octahedral shear strain and octahedral normal strain.

The functions ϕ and F_H are determined from the hydrostatic compression data shown in Figure 9.1(a), where the data for $\epsilon_o > 3 \times 10^{-3}$ are assumed to be linear. Then F_H, whose form in the linear range is given by Eq. (4-45), is determined by evaluating β from the linear portion of the hydrostat, in accordance with Eq. (4-46). The function ϕ, which is represented by the series (9.8), is determined in accordance with the approach described in Section 4.2.2. The hydrostatic compression curve actually used for this purpose is shown by the solid line in Figure 9.1(a). Also depicted by a dashed line in this figure is a specific hydrostatic curve from the data. An examination of the purely hydrostatic portion of the many tests with complex strain paths reported in Reference [9.1] revealed that the dashed curve appeared to be too low, while the solid line provided a more accurate portrayal of the hydrostatic behavior. In this manner, the following material parameters associated with the hydrostatic component were determined:

$$
\begin{aligned}
K &= 2.1 \times 10^3 \text{ ksi} \ , \quad \beta = 64.8 \\
B_1 &= 1.55 \times 10^3 \text{ ksi} \ , \quad \beta_1 = 570 \\
B_2 &= 5.87 \times 10^3 \text{ ksi} \ , \quad \beta_2 = 2.224
\end{aligned}
\tag{9-9}
$$

where

$$
\phi = \sum_{r=1}^{2} B_r e^{-\beta_r z_H}
\tag{9-10}
$$

and

$$
F_H = 1 + \beta \epsilon^p \ .
\tag{9-11}
$$
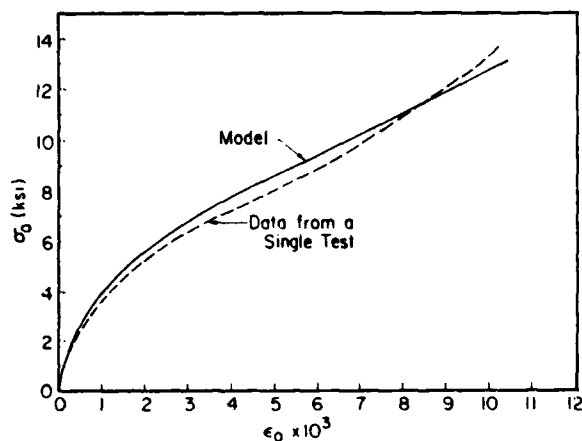
(a) Pure hydrostatic compression
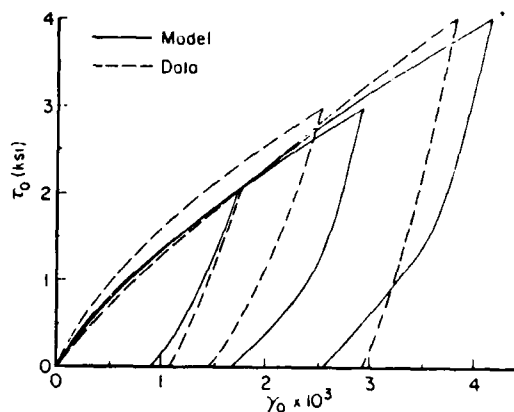
(b) Shear response at constant σ.
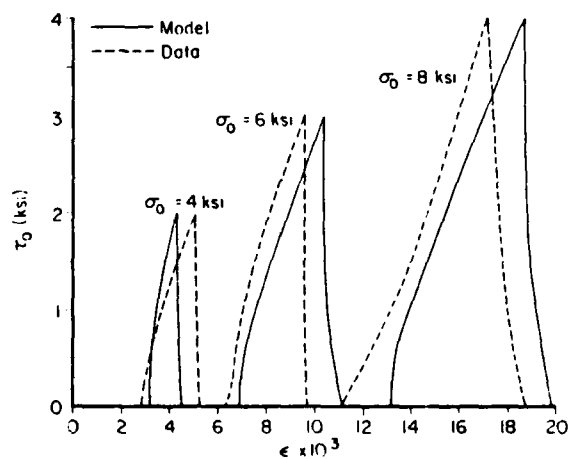
(c) Volumetric change during shear at
various values of constant σ.
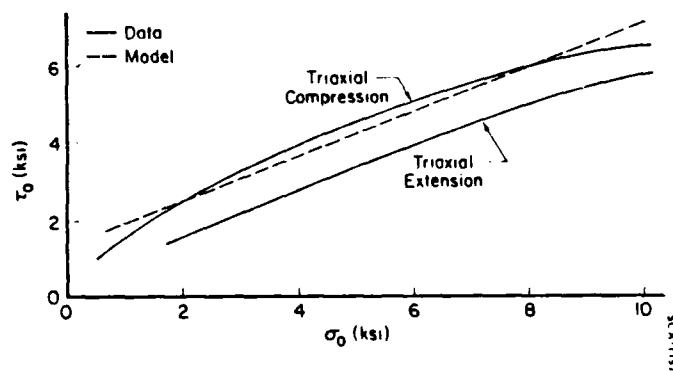
(d) Hydrostatic section of failure envelope.

Figure 9.1 Data used to fit model.

9-5

Turning now to the function $\rho(z_s)$, it was noted in Section 4.3 that the most direct way of determining $\rho(z_s)$ is from data on shear behavior under zero hydrostatic stress. However, this case was not investigated experimentally and, even if it had been, it would be of little use since the inelastic behavior of plain concrete under zero hydrostatic stress is due more to cracking than plastic flow. Therefore, $\rho(z_s)$ was determined from the curves of τ_o vs γ_o depicted in Figure 9.1(b). An inspection of the data reveals some apparent discrepancies. According to the trends of the plain concrete data reported in the literature, the initial slope of typical τ_o vs γ_o curves increase with confining pressure, and the corresponding τ_o vs γ_o curves tend to lie above each other -- not intersect -- as the confining pressure increases. The τ_o vs γ_o curve at a confining pressure of 8 ksi, which was selected for fitting the parameters, did not follow this pattern. There is the expected scatter in the data but the degree of scatter is not known. In view of this, we used our best judgement to construct a curve (close to the measured one) which provides a description of the shear response at $\sigma_o = 8$ ksi that is consistent with the expected trends. This curve is shown by a solid line in Figure 9.1(b).

The determination of $\rho(z_s)$ hinges on knowledge of the shear modulus μ and the shear hardening function F_s. The former is necessary for establishing the dependence of τ on γ^p when τ as a function of γ is known. The latter is essential because of the dependence of the τ vs γ^p curve on F_s, as is apparent from Eqs. (4-110) and (4-149). In addition, it is necessary that the coupling parameter k be known.

Let us consider, first, the shear modulus. An inspection of the data given in Figure 9.1(b) shows that the slopes of the τ_o vs γ_o curves at the points of unloading are an increasing function of the shear strain γ_o at unloading. Inasmuch as the model stipulates that the initial unloading increment is purely elastic, it follows that the shear modulus μ is not a constant. Its variation with the state of deformation can be found from the initial slopes of the loading and unloading curves given in Figure 9.1(b).

Attempts were made to correlate the values of 2μ determined in this manner with various deformation variables, such as the plastic volumetric strain ϵ^p, the total volumetric strain ϵ, the total octahedral strain γ, and the plastic octahedral shear strain γ^p. The latter two provided the best correlation, but the last one was chosen

because of its greater physical plausibility. Specifically, it seems more reasonable to assume that μ is a function of internal changes associated with permanent shear deformation, i.e., the plastic shear strain. Proceeding in this manner, it was found that the relationship between 2μ and γ^p was essentially linear and of the form:

$$2\mu = 2\mu_o + m\gamma_o^p \quad . \tag{9-12}$$

where $2\mu_o = 1.83 \times 10^3$ ksi and $m = 1.42 \times 10^6$ ksi.

From physical considerations, one expects μ to first increase during the initial pure hydrostatic compression phase of the shear tests due to closure of existing microcracks. But as shearing takes place under constant pressure, existing microcracks will open while new microcracks will develop, leading to a decrease in μ with increasing shear strain. As the level of the fixed hydrostatic stress is increased, the growth and nucleation of microcracks will begin at an increasingly larger value of shear strain. Based upon this picture, it is difficult to conclude whether the values of the initial unloading slopes obtained from the data in Figure 9.1(b) are realistic or clouded by system effects. For example, the apparent increase in μ with γ_o implied by Figure 9.1(b) may simply be due to creep, which is expected to increase with the magnitude of the shear stress.

The determination of the shear hardening function $F_s(\sigma)$ is straightforward. It was shown in Section 4.3.3 that, for the case of shear in the pressure of a fixed hydrostatic stress, F_s is given by the following expression:

$$F_s(\sigma) = \frac{\tau_\infty(\sigma)}{\tau_\infty(\sigma_R)} \quad , \tag{9-13}$$

where $\tau_\infty(\sigma)$ and $\tau_\infty(\sigma_R)$ denote, respectively, the shear stresses at failure corresponding to the hydrostatic stresses σ and σ_R. Recall that σ_R is a reference hydrostatic stress, which has been selected here to be 8 ksi. Also note that since $\tau_o = \sqrt{2/3}\ \tau$, we can rewrite Eq. (9-13) in terms of the octahedral shear stress at failure, τ_o^∞, as follows:

$$F_s(\sigma) = \frac{\tau_o^\infty(\sigma)}{\tau_o^\infty(\sigma_R)} \quad . \tag{9-14}$$

Figure 9.1(d) depicts the triaxial compression and triaxial extension failure envelopes for the plain concrete considered. Inasmuch as the present application is concerned with the non-cracking behavior of plain concrete, the fine details of the failure surface are not important. Accordingly, we shall adopt the linear approximation for the triaxial compression failure envelope shown by the dashed line in Figure 9.1(d) as the failure envelope for the model. On this basis, and in view of Eq. (9-14) with $\tau_o^{\infty}(\sigma_R) = 6$ ksi, we find that

$$F_s = \delta_o + \eta_o \sigma . \tag{9-15}$$

where $\delta_o = 0.336$ and $\eta_o = 0.083$ ksi^{-1}. It can be shown that when F_s depends on σ in the form of Eq. (9-15), the failure surface exhibited by the model is of the Drucker-Prager type, in which the trace of the failure surface in the π-plane is a circle.

To determine the shear-volumetric coupling parameter k, consider Figure 9.1(c) which shows the manner in which ϵ_o varies with τ_o during shearing at several different values of fixed hydrostatic stress. In the absence of contrary information, it is assumed that the volumetric changes that occur during shear are irreversible. On this basis, and using the data in Figure 9.1(b) and (c) for the reference stress $\sigma_o = 8$ ksi, the measured dependence of ϵ^p on γ_o^p can be constructed, as shown in Figure 9.2.

Equation (4-135), derived earlier in Section 4.3.3, provides a theoretical relation between ϵ^p and γ_o^p for shear at constant hydrostatic stresses which are located on the linear portion of the hydrostat; this becomes evident by noting that

$$\gamma_o^p = \varsigma_s / \sqrt{3} \quad ,$$

$$\tag{9-16}$$

$$\epsilon^p = (x-1)/(ak) .$$

The variation of ϵ^p with γ_o^p is therefore obtained in terms of the parameter k, since the constant a is given in terms of k by Eq. (4-131). In this manner, the dependence of ϵ^p on γ_o^p, as shown in Figure 9.2, was determined for several selected
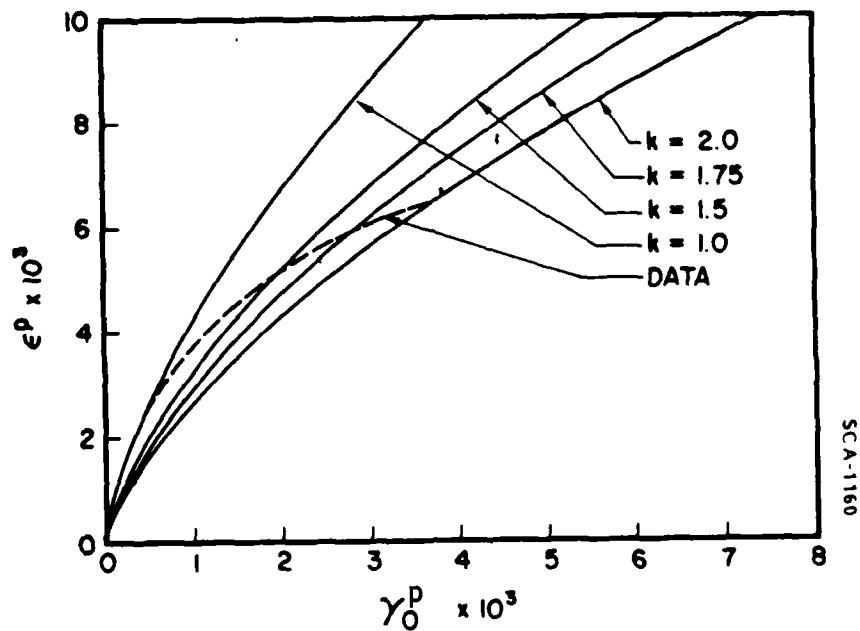
Figure 9.2 Shear-volumetric coupling at a constant hydrostatic pressure of 8 ksi. Data are from Test 4-11 Reference [9.1].
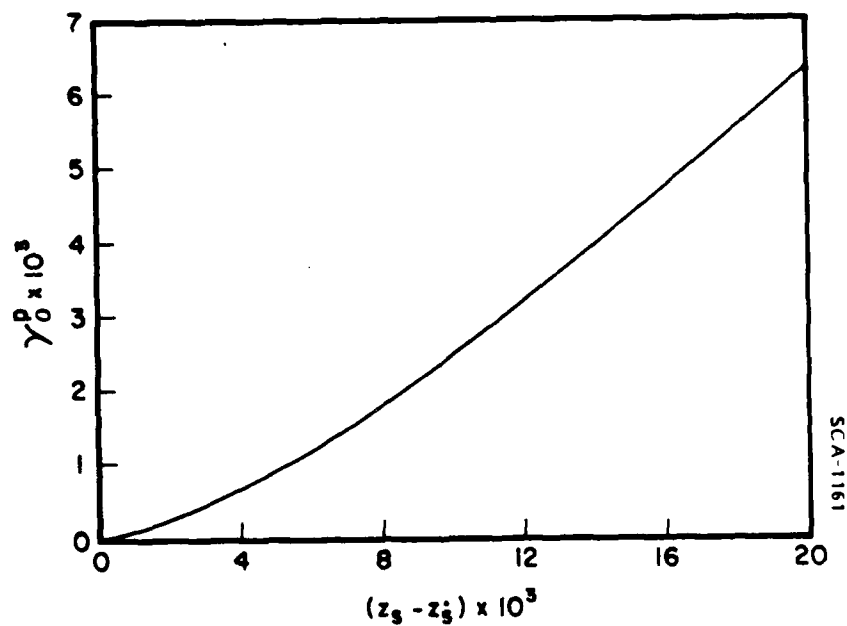

Figure 9.3 Dependence of γ_0^p on $z_s - z_s^*$ predicted by Eqs. (9-18) and (9-19) for shear at a constant pressure of 8 ksi.

values for k. An inspection of the figure reveals that the curve for $k = 1.5$ provides the best overall representation of the data, so we set

$$k = 1.5 . \tag{9-17}$$

Finally, to determine the function $\rho(z_s)$, we recall Eq. (4-139) which is valid during shear at constant hydrostatic stress:

$$\varsigma_s = \frac{1}{2a} \left\{ \sqrt{2ay} \ \sqrt{1+2ay} - \log \left| \sqrt{2ay} + \sqrt{1+2ay} \right| \right\} , \tag{9-18}$$

where $y = z_s - z_s^*$ and z_s^* denotes the value of z_s at the completion of the pure hydrostatic loading phase. Also, during shear at constant hydrostatic stress, we can write

$$\dot{\varsigma}_s = \sqrt{3} \ \dot{\gamma}_o^p , \tag{9-19}$$

which can be combined with Eq. (9-18) to yield a relationship between γ_o^p and z_s for a prescribed value of a. Adopting the value of k given in Eq. (9-4), the constant a is then known. In this manner, the relationship between γ_o^p and $z_s - z_s^*$ shown in Figure 9.3 was obtained. Upon using this result, together with the relationship between τ_o and γ_o^p obtained from Figure 9.1(b), the dependence of τ_o on z_s during shear at constant hydrostatic stress was determined. The numerical method described in Section 10.2 can then be used to obtain $\rho(s_s)$. The resulting function $\rho(z_s)$ was represented by a two-term exponential series of the form:

$$\rho(z_s) = \sum_{r=1}^{2} A_r e^{-a_r z_s} \tag{9-20}$$

where

$$A_1 = 1.46 \times 10^3 \ \text{ksi} \quad , \quad a_1 = 100 .$$
$$\tag{9-21}$$
$$A_2 = 19.0 \times 10^3 \ \text{ksi} \quad , \quad a_2 = 6.554 .$$

The extent to which the model, with the values of the parameters given in this section, represents the data to which it was fitted is illustrated in Figure 9.1.

9.3 Proof Tests of Model.

In the preceding section, the endochronic constitutive model described in Section 9.1 was applied to the plain concrete data reported in Reference [9.1], with the model parameters evaluated from a small subset of these data. The ability of the resulting model to accurately portray the data to which it was fitted was described. In this section, the capability of the model to predict measured behavior for a variety of prescribed complex stress paths that were not used in determining the model parameters is examined. For this purpose, a number of complex stress path tests experimentally studied in Reference [9.1] is considered. The specific tests selected for consideration below were chosen because they reveal a variety of different response features exhibited by plain concrete and therefore allow various features of the model to be exercised and tested. None of the proof-tests considered below were used in fitting the model parameters, and no optimization techniques were employed to achieve the results presented below.

Test 1

This test was designed to explore the response of plain concrete to triaxial load cycles which do not exhibit stress reversals. The loading history, shown in Figure 9.4(a) and (b), consists first of cyclic hydrostatic loading up to 8 ksi, followed by cyclic deviatoric loading along the triaxial compression path, as indicated in Figure 9.4(b). The predicted and measured responses for this loading history are given in Figure 9.4(c). As this figure reveals, the predicted and measured behaviors are in good agreement, considering the usual data scatter for plain concrete. Note that if the predicted response was simply translated to the right a small amount, the agreement would be excellent. Such a shift appears justified in view of the fact that the measured hydrostatic response for this particular test is somewhat stiffer than the hydrostatic data to which the model was fit (see Figure 9.1(a)). Aside from this difference, however, the qualitative features of the plain concrete behavior are obviously captured very well by the model.
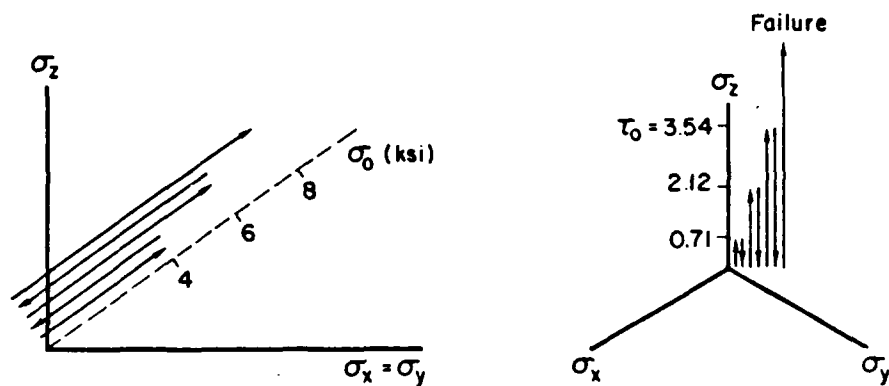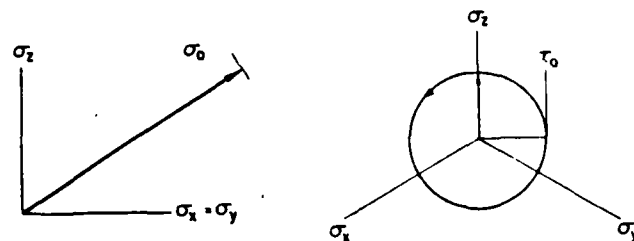
(a) Prescribed stress path
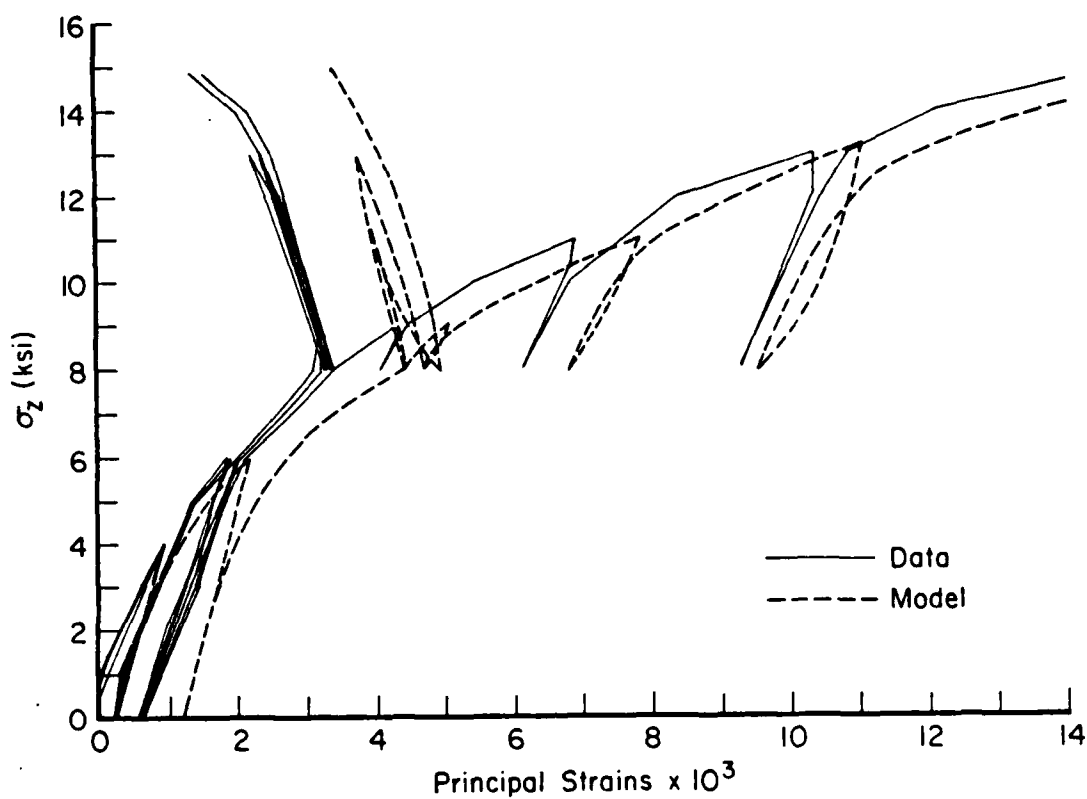
(b) Major principal stress versus principal strains.

Figure 9.4   Cyclic triaxial loading (Test 1).

Tests 2 and 3

These tests were designed to explore the behavior of plain concrete for circular stress paths in the deviatoric plane. The stress path, which is shown in Figure 9.5(a), consisted first of monotonic hydrostatic compression to some pressures σ_o, followed by a circular load path in the deviatoric plane at some fixed value of the octahedral shear stress, τ_o. Comparisons between model predictions and data for the deviatoric loading portions of these tests are shown in Figure 9.5(b) and (c). The overall agreement is quite good. Note that if the data in Figure 9.5(c) were translated vertically upward by a sufficient amount, the predicted and measured results would be in reasonably good agreement. However, such a translation does not appear to be justified on the basis of the data from replicate tests (not shown), which had identical stress paths to Test 3. Therefore, the model appears to be somewhat too soft during the proportional deviatoric loading leg of the test.

The results depicted in Figure 9.5 are also of interest for another reason. Recently, the modern version of the endochronic theory - which forms the basis of the model presented here - was criticized in the literature as being unable to properly describe the response of concrete to what has been termed "loading-to-the-side". Such loading is said to occur when the strain increment $d\varepsilon$ is tangent to the loading surface in strain space. To the authors' knowledge, no data are currently available for plain concrete which define its response to loading-to-the-side. Despite this, it is claimed that plain concrete exhibits inelastic behavior for such loading. We note that while the model's response to infinitesimal loading-to-the-side is purely elastic, its response to finite loading-to-the-side is inelastic. In Tests 2 and 3, the plain concrete was subjected to loading-to-the-side, at least at the beginning of the circular stress path and possibly when it crossed over the other two principal stress axes. The uncertainty arises because the location and shape of the "loading surface" are not known. In view of these considerations and the reasonably good agreement between the data and the model for the circular stress paths, criticism of the model based on perceived notions of the response of concrete to loading-to-the-side appears to be unjustified.

(a) Prescribed stress path
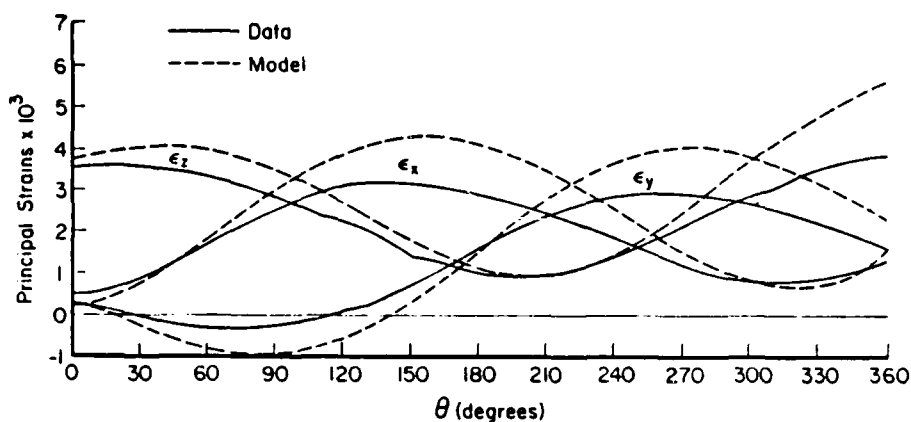
(b) Test 2 in which $\sigma_o = 4$ ksi and $\tau_o = 2$ ksi.
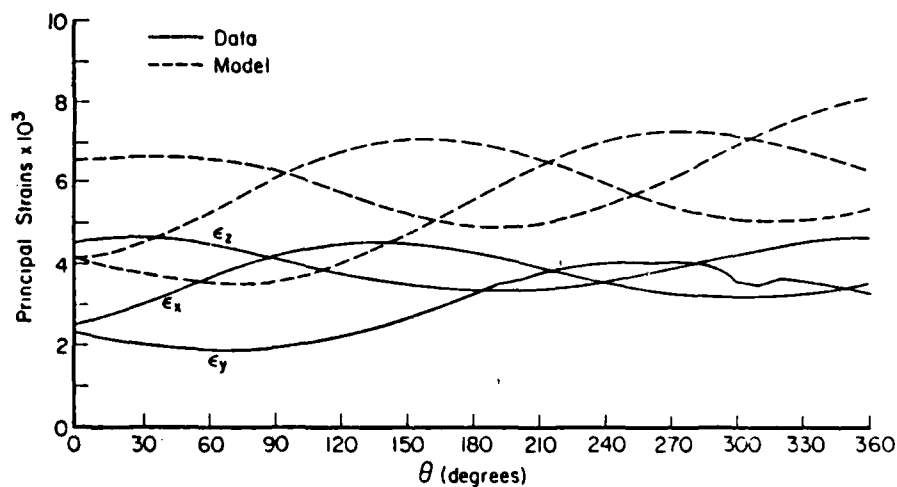
(c) Test 3 in which $\sigma_o = 8$ ksi and $\tau_o = 1.5$ ksi.

Figure 9.5 Circular stress paths in the deviatoric planes.

Tests 4, 5 and 6

These tests were part of a larger group of tests designed to explore several aspects of the response of plain concrete to complex stress paths for which two of the principal stresses are equal. While the stress paths for Tests 4, 5 and 6 were quite different, they nevertheless had a common stress state of $\sigma_o = 8$ ksi and $\tau_o = 4$ ksi. A comparison of the strains developed in these tests at this common stress state revealed the very significant dependence of the deformation on the stress-path. Comparisons between the predicted and measured behavior of Tests 4, 5 and 6 are shown in Figures 9.6 to 9.8, where the prescribed stress histories are also depicted. An inspection of these figures reveals that the model describes the observed behavior quite well, with an accuracy that appears to be well within the data scatter. This demonstrates the ability of the model to realistically account for the effect of stress path on the behavior.

Tests 7, 8 and 9

The purpose of these tests was to investigate the response of plain concrete to unsymmetric stress paths in a fixed deviatoric plane. The stress paths consisted of hydrostatic compression to the 4 ksi deviatoric plane, then proportional loading in the π-plane along the s_z-axis until $\tau_o = 2$ ksi, followed by linear load paths which made angles of 30°, 60° and 90° with the triaxial compressive axis, as shown in Figure 9.9(a). The predicted and measured responses for these tests are shown in Figure 9.9(b), (c) and (d). From an inspection of the figures, it is apparent that the location on the e_z-axis at which the non-proportional portion of the deviatoric loading begins is consistently higher than the data in all three tests. It appears, therefore, that the model is too soft for proportional excursions from the hydrostatic axis out along the triaxial compression axis, confirming the same conclusion drawn earlier in conjunction with the circular stress paths. Despite these small differences the model provides an excellent description of the observed behavior of plain concrete in the deviatoric plane.
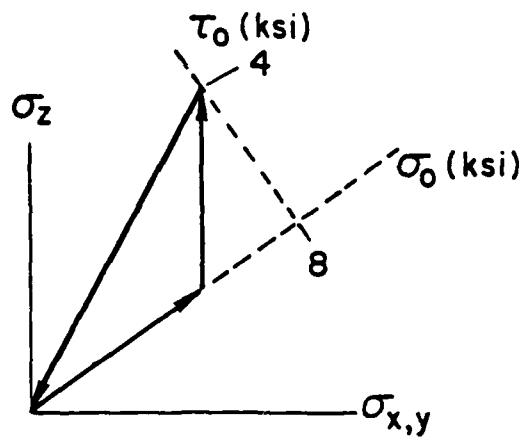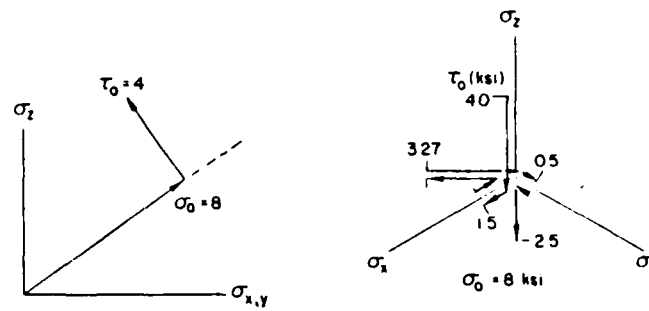
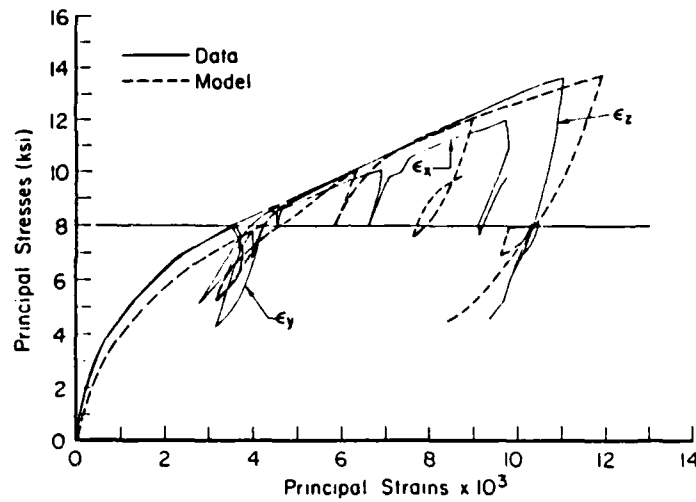(a) Prescribed stress path
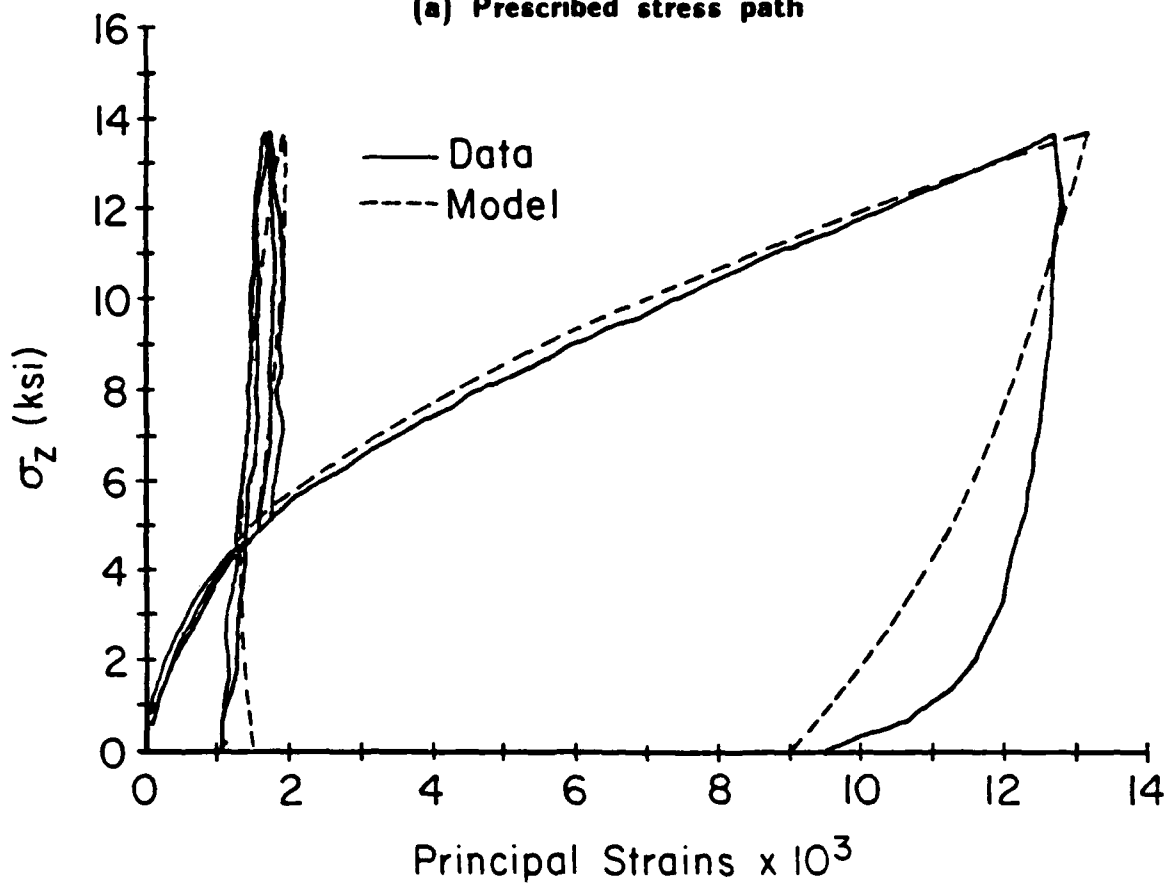
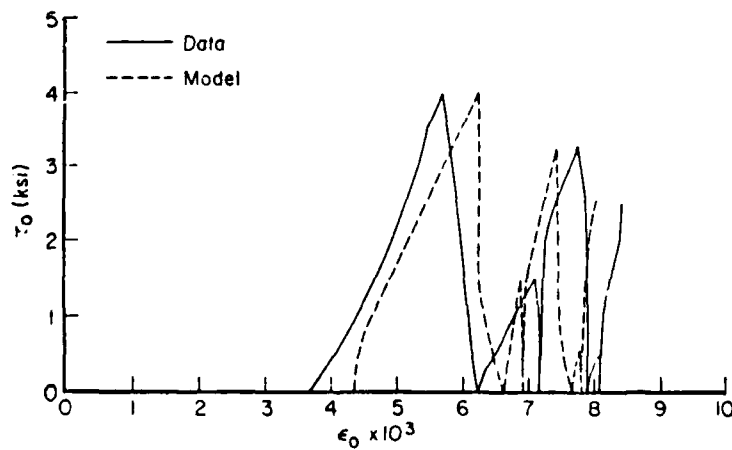(b) Predicted and measured deformations.

Figure 9.6.   Measured and predicted responses for Test 4.
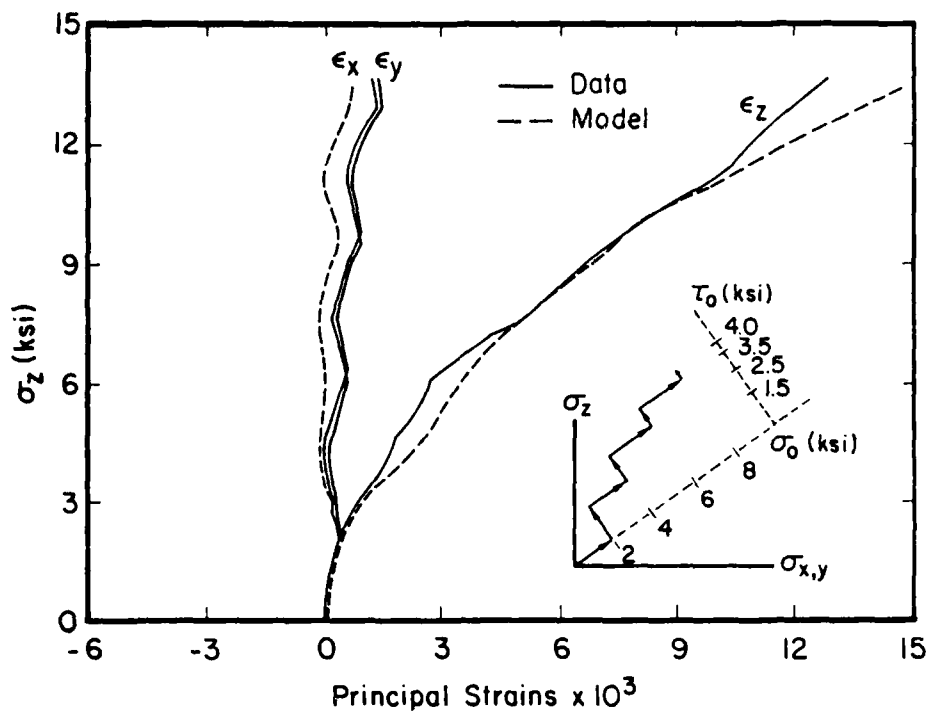
(a) Prescribed stress path.

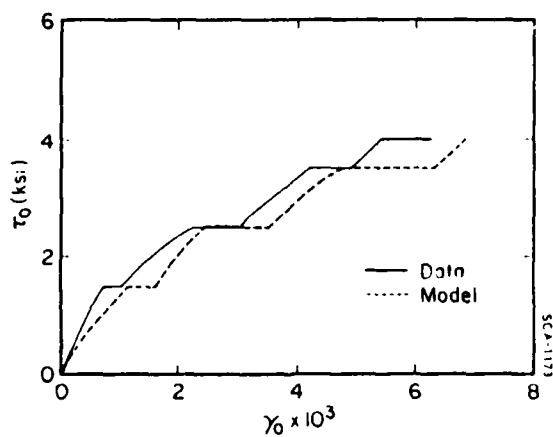(b) Major principal stress versus principal strains.

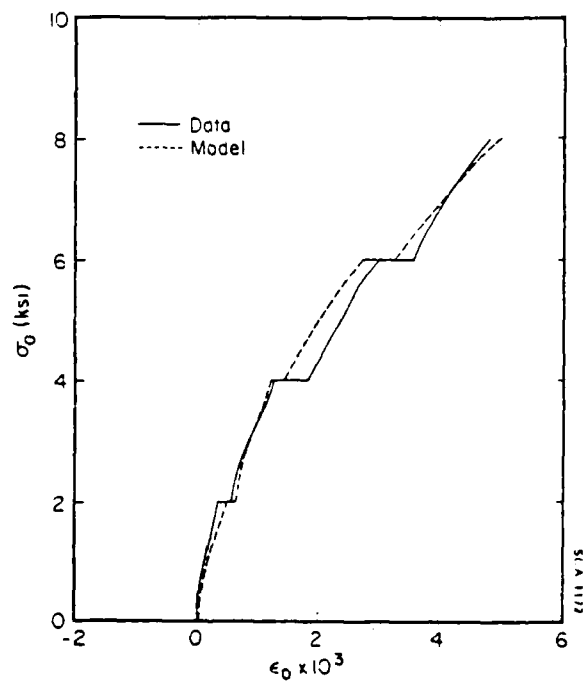(c) Octahedral shear stress versus octahedral normal strain.

Figure 9.7 Measured and predicted responses for Test 5.

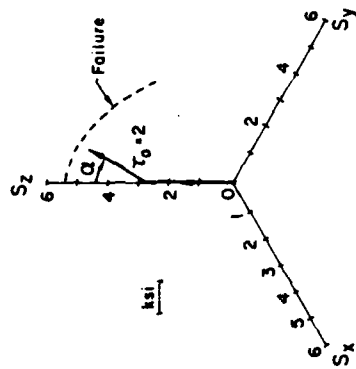(a) Major principal stress versus principal strains.

(b) Octahedral shear stress vs. octahedral shear strain

(c) Octahedral normal stress versus octahedral normal strain.
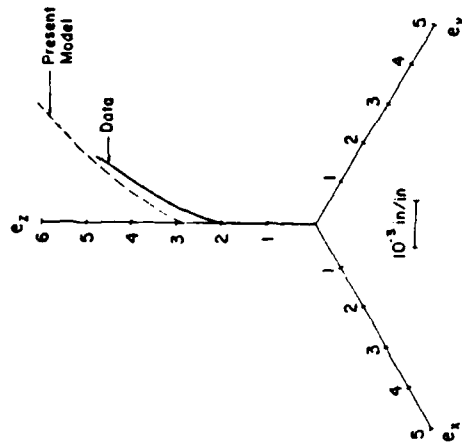
Figure 9.8. Measured and predicted responses for Test 6.
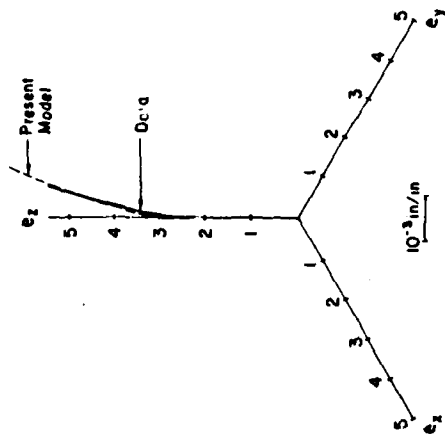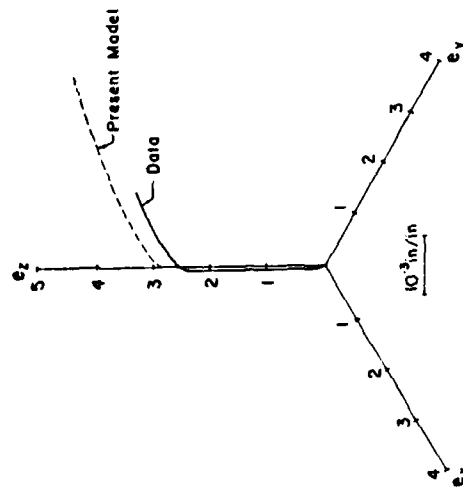
Figure 9.9 Measured and predicted responses for Tests 7, 8 and 9.

(a) Prescribed stress path

(b) Test 7 ($a = 30°$)

(c) Test 8 ($a = 60°$)
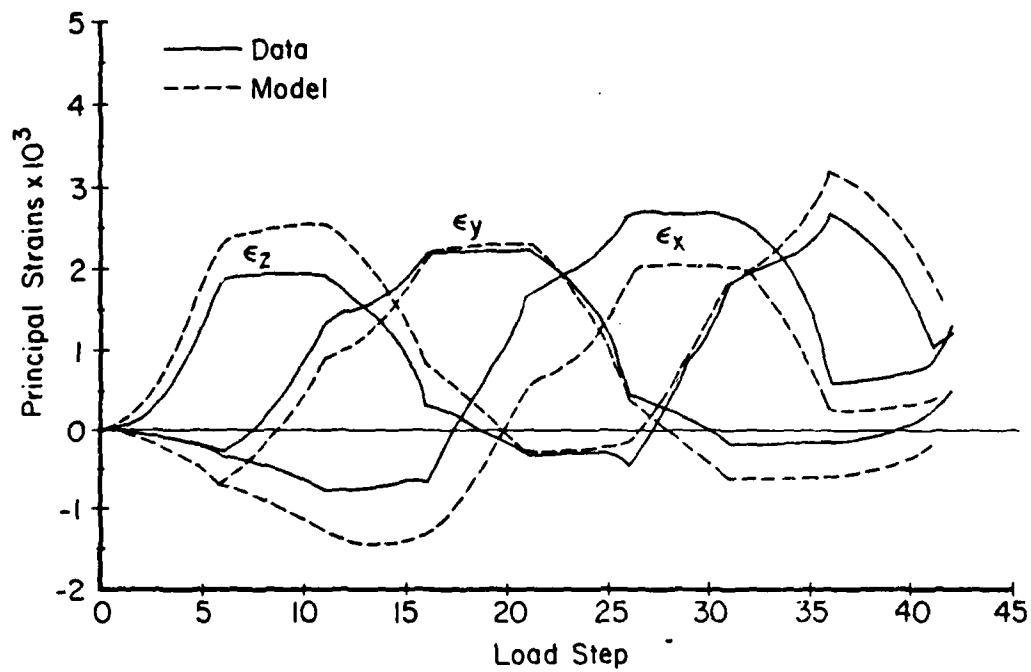
(d) Test 9 ($a = 90°$)
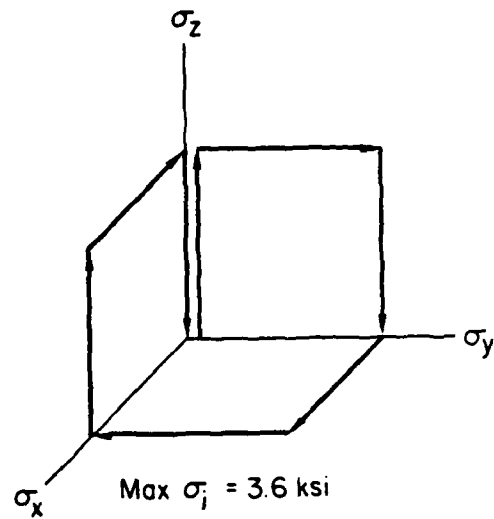
(a) Prescribed stress path

(b) Principal strains versus load step.

Figure 9.10   Measured and predicted behavior for Test 10.

Test 10

In this test, the response of plain concrete to the piece-wise linear loading path shown in Figure 9.10(a) was explored. The loading history was designed so that all possible uniaxial and equibiaxial stress states at a peak stress of 3.6 ksi was achieved. The predicted and measured responses to this applied stress history are depicted in Figure 9.10(b). Considering the usual scatter in concrete data, and the complexity of the stress path, the agreement between the model and experiment is considered excellent.

9.4 Remarks.

The success with which the endochronic model passed the various proof-tests described above reveals that the model provides an excellent description of the nonlinear, inelastic behavior of plain concrete for stress states below failure. There are, however, several limitations of the model that should be kept in mind. First, by virtue of the linear expression adopted for the function $F_H(\epsilon^P)$ in Eq. (9-11), the model is limited to hydrostatic pressures which lie on or below the linear portion of the virgin hydrostat. For the medium strength concrete considered here, the peak pressures are therefore limited to about 15 ksi. To extend the model to encompass a much wider range of pressures, a more general expression for $F_H(\epsilon^P)$ is required. Such an expression is discussed in Section 9.6, where the application to plain concrete data covering a wider range of hydrostatic pressure is illustrated.

Secondly, because the fine details of the failure surface are not expected to have a significant effect on the behavior of the model for peak stress states that are sufficiently far from failure, a simple failure surface was adopted in which the function F_s was taken to depend linearly on σ. It can be shown that such a failure surface is of the Drucker-Prager type, with the trace of the surface in the π-plane being a circle. A more realistic failure surface for plain concrete would allow F_s to depend not only on σ but also on J_3'. The incorporation of such a failure surface into the endochronic model is described in Section 9.5 and illustrated through application to a variety of plain concrete failure data.

Inasmuch as the above model is isotropic, it cannot account for the anisotropy that develops when significant macrocracking with preferred orientation occurs. Also, when there is shearing under a fixed hydrostatic pressure, the model exhibits only

compaction. Thus, the dilatant behavior usually observed when cracked concrete is sheared cannot be described by the above model.

The model described above, however, has been recently extended by Valanis [9.3] to include the capability to treat developing damage, fracture and dilatancy. The evolution of damage is described by a differential equation which depends upon the tensile strain state. As damage develops in preferred directions, the model becomes anisotropic and exhibits dilatancy. Inasmuch as this model is in the early stages of development, a more detailed discussion of it will be given in the upcoming second volume of Endochronic Plasticity by the present co-authors.

9.5 A Third Invariant Failure Surface for Plain Concrete.

When the shear kernel $\rho(z_s)$ is of such a form that a failure surface exists (see Section 3.2.6 for requirements), the shear hardening function F_s defines the properties of the failure surface. For isotropic media, the most general form of the failure criterion can be expressed in terms of the three independent invariants of the stress tensor, namely:

$$\sigma = \text{tr} \ (\underline{\sigma})$$

$$J_2 = \frac{1}{2} \ \underline{s} : \underline{s} \tag{9-22}$$

$$J = \frac{3\sqrt{3}}{2} \ \frac{J_3}{\left(J_2\right)^{2/3}} \quad ,$$

where

$$J_3 = \frac{1}{3} \ \text{det} \ (\underline{s}) \tag{9-23}$$

Here, the notation $\text{det}(\underline{s})$ denotes the determinant of the components of $\underline{s}$. The most general form of the failure criterion for isotropic media can therefore be expressed in the form:

$$\sqrt{J_2} = \psi(\sigma, J). \tag{9-24}$$

To determine the relation between the functons F_s and ψ, consider the case of radial deformation at constant hydrostatic pressure of a plastically incompressible solid. For this case, we can write

$$d\underset{\sim}{e}^p = \underset{\sim}{n} \left|\left| d\underset{\sim}{e}^p \right|\right| = \underset{\sim}{n} \, d\varsigma_s \tag{9-25}$$

so that

$$\underset{\sim}{s} = \int_0^{z_s} \rho(z_s - z') \frac{d\underset{\sim}{e}^p}{dz'} \, dz' = \underset{\sim}{n} \int_0^{z_s} \rho(z_s - z') \frac{d\varsigma_s}{dz'} \, dz' \tag{9-26}$$

During the initial hydrostatic loading process for which $0 \leq z_s \leq z_s^o$, we have $\varsigma_s = 0$. Thus, if we set

$$w = z_s - z_s^o . \tag{9-27}$$

it follows that

$$z_s - z_s' = w + z_s^o - z_s' = w - w' \tag{9-28}$$

As a result. Eq. (9-26) can be rewritten in the form

$$\underset{\sim}{s} = \underset{\sim}{n} \int_0^{z_s} \rho(z_s - z') \frac{d\varsigma_s}{dz'} \, dz' = \underset{\sim}{n} \int_0^w \rho(w - w') \frac{d\varsigma_s}{dw'} \, dw' \tag{9-29}$$

It was shown earlier in Section 4.3.2 (Eq. (4-74)) that when the hydrostatic hardening function F_H is of the form:

$$F_H = e^{\beta \varsigma_H} \tag{9-30}$$

where β is a positive constant. we have

$$\frac{d\varsigma_s}{dw} = \frac{F_s \left(2cw + c^2 w^2\right)^{1/2}}{(1 + cw)} \quad , \tag{9-31}$$

where

$$c = \frac{\beta}{k} F_s \tag{9-32}$$

and β. k are material constants. Substitution of Eq. (9-31) into Eq. (9-29) gives

$$\underset{\sim}{\varsigma} = \underset{\sim}{n} F_s \int_0^w \rho(w - w') \frac{\left[2 \, cw' + c^2 (w')^2\right]^{1/2}}{(1 + cw')} \, dw' \tag{9-33}$$

Using the results of Section 4.3.4. it can be shown that

$$\lim_{w \to \infty} \int_0^w \rho(w - w') \frac{\left[2 \, cw' + c^2 (w')^2\right]^{1/2}}{(1 + cw')} \, dw' = M_\infty \quad , \tag{9-34}$$

where

$$M_\infty = \int_0^\infty \rho(x) \, dx \tag{9-35}$$

Thus. from Eqs. (9-33) and (9-34). we can write

$$\underset{\sim}{\varsigma}^f = \lim_{w \to \infty} \underset{\sim}{\varsigma} = \underset{\sim}{n} F_s M_\infty \quad , \tag{9-36}$$

where the superscript f denotes failure. It then follows that at failure we have

$$\sqrt{J_2} = \frac{1}{\sqrt{2}} F_s M_\infty \qquad (9\text{-}37)$$

The relation between the functions F_s and ψ is then obtained by eliminating $\sqrt{J_2}$ between Eqs. (9-24) and (9-37), with the result:

$$F_s = \frac{\sqrt{2}\ \psi(\sigma,\theta)}{M_\infty} \qquad (9\text{-}38)$$

Therefore, to define F_s for a particular material, the function $\psi(\sigma,J)$ must be specified. This is done below for plain concrete.

There are a number of advanced failure criteria for plain concrete which have been proposed in the literature that have the general form of Eq. (9-24) (see Refs. [9.4] to [9.9]). Considering the large scatter in data between experimenters, as well as between different testing devices (see Ref. [9.10]), most of the advanced failure criteria noted above provide satisfactory descriptions of existing plain concrete failure data. For critical assessments of most of the above failure models, the reader is referred to References [9.6] and [9.9].

Inasmuch as all of the failure models noted above are reasonably accurate, and none appear to have significant advantages in predictive capability over the others, we select the model proposed by Peyton [9.8] for specific consideration in this section because of our greater familiarity with it. A description of this failure model is given below, where the corresponding form of the function $\psi(\sigma,\theta)$ is defined. The model is then applied to failure data for plain concrete.

The failure criterion proposed in Reference [9.8] is given by the expression:

$$\frac{J_2}{\tau^2} - \alpha\,\frac{J_3}{\tau^3} = 1 \ , \qquad (9\text{-}39)$$

where τ and α are, in general, smooth monotonic functions of the hydrostatic stress σ, i.e.,

$$\tau = \tau(\sigma) .$$

$$\alpha = \alpha(\sigma) .$$

(9-40)

The role of the function $\tau(\sigma)$ is to describe the effect of pressure on the meridians of the failure surface, while the function $\alpha(\sigma)$ determines the manner in which the trace of the failure surface in the π-plane changes with σ. In order for the trace to be convex, it is necessary that $0 \leq \alpha \leq 1$. If α is a continuous decreasing function of σ, the trace of the failure surface in the π-plane changes smoothly from a triangle ($\alpha = 1$) to a circle ($\alpha = 0$) with increasing σ.

To express Eq. (9-39) in the form of Eq. (9-24), we note that by defining an angle θ in the π-plane as shown in Figure 9.11 it follows that:

$$J = -\sin 3\theta$$

(9-41)

Solving Eq. (9-22b) for J_3 and combining the result with Eq. (9-27) gives

$$\frac{J_2}{\tau^2} - \alpha \, \frac{2J}{3\sqrt{3}} \left(\frac{J_2}{\tau^2}\right)^{3/2} = 1 ,$$

(9-42)

which is of the form:

$$x^2 - q \, x^3 = 1.$$

(9-43)

if we set:

$$q \equiv \frac{2\alpha J}{3\sqrt{3}} \quad , \quad x \equiv \sqrt{\frac{J_2}{\tau^2}} \ .$$

(9-44)

With the change of variable

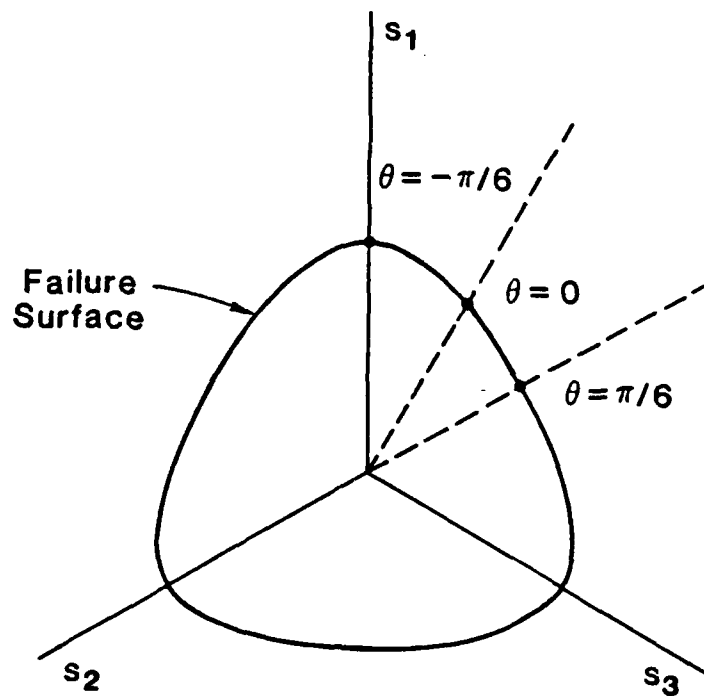$$x \equiv \frac{1}{y} \quad ,$$

(9-45)

Figure 9.11 Deviatoric stress plane, showing the manner in which the angle θ is defined.

Eq. (9-43) can be written in the form:

$$y^3 - y + 1 = 0 .$$ (9-46)

With a further change of variable,

$$y = \lambda \sin \phi .$$ (9-47)

Eq. (9-46) becomes

$$\sin^3 \phi - \frac{1}{\lambda^2} \sin \phi + \frac{q}{\lambda^3} = 0 .$$ (9-48)

We observe that this equation has the form of the following trigonometric identity:

$$\sin^3 \phi - \frac{3}{4} \sin \phi + \frac{1}{4} \sin 3 \phi = 0 ,$$ (9-49)

if we set

$$\lambda = \frac{2}{\sqrt{3}} \quad , \quad \sin 3 \phi = a J .$$ (9-50a,b)

From Eq. (9-50b), it follows that

$$\phi = \frac{1}{3} \left[\sin^{-1} (aJ) + 2 \pi \right] .$$ (9-51)

Upon combining Eqs. (9-44b), (9-45), (9-47), (9-50) and (9-51), we can write

$$\sqrt{J_2} = \frac{\sqrt{3} \, \tau}{2 \sin \left[\frac{1}{3} \sin^{-1}(aJ) + \frac{2\pi}{3} \right]} ,$$ (9-52)

which is of the form of Eq. (9-24). To apply this expression to a specific set of data, the functions $a(\sigma)$ and $\tau(\sigma)$ must be specified. A procedure for doing this is described below.

Generally, failure data are obtained from triaxial compression and triaxial extension tests and, with this in mind, we define the ratio r as

$$r \equiv \frac{\left(\sqrt{J_2}\right)_c}{\left(\sqrt{J_2}\right)_e} \quad , \tag{9-53}$$

where the subscripts c and e refer, respectively, to compression and extension and both values of $\sqrt{J_2}$ are taken at the same hydrostatic pressure. Considering Eq. (9-52) with $J = +1$ for compression and $J = -1$ for extension, it can be shown that

$$r = \frac{\left(\sin \frac{2\pi}{3} - \frac{1}{3} \sin^{-1} \alpha\right)}{\left(\sin \frac{2\pi}{3} + \frac{1}{3} \sin^{-1} \alpha\right)} \quad . \tag{9-54}$$

Upon solving for α, we find

$$\alpha = \sin \left\{ 3\tan^{-1} \left[\sqrt{3} \, \frac{r-1}{r+1} \right] \right\} \quad . \tag{9-55}$$

Therefore, if we know the manner in which $\left(\sqrt{J_2}\right)_c$ and $\left(\sqrt{J_2}\right)_e$ depend on σ from data, then $r(\sigma)$ is known from Eq. (9-53) and $\alpha(\sigma)$ can be found from Eq. (9-55).

To determine $\tau(\sigma)$, we solve Eq. (9-52) for $\tau(\sigma)$ and set $J = +1$ to obtain

$$\tau(\sigma) = \frac{2}{\sqrt{3}} \sin \left[\frac{1}{3} \sin^{-1} \alpha + \frac{2\pi}{3} \right] \left(\sqrt{J_2}\right)_c \quad . \tag{9-56}$$

Therefore, since $\alpha(\sigma)$ and the variation of $\left(\sqrt{J_2}\right)_c$ with σ are known, the function $\tau(\sigma)$ can be found.

The procedure described above was used to determine the forms of $\alpha(\sigma)$ and $\tau(\sigma)$ for plain concrete, using the failure data shown in Figure 9.12. Here, data from both triaxial compression and triaxial extension tests on plain concretes conducted by several investigators on several different strengths of concrete are depicted. In this manner, it was found that the data could be well represented by setting
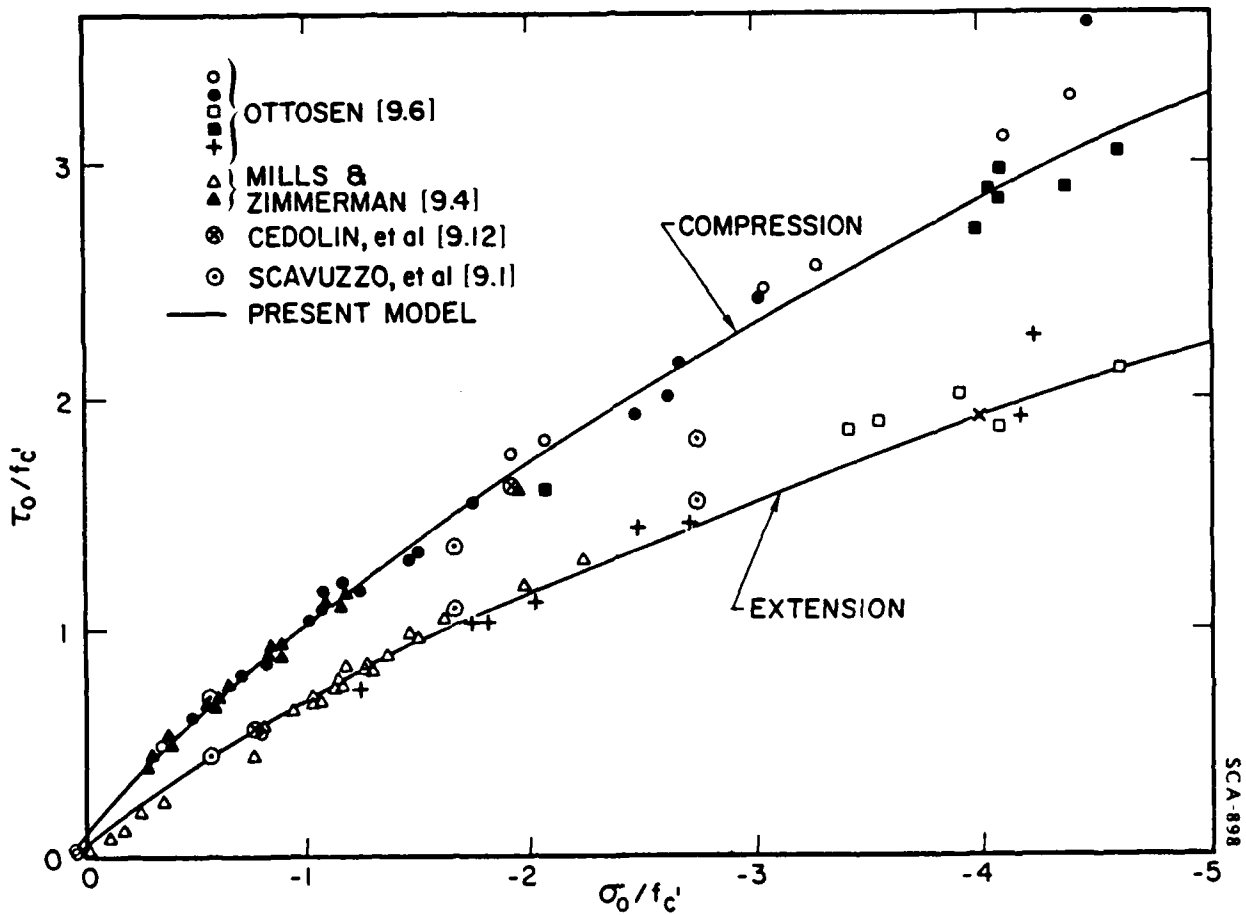
Figure 9.12 Comparison between predicted and measured failure states for plain concrete.

$$\alpha = \alpha_o$$

$$\tau = \tau_o + \beta_o \sqrt{\sigma - \gamma_o} \, , \qquad\qquad (9\text{-}57a,b)$$

where

$$\alpha_o = 0.83$$

$$\tau_o = -1.91 \, f'_c$$

$$\qquad\qquad (9\text{-}58)$$

$$\beta_o = 1.24 \, \sqrt{f'_c}$$

$$\gamma_o = -2.69 \, f'_c$$

The excellent ability of the failure model, with only four material parameters, to correlate the failure data is shown in Figure 9-12.

To determine the corresponding expression for the shear hardening function F_s, we first note that, since the shear kernel function $\rho(z_s)$ is assumed to be of the form of Eq. (9-7), it follows from Eq. (9-26) that

$$M_\infty = \sum \frac{A_r}{\alpha_r} \qquad\qquad (9\text{-}59)$$

Upon substituting the values for A_r and α_r given earlier in Eq. (9-21), we find

$$M_\infty = 17.5 \text{ ksi} . \qquad\qquad (9\text{-}60)$$

Equations (9-24), (9-25) and (9-40) may be combined to give the following expression for F_s:

$$F_s = \frac{c_o \tau}{\sin \left[\frac{1}{3} \sin^{-1}(\alpha J) + \frac{2\pi}{3} \right]} \, , \qquad\qquad (9\text{-}61)$$

where $\alpha(\sigma)$ and $\tau(\sigma)$ are defined by Eqs. (9-57) and (9-58) and $c_o = 0.07$ ksi⁻¹.

9.6 A Hydrostatic Model for High Pressures.

Under monotonically increasing pressure, it is observed that the hydrostatic behavior of plain concrete is characterized by an initially convex stress-strain curve, which eventually becomes concave and finally (asymptotically) linear as depicted earlier in Figure 4.1. The linear portion is reversible, indicating that the material has reached an elastic state. As the elastic state is approached, the stress and slope of the hydrostatic pressure - plastic volumetric strain curve tend to infinity as the plastic volumetric strain tends toward a critical value, ϵ_c^P, which corresponds to complete compaction. Further compression occurs elastically with $d\epsilon^P = 0$.

The role of the hardening function F_H is to account for the effect of compaction on the hydrostatic behavior and, since compaction is reflected through the plastic volumetric strain, ϵ^P, it is natural to take $F_H = F_H(\epsilon^P)$. It can be shown that, for monotonic loading above the initial convex portion of the stress-strain curve, the hydrostatic stress σ and $F_H(\epsilon^P)$ are related by an expression of the form:

$$\sigma = \phi_o\, F_H(\epsilon^P) \ . \tag{9-62}$$

where ϕ_o is a positive material constant. Therefore, except for the constant multiplier ϕ_o, the function $F_H(\epsilon^P)$ describes the monotonic hydrostatic loading curve for all pressures above the initial convex part of this curve.

The general restrictions that the function F_H must satisfy, in addition to being a monotonically increasing function of ϵ^P, are:

$$F_H(0) = 1$$

$$\lim_{\epsilon^P \to \epsilon_c^P} F_H = \infty \tag{9-63}$$

The first restriction follows simply from convenience and allows us to set $\phi_o = \sigma_o$. where σ_o is the intercept on the σ-axis shown in Figure 4.4. With ϕ_o set to σ_o in Eq. (9-62), the virgin hydrostatic compression curve from A to C is then described by the equation

$$\sigma = \sigma_o \, F_H(\epsilon^P) \ . \tag{9-64}$$

which proves convenient in applying the model to specific materials. The second restriction arises from the fact that it takes an infinite pressure to close all pores, that is:

$$\lim_{\epsilon^P \to \epsilon^P_c} \sigma \; = \; \infty \tag{9-65}$$

In view of Eq. (9-64), condition (9-65) is satisfied by taking F_H such that condition (9-63b) is fulfilled.

The hydrostatic data to which the endochronic model was applied in Section 9.2 covered the range of pressures up to 15 ksi. Over this range, it was found that the simple linear expression given by Eq. (9-11), which satisfies condition (9-63a), led to an excellent description of the hydrostatic data. For higher pressures, however, this linear form for F_H is inadequate and a more general expression which also satisfies condition (9-63b) is required.

To extend the range of the model to high pressures, including elastic behavior beyond full compaction, a suitable expression for F_H is as follows:

$$F_H = 1 + \beta_o \epsilon^P + \gamma_o \, (\epsilon^P_c - \epsilon^P)^{-m} \tag{9-66}$$

where β_o, γ_o and m are positive constants. This expression satisfies conditions (9-63) and is a monotonically increasing function of ϵ^P. There are, of course, other expressions that satisfy these general requirements, also, but that given by Eq. (9-66) appears to capture the behavior of plain concrete quite well, as shown in Figure 9.13. Here, the response of the endochronic hydrostatic model, with F_H defined according to Eq. (9-66), to pure hydrostatic compression of plain concrete up to 65 ksi is compared with the corresponding data reported in Reference [9.11], which unfortunately provided very limited unloading data. The agreement between the model and the data is considered quite good.

Finally, if high pressures that nearly cause complete compaction are not of interest, the following simple expression for F_H has been found to be adequate in many cases:

$$F_H = e^{\beta \epsilon^p} \qquad\qquad (9\text{-}67)$$

This expression satisfies only the first of the two conditions in Eq. (9-63). Also, it reduces, for small ϵ^p, to the linear expression for F_H adopted in Section 9.2.
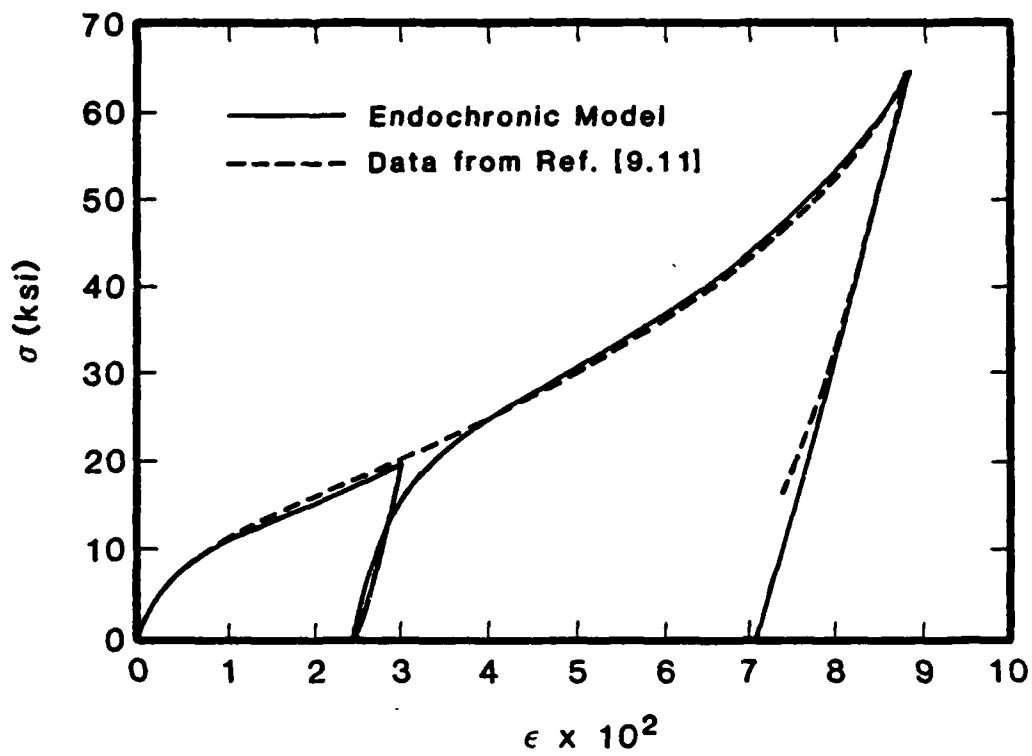
Figure 9.13   Hydrostatic compression of plain concrete to high pressures.

REFERENCES FOR CHAPTER 9.

9.1   Scavuzzo, R., T. Stankowski, K. H. Gerstle and H. Y. Ko, "Stress-Strain Curves for Concrete Under Multiaxial Load Histories," CEAE Department, University of Colorado, Boulder, (1983).

9.2   Valanis, K. C., and H. E. Read, "An Endochronic Plasticity Theory for Concrete," *Mechanics of Materials*, 5, (1986), 277.

9.3   Valanis, K. C., "A Damage Theory for Brittle and Ductile Solids," in preparation.

9.4   Mills, L. L., and R. M. Zimmerman, "Compressive Strength of Plain Concrete Under Multiaxial Loading Conditions," *ACI Journal*, October, (1970), 802.

9.5   Willam K. J., and E. P. Warnke, "Constitutive Model for the Triaxial Behavior of Concrete," *Proc. Intl. Assoc. Bridge and Structural Engrs., Seminar on Concrete Structs. Subjected to Triaxial Stresses*, Bergamo, Italy, May 17-19, (1974).

9.6   Ottosen, N. S., "A Failure Criterion for Concrete," *J. Engr. Mechs. Div.*, ASCE, 103 (EM5), October, (1977), 850.

9.7   Lade, P. V., "Three Parameter Failure Criterion for Concrete," *J. Engr. Mechs. Div.*, ASCE, 108, October, (1982), 850.

9.8   Peyton S., "A Failure Criterion for Rocks, Soils and Concrete," S-CUBED, La Jolla, California, unpublished report, (1983).

9.9   Podgorski, J., "General Failure Criterion for Isotropic Media," *J. Engr. Mechs. Div.*, ASCE, 111, (1985), 188.

9.10   Hegemier, G. A., and H. E. Read, "On Deformation and Failure of Brittle Solids: Some Outstanding Issues," *Mechanics of Materials*, 4, (1986), 215.

9.11   Green, S. J., and S. R. Swanson, "Static Constitutive Relations for Concrete," Terra Tek, Inc., Salt Lake City, Utah, Report AFWL-TR-782-244, (1973).

9.12   Cedolin, L., R. J. Crutzen and S. Dei Poli, "Triaxial Stress-Strain Relationship for Concrete," *J. Engr. Mechs. Div.*, ASCE, 103 (EM5), (1977), 423.

10. NUMERICAL METHODS

In this chapter, numerical methods for computationally dealing with several aspects of the endochronic theory are presented. Included are an incremental approach for integrating the endochronic equations for the case in which there is no yield surface, and a numerical approach for determining the shear kernel function $\rho(z)$, using data obtained from shear tests conducted at fixed hydrostatic stress. A numerical algorithm developed by Valanis and Fan [10.1]) to deal with the endochronic equations within a finite element framework under the conditions of plane stress and plane strain was described earlier in Section 3.5.1. A much more extensive discussion of numerical methods for computationally treating the endochronic equations is given in the upcoming second volume of Endochronic Plasticity by the present authors.

10.1 An Incremental Approach for Numerically Integrating the Endochronic Equations.

An incremental scheme is presented in this section for numerically integrating the system of equations which govern the basic endochronic plasticity model without a yield surface. The scheme is explicit and based on Euler's method. Accordingly, care *must be taken in applying the method to ensure that the prescribed increments are* sufficiently small so that the computed behavior does not depend upon the increment size.* Otherwise, the scheme is straightforward, efficient and easy to implement.

Two different versions of the scheme are described below, namely, one which assumes prescribed strain increments as input and one which assumes prescribed stress increments as input. Both versions have had widespread application in the past in studies of various materials.

The basic equations which govern the endochronic model under consideration have been given earlier in Eqs. (3-1) to (3-8), but are repeated below for ready reference:

$$\underset{\sim}{s} = \int_0^{z_s} \rho\left(z_s - z'\right)\frac{d\underset{\sim}{e}^p}{dz} \, dz' \qquad (10\text{-}1)$$

---

* An approach for increasing the computational speed of this method by over an order of magnitude has been developed by Murakami and Read [10.2].

$$\sigma = \int_{0}^{z_H} \phi\left(z_H - z'\right)\frac{d\epsilon^P}{dz'} \, dz' \tag{10-2}$$

$$d\underset{\approx}{s} = 2\mu\left(d\underset{\approx}{e} - d\underset{\approx}{e}^P\right) \tag{10-3}$$

$$d\sigma = K\left(d\epsilon - d\epsilon^P\right) \tag{10-4}$$

$$dz^2 = \left|\left|d\underset{\approx}{e}^P\right|\right|^2 + k^2\left(d\epsilon^P\right)^2 \tag{10-5}$$

$$dz_s = dz/F_s$$

$$\tag{10-6a,b}$$

$$dz_H = dz/\left(kF_H\right)$$

The weakly singular kernel functions can be expressed in terms of Dirichlet series:

$$\rho(z) = \sum_{r=1}^{\infty} A_r e^{-\alpha_r z} \tag{10-7}$$

$$\phi(z) = \sum_{i=1}^{\infty} B_i e^{-\beta_i z} \quad , \tag{10-8}$$

where in order to satisfy the Clausius-Duhem inequality. it is necessary that $\alpha_r \geq 0$. $\beta_i \geq 0$ and $A_r \geq 0$. $B_i \geq 0$. Moreover. to ensure that $\rho(z)$ and $\phi(z)$ are singular at the origin and integrable over a finite domain. we must have

$$\sum_{r=1}^{\infty} A_r = \sum_{i=1}^{\infty} B_i = \infty \tag{10-9}$$

and

$$\sum_{r=1}^{\infty} A_r/\alpha_r < \infty \; , \quad \sum_{i=1}^{\infty} B_i/\beta_i < \infty \; . \tag{10-10}$$

In applications of the theory to date, it has been found that two or three terms of the series (10-7) and (10-8) are usually quite adequate for representing the kernel functions. In such cases, however, care must be taken to ensure that the infinitely large values of $\rho(0)$ and $\phi(0)$ are approximated by suitably large finite values. When this is done, we can write:

$$\rho(z) \doteq \sum_{r=1}^{n} A_r \; e^{-\alpha_r z} \tag{10-11}$$

$$\phi(z) \doteq \sum_{i=1}^{n} B_i e^{-\beta_i z} \; , \tag{10-12}$$

where n is finite.

It then follows that the expressions for $\underset{\sim}{s}$ and σ given by Eqs. (10-1) and (10-2) can be alternately written as

$$\underset{\sim}{s} = \sum_{r=1}^{n} \underset{\sim}{Q}_r \tag{10-13}$$

$$\sigma = \sum_{i=1}^{n} P_i \; , \tag{10-14}$$

where $\underset{\sim}{Q}_r$ and P_i satisfy the following ordinary differential equations:

$$\frac{d\underset{\sim}{Q}_r}{dz_s} + \alpha_r \; \underset{\sim}{Q}_r = A_r \; \frac{d\underset{\sim}{e}^P}{dz_s} \tag{10-15}$$

$$\frac{dP_i}{dz_H} + \beta_i \; P_i = B_i \; \frac{de^P}{dz_H} \tag{10-16}$$

From Eqs. (10-13) to (10-14), we can write:

$$d\underset{\sim}{s} = A \, d\underset{\sim}{e}^{p} - \underset{\sim}{Q} \, dz_{s} \qquad (10\text{-}17)$$

$$d\sigma = B \, d\epsilon^{p} - P \, dz_{H} \qquad (10\text{-}18)$$

where

$$A = \sum_{r=1}^{n} A_{r}$$

$$\underset{\sim}{Q} = \sum_{r=1}^{n} \alpha_{r} \, \underset{\sim}{Q}_{r}$$

$$\qquad (10\text{-}19)$$

$$B = \sum_{i=1}^{n} B_{i}$$

$$P = \sum_{i=1}^{n} \beta_{i} \, P_{i}$$

Equations (10-17) to (10-19) provide a simple approach for incrementally integrating the stresses $\underset{\sim}{s}$ and σ, which is considerably more attractive from a computational standpoint then numerically coping with the hereditary integrals in Eqs. (10-1) and (10-2).

In that which follows, explicit numerical schemes are presented for incrementally updating the endochronic equations given above when either the strain increments or the stress increments are given. Because of the explicit nature of the scheme, it is necessary that the increments be taken sufficiently small to ensure accuracy.

10.1.1 Prescribed Strain Increments $\Delta\underset{\sim}{\epsilon}$.

It is assumed that $\underset{\sim}{s}$, σ, $\underset{\sim}{e}$, $\underset{\sim}{e}^{p}$, ϵ, ϵ^{p}, $\underset{\sim}{Q}_{r}$ and P_{i} are known at the beginning of each prescribed strain increment, $\Delta\underset{\sim}{\epsilon}$. From Eqs. (10-17) and (10-18), we can write

10-4

$$\Delta \underset{\sim}{s} = A \, \Delta \underset{\sim}{e}^P - \underset{\sim}{Q} \, \Delta z_s \tag{10-20}$$

$$\Delta \sigma = B \, \Delta \epsilon^P - P \, \Delta z_H \tag{10-21}$$

If we now combine these equations with the incremental Hooke's Law, Eqs. (10-3) and (10-4), and introduce Eqs. (10-6a,b), it follows that

$$\Delta \underset{\sim}{e}^P = \frac{1}{(A + 2G)} \left[2G \, \Delta \underset{\sim}{e} + \underset{\sim}{Q} \, \frac{\Delta z}{F_s} \right] \tag{10-22}$$

$$\Delta \epsilon^P = \frac{1}{(B + K)} \left[K \Delta \epsilon + P \, \frac{\Delta z}{k F_H} \right] \tag{10-23}$$

Upon substituting these results into Eq. (10-5), the following quadratic expression for Δz is obtained:

$$a \, \Delta z^2 + b \, \Delta z + c = 0 \quad , \tag{10-24}$$

where

$$a = 1 - \frac{\underset{\sim}{Q} \cdot \underset{\sim}{Q}}{(A + 2G)^2 F_s^2} - \frac{P^2}{(B + K)^2 F_H^2}$$

$$b = -2 \left\{ \frac{2G \, \underset{\sim}{Q} \cdot \Delta \underset{\sim}{e}}{(A + 2G)^2 F_S} + \frac{kKP}{(B + K)^2 F_H} \, \Delta \epsilon \right\} \tag{10-25}$$

$$c = - \left\{ \left(\frac{2G}{A + 2G} \right)^2 \Delta \underset{\sim}{e} \cdot \Delta \underset{\sim}{e} + \left(\frac{kK}{B + K} \right)^2 \Delta \epsilon^2 \right\}$$

Equation (10-24) provides two roots $\Delta z_{1,2}$, the one of interest being the one for which $\Delta z \geq 0$. Once Δz is known, $\Delta \underset{\sim}{e}^P$ and $\Delta \epsilon^P$ can be obtained from Eqs. (10-22) and (10-23), after which $\Delta \underset{\sim}{s}$ and $\Delta \sigma$ can be obtained from Eqs. (10-20) and (10-21). Finally, Eqs. (10-15) and (10-16) are used to update the $\underset{\sim}{Q}_r$ and P_i. This approach, therefore, permits one to determine the stress increments, $\Delta \underset{\sim}{\sigma}$, for prescribed increments in the strain $\Delta \underset{\sim}{\epsilon}$.

10.1.2   Prescribed Stress Increments $\Delta\underset{\sim}{\sigma}$.

In this case. $\underset{\sim}{s}$, σ, $\underset{\sim}{\varepsilon}$, $\underset{\sim}{\varepsilon}^P$, ϵ, ϵ^P, Q_r and P_i are assumed to be known at the beginning of each prescribed stress increment $\Delta\underset{\sim}{\sigma}$. From Eqs. (10-6a,b). (10-17) and (10-18). we can obtain the expressions:

$$\Delta\underset{\sim}{\varepsilon}^P = \frac{1}{A}\left[\Delta\underset{\sim}{s} + \frac{\underset{\sim}{Q}}{F_s}\,\Delta z\right] \tag{10-26}$$

$$\Delta\epsilon^P = \frac{1}{B}\left[\Delta\sigma + \frac{P}{kF_H}\,\Delta z\right] \tag{10-27}$$

Upon substituting these results into Eq. (10-5). the following quadratic expression for Δz results:

$$a\,\Delta z^2 + b\,\Delta z + c = 0 \tag{10-28}$$

where

$$a = 1 - \frac{\underset{\sim}{Q}\cdot\underset{\sim}{Q}}{(A\,F_s)^2} - \left(\frac{P}{B\,F_H}\right)^2$$

$$b = -2\left[\frac{\underset{\sim}{Q}\cdot\Delta\underset{\sim}{s}}{A^2\,F_s} + \frac{k\,P}{B^2\,F_H}\,\Delta\sigma\right] \tag{10-29}$$

$$c = -\left[\frac{\Delta\underset{\sim}{s}\cdot\Delta\underset{\sim}{s}}{A^2} + \left(\frac{k\,\Delta\sigma}{B}\right)^2\right]$$

Again. the root of interest from Eq. (10-28) is that for which $\Delta z \geq 0$. Once Δz is found from Eq. (10-28). $\Delta\underset{\sim}{\varepsilon}^P$ and $\Delta\epsilon^P$ can be determined from (10-26) and (10-27). after which $\Delta\underset{\sim}{\varepsilon}$ and $\Delta\epsilon$ may be found from Eqs. (10-3) and (10-4). The Q_r and the P_i are updated on the basis of Eqs. (10-15) and (10-16). This approach. therefore. permits one to determine the strain increments $\Delta\underset{\sim}{\varepsilon}$ for prescribed increments in the stress $\Delta\underset{\sim}{\sigma}$.

10-6

10.2. A Numerical Procedure for Determining the Shear Kernel Function.

In Section 4.3, it was shown that in the case of shear at a fixed hydrostatic stress σ, the shear stress τ is given by an expression of the form

$$\tau(y) = \int_0^y \rho(y - y')\, G(y')\, dy' \tag{10-30}$$

where

$$dy = dw = dz \tag{10-31}$$

From experimental data obtained from shear tests at fixed σ, the functions $\tau(y)$ and $G(y)$ can be found When this has been done, Eq. (10-30) becomes a Volterra equation of the first kind for the unknown kernel function $\rho(y)$. In that which follows, a numerical procedure is given for obtaining $\rho(y)$ from Eq. (10-30), given the functions $\tau(y)$ and $G(y)$.

Let y_n be a generic value of the variable y. We divide the interval $[0,y]$ into suitably small equal subintervals Δ such that

$$y_n = n\Delta \tag{10-32}$$

The integral on the right-hand side of Eq. (10-30) can then be written in the form

$$\tau(y_n) = \tau_n = \int_0^\Delta \rho(y_n - y')\, g(y')\, dy' + \ldots \tag{10-33}$$

$$\ldots + \int_{(n-1)\Delta}^{n\Delta} \rho(y_n - y')\, g(y')\, dy'$$

or

$$\tau_n = \sum_{r=1}^n g_r \left\{ M[(n - r + 1)\Delta] - M[(n - r)\Delta] \right\}, \tag{10-34}$$

where by virtue of the mean value theorem

$$g_r = g\left(y_r^*\right) \quad , \tag{10-35}$$

$$(r - 1)\Delta \leq y_r^* \leq r\Delta \tag{10-36}$$

and

$$M(r\Delta) \approx \int_0^{r\Delta} \rho(y')dy' \tag{10-37}$$

The function g_r may be determined to the required degree of accuracy by making the interval Δ sufficiently small.

In consequence, we have the relations

$$\tau_1 = \Delta g_1 M(\Delta)$$

$$\tau_2 = \Delta g_1 M(2\Delta) + \Delta g_2 M(\Delta) \tag{10-38}$$

$$\tau_n = \Delta g_1 M(n\Delta) + \Delta g_2 M[(n - 1)\Delta] + \ldots + \Delta g_n M(\Delta)$$

where

$$\Delta g_r = g_r - g_{r-1} \tag{10-39}$$

This is a system of a linear simultaneous equations in $M(\Delta)$, $M(2\Delta)$ ... $M(n\Delta)$. Since the Δg_r are known, then knowing τ_1, τ_2 ... τ_n allows one to determine $M(r\Delta)$, $r = 1, 2$ ... n, by successive substitution. The following algorithm applies:

If

$$\bar{\tau}_n = \sum_{m=1}^{n-1} \Delta g_{n+1-m} M(m\Delta) \quad , \tag{10-40}$$

10-8

then

$$M(r\Delta) = \frac{\tau_n - \bar{\tau}_n}{\Delta g_1} \qquad (10\text{-}41)$$

Knowledge of $M(y)$ thus allows the determination of $\rho(y)$ since

$$\rho(y) = \frac{dM(y)}{dy} \qquad (10\text{-}42)$$

REFERENCES FOR CHAPTER 10.

10.1 Valanis, K. C., and J. Fan, "A Numerical Algorithm for Endochronic Plasticity and Comparison with Experiment," *Intl. J. Computs. and Structs.*, Vol. 19, 717., (1984).

10.2 Murakami, H., and H. E. Read, "A Second-Order Accurate Numerical Scheme for Integrating the Endochronic Equations," submitted to *Intl. J. Computs. and Structs.*, (1987).